UNIVERSITÀ DEGLI STUDI DI PADOVA

DIPARTIMENTO DI SCIENZE CHIMICHE

CORSO DI LAUREA MAGISTRALE IN CHIMICA

TESI DI LAUREA MAGISTRALE

Asymmetric Olefinative Conjugate Addition (AOCA): a New Tandem Transformation

Relatore: Dr. Orlandi Manuel

Controrelatore: Prof. Biffis Andrea

Laureando: Soppelsa Piero

ANNO ACCADEMICO 2022/2023

Table of Contents

1. ABSTRACT

The Asymmetric Allylic Substitutions (AAA) provide an invaluable synthetic tool in organic synthesis that is commonly employed for the synthesis of drugs and natural products, with high levels of regio- and stereoselectivity. Notwithstanding the widespread utilization of this reaction, certain drawbacks arise due either to the employment of precious metals or to intrinsic mechanistic constraints. In order to overcome these limitations, we developed a new tandem transformation named Asymmetric Olefinative Conjugate Addition (AOCA) for the generation of a stereocenter in α-position with respect to an internal, functionalized olefin. High yields and enantioselectivities are obtained by the use of an inexpensive and abundant copper catalyst, making this new methodology a valuable alternative to existing methods. The reaction has been optimized and the reaction scope has been evaluated within this thesis project work.

2. INTRODUCTION

2.1. Asymmetric Allylic Substitution

Asymmetric catalysis, since its inception in the 1960s, has brought a dramatical transformation of chemical synthesis protocols, achieving an impressive progression to a level that technically approximates or sometimes even exceeds that of natural biological processes. At its core, this discipline focuses on obtaining chiral products in highly enantiomerically enriched fashion starting from substrates that are achiral or racemic.[1] The magnitude of this science relies on the fact that molecular chirality plays a key role in science and technology. In particular, life depends on molecular chirality, with many biological functions being inherently asymmetric. Most physiological phenomena arise from highly precise molecular interactions, in which chiral host molecules discern two enantiomeric guest molecules in distinct manner.[2] This is only one example that show the importance of asymmetric catalysis and why it has experienced considerable progress over the last decades, resulting in the assignation of Nobel prizes in 2001 and 2021, and in the development of a broad array of novel methodologies. Among these, asymmetric allylic substitutions (AAA) are often employed in natural products synthesis.

AAA-type reactions facilitate the formation of a stereocenter in α-position with respect to an olefin by the formal nucleophilic substitution of a nucleophile to an allyl electrophile (Figure 1). These can be accomplished with soft nucleophiles employing several metal catalysts (usually Pd or Ir), or with hard nucleophiles typically employing Cu catalysts.[3-6] The latter is particularly attractive because it allows accessing a large variety of chiral products by the use of C-nucleophiles (e.g. organozinc, Grignard, organoboron, organolithium),[5,7-9] as well as Si-nucleophiles [10] and B-nucleophiles,[9,11] in addition to hydride.[12] These are useful in the synthesis of stereochemically complex targets, considering also the subsequent possibility of downstream functionalizations. Furthermore, the achievement of this goal is attained by the use of abundant and inexpensive metal catalysts. Such strategic approach holds significant foresight considering the expected low availability of chemical elements in future society and the need to utilize base metals instead of precious once.

A typical Cu-catalyzed AAA cycle (Figure 1) involves three elementary steps: (i) *transmetalation* between a copper(I) salt **1** and an organometallic reagent to give either a mono- or diorganocuprate(I) nucleophilic intermediate **2**; (ii) after coordination to the substrate **3**, the nucleophilic attack of the d-orbital of the copper(I) atom produces an organocopper(III)

intermediate **4**, which occurs driven by a key $d_{Cu} \rightarrow \sigma^*_{C\text{-}X}$ (*oxidative addition*);[13] and (iii) *reductive elimination* of the copper(III) intermediate to generate the product **5** and giving back the neutral copper(I) species. In a catalytic reaction, the last specie takes part in the subsequent catalytic cycle.[14]

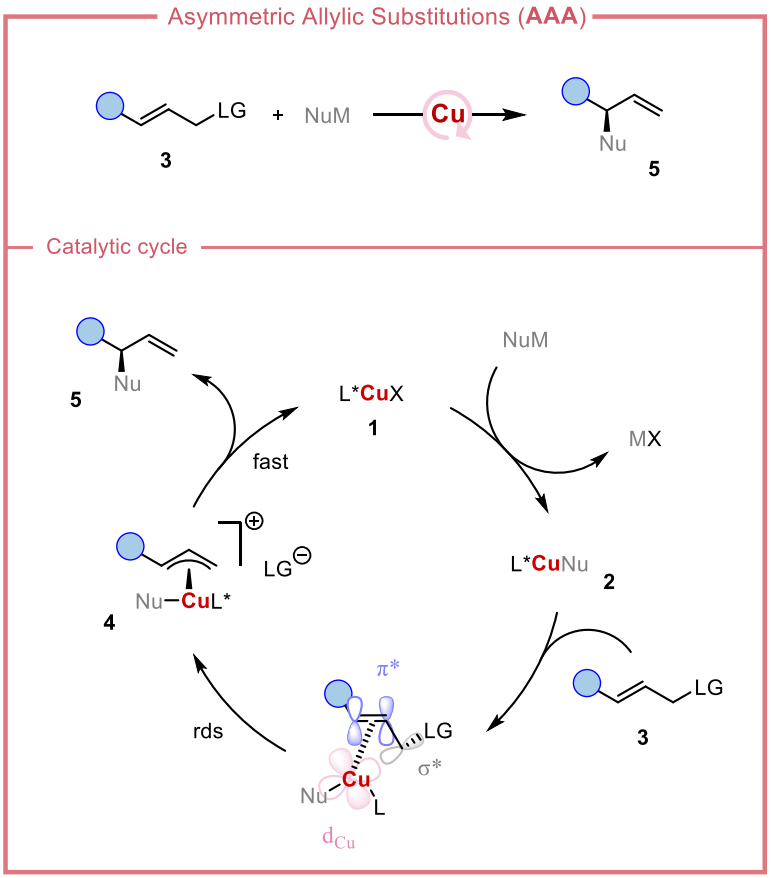

Figure 1. Asymmetric Allylic Substitution catalytic cycle

From a stereochemical standpoint, the following key conclusions can be drawn that can be rationalized with the reaction mechanism depicted in Figure 1. The oxidative addition step occurs with the nucleophilic/electron-rich ligand (Nu) in *trans* with respect to the leaving group (LG). This S_N2' selectivity is favoured since it maximizes the $d_{Cu} \rightarrow \sigma^*_{C\text{-}X}$ orbital overlap. Moreover, because Cu(III) complexes are relatively instable and reactive species, reductive elimination occurs fast from intermediate **4** without dissociation and reassociation of the allyl ligand. As a result, in the case of chiral allylic electrophiles such as **6**, the reaction is stereospecific (meaning that a single and specific enantiomer of the substrate results in a single and specific enantiomer of the product) (Figure 2-3).[15] This fact translates into two different synthetic scenarios:

1) The use of a chiral and enantiopure alkyl electrophile in the presence of an achiral Cu catalyst results in the selective generation of one out of four possible diastereosimers. Beyond the before mentioned S_N2' selectivity, this is due the high 1,3-allylic strain observed in one of the two possible transition states **7** and **8** that are generated from two distinct substrate conformations as depicted in Figure 2. This strategy annihilate the advantage of the asymmetric synthesis of obtaining highly enantiomerically enriched products starting from a racemic mixture of the substrate, given that an enantiomerically pure starting material must be employed (Figure 2).[r-v]

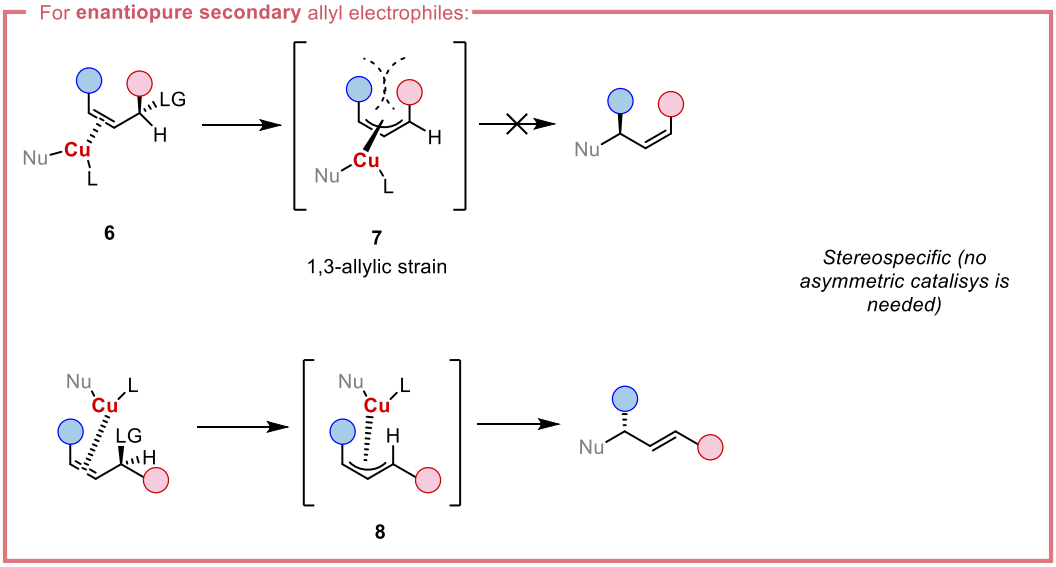

Figure 2. Stereospecificity of the AAA reaction

2) The use of a racemic chiral substrate in combination with a chiral Cu catalyst - according to the principles of asymmetric catalysis - leads to the formation of a nearly equimolar mixture of (*E*) and (*Z*)-products. Indeed, the use of a chiral ligand for the Cu catalyst allows for the preferential coordination of one of the two olefinic diastereotopic faces of the substrate. This leads to the selective production of one configuration of the new stereocenter but results in loss of control over the olefin configuration, generating the (E) and the (Z) configurations in equal proportions (because of the racemic nature of the substrate). In other words, the coupling between the formation of the new stereocenter and the olefination forbids the formation of a stereochemically pure internal olefin starting from a racemic substrate (Figure 3).[16-20]

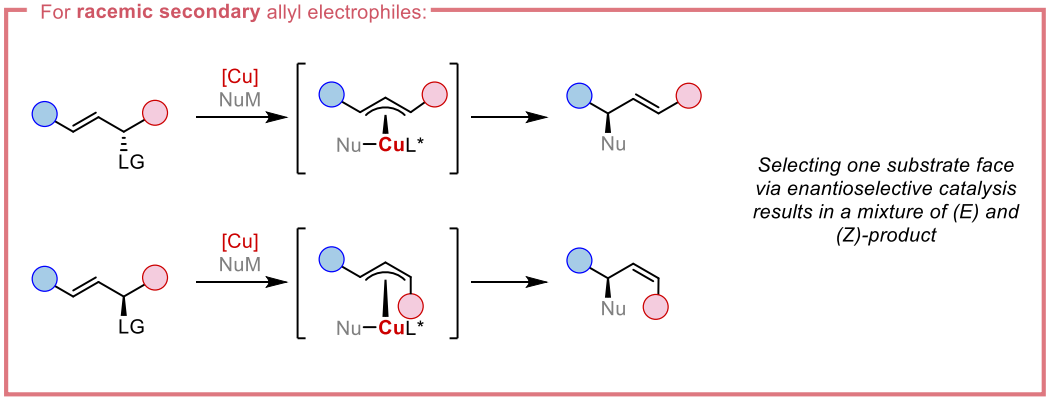

Figure 3. Enantioselective catalysis in AAA of racemic secondary allyl electrophiles

Thus, in these Cu-catalyzed AAA reactions the formation of the stereocenter and of the olefin are intrinsically coupled, which poses a major limitation in the context of asymmetric catalysis when compared to precious metals catalyzed analogues: *only primary allyl electrophiles can be employed to give terminal olefinic products* (Figure 4).

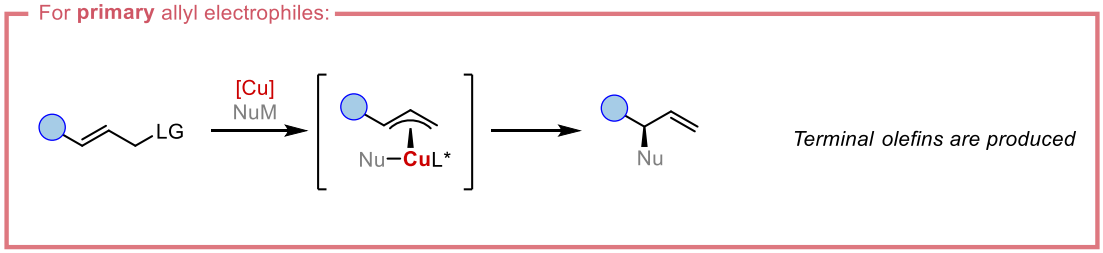

Figure 4. Enantioselective catalysis in AAA of racemic primary allyl electrophiles

In order to overcome this limitation, we propose a new synthetic methodology that we named Asymmetric Olefinative Conjugate Additions (AOCA). The underlying strategy relies on the decoupling of the addition and olefination steps, resulting in a separate control over the configuration of the two new stereochemical elements (i.e. the stereocenter and the olefin). As will be discussed in more detail in the next paragraphs, this method is based on the Asymmetric Conjugate Addition (ACA). To enhance the comprehension of our new methodology, a brief overview of ACA reactions is given below, with particular emphasis on the employment of Cu catalysts.

2.2. Asymmetric Conjuate Addition (ACA)

The conjugate addition reaction of organocuprates to α,β-unsaturated carbonyl compounds is arguably the most versatile organocopper reaction. Indeed, ACA reactions allow to introduce C(sp^3), C(sp^2), C(sp), H, Si, and B-nucleophiles in β-position with respect to a variety of electron withdrawing groups (EWG) under basic conditions.[9-11] For this reason, its mechanism (Figure 5) has been extensively studied. Similarly to the mechanism of AAA reactions, the ACA mechanism involves a first transmetallation step in which the active chiral – if a chiral ligand is used – organocopper reagent **2** is formed. Then the reversible formation of a cuprate-alkene complex **9** occurs. Again, this is a π-complexation of the C=C to the Cu atom. The subsequent oxidative addition step creates a new stereocenter in β-position, while the effective addition of the nucleophile is given through the reductive elimination at the Cu center. The anionic intermediate **10** that is generated as the reaction product can finally be quenched with an electrophile E^+ giving the desired unsaturated product **11**.[5,21-25]

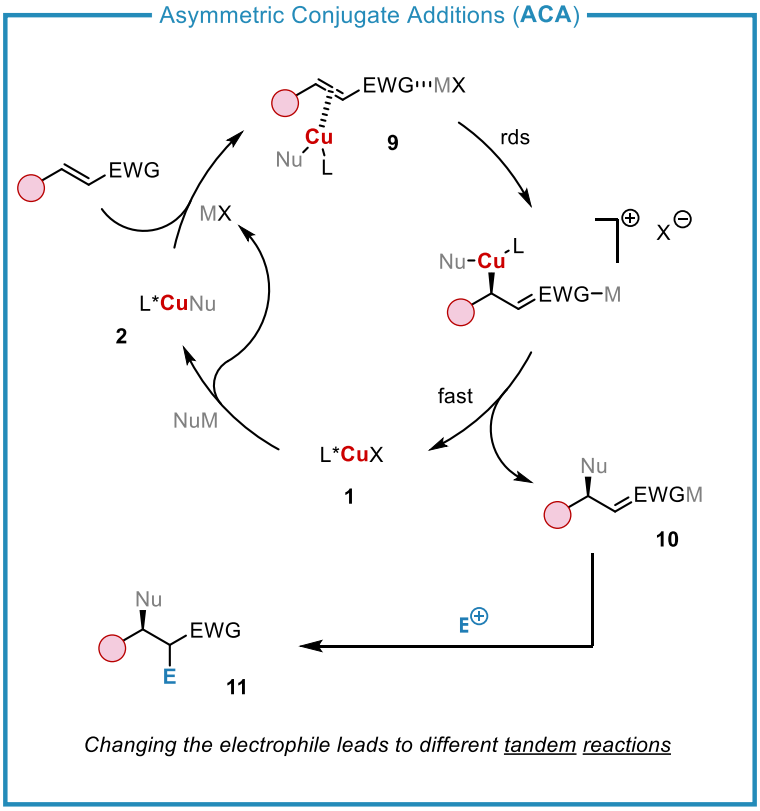

Figure 5. Asymmeyric Conjugate Addition catalytic cycle

This final step (the reaction quench) can lead to various catalytic asymmetric tandem transformations, i.e. transformations initiated by a catalytic ACA followed by many different

reactions involving the aforementioned anionic intermediate **10** with an electrophile of choice E^+. Asymmetric tandem reactions are a very appealing strategy because it enables the generation of complex products from readily available starting materials. Indeed, such multistep transformation allows for a rapid increase in molecular complexity of common substrates in a single reaction pot. The main advantage of this synthetic strategy is the formation of several bonds and the generation of two or more contiguous stereocenters through a one pot multistep reaction, eliminating the need for the isolation of the intermediates. The use of prochiral substrates and a chiral Cu catalyst in the first step provides the formation of a new stereogenic center with a high and *fixed* enantiomeric excess. *Fixed* means that the enantioselectivity with which the anionic intermediate **10** is obtained remains unchanged independently from the reaction employed to quench the intermediate after the ACA step. This makes it possible to obtain a plethora of complex products with the same *ee* at the β-position.

Because of these valuable features, a big effort has been made in recent years to extend the versatility of ACAs-initiated tandem transformations by matching different quenching reactions. Conjugate addition-triggered sequential transformations can be divided into anionic and radical processes, as a consequence of the addition mechanism. In Figure 6 are reported some examples in the field of copper-catalyzed ACA tandem processes of α,β-unsaturated compounds.[26] Only anionic processes are taken into account, since our methodology (AOCA) belongs to this category.

The first case makes use of the simplest electrophile, i.e. the proton. The required H^+ to quench the aforementioned anionic intermediate **12** is provided by a simple acidic work-up after the conjugate addition step. This methodology was developed in the '90 by several authors including Feringa and co-workers, who employing the chiral phosphoramidite ligands **L1**-**L5** provided the first examples of Cu-catalyzed ACA with high enantioselectivities (Figure 6a).[27]

Immediately, the authors understood the possibility of performing more complex tandem transformations, i.e. the possibility of exploiting anionic intermediate **10** in more elaborate reactions. This led Feringa and co-workers to report the first example of this bipartite methodology, performing a catalytic tandem 1,4-addition/aldol reaction (Figure 6b). This was a regio- and enantioselective three-component coupling of organozinc reagents with α,β-unsaturated ketones and aldehydes to afford *trans*-2,3-disubstituted carbonyl products with more than 90% *ee* in all cases. Such a good selectivity was achieved with only 2 mol% of a chiral catalyst which was prepared in situ from $Cu(OTf)_2$ and an enantiopure phosphoramidite ligand **L2**. The reaction gave β-hydroxy ketones **13** with three contiguous stereogenic centers. Based

on the reaction mechanism, full stereocontrol was achieved in the ACA step and nearly complete stereocontrol was obtained also in the formation of the two consecutive stereocenters in the subsequent aldol step, providing almost enantiomerically and diastereoisomerically pure products.[28]

Alexakis et al. extended the scope of the method demonstrating that Lewis acid activated acetals, ketals, and ortho esters could also be used to functionalize the zinc enolate intermediate, instead of the above mentioned aldehydes, affording aldol-type products.[29]

Related to the use of aldehydes as the electrophile, is the use of iminium ions **14** to access aminated products such as **15**, which is namely an ACA/Mannich tandem reaction (Figure 6c).

Alkylation can also be easily performed using alkyl halides. Compared with aldehydes, alkyl chlorides and bromides react with difficulty since they are less electrophilic. Even the use of alkyl iodides is not highly effective and works only under particular conditions such as the excess of the halide and the use of HMPA as an additive that favors an SN_2 reaction by carbocation solvation. Hoveyda and co-workers were able to employ this methodology in the synthesis of the anticancer drug Clavularin B **16**, obtaining 80% yield in the tandem addition/alkylation step using 10 eq. of alkyl iodide in the presence of 10 eq. of HMPA (Figure 6d).[30]

Tandem ACA/allylation reactions were developed by Alexakis and co-workers. The direct trapping of zinc enolates with activated allylic electrophiles was in fact known to be catalysed by Pd-complexes as in the known Tsuji-Trost reaction (Figure 6e).[31] This di-catalytic tandem transformation allows to extend the scope of the alkyl electrophiles.

Further tandem reactivity included ACA/halogenation (Figure 6f), ACA/silylation (Figure 6g) and ACA/hydroxylation (Figure 6h) to give products **17**, **18** and **20** respectively.

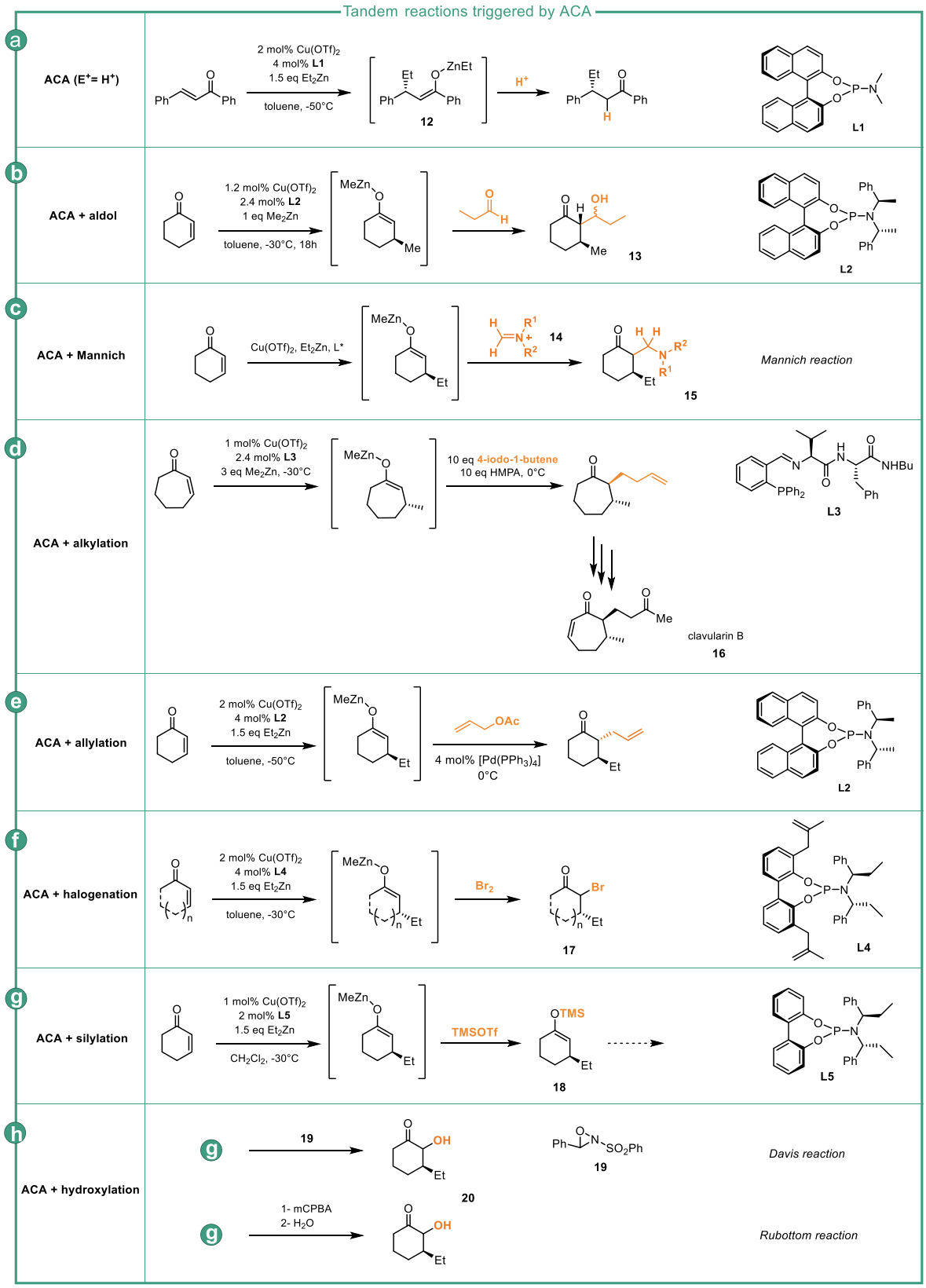

Figure 6. Catalytic Asymmetric Tandem Transformations Triggered by Conjugate Addition

As seen, trapping of the carbanionic intermediates resulting from ACA reactions with different electrophiles is well documented. However, *the one pot combination of ACAs with olefination reactions has no precedents*. Our innovative AOCA methodology aims at fulfilling this vacancy.

2.3. Asymmetric Olefinative Conjugate Addition (AOCA)

This innovative approach originates from the need for new catalytic protocols relying on abundant and inexpensive first-row transition metal catalysts that would allow accessing similar reactivity than their precious counterparts (Pd, Ir, Rh, etc.). As mentioned before, Cu-catalyzed AAA partly allow to reach this goal but two main drawbacks that make this synthetic methodology lag behind with respect to Tsuji-Trost type reactions:

1- Because the net process is stereospecific, selecting one of the two olefinic diastereotopic faces (by achiral catalyst) for *racemic* secondary allylic substrates leads to the formation of a nearly equimolar mixtures of *E* and (*Z*)-products. In other words, because the stereocenter and olefin formation are coupled, allylic substitutions to give stereochemically pure internal olefins are only possible starting from enantiomerically pure allylic electrophiles, whereas attainment of the same products by asymmetric catalysis has yet to be reported.

2- Therefore, when compared to precious metal analogues, Cu-catalyzed AAA suffer a major limitation: only primary allylic electrophiles can be employed leading to terminal olefinic products. In other words, only terminal olefins can be accessed by Cu-catalyzed AAA.

In order to overcome these limitations and obtain the desired internal olefins exploiting asymmetric catalysis, we propose a new synthetic methodology that we named Asymmetric Olefinative Conjugate Additions (AOCA) (Figure 7). This one-pot tandem reaction allows to decouple the asymmetric addition and the olefination steps thus resulting in a separate control over the configuration of the two stereochemical elements (i.e. the stereogenic center and the olefin). Such decoupling is crucial and possible - in principle - within the domain of the aforementioned catalytic asymmetric tandem transformations triggered by an asymmetric conjugate addition. Cu-catalysts provide effective ACA to not only α,β-unsaturated carbonyl compounds but also vinyl phosphonates.[12,32-41] Since this transformations proceed via formation of a carbanionic intermediate, we envisioned that this could be trapped with a carbonyl compound in the second step of AOCA thus undergoing an olefination via a Horner-Wadsworth-

Emmons (HWE) reaction.[42,43] Examples of conjugate addition to these starting materials have been already reported. [12,32-41] Thus, even though never realized in conjunction with an ACA reaction, it seems to be feasible for the resulting anions to undergo stereoselective olefination with the almost exclusive production of the (*E*) or (*Z*) diastereoisomer, thereby satisfying our objective.

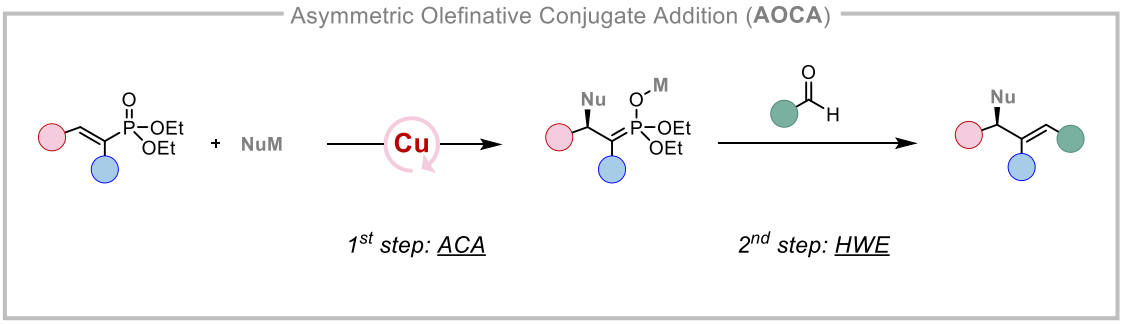

Figure 7. Asymmetric Olefinative Conjugate Addition methodology

Overall, if realized AOCA would be a new synthetic methodology filling gaps in organic synthesis and granting the following advantages:

1- A plethora of nucleophiles should work in this reaction thus giving AOCA good generality. Indeed, Grignard reagents, dialkyl zinc reagents, and organoboranes can be employed in Cu-catalyzed ACAs, also considering various activating groups and possible additional stabilizing EWG-groups necessary in the olefination step.

2- AOCA is formally a multicomponent transformation. This will allow to build libraries of chiral compounds by only selecting the appropriate substrate, nucleophile, and carbonyl compound. This possibility will be investigated and confirmed during the expansion of the scope of the reaction.

3- The key point of the innovative idea is the decoupling between the enantioselective conjugate addition step and the olefination, which could make it possible to obtain selectively one diastereoisomer of the olefin (*E* or *Z*). Additionally, it is expected that once that optimal reaction conditions are identified for a given substrate/nucleophile pair in the ACA step, any products attainable by variation of the third component (i.e. the carbonyl compound) should be accessed with the same (*fixed*) high enantioselectivity. In other words, the olefination step occurs after the conjugate addition, when the *ee* of the first steroecenter has already been irreversibly set. This is

an ideal feature in the context of the high-fidelity construction of libraries useful compounds in medicinal chemistry as an example.

4- AOCA should allow performing a formal AAA reaction with direct installation of functional groups that are normally poorly compatible with AAAs (e.g. a second Michael acceptor with a similar reactivity to the original substrate) even for precious metal catalysts.

All of these features are indicative of a synthetic methodology that has the potential to effectively address gaps in organic synthesis and testing its validity and feasibility is the core of the present master thesis.

3. SYNTHESIS METHODS

In this section, the theoretical aspects of the synthetic methods that have been employed in this project are described. The adopted experimental procedures are reported in detail in the *Experimental Section* chapter.

3.1. Synthesis of the Ligands

There are three main synthetic routes for the synthesis of phosphoramidites reported in the literature, and they differ for the order of formation of the P-O and P-N bonds.[44] The first and most frequently used one involves a first step in which the appropriate diol **21** is treated with phosphorus trichloride to obtain the corresponding chlorophosphite **22**. This intermediate is then stirred in the presence of the desired amine and a base yielding the target phosphoramidite **23** (Figure 8, Route 1). Most of the chiral ligands that have been synthesized within this project require the use of sterically hindered amines. In these cases, the initial synthesis of the dichloroaminophosphine **24** can provide a better alternative to Route 1 in terms of yield. Thus the amine is first treated with PCl_3, and the desired diol is then added (Figure 8, Route 2). The third possible pathway involves the treatment of BINOL **21** with hexamethylphosphorus triamide (HMPT) to give the dimethylamine-derived phosphoramidite ligand **25** known as MonoPhos. This can further be reacted to give an amine exchange under basic conditions to render different phosphoramidites (Figure 8, Route 3). It should be emphasized that in our experience, most phosphoramidite ligands are air-stable for months and do not require handling and storing under stringent inert conditions, representing a good feature of our methodology in terms of practicality. Many of the phosphoramidites that have been produced and tested within this thesis work involve non commercially available diols and amines. Therefore, the synthesis of the desired diols and amines was necessary and it is described below.

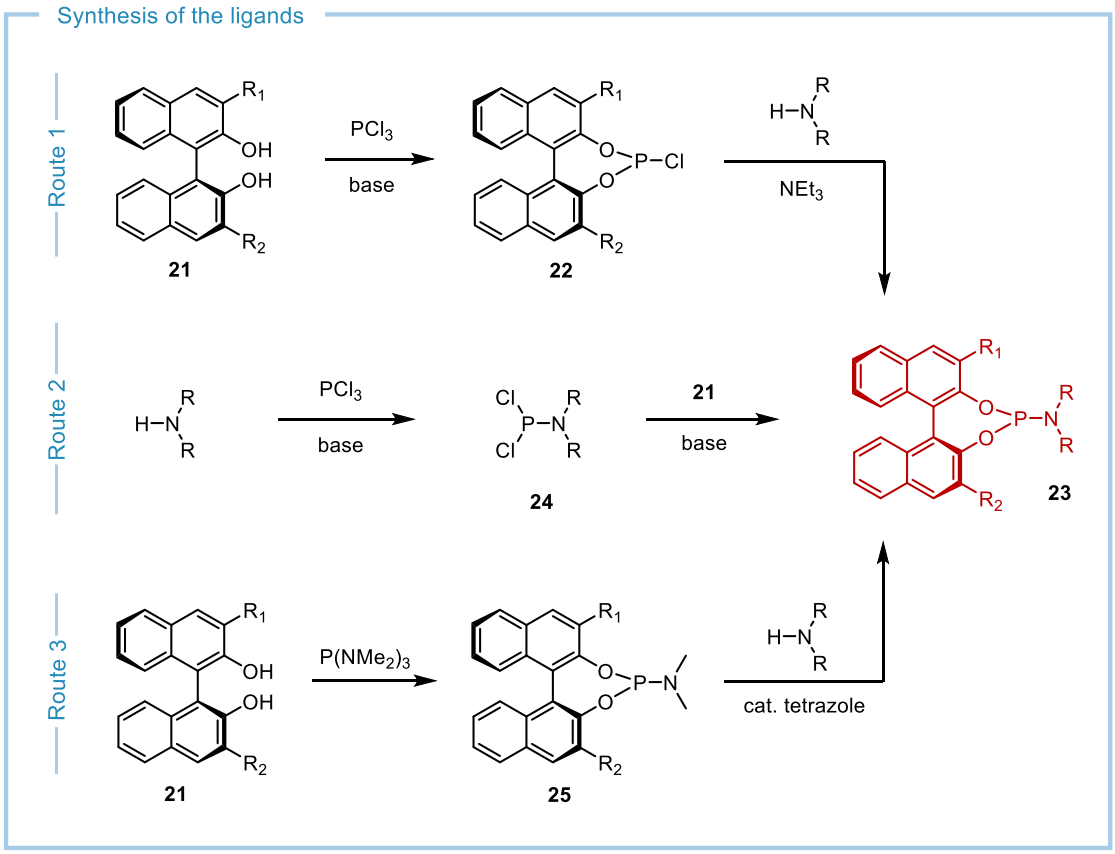

Figure 8. Synthesis of BINOL-based phosphoramidites

3.2. Synthesis of the Diols

Most of the ligands that have been tested feature an *ortho*-substituted BINOL moiety. Three different procedures were exploited in order to access these substituted diols starting from BINOL **21** (Figure 9). For all of them, a first step of protection of the two hydroxyl groups with chloromethyl methyl ether (MOMCl) was needed, giving compound **26**.[45] The *ortho*-functionalization with small alkyl substituents (e.g. methyl, ethyl, or butyl) involved a first *ortho*-lithiation by the use of BuLi and a second step of nucleophilic substitution of the resulting aryl lithium intermediate with the appropriate alkyl halide (CH_3I, EtBr, or BuBr).[46] Good yields were obtained for the mono- and di-substitution for the methyl group, while moderate to low amounts of the desired products have been obtained when ethyl or *n*-butyl bromide were used. In these cases, the *Negishi coupling* assured higher substitution yields, representing a convenient alternative for the BINOL substitution. This synthetic route involves a first step of *ortho*-lithiation of the MOM-protected diol and the subsequent addition of I_2 or Br_2 to obtain

the *ortho*-halogenated product **27**.[47] The obtained aryl halide is finally employed in a *Negishi coupling* with the desired dialkyl zinc and a catalytic amount of $Pd(OAc)_2$ and the monodentate phosphine S-Phos to give the desired products after the cleavage of the MOM-protecting group by acidic hydrolysis.[46]

The aforementioned aryl iodide can also be involved in a *Suzuki coupling* with an arylboronic acid to introduce an aryl substituent in the *ortho*-position. This coupling was performed in the presence of $Pd(PPh_3)_4$ as the catalyst and K_2CO_3 as the base.[48]

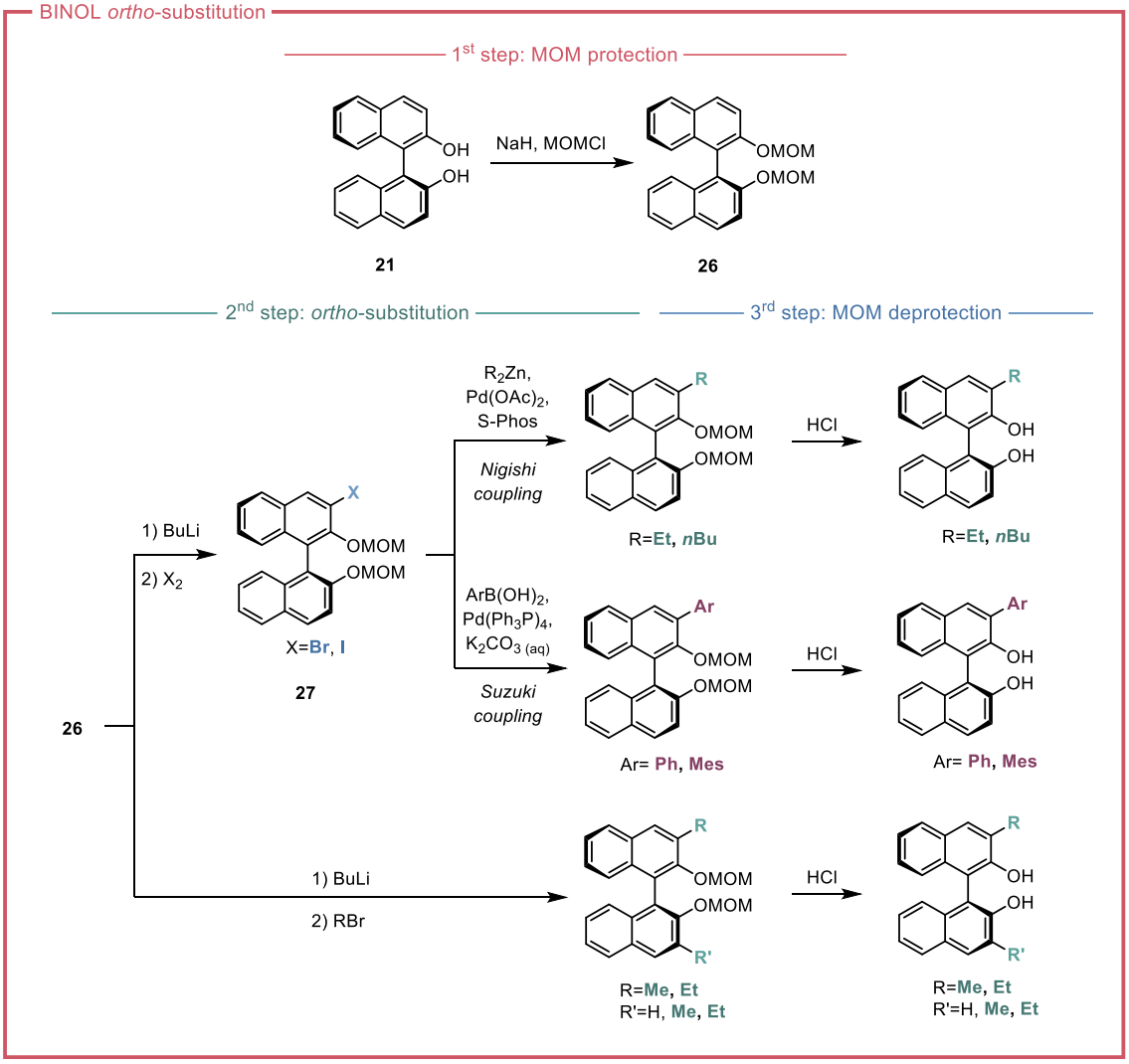

Figure 9. Possible synthetic routes for the BINOL *ortho*-substitution

3.3. Synthesis of the Amines

Phosphoramidite ligands featuring a chiral C_2-symmetric amine often provide superior performances in terms of stereoselectivity. Thus, the possibility of accessing different of these amines and assessing their effect on the ligand performances was taken. One of the possible synthesis of this class of chiral amines consists in the reductive amination of a ketone **28** with an enantiopure primary amine **29**. The first step involves the addition of an excess of titanium isopropoxide to an equimolar mixture of the mentioned starting materials with the formation of an imine intermediate **30**. This intermediate is finally reduced to the desired secondary amine via hydrogenation catalyzed by Pd/C and H_2 at atmospheric pressure.[49] This process can result in the formation of two diastereomeric products, which is due to the presence of two stereogenic carbon atoms in the secondary amine products. The configuration of one of them is fixed since an enantiomerically pure primary amine is involved in the synthesis, while the other one is formed from the pro-stereogenic iminic carbon after the C=N bond reduction. Both the (*R*) and the (*S*)-configuration for this second stereocenter can result, thus generating two possible diastereoisomers (the (*R*,*R*) and the (*R*,*S*), if the primary amine (*R*)-**28** is employed in the synthesis). In most cases, the mixture of diastereoisomers is obtained after this step with a diastereoselectivity of ca. 9:1 dr (see below for a discussion concerning the origin of this selectivity). However, their separation can be attempted by fractional recrystallization of the amine hydrochloride, which is simply generated through the addition of HCl. In a few cases, a single diastereoisomer could not be obtained by recrystallization. However, we found that using the mixture of stereoisomers in the synthesis of phosphoramidites resulted in diastereomerically pure ligands. Indeed, because of the diastereoisomeric relationship between the two isomers, these react in the formation of the phosphoramidite with the chiral BINOL derivative with different rates, allowing for the kinetic resolution of the amine.

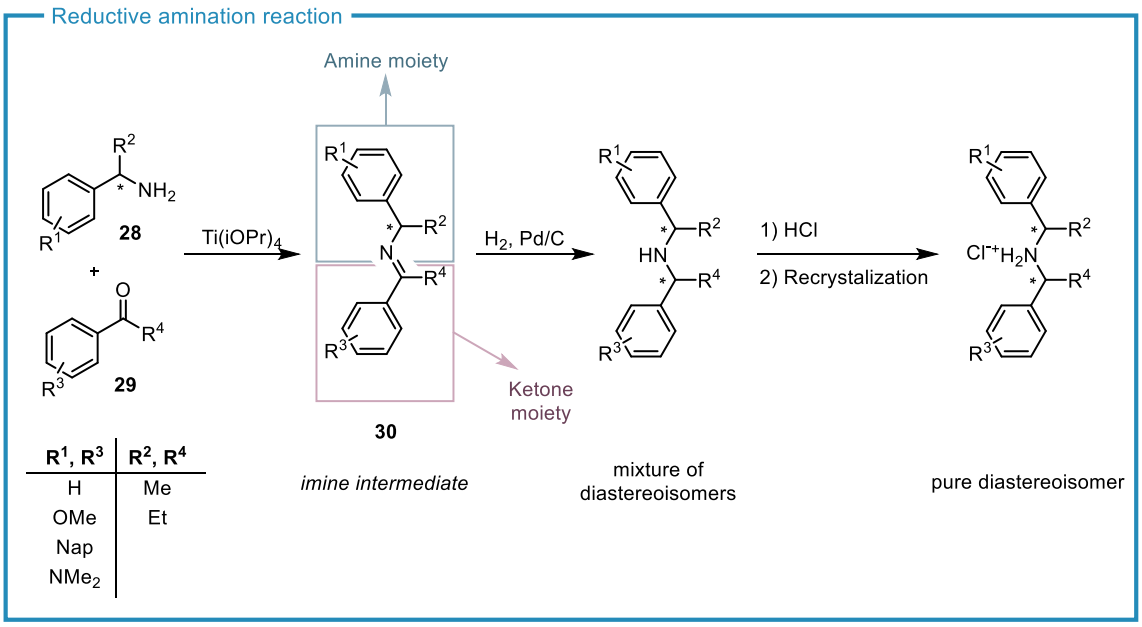

Figure 10. Synthesis of the secondary amines

In order to rationalize the hydrogenation diastereoselectivity, the Felkin-Anh model can be used. This is a stereochemical model for the rationalization of the stereochemistry of some reactions that involve a diastereoselective transformation at a pro-stereogenic π-reaction site (e.g. a carbonyl or an olefin) next to a stereocenter. The addition of two H-atoms to the imine intermediate **30** falls within this cases. The first aspect that the model takes into account is the substrate's conformation (i.e. the spatial disposition of the molecule's atoms resulting from single bonds rotations). For the same configuration of the imine, two possible conformations **31** and **32** can be considered as starting point in accordance with the model. The most stable one (**31**) has more possibilities to undergo the transformation because most of the reacting molecules are in that conformation and because the same energy difference between **31** and **32** is supposed to be transferred also to the reduction TS. After having identified the most probable configuration for the reagent, a qualitative estimation of the energies for the two possible H_2 addition TSs has to be done. These two options differ for the face of the imine that is approached by the nucleophile (Pd-H in our case). Since this substrate is chiral, the attack at the pro-R face has a different energy with respect to the attack at the pro-S face because the two TSs involved are diastereomeric. The most likely addition occurs at the less hindered face, in accordance with the Felkin-Ahn model. Thus, the higher is the difference in the steric hindrance between the

small and medium groups (Figure 11), the higher the diastereoselectivity of the reaction.

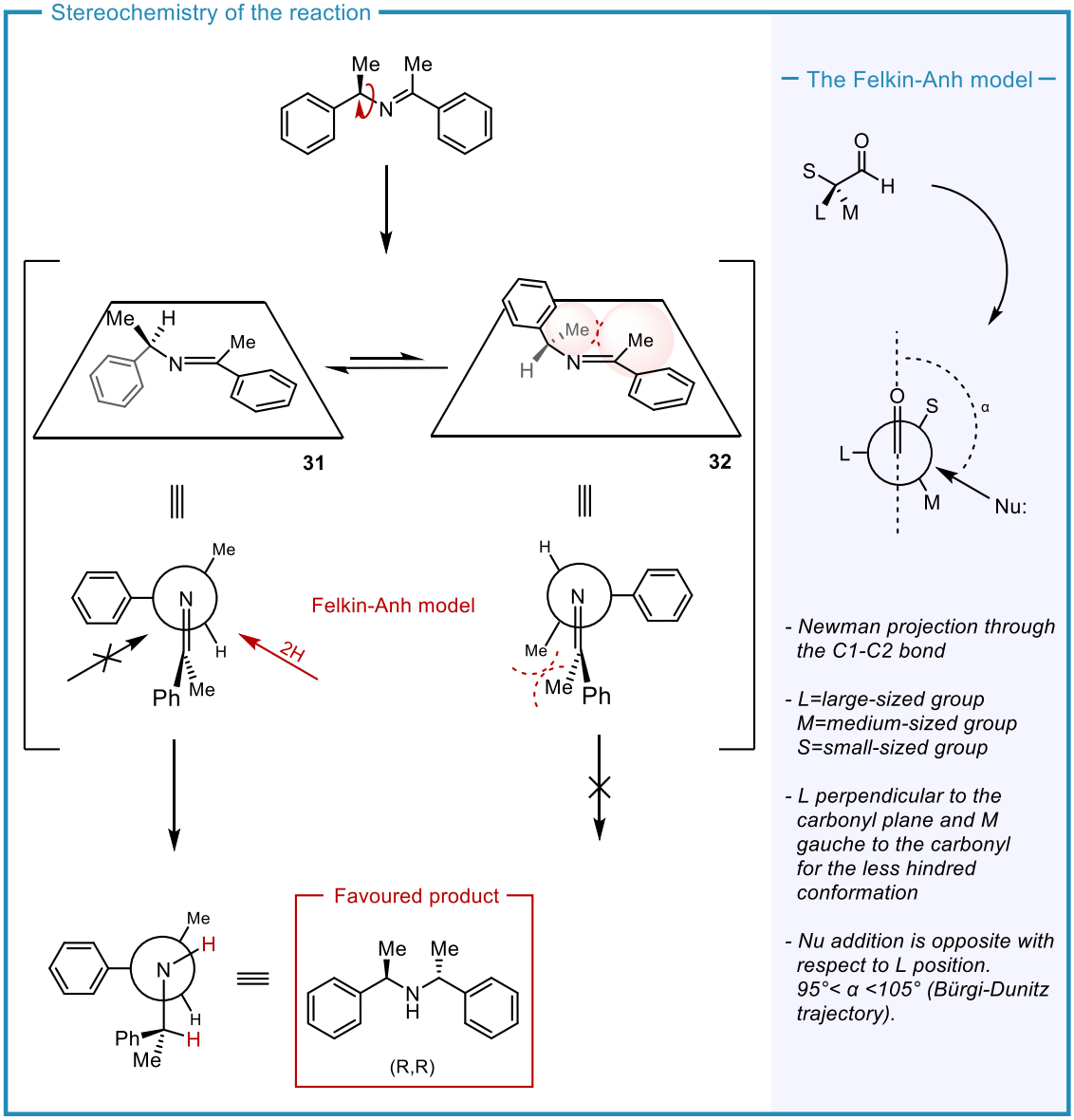

Figure 11. Stereochemistry of the reductive amination reaction and rationalization via the Felkin-Ahn model

3.4. Synthesis of the Substrates

The scope of the reaction has been extended by employing different aldehydes in the HWE step (the second step of AOCA) but also by trying substrates that differ from each other for either the phosphonate substituent, the electron withdrawing group, or the β-substituent. The EWG groups explored are the CN and CO_2Me groups, which have been paired with different

phosphonates (i.e. $P(O)(OMe)_2$, $P(O)(OEt)_2$, or $P(O)(OiPr)_2$). Whenever not commercially available, the desired phosphonoacetonitrile **33** was synthesized by heating a mixture of the corresponding trialkyl phosphite and chloroacetonitrile.[50] The obtained compound is then reacted in the *Knoevenagel* condensation with the desired aldehyde **34** mediated by NEt_3 and $ZnCl_2$, yielding the final (*E*)-vinylphosphonate **35** (Figure 12).[51] In order to vary the β-substituent of the substrate, the appropriate aldehyde was employed in this second reaction step.

For the synthesis of substrates with different EWG groups, a similar synthetic route was employed with the replacement of the cyano group with other electron withdrawing groups.

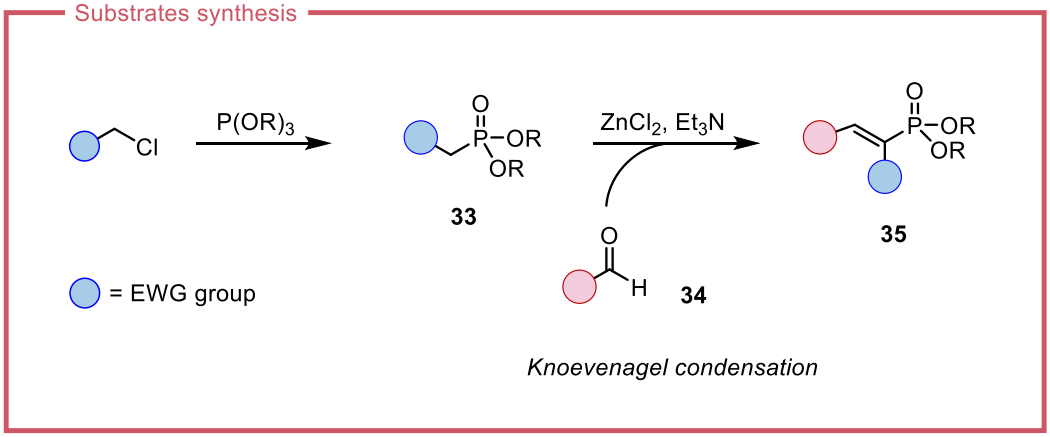

Figure 12. Synthetic methodology for the production of the starting materials

4. RESULTS AND DISCUSSION

4.1. Preliminary Data and Conditions Optimization

This master thesis work relies on reaction conditions previously optimized in our research group. In order to maximise both the enantioselectivity and yield of the benchmark reaction depicted in Figure 13, different parameters have been screened such as temperature T_1, solvent, Cu source, concentration, catalyst loading, phosphonate activating group, and reaction time. All the attempts are reported in Table 1, which highlights the optimized conditions in entry 17 that were used in the subsequent ligand screening. These conditions allowed to obtain product **36** in 77% *ee* and 76% yield, thus giving us a good starting point for further optimization by the identification of an optimal ligand for accessing >90% *ee* range. The screening of a wide range of different ligands synthetized according to the procedures described in the previous chapter, allowed to identify **L26** as the most effective one. While the ligands screening is discussed in more detail in the next paragraph, we anticipate that after the identification of **L26** as the optimal ligand, a fine tuning of the catalyst loading was further undertaken in order to minimize its concentration thus improving the appeal of the AOCA methodology. More specifically, we found that halving the catalyst loading from 4 mol% CuTC and 10 mol% **L26** to 2 mol% CuTC and 5 mol% **L26** led to the same levels of yield and enantioselectivity.

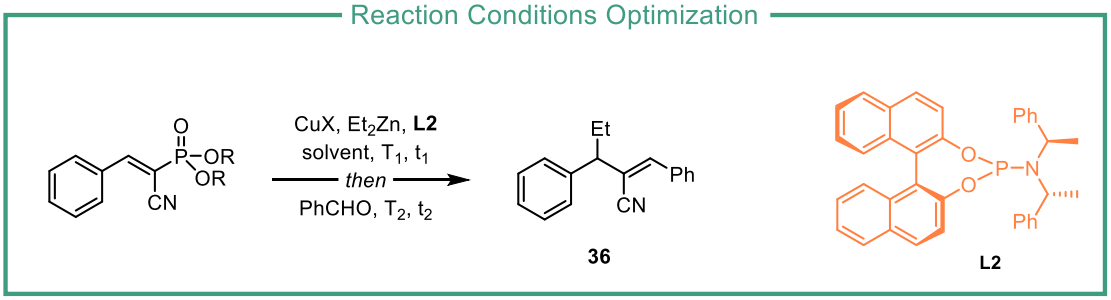

Figure 13. Reference reaction for the optimization of the reaction conditions

	R	L2 (mol%)	CuX	t_1 (h)	T_1 (°C)	Solvent	[M]	y (%)	e.r.
1	Me	8%	CuTc (4%)	4.5	-40°C	Toluene	0.15	94	68:32
2	iPr	8%	CuTc (4%)	4.5	-40°C	Toluene	0.15	84	65:35
3	Et	8%	CuTc (4%)	4.5	-40°C	Toluene	0.15	96	72.5:27.5
4	Et	10%	CuTc (4%)	4.5	-40°C	Toluene	0.15	99	74.5:25.5
5	Et	10%	$Cu(OTf)_2$ (4%)	4.5	-40°C	Toluene	0.15	84	68.5:31.5
6	Et	10%	CuBr (4%)	4.5	-40°C	Toluene	0.15	79	69.5:30.5
7	Et	10%	$Cu(OAc)_2$ (4%)	4.5	-40°C	Toluene	0.15	76	76:24
8	Et	10%	CuTc (4%)	O/N	-78°C	Toluene	0.15	90	59:41
9	Et	10%	CuTc (4%)	O/N	-60°C	Toluene	0.15	79	64.5:35.5
10	Et	10%	CuTc (4%)	4.5	-20°C	Toluene	0.15	80	68.5:31.5
11	Et	10%	CuTc (4%)	4.5	0°C	Toluene	0.15	82	56.5:43.5
12	Et	10%	CuTc (4%)	4.5	-40°C	DCM	0.15	75	65:35
13	Et	10%	CuTc (4%)	4.5	-40°C	MTBE	0.15	79	59.5:40.5
14	Et	10%	CuTc (4%)	4.5	-40°C	Toluene	0.12	70	76:24
15	Et	10%	CuTc (4%)	4.5	-40°C	Toluene	0.24	78	85.5:14.5
16	Et	10%	CuTc (4%)	4.5	-40°C	Toluene	0.35	79	88:12
17	Et	10%	CuTc (4%)	4.5	-40°C	Toluene	0.5	76	88.5:11.5

Table 1. First optimization of the reaction conditions

The product **36** resulting from our benchmark reaction was always obtained as (*Z*)-isomer with dr >20:1. However, during the reaction scope evaluation we observed that in some cases, when different substrates or aldehydes were employed, a small amount of product with (*E*)-configuration at the olefin was formed (in the range of 5-20% depending on substrate and aldehyde). In order to improve the reaction diastereoselectivity (i.e. the (Z)/(*E*) ratio), different temperatures T_2 and olefination times t_2 were screened within the reaction depicted in Figure 14. We found that performing the HWE reaction step at -40°C for 12h instead of 25 °C for 2 h provided the highest (*Z*)-selectivity without decreasing the reaction yield, thus granting us the full optimization of the AOCA conditions. All the results are reported in Table 2. It is worth noticing that, within the scope of this thesis work, the (*Z*)-configuration of the olefin is the most stable as result of the spatial separation of the most hindered substituents.

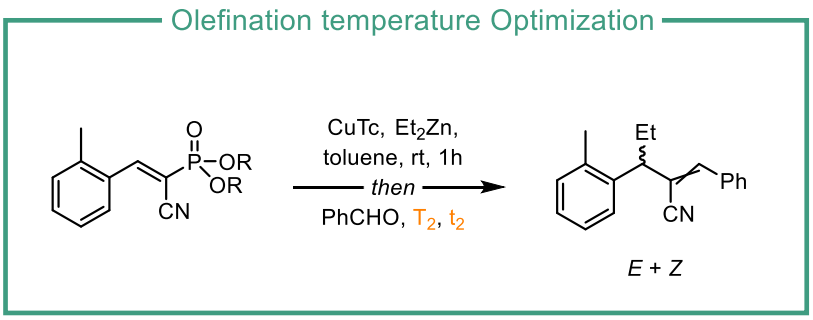

Figure 14. Reference reaction for the olefination temperature optimization

	T_2 (°C)	t_2 (h)	(*Z*)/(*E*) ratio
1	25°C	1	88:12
2	0°C	2	93:7
3	-40°C	16	99:1

Table 2. Optimization of the olefination step temperature

4.2. Ligand Screening

After optimizing the reaction conditions, the screening of the ligands was performed starting from Feringa's phosphoramidite **L2** with systematic variations introduced in both the diol and the amine moieties. These modifications were aimed at rationalizing the effects of the substituents, thereby facilitating the assessment of electronic and/or steric trends and enabling straightforward predictions regarding the optimal ligand structure.

First, the investigation of the amine moiety effects was performed (Figure 15). During the series **L1**, **L6**, **L7**, **L2**, **L8**, **L9** the size of the amine and the number of its stereogenic carbon atoms increase. It's possible to notice that the presence of two stereocenters in the amine provided the highest enantiomeric excesses. Furthermore, a trend for the steric hindrance of this moiety of the ligand can be visualized, with both the yield and the enantiomeric excess reaching their maximum values for the ligand **L2**. Then the electronic effects were investigated by substituting the ligand **L2** phenyl groups with either electron-withdrawing or electron-donating substituents. Since an improvement of the *ee* has been obtained through the substitution with one or two OMe groups (**L10** and **L12**) up to 92.5:7.5 er, it seemed that having EDG substituents on the amine aryl rings increases the selectivity of the reaction. Thus, this electron-donating effect was emphasized by using the NMe_2 substituent with a higher electron-donating effect (**L14**, **L15**).

These also provided high enantioselectivities, with er up to 94.5:5.5 with **L15**. Thus, it is possible to conclude that there seems to be a trend for the electronic effects of these substituents even though this is subjected to the number of substitutions as **L14** gave lower er than **L10**.

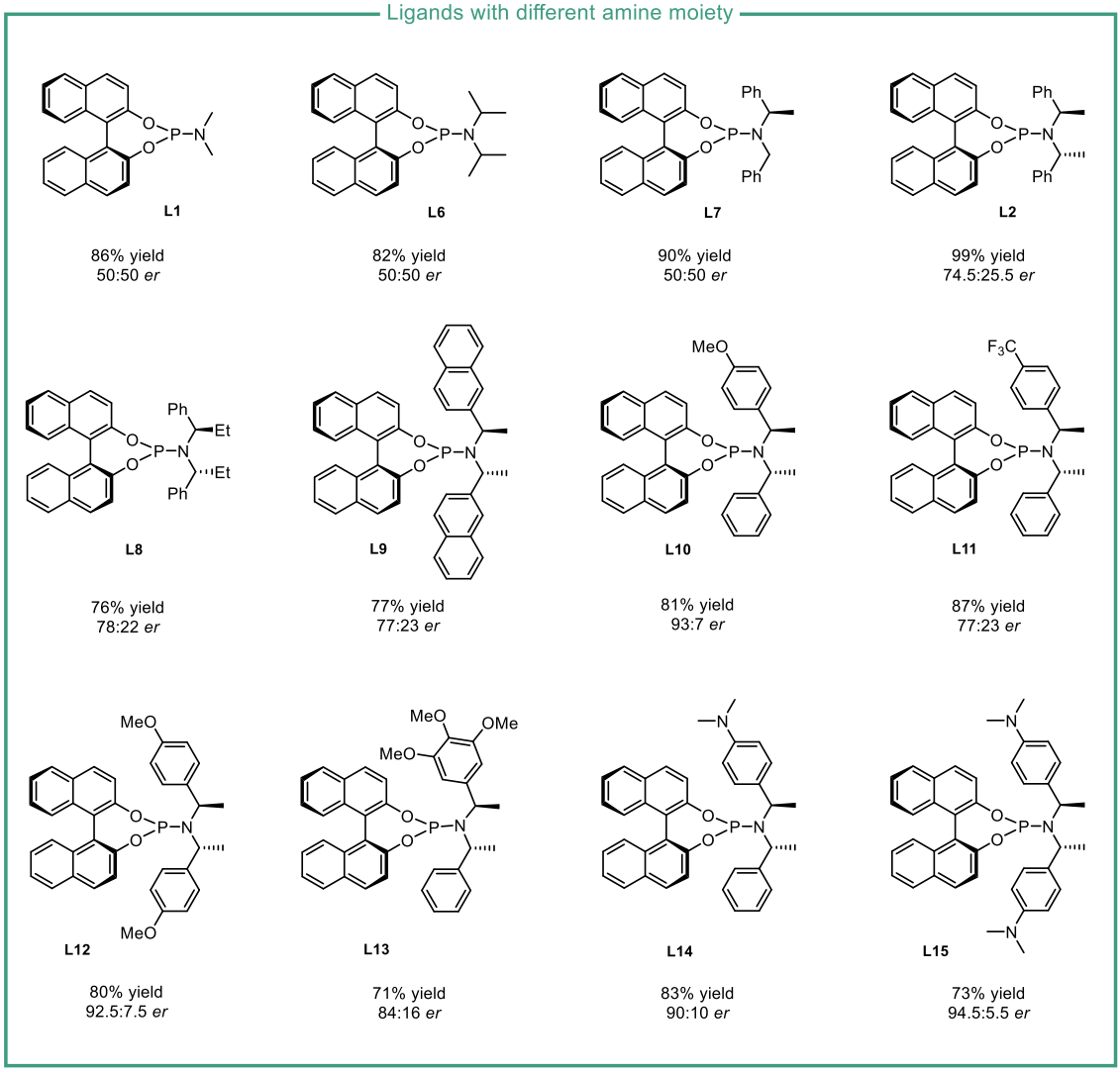

Figure 15. Screening of phosphoramidites featuring diverse amine moieties

A second stage investigation of the ligand structure was made by varying the BINOL moiety (Figure 16). First, another diastereoisomer of ligand **L2** was synthesized, employing the (*R*)-BINOL thus forming ligand **L16**. In our benchmark reaction **L16** resulted in the formation of product **36** in 45.5:54.5 er in favour of the opposite product enantiomer with respect to **L2**, which suggests a dominance of the binaphthyl moiety in controlling the reaction stereochemical course with respect to the amine moiety. Then, other diols were tested, such as the partially unsaturated octahydrobinaphtol or biphenyl, resulting in ligands **L17** and **L18** respectively. Since

these attempts did not improve the reaction enantioselectivity, additional trials were made by introducing different substituents in the BINOL *ortho*-position(s). The steric effect of this substitution was tested with the series of ligands **L19**-**L21**, reaching a maximum of selectivity with the methyl disubstituted ligand **L19**. Instead, the electronic effect of the substituent was tested through a di-*ortho*-bromination generating the ligand **L22**. The use of these EWG substituents decreases the reaction *ee* with respect to simple alkyl groups with similar steric properties. Consequently, our work was directed towards the investigation of these alkyl substituents. For instance, assessing the influence of the mono-substitution to give **L23** provided product **36** with improved stereoselectivity (80% yield and 96:4 er). This result suggested that higher selectivity could be accessed with ligands featuring mono-substituted binaphtols compared to their di-substituted counterparts. Thus, modifications of this ligand general structure were finally investigated. Because **L19** gave better results in term of selectivity with respect to **L20**, we synthesized and tested ligand **L24**. This resulted in an unexpected decrease of the *ee* but, on the other hand, suggested a trend for the steric hindrance of the alkyl substituent. For this reason, ligands **L25**, **L26**, and **L27** with enhanced bulky steric properties for the mono-*ortho*-substituent have been synthesized and tested. Amon these, the mono-phenyl-substituted ligand **L26** provided product **36** in 79% yield and 98:2 er.

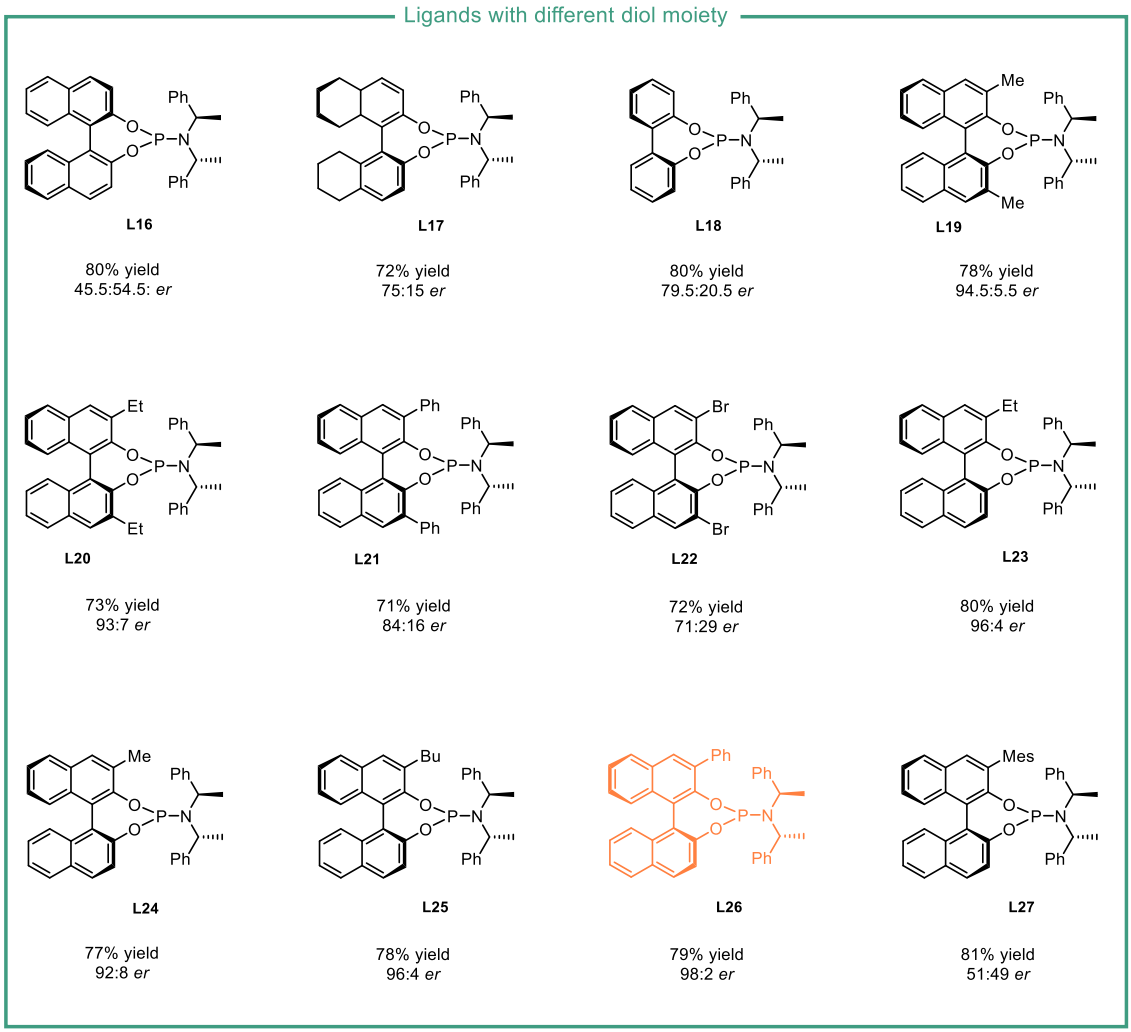

Figure 16. Screening of phosphoramidites with different diol moieties

In addition to optimizing the amine and the diol moieties separately, some cross experiments have also been conducted combining different optimized diol and amine moieties (Figure 17). A first experiment was made with ligand **L28** in order to assess whether a hindered diol could compensate for the steric vacancies of the amine. However, this provided a racemic mixture of the product **36**. Then, other experiments featuring the combination of diols and amines that gave the highest selectivities were undertaken. Thus, ligands **L29** and **L30** were synthesized and tested. Despite these ligands provided high enantioselectivities (93:7 and 94:6 er respectively), these could not improve the results obtained with ligands **L19** and **L23** respectively. This suggests that the amine and the diol moieties of these phosphoramidite ligands operate through distinct and separate effects rather than synergistically.

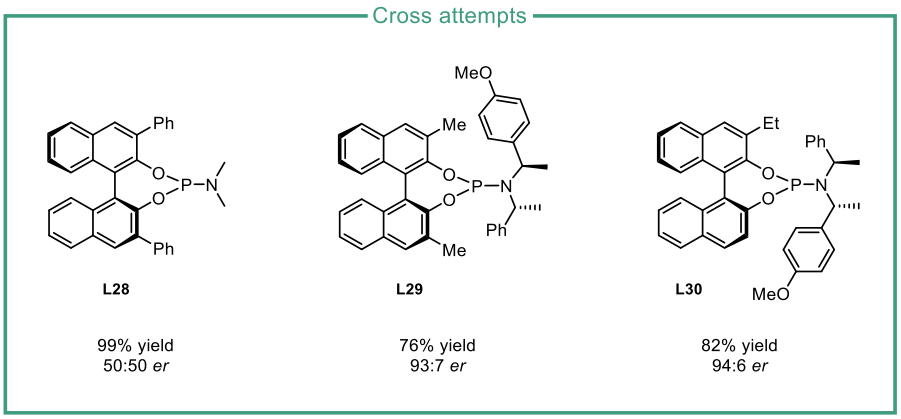

Figure 17. Screening of phosphoramidites with combinations of different amine and diol moieties

Overall, among the tested phosphoramidites, **L26** provided the best outcomes in terms of enantioselectivity coupled with a high yield. Therefore, this was selected as the ligand of choice for further studies of our AOCA methodology and in particular for the evaluation of the reaction scope.

4.3. Reaction Scope

One of the main advantages of our novel methodology is that the AOCA reaction is formally a multicomponent transformation. Indeed, since the formation of the two stereogenic elements (i.e. the stereogenic carbon atom and the olefin) is decoupled in two different steps, this allows to easily build libraries of chiral compounds by only selecting the appropriate substrate, nucleophile, and carbonyl compound (Figure 18). This possibility was explored while expanding the scope of the reaction, confirming the possibility of generating a wide range of different compounds with very high standards of yield and enantioselectivity.

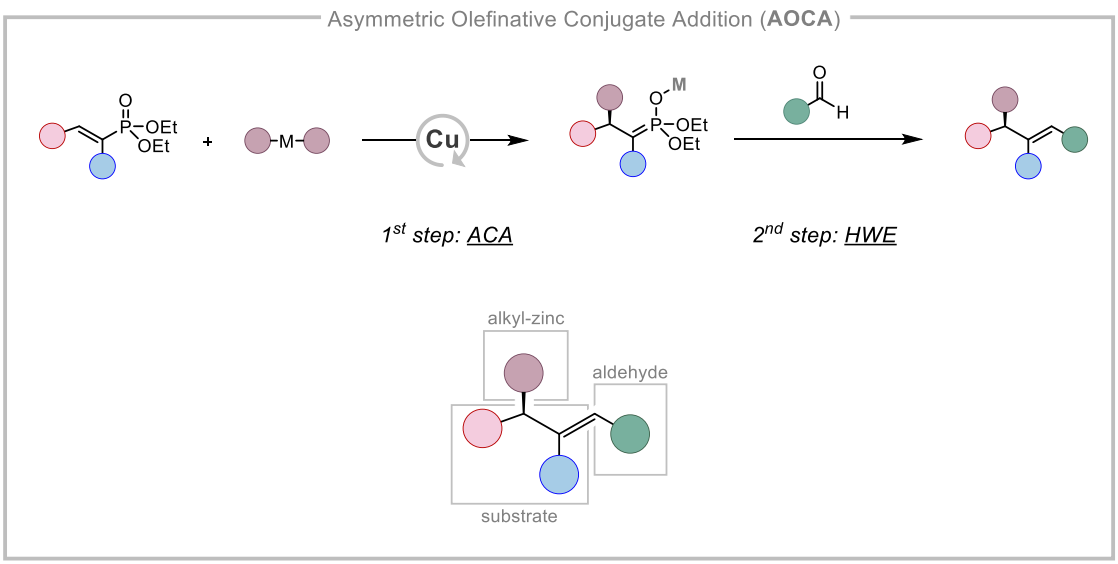

Figure 18. AOCA methodology with emphasis on the multicomponent character

4.3.1. Aldehyde Scope

The key point of our methodology is the decoupling between the enantioselective conjugate addition step and the olefination, which could make it possible to have full control on the configuration of both the new stereogenic carbon atom (R or S) and the olefin (*E* or Z). As predicted, through the HWE olefination it has been possible to selectively obtain the *Z*-olefin for all of the cases reported below. It is worth highlighting that for the products obtained via the AOCA reaction with the substrates employed in this thesis work, the *Z*-products are those that present a reduced steric repulsion between the olefins substituents, and therefore this has to be considered the most stable configuration.

Another advantage derives from the decoupling between the formation of the two stereogenic elements (i.e. the stereogenic carbon atom and the olefin). Indeed, once that optimal reaction conditions are identified for a given substrate/nucleophile pair in the first step (ACA), any products attainable by variation of the third component (i.e. the carbonyl compound) should be accessed with the same (*fixed*) high enantioselectivity. In other words, the olefination step occurs after the conjugate addition, when the *ee* of the new steroeogenic carbon has already been irreversibly set. This possibility was confirmed by expanding the scope using different aldehydes in the HWE olefination step, obtaining always the same high enantiomeric ratio of

98:2. Small variations are in a few cases observed but they can be ascribable to experimental errors.

Finally, this methodology allows the production of functionalised olefins without any major limitation in terms of compatibility of functional groups. Indeed, functionalised carbonyl compounds can be involved in the HWE olefination while in the Tsuji-Trost reaction these functional groups need to be already in the starting material or introduced by subsequent synthetic steps, avoiding in some cases the possibility of performing the desired conjugate addition. In other words, AOCA allows performing a formal AAA reaction with direct installation of functional groups that would be poorly compatible with AAA (e.g. a second Michael acceptor with similar reactivity to the original substrate). Also this reaction feature was confirmed while expanding the aldehyde scope (see entries **A7**, **A10**).

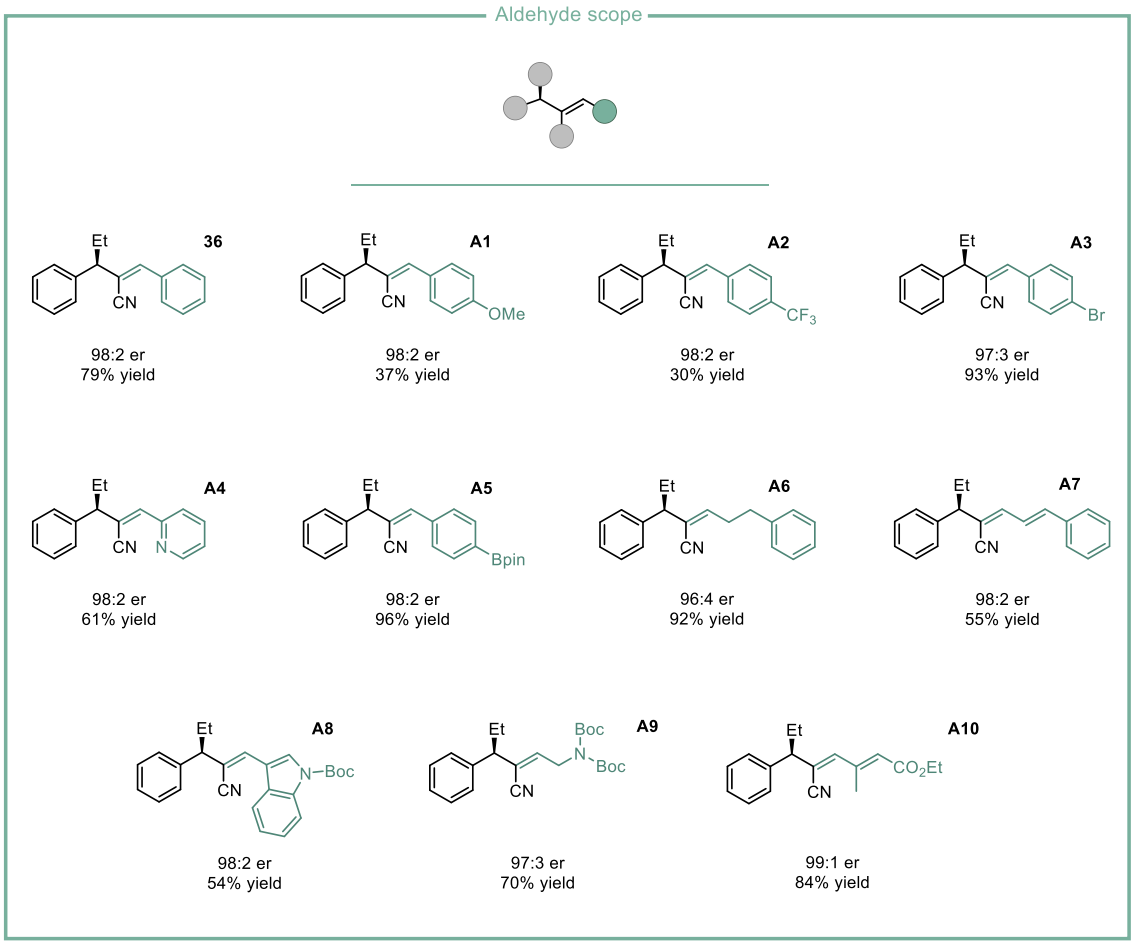

Figure 19. Aldehyde scope

4.3.2. Substrate Scope

The starting materials involved in the reaction can differ for either the γ-position substituent or the EWG group. Therefore, both the substitution of the new stereogenic carbon atom and the olefin in the product are dependent on the substrate.

While expanding the starting material scope, the focus was directed towards varying the substituent in the γ-position. This was done not only by modifying the substrate aromatic ring used in the reference reaction, but also by replacing such aryl substituent with alkyl, alkenyl, and alkynyl groups in the substrate (Figure 20). In all these cases the selectivity of the reaction decreased with respect to our benchmark reaction. This is due to the fact that the enantioselectivity of the reaction is determined by the spatial disposition of the chiral ligand and the substrate in the stereo-determining step, i.e. the conjugate addition of the nucleophile to the substrate. Even if it has not been rationalized yet, this arrangement mainly relies on the steric hindrance of the molecules involved in this interaction (i.e. the starting material, the nucleophile and the ligand). This became experimentally evident during the optimization of the ligand when phosphoramidite substituent with different size were screened, even if in this and other reported cases a clear trend is never shown.[44] Therefore, the enantioselectivity will in principle change also by changing the scaffold of the starting material as observed while expanding the substrate scope.

Based on the data presented in Figure 20, it can be inferred that the AOCA conducted with the presence of the chiral ligand **L26** shows very high levels of enantioselectivity for most 2-aryl-vinylphosphonates. Pleasingly, also *ortho*-substituted arenes were tolerated with products **S6** and **S8** being obtained in high yield and >88% *ee*. *Ortho*- and *para*-anisyl groups resulted in low enantioselectivity (**S3** and **S1**). While a reason for such drop in selectivity has not been rationalized yet, we speculate that resonance effects are in place. This hypothesis is in agreement with the obtainment of product **S2** in 94:6 er and 48% yield, where the OMe group was placed in the *meta* position. Moreover, other groups that are electron donating by inductive effect rather than resonance effects proved good substrates as exemplified with products **S4**, **S5** and **S6**, which were all obtained in high yields and enantioselectivities.

Unfortunately, the enantioselectivity of the reaction when some other aryl-vinylphosphonates were employed was not satisfying, with <71% *ee* for naphtyl-, thiophenyl-, and furyl-vinylphosphonate (products **S9**, **S10**, **S11**, and **S12**). Even worse results in term of selectivity were obtained for alkyl-, alkenyl-, and alkynyl-substituted vinylphosphonates, with the obtainment of almost racemic mixtures of products. This can be ascribed to the major

modification of the substrate scaffold, causing the aforementioned variation of the interactions with the chiral complex at the reaction stereo-determining step. In order to improve the enantioselectivity for these classes of substrates, the re-optimization of the chiral ligand would be necessary. Lastly, a few of the substrates exhibited a low or very low NMR yield. In most cases the origin of the problem can be ascribed to the low solubility of the substrates in the rather non-polar solvent mixture employed (Hexane/Toluene 3:1). Unfortunately, rising the polarity of the reaction solvent results in higher yields but decreased selectivity as tested during the reaction conditions optimization (vide infra).

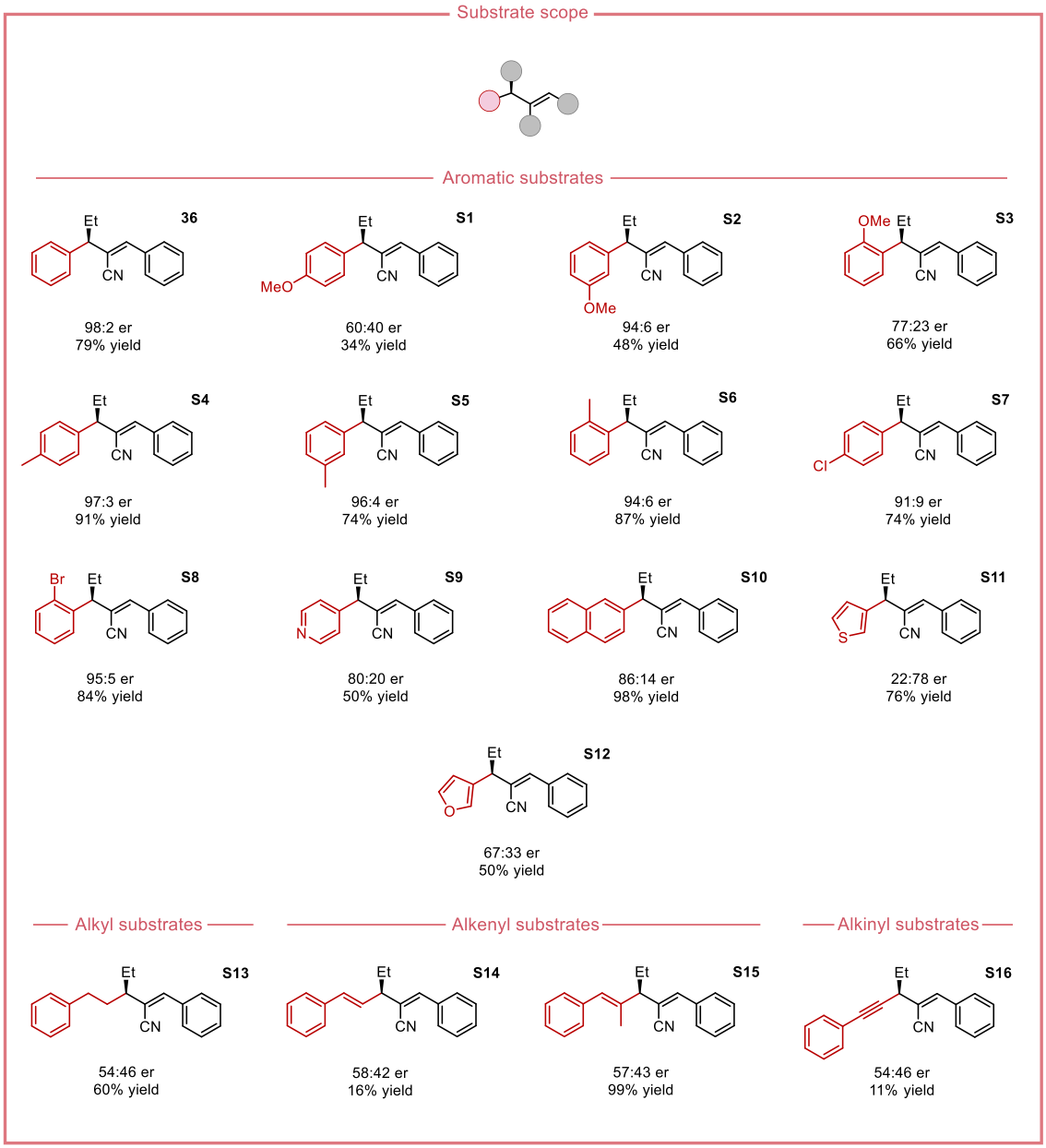

Figure 20. Substrate scope with variation of the γ-substituent

A short investigation on the starting material has been made also by varying the EWG with respect to the CN group (Figure 21), which was constant for all of the aforementioned substrates. In particular, the methyl-ester group was tested. This gave a satisfying result in terms of enantioselectivity reaching 95:5 er, but the reaction yield was low (10%). Under the optimized reaction conditions for our benchmark reaction, the major product of this reaction was the pre-olefination intermediate, suggesting that the conjugate addition step occurs but the olefination step is sluggish. Future efforts will be directed to the re-optimization of this step for substrates bearing an ester EWG, which seems possible based on the data shown here. Moreover, this limitation is a minor one in our opinion, as the cyano-group is synthetically very modular and can undergo various transformations generating a plethora of other functional groups in one step (e.g. amine, amide, aldehyde, carboxylic acid, ketone, ester). Therefore, considering the excellent enantioselectivity levels obtained with the this EWG group and its versatility in organic synthesis, the results obtained with other EWG groups do not diminish the appeal of the AOCA methodology.

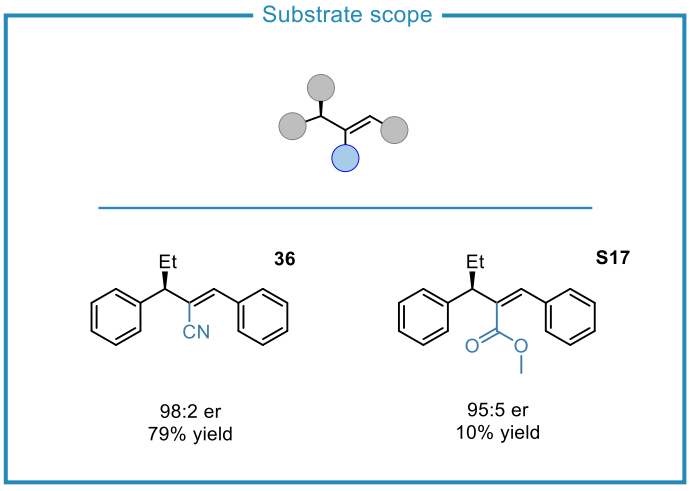

Figure 21. Substrate scope with variation of the EWG α-substituent

4.3.3. Alkyl-zinc Scope

Finally, the last possibility for changing the scaffold of the product relies on the use of different alkyl-zinc nucleophiles. By varying this element, different substitutions on the new stereogenic carbon atom can be obtained. Only a few dialkylzinc reagents have been employed in the AOCA reaction so far, and the scope will be more widely extended in the near future. In addition to

Et_2Zn involved for all the experiments reported above, the commercially available Me_2Zn has been tested (**Z1**, **Z3**-**Z6**). The asymmetric conjugate methylation has been performed with different substrates but also using various aldehydes in the HWE olefination step, in order to exhaustively demonstrating the multicomponent character of the methodology. As reported in Figure 22, the same high enantioselectivity for the AOCA reaction is obtained also when Me_2Zn is used. Finally, the butylation has been tested replacing Et_2Zn with Bu_2Zn in the reference reaction, obtaining the product **Z2**. In this case, a synthesis of the non-commercially available organozinc reagent has to be undertaken. The employment of the Bu_2Zn currently obtained in our lab caused a decrease of selectivity compared to analogous AOCA reactions where Et_2Zn or Me_2Zn were used. Studies are still ongoing that aims at assessing the quality of the Bu_2Zn reagent obtained and at the optimization of the synthesis of this class of organometallic reagents.

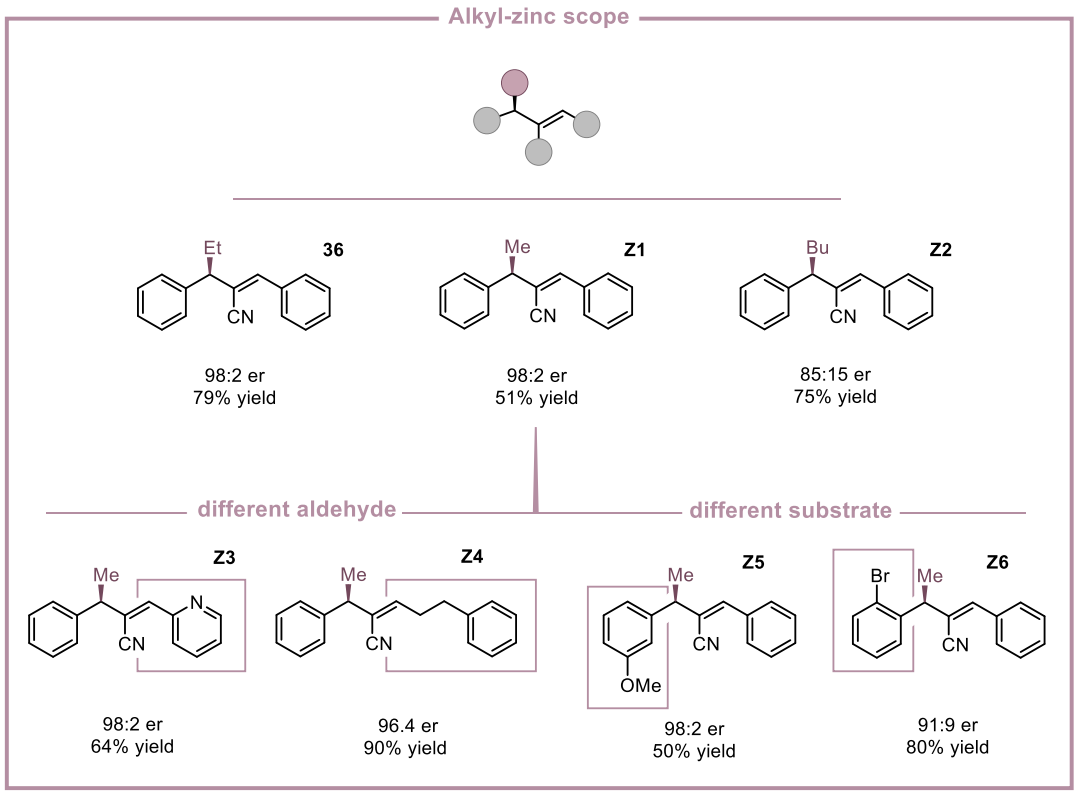

Figure 22. Alkyl-zinc scope with emphasis on the multicomponent character

5. CONCLUSIONS

This master thesis relies on the development of a novel tandem methodology named Asymmetric Olefinative Conjugate Addition (AOCA), designed for the synthesis of a new stereocenter in α-position to an internal olefin. This project was motivated by the desire to find a sustainable alternative to the extensively reported Pd/Ir-based Tsuji-Trost methodology, employing the principles of asymmetric catalysis. Compared to the existing asymmetric copper-catalyzed asymmetric allylic substitution (AAA), which is limited by its mechanism, the AOCA methodology achieve selective control over the configuration of both the new stereogenic elements (e.g. the stereogenic carbon atom and the olefin). This possibility is achieved through the decoupling between their formation in two different steps, an asymmetric conjugate addition (ACA) followed by a Horner-Wadsworth-Emmons (HWE) reaction. Remarkably yileds and enantioselectivity are achieved through the involvement of an inexpensive and abundant copper catalyst in the first step. The AOCA methodology offers a multitude of additions advantages related to the compatibility with a broad spectrum of nucleophiles, the multicomponent character, the enantio- and diastereoselectivity control, as well as the compatibility with various functional groups. The feasibility of this methodology has been investigated by expanding the scope of the reaction, finding that a high level of enantioselectivity can be obtained for 2-aryl-vinylphosphonates. Future research will involve the optimization of the phosphoramidite ligand for other substrate classes (alkyl-, alkenyl-, and alkynyl-vinylphosphonates), in addition to the ongoing expansion of the substrate and nucleophile scope. In conclusion, the potential of AOCA to offer a sustainable and strategic methodology to address vacancies in organic synthesis is a promising avenue for the future research in the field of asymmetric catalysis.

6. EXPERIMENTAL SECTION

6.1. Materials and Methods

All reactions were carried out in oven- or flame-dried glassware under an atmosphere of dry Nitrogen unless otherwise noted. Except as otherwise indicated, all reactions were magnetically stirred and monitored by analytical thin layer chromatography (TLC) using Merck pre-coated silica gel plates with F254 indicator. Visualization was accomplished by UV light (254 nm), with combination of Potassium Permanganate solution as an indicator. Flash column chromatography was performed using silica gel pore size 60 Å, 230-400 mesh particle size, 40-63 µm particle size. Yields refer to chromatographically and spectrographically pure compounds, unless otherwise noted. Commercial grade reagents and solvents were used without further purification. 1H NMR, 13C NMR, 31P NMR and 19F spectra were recorded on Bruker Avance300 spectrometer and Bruker 400 AVANCE III HD. The proton spectra are reported as follows: δ (position of proton, multiplicity, coupling constant J, number of protons). Multiplicities are indicated by s (singlet), d (doublet), t (triplet), q (quartet), p (quintet), h (sextet), m (multiplet) and broad (broad). Enantiomeric excess was determined on a Shimadzu HPLC SPD-10A with a variable wavelength detector or a Shimadzu LC-40D with a SPD-M40 detector using chiral stationary phase columns (0.46 cm x 25 cm) from Phenomenex. NMR yields were collected using dimethyl terephthalate as internal standard.

6.2. General Procedures

General Procedure A

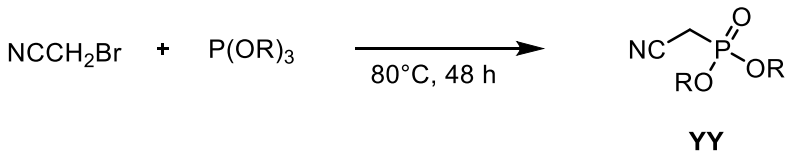

YY

A mixture of bromoacetonitrile (1.0 equiv) and trimethyl phosphite (1.1 equiv) was heated at ca. 80 °C for 48 h. The volatile component was evaporated under reduced pressure and the residue was purified by column chromatography (EtOAc).

General procedure B

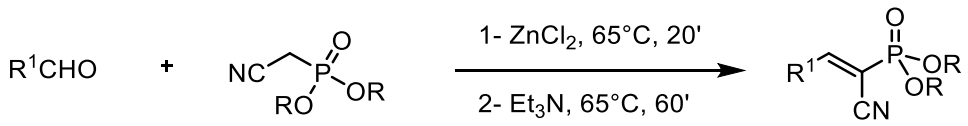

LL **YY** **MM**

Aldehyde (1.0 equiv) was added to a solution of $ZnCl_2$ (1.0 equiv) in 1,4-dioxane (0.5 M). Cyanomethylphosphonate (1.0 equiv) was added to the mixture and the mixture was stirred for 20 min at 65 °C without using any inert gas. Et_3N (1.5 equiv) was added to the mixture and stirred for 30–60 min at 65 °C (in an oil bath). Ethyl acetate was added to the reaction mixture and the solution was washed two times with distilled water and dried over sodium sulfate. The solvent was evaporated and the crude product was purified by short column chromatography (Hex/EtOAc 9 : 1 to 3 : 7) to give the product as a viscous oil or a white solid.

General Procedure C

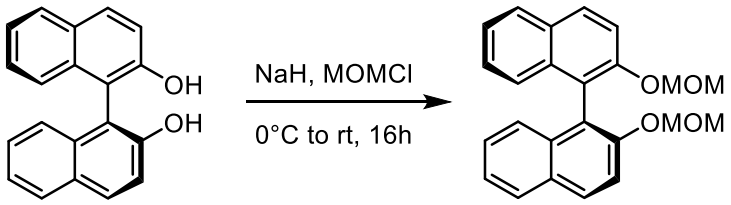

AA **EE**

To a solution of NaH (60 wt%, 4 equiv) in a solution of dry THF (1.33 M) was added dropwise a solution of (*R*)-BINOL (1 equiv) in dry THF (0.33 M) at 0°C. The mixture was stirred at 0°C until the evolution of gas ceased. After stirring for 30' at room temperature, chloromethyl methyl ether (MOMCl, 2.1 equiv) was introduced to the resultant mixture. A white precipitate immediately appeared and the reaction was further stirred for 16 h at room temperature. Then the mixture was diluted with diethyl ether, extracted three times with ethyl water, dried with Na_2SO_4, and condensed *in vacuo*. The resultant residue was purified by column chromatography (Hex/EtOAc 8:2) to give the aimed product as with crystal.

General Procedure D

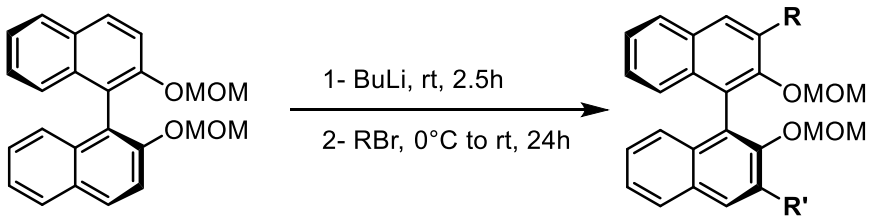

EE

2,2'-bis(MOM)-1,1'-binaphtyl (1 equiv) was dissolved in dry Et_2O under nitrogen atmosphere. BuLi (2.5 M, 3.5 equiv) was slowly added into the solution turning its colour into light brown. It was stirred for 2.5 h at room temperature. Dry THF was added and the mixture was stirred for 1 h at room temperature. After cooling the reaction mixture to 0°C, the bromoalkane (3.5 equiv) was introduced and the mixture assumed a transparent yellow colour. It was stirred at 0°C for 15' and then 24h at rt. The reaction was quenched with aqueous saturated NH_4Cl, extracted three times with Et_2O, combined the organic phases and washed it with little brine, then dried

over anhydrous Na_2SO_4 and condensed under reduced pressure. The residue was purified by column (Hex/EtOAc 95:5) to give the targeted compound.

General Procedure E

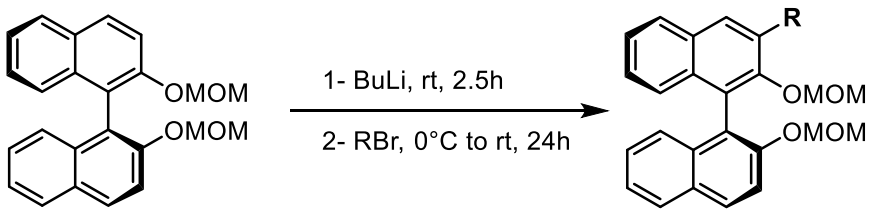

EE

2,2'-bis(MOM)-1,1'-binaphtyl (1 equiv) was dissolved in dry Et_2O under nitrogen atmosphere. BuLi (2.5 M, 1 equiv) was slowly added into the solution turning its colour into light brown. It was stirred for 2.5 h at room temperature. Dry THF was added and the mixture was stirred for 1 h at room temperature. After cooling the reaction mixture to 0°C, the bromoalkane (1 equiv) was introduced and the mixture assumed a transparent yellow colour. It was stirred at 0°C for 15' and then 24h at rt. The reaction was quenched with aqueous saturated NH_4Cl, extracted three times with Et_2O, combined the organic phases and washed it with little brine, then dried over anhydrous Na_2SO_4 and condensed under reduced pressure. The residue was purified by column (Hex/EtOAc 95:5) to give the targeted compound.

General Procedure F

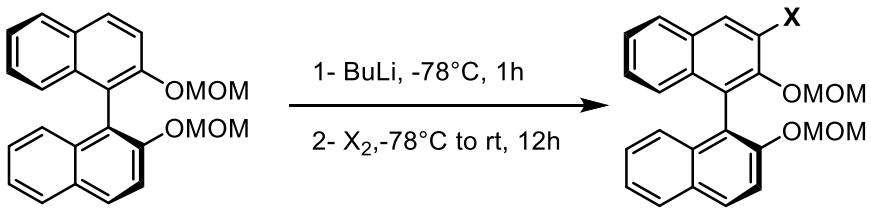

EE **XX**

A flame-dried two-necked flask was charged with 2,2'-bis(MOM)-1,1'-binaphtyl (1 equiv) and dry THF (0.075 M) under nitrogen atmosphere. The mixture was cooled down to -78°C and BuLi

(1.2 equiv) was added dropwise over a period of 30'. The solution was stirred 1 h at the same temperature. A solution of X_2 (1.2 equiv) in dry THF (1 M) was added dropwise and the solution was stirred for 1 h at -78°c and 12 h at room temperature. The excess of X_2 was reduced with an aqueous solution 5% in $Na_2S_2O_3$. The reaction was extracted three times with EtOAc, dried over Na_2SO_4 and condensed under reduced pressure. The residue was purified by column (Hex/EtOAc 9:1) to give the targeted compound.

General Procedure G

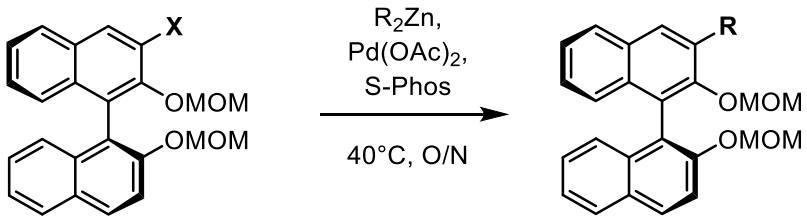

XX

In a two-necked flask, the starting material (1 equiv), $Pd(OAc)_2$ (4 mol%) and S-Phos (8 mol%) were added and dissolved in dry THF (0.5 M) under nitrogen atmosphere. R_2Zn (3 equiv) was added and the mixture was stirred overnight at 40°C. the reaction was quenched with water, extracted three times with Et_2O, dried over Na_2SO_4 and condensed under reduced pressure. The residue was purified by column (Hex/EtOAc 8:2) to give the targeted compound.

For the synthesis of alkyl-zinc solutions that were not commercially available, LiCl (4 equiv) and Zn (5 equiv) were mixed in a two-necked flask and heated up to 180°C for 1 h, while performing vacuum/N_2 cycles. The solids were then cooled down to room temperature and THF (1 M in the alkyl iodide), 1,2-dibromoethane (0.4 equiv) and TMSCl (0.1 equiv) were added in this order. When the effervescence ceased, the alkyl iodide (4 equiv) was added and the mixture was stirred for 3 h at 60°C. The alkyl-zinc solution was then titrated with a I_2 solution in THF.

General Procedure H

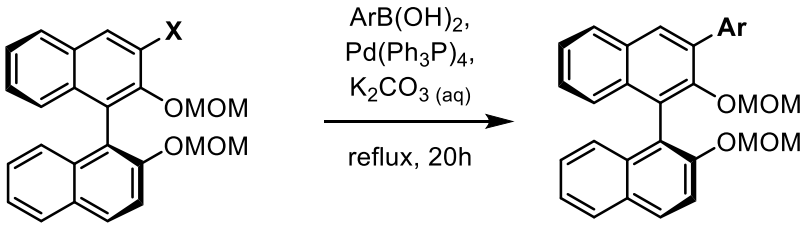

XX

The starting material (1 equiv), $ArB(OH)_2$ (2 equiv) and $Pb(Ph_3P)_4$ (10 mol%, quick weighed) were dissolved in DME (0.5 M) under nitrogen atmosphere. A 2 M aqueous solution of K_2CO_3 (1 equiv) was added and the mixture was stirred at reflux for 20 h. the reaction mixture was then cooled down to room temperature, quenched with NH_4Cl, extracted three times with Et_2O, dried over Na_2SO_4 and condensed under reduced pressure. The residue was purified by column (Hex/EtOAc 9:1) to give the targeted compound.

General Procedure I

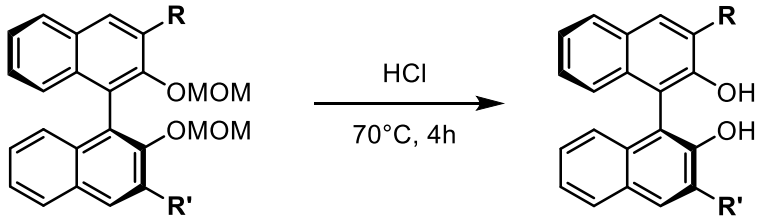

The starting material (1 equiv) was dissolved in dioxane (0.25 M) and HCl was added (4 N, 10 equiv). the reaction mixture was stirred 4 h at 70°C. When a transparent mixture was obtained, it was cooled down to room temperature and water was added to quench the reaction. The resulting mixture was extracted three times with CH2Cl2, combined the organic layers, dried over Na_2SO_4 and condensed under reduced pressure. The residue was used in the subsequent reactions without purification.

General procedure J

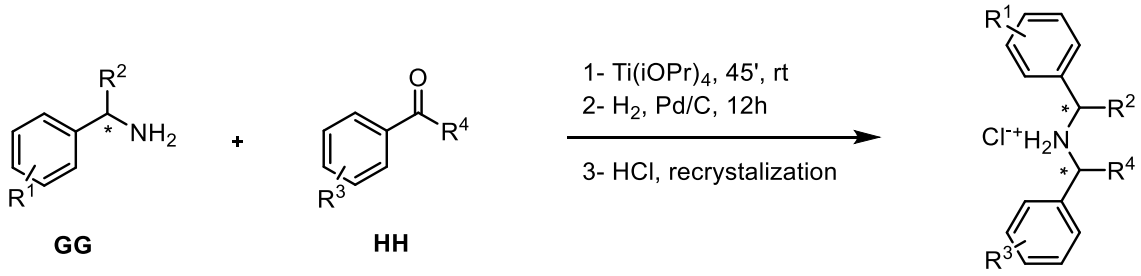

GG **HH**

The primary amine (1 equiv) and the ketone (1 equiv) were added in a two-necked flask under nitrogen atmosphere. $Ti(iOPr)_4$ (3 equiv) was added and the reaction mixture was stirred 45' at room temperature. EtOAc could be added if the mixture turns solid in order to dissolve the product. Pd/C (0.5 mol%) was added, 2 cycles vacuum/H_2 were performed, then the reaction mixture was finally stirred for 12 h under H_2 atmosphere. After this period the H_2 atmosphere was removed with vacuum/N_2 cycles. A solution of NaOH 1 M was added and the mixture was stirred for 45' to quench the catalyst. After this addition, the N_2 atmosphere was removed. EtOAc was added and the heterogeneous mixture was filtered through a celite filter, the organic phase was separated, dried over Na_2SO_4 and condensed under reduced pressure. The raw product was diluted with DCM and concentrated HCl was added. The solvent was evaporated under reduced pressure and the product precipitated in form of chloride salt. After recrystallization with EtOAc/MeOH 75:25, the desired product was obtained as a pure diastereoisomer.

General Procedure K

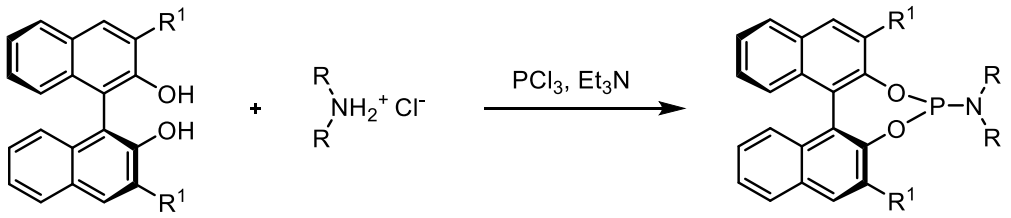

AA **CC**

PCl_3 (1 equiv) and Et_3N (3 equiv) were added in anhydrous CH_2Cl_2 (0.2 M) in a two-necked flask under N_2 atmosphere and the mixture was cooled down to 0°C. The chlorohydrate amine (1 equiv) was added under great flux of nitrogen and the mixture was stirred for 4.5 h at room

temperature. A solution of substituted BINOL (1 equiv) in anhydrous CH_2Cl_2 (0.3 M) was added dropwise and the reaction mixture was stirred overnight at room temperature. The mixture was then washed with water and the solvent was evaporated under reduced pressure. The residue was purified by column (Hex/EtOAc 100:1) to give the targeted compound.

General Procedure L

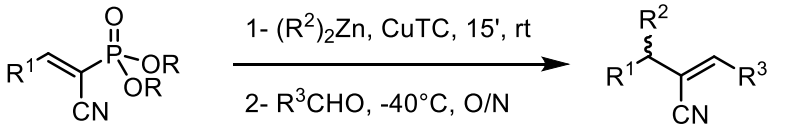

MM racemic mixture

In a flame-dried round-bottom flask CuTC (4 mol%) and anhydrous toluene (0.5 M) were added under nitrogen atmosphere. The alkyl-zinc (1 M in hexane, 1.5 equiv) was added and the reaction mixture was stirred for 15' at room temperature. The starting material (1 equiv) was added and the mixture was stirred for 1 h. Then the solution was cooled down to -40°C, the aldehyde (3 equiv) was added, and the mixture was stirred overnight at this temperature. Hexane was added to quench the reaction. The solution was filtered through a silica filter with Hex/Et_2O 6:4. After evaporation of the solvent under reduced pressure, the product was purified by column chromatography (Hex/EtOAc 95:5).

General Procedure M

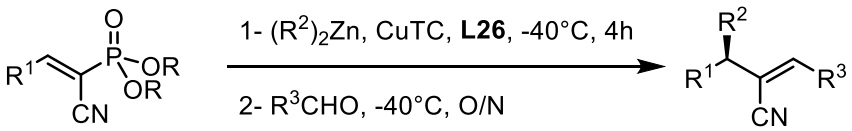

MM

In a flame-dried round-bottom flask CuTC (2 mol%), the ligand **L26** (5 mol%), and anhydrous toluene (0.5 M) were added under nitrogen atmosphere and the mixture was stirred for 10' at room temperature. Then the reaction mixture was cooled down to -40°C. The alkyl-zinc (1 M in

hexane, 1.5 equiv) was added and the reaction mixture was stirred for 15' at -40°C. The starting material (1 equiv) was added and the mixture was stirred for 4 h at the same temperature. The aldehyde (1.5 equiv) was added, and the mixture was stirred overnight at -40°C. Hexane was added to quench the reaction and the mixture was warmed to room temperature. The solution was filtered through a silica filter with Hex/Et_2O 6:4 and the solvent was evaporated under reduced pressure.

6.3. Synthesis and Characterization

6.3.1. Diols Synthesis and Characterization

(S)-2,2'-bis(MOM)-1,1'-binaphtyl

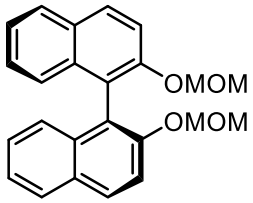

Following **General Procedure C**, (S)-BINOL (6.007 g, 23.0 mmol), NaH (60 wt%, 3.353 g, 83.8 mmol) and choloro(methoxy)methane (4.8 mL, 44.0 mmol) in dry THF (60 mL). The purification by flash chromatography column (silica gel, Hex/EtOAc 8:2) afforded the name compound (6.53 g, 83%).[52]

R_f (Hex/EtOAc 8:2)= 0.26

(S)-3-iodo-2,2'-bis(MOM)-1,1'-binaphtyl

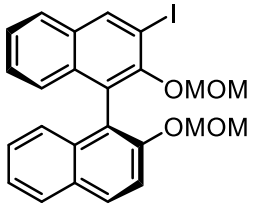

Following **General Procedure F**, (S)-2,2'-bis(MOM)-1,1'-binaphtyl (3.001 g, 8.0 mmol), BuLi (2.5 M, 4.0 mL, 10.0 mmol) and I_2 (2.457 g,9.7 mmol) in dry THF (120 mL). The purification by flash chromatography column (silica gel, Hex/EtOAc 9:1) afforded the name compound (2.96 g, 74%).[47]

R_f (Hex/EtOAc 9:1)= 0.17

(S)-3-methyl-2,2'-bis(MOM)-1,1'-binaphtyl

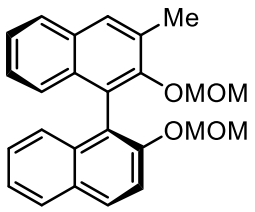

Following **General Procedure E**, (S)-2,2'-bis(MOM)-1,1'-binaphtyl (501 mg, 1.3 mmol), BuLi (2.5 M, 0.54 mL, 1.35 mmol) and iodomethane (d=2.28 g/mL, 0.083 mL, 1.3 mmol) in dry THF (23 mL). The purification by flash chromatography column (silica gel, Hex/EtOAc 85:15) afforded the name compound (162 mg, 31%).[46]

R_f (Hex/EtOAc 85:15)= 0.30

(S)-3-methyl-1,1'-binaphtyl

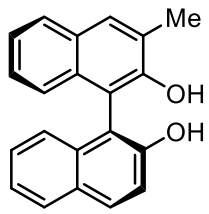

Following **General Procedure I**, (S)-3-methyl-2,2'-bis(MOM)-1,1'-binaphtyl (162 mg, 0.4 mmol) and HCl (4 N, 1 mL) in dioxane (2 mL). The purification by flash chromatography column (silica gel, Hex/EtOAc 85:15) afforded the name compound (125 mg, 99%).[46]

R_f (Hex/EtOAc 85:15)= 0.27

(S)-3-ethyl-2,2'-bis(MOM)-1,1'-binaphtyl

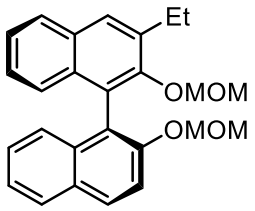

Following **General Procedure G**, (S)-3-iodo-2,2'-bis(MOM)-1,1'-binaphtyl (500 mg, 1.0 mmol), $Pd(OAc)_2$ (9 mg, 0.04 mmol), S-Phos (33 mg, 0.08 mmol) and Et_2Zn (1 M, 3 mL, 3.0 mmol) in dry THF (2 mL). The purification by flash chromatography column (silica gel, Hex/EtOAc 8:2) afforded the name compound (238 mg, 59%).[46]

R_f (Hex/EtOAc 8:2)= 0.34

(S)-3-ethyl-1,1'-binaphtyl

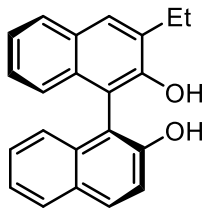

Following **General Procedure I**, (S)-3-ethyl-2,2'-bis(MOM)-1,1'-binaphtyl (238 mg, 0.6 mmol) and HCl (4 N, 1.5 mL) in dioxane (2.5 mL). The purification by flash chromatography column (silica gel, Hex/EtOAc 8:2) afforded the name compound (180 mg, 97%).[46]

R_f (Hex/EtOAc 8:2)= 0.43

(S)-3,3'-diethyl-2,2'-bis(MOM)-1,1'-binaphtyl

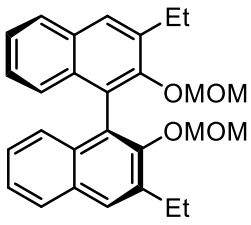

Following **General Procedure D**, (S)-2,2'-bis(MOM)-1,1'-binaphtyl (502 mg, 1.3 mmol), BuLi (2.5 M, 1.9 mL, 4.7 mmol) and bromoethane (d=1.46 g/mL, 0.35 mL, 4.7 mmol) in dry THF (23 mL). The purification by flash chromatography column (silica gel, Hex/EtOAc 95:5) afforded the name compound (177 mg, 31%).[46]

R_f (Hex/EtOAc 8:2)= 0.7

(S)-3,3'-diethyl-1,1'-binaphtyl

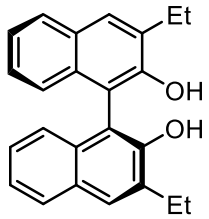

Following **General Procedure I**, (S)-3,3'-diethyl-2,2'-bis(MOM)-1,1'-binaphtyl (177 mg, 0.4 mmol) and HCl (4 N, 1 mL) in dioxane (2 mL). The purification by flash chromatography column (silica gel, Hex/EtOAc 85:15) afforded the name compound (140 mg, 99%).[46]

R_f (Hex/EtOAc 8:2)= 0.50

(S)-3-buthyl-2,2'-bis(MOM)-1,1'-binaphtyl

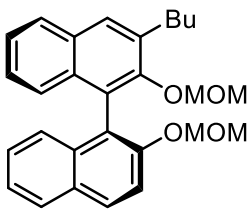

Following **General Procedure G**, (S)-3-iodo-2,2'-bis(MOM)-1,1'-binaphtyl (499 mg, 1.0 mmol), $Pd(OAc)_2$ (10 mg, 0.04 mmol), S-Phos (33 mg, 0.08 mmol), LiCl (170 mg, 4.0 mmol), Zn (336 mg, 5.0 mmol), BuI (d=1.64 g/mL, 0.45 mL, 4.0 mmol), TMSCl (d=0.856 g/mL, 0.013 mL, 0.1 mmol) and 1,2-dibromoethane (d=2.15 g/mL, 0.035 mL, 0.4 mmol) in THF (4 mL). The purification by flash chromatography column (silica gel, Hex/EtOAc 8:2) afforded the name compound (393 mg, 92%).

R_f (Hex/EtOAc 8:2)= 0.38

^{1}H NMR (400 MHz, Chloroform-*d*) δ 7.99 (d, *J* = 9.0 Hz, 1H), 7.92 – 7.81 (m, 3H), 7.62 (d, *J* = 9.1 Hz, 1H), 7.39 (t, *J* = 7.0 Hz, 2H), 7.33 – 7.27 (m, 1H), 7.20 (q, *J* = 8.3, 7.5 Hz, 3H), 5.14 (d, *J* = 6.9 Hz, 1H), 5.07 (d, *J* = 6.9 Hz, 1H), 4.64 (d, *J* = 5.5 Hz, 1H), 4.57 (d, *J* = 5.5 Hz, 1H), 3.22 (s, 3H), 2.96 (s, 3H), 1.89 – 1.79 (m, 2H), 1.60 – 1.46 (m, 2H), 1.33 – 1.29 (m, 2H), 1.04 (t, *J* = 7.3 Hz, 3H).

^{13}C NMR (125 MHz, $CDCl_3$) δ 154.58, 152.94, 133.43, 133.04, 129.96, 129.68, 128.75, 128.13, 128.06, 127.97, 127.95, 127.86, 127.83, 127.43, 126.43, 126.07, 124.89, 124.26, 113.08, 98.80, 96.52, 57.94, 56.53, 31.20, 30.29, 22.56, 13.93.

(S)-3-buthyl-1,1'-binaphtyl

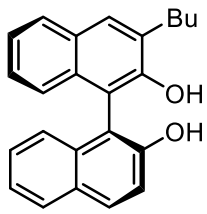

Following **General Procedure I**, (S)-3-buthyl-2,2'-bis(MOM)-1,1'-binaphtyl (393 mg, 0.9 mmol) and HCl (4 N, 2.3 mL) in dioxane (4 mL). The purification by flash chromatography column (silica gel, Hex/EtOAc 8:2) afforded the name compound (140 mg, 99%).

R_f (Hex/EtOAc 8:2)= 0.46

^{1}H NMR (300 MHz, Chloroform-*d*) δ 7.99 (d, *J* = 8.9 Hz, 1H), 7.95 – 7.80 (m, 3H), 7.46 – 7.32 (m, 4H), 7.32 – 7.23 (m, 1H), 7.15 (ddd, *J* = 19.5, 8.3, 1.3 Hz, 2H), 5.13 (s, 1H), 5.09 (s, 1H), 3.01 – 2.81 (m, 2H), 1.80 (tt, *J* = 7.6, 6.3 Hz, 2H), 1.50 (tq, *J* = 14.7, 7.3 Hz, 2H), 1.03 (t, *J* = 7.3 Hz, 3H).

^{13}C NMR (125 MHz, $CDCl_3$) δ 153.93, 150.75, 132.22, 132.19, 130.41, 128.79, 128.58, 128.13, 127.92, 127.86, 127.85, 127.36, 126.86, 126.45, 125.59, 125.48, 124.57, 121.90, 120.19, 114.08, 31.38, 31.24, 22.56, 13.93.

(S)-3-phenyl-2,2'-bis(MOM)-1,1'-binaphtyl

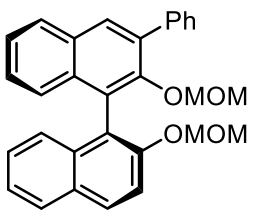

Following **General Procedure H**, (S)-3-iodo-2,2'-bis(MOM)-1,1'-binaphtyl (2.06 g, 4.11 mmol), phenylboronic acid (1.004 g, 8.23 mmol), $Pd(PPh_3)_4$ (476 mg, 0.4 mmol) and NaOH (1 M, 4.2 mL, 4.2 mmol). The product was involved in the subsequent steps without purification.

R_f (Hex/EtOAc 9:1)= 0.25

(S)-3-phenyl-1,1'-binaphtyl

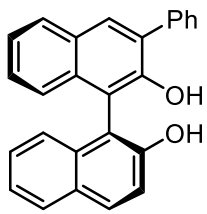

Following **General Procedure I**, (S)-3-phenyl-2,2'-bis(MOM)-1,1'-binaphtyl (1.85 g, 4.0 mmol) and HCl (4 N, 4.0 mL) in dioxane (20 mL). The purification by flash chromatography column (silica gel, Hex/EtOAc 8:2) afforded the name compound (1.571 g, 99%).[53]

R_f (Hex/EtOAc 8:2)= 0.20

(S)-3-mesityl-2,2'-bis(MOM)-1,1'-binaphtyl

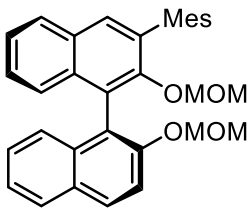

Following **General Procedure H**, (S)-3-iodo-2,2'-bis(MOM)-1,1'-binaphtyl (301 mg, 0.6 mmol), 2,4,6-trimethylphenylboronic acid (200 mg, 1.2 mmol), $Pd(PPh_3)_4$ (76 mg, 0.07 mmol) and K_2CO_3 (2 M, 0.3 mL, 0.6 mmol). The product was involved in the subsequent steps without purification.

R_f (Hex/EtOAc 9:1)= 0.30

(S)-3-mesityl-1,1'-binaphtyl

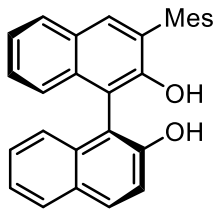

Following **General Procedure I**, (S)-3-mesityl-2,2'-bis(MOM)-1,1'-binaphtyl (255 mg, 0.5 mmol) and HCl (37%, 0.5 mL) in dioxane (2.5 mL). The purification by flash chromatography column (silica gel, Hex/EtOAc 7:3) afforded the name compound (100 mg, 48%).[53]

R_f (Hex/EtOAc 7:3)= 0.35

6.3.2. Amines Synthesis and Characterization

(R,R)-N,N-bis(1-phenylethyl)amine hydrochloride

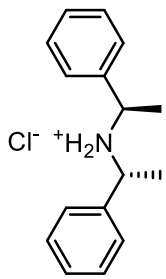

Following **General Procedure J**, (R)-1-phenylethylamine (d=0.952 g/mL, 6.3 mL, 49.5 mmol), acetophenone (d=1.030 g/mL, 5.8 mL, 49.5 mmol), $Ti(iOPr)_4$ (d=0.96 g/mL, 44 mL, 149 mmol) and Pd/C (10% w/w, 900 mg). The recrystallization of the raw product afforded the name product as pure diastereoisomer (6.594 g, 51%).[54]

R_f (Hex/EtOAc 65:35)=0.36

(R,R)-N,N-dimethyl-4-(1-(1-phenylethylamino)ethyl)aniline hydrochloride

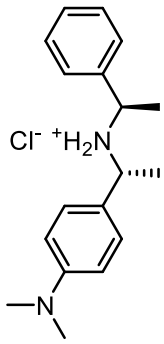

Following **General Procedure J**, (R)-1-phenylethylamine (d=0.952 g/mL, 2.1 mL, 16.5 mmol), 4'-dimethylaminoacetophenone (2.708 g, 16.5 mmol), $Ti(iOPr)_4$ (d=0.96 g/mL, 14.7 mL, 49.5 mmol) and Pd/C (10% w/w, 300 mg). The product was obtained and used as a mixture of the two diastereoisomers (*dr*=0.85, 1.907 g, 43%).

R_f (Hex/EtOAc 65:35)=0.2

^{1}H NMR (400 MHz, $CDCl_3$) δ 7.40 – 7.36 (m, 2H), 7.32 – 7.28 (m, 3H), 7.17 – 7.11 (m, 2H), 6.82 – 6.73 (m, 2H), 3.59 (q, *J* = 6.7 Hz, 1H), 3.48 (q, *J* = 6.7 Hz, 1H), 3.00 (s, 6H), 1.32 (dd, *J* = 6.7, 3.6 Hz, 6H).

^{13}C NMR (125 MHz, $CDCl_3$) δ 150.59, 143.15, 134.02, 129.29, 128.51, 128.02, 126.08, 112.66, 54.45, 52.70, 40.30, 21.23, 21.13.

6.3.3. Ligands Synthesis and Characterization

(S)-2,2'-binaphtoyl-(R,R)-N-(1-phenylethyl)-N-(1-(N,N-dimethyl-4'-aniline)ethyl)aminoylphosphine (L14)

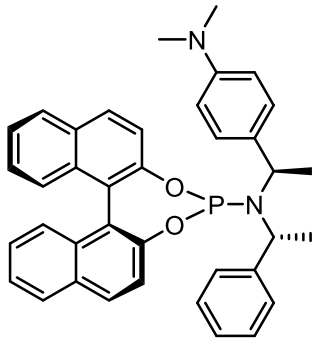

Following **General Procedure K**, (S)-BINOL (200 mg, 0.7 mmol), (R,R)-N-(1-phenylethyl)-N-(1-(N,N-dimethyl-4'-aniline)ethyl)amine (187 mg, 0.7 mmol), PCl_3 (d=1.57 g/mL, 0.061 mL, 0.7 mmol) and Et_3N (d=0.726 g/mL, 0.78 mL, 5.6 mmol) in anhydrous CH_2Cl_2 (5 mL). The purification by flash chromatography column (silica gel, Hex/EtOAc 7:3) afforded the name compound (90 mg, 22%).

R_f (Hex/EtOAc 1:1)= 0.60

^{1}H NMR (300 MHz, $CDCl_3$) δ 8.00 (ddd, J = 10.5, 8.8, 6.4 Hz, 6H), 7.69 (d, J = 8.8 Hz, 1H), 7.53 – 7.44 (m, 4H), 7.43 – 7.34 (m, 4H), 7.10 – 7.03 (m, 2H), 6.86 – 6.74 (m, 2H), 6.66 – 6.50 (m, 2H), 4.56 (dq, J = 13.7, 7.0 Hz, 2H), 2.98 (s, 9H), 1.80 (t, J = 6.6 Hz, 6H).

^{13}C NMR (75 MHz, $CDCl_3$) δ 150.30, 150.21, 149.74, 149.51, 143.32, 132.84, 132.81, 131.40, 130.90, 130.51, 130.21, 129.42, 128.82, 128.34, 128.13, 128.10, 127.80, 127.18, 126.62, 125.96, 124.71, 124.44, 124.17, 124.14, 124.09, 122.57, 121.85, 112.20, 52.13, 51.97, 51.83, 51.67, 40.80.

^{31}P NMR (122 MHz, $CDCl_3$) δ 146.58 (t, J = 11.0 Hz).

(S)-3-methyl-2,2'-binaphtoyl-(R,R)-N,N-bis(1-phenylethyl)aminoylphosphine (L24)

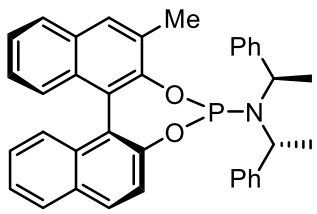

Following **General Procedure K**, (S)-3-methyl-1,1'-binaphtyl (125 mg, 0.45 mmol), (R,R)-N,N-bis(1-phenylethyl)amine (119 mg, 0.45 mmol), PCl_3 (d=1.57 g/mL, 0.040 mL, 0.45 mmol) and Et_3N (d=0.726 g/mL, 0.505 mL, 3.6 mmol) in anhydrous CH_2Cl_2 (5 mL). The purification by flash chromatography column (silica gel, Hex/EtOAc 99:1) afforded the name compound (63 mg, 27%).

R_f (Hex/EtOAc 99:1)= 0.33

^{1}H NMR (400 MHz, $CDCl_3$) δ 7.90 (dd, J = 17.4, 8.5 Hz, 2H), 7.83 (m, 2H), 7.47 (d, J = 8.8 Hz, 1H), 7.44 – 7.28 (m, 4H), 7.22 – 7.14 (m, 3H), 7.08 (m, 9H), 4.53 (s, broad, 2H), 2.72 (s, 3H), 1.62 (s, 6H).

^{13}C NMR (75 MHz, $CDCl_3$) δ 149.56, 149.12, 132.86, 131.81, 131.40, 130.34, 130.10, 129.53, 128.29, 127.96, 127.92, 127.72, 127.37, 127.03, 126.94, 126.59, 125.93, 125.13, 124.62, 124.50, 124.17, 124.10, 122.19, 121.94, 52.25, 52.10, 18.46.

^{31}P NMR (162 MHz, $CDCl_3$) δ 146.23 (t, J = 11.2 Hz).

(S)-3-ethyl-2,2'-binaphtoyl-(R,R)-N,N-bis(1-phenylethyl)aminoylphosphine (L23)

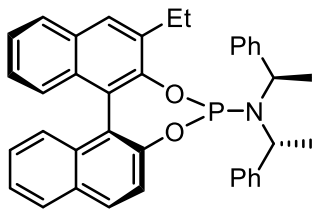

Following **General Procedure K**, (S)-3-ethyl-1,1'-binaphtyl (127 mg, 0.4 mmol), (R,R)-N,N-bis(1-phenylethyl)amine (106 mg, 0.4 mmol), PCl_3 (d=1.57 g/mL, 0.035 mL, 0.4 mmol) and Et_3N (d=0.726 g/mL, 0.33 mL, 2.4 mmol) in anhydrous CH_2Cl_2 (4 mL). The purification by flash chromatography column (silica gel, Hex/EtOAc 99:1) afforded the name compound (98 mg, 43%).

R_f (Hex/EtOAc 100:1)= 0.23

^{1}H NMR (400 MHz, $CDCl_3$) δ 7.96 – 7.79 (m, 4H), 7.47 (dd, J = 8.8, 1.0 Hz, 1H), 7.43 – 7.28 (m, 4H), 7.23 – 7.15 (m, 3H), 7.08 (m, 9H), 4.51 (s, broad, 2H), 3.32 (dq, J = 14.9, 7.4 Hz, 1H), 3.01 (dq, J = 15.0, 7.5 Hz, 1H), 1.93 – 1.47 (m, 6H), 1.43 (t, J = 7.5 Hz, 3H).

^{13}C NMR (75 MHz, $CDCl_3$) δ 149.56, 148.74, 148.66, 136.08, 132.91, 131.71, 131.43, 130.49, 130.09, 129.06, 128.31, 127.91, 127.73, 127.61, 127.13, 126.93, 126.60, 125.93, 125.17, 124.65, 124.49, 124.34, 124.27, 122.24, 121.97, 121.94, 52.13, 25.07, 14.06, 1.08.

^{31}P NMR (162 MHz, $CDCl_3$) δ 146.04 (t, J = 11.1 Hz).

(S)-3,3'-diethyl-2,2'-binaphtoyl-(R,R)-N,N-bis(1-phenylethyl)aminoylphosphine (L20)

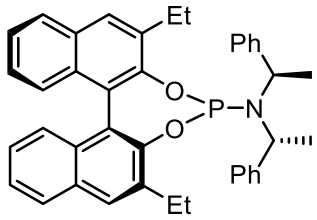

Following **General Procedure K**, (S)-3,3'-diethyl-1,1'-binaphtyl (140 mg, 0.41 mmol), (R,R)-N,N-bis(1-phenylethyl)amine (107 mg, 0.41 mmol), PCl_3 (d=1.57 g/mL, 0.036 mL, 0.41 mmol) and Et_3N (d=0.726 g/mL, 0.34 mL, 2.45 mmol) in anhydrous CH_2Cl_2 (4 mL). The purification by flash chromatography column (silica gel, Hex/EtOAc 99:1) afforded the name compound (123 mg, 51%).

R_f (Hex/EtOAc 100:1)= 0.26

^{1}H NMR (400 MHz, $CDCl_3$) δ 7.89 – 7.79 (m, 4H), 7.35 (dtd, J = 8.7, 6.8, 2.5 Hz, 4H), 7.26 – 6.60 (m, 12H), 4.51 (s, broad, 2H), 3.32 (dq, J = 14.9, 7.4 Hz, 1H), 3.01 (dq, J = 15.0, 7.5 Hz, 1H), 2.78 (dq, J = 14.8, 7.5 Hz, 1H), 2.70 (dq, J=14.9, 7.5, 1H), 1.53 (s, broad, 6H), 1.41 (t, J = 7.5 Hz, 3H), 1.27 (t, J = 7.5 Hz, 3H).

^{13}C NMR (75 MHz, $CDCl_3$) δ 148.64, 148.56, 148.51, 136.23, 135.97, 131.81, 131.65, 131.38, 130.49, 128.30, 127.69, 127.57, 127.41, 127.07, 126.90, 126.61, 126.57, 125.08, 125.01, 124.57, 124.41, 124.14, 124.08, 122.34, 52.26, 25.14, 24.19, 14.68, 14.13, 1.06.

^{31}P NMR (162 MHz, $CDCl_3$) δ 144.34 (t, J = 11.6 Hz).

(S)-3-buthyl-2,2'-binaphtoyl-(R,R)-N,N-bis(1-phenylethyl)aminoylphosphine (L25)

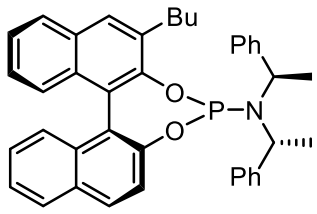

Following **General Procedure K**, (S)-3-buthyl-1,1'-binaphtyl (253 mg, 0.74 mmol), (R,R)-N,N-bis(1-phenylethyl)amine (193 mg, 0.74 mmol), PCl_3 (d=1.57 g/mL, 0.065 mL, 0.74 mmol) and Et_3N (d=0.726 g/mL, 0.618 mL, 4.43 mmol) in anhydrous CH_2Cl_2 (8 mL). The purification by flash chromatography column (silica gel, Hex/EtOAc 9:1) afforded the name compound (130 mg, 30%).

R_f (Hex/EtOAc 8:2)= 0.60

^{1}H NMR (400 MHz, $CDCl_3$) δ 7.90 (dd, J = 15.5, 8.5 Hz, 2H), 7.84 (d, J = 8.1 Hz, 1H), 7.81 (s, 1H), 7.47 (d, J = 8.7 Hz, 1H), 7.44 – 7.26 (m, 4H), 7.18 (m, 3H), 7.08 (m, 9H), 4.51 (s, broad, 2H), 3.38 (ddd, J = 14.7, 9.9, 5.3 Hz, 1H), 2.93 – 2.79 (m, 1H), 2.02 – 1.80 (m, 2H), 1.71 (s, 6H), 1.53 – 1.44 (m, 2H), 1.00 (t, J = 7.3 Hz, 3H).

^{13}C NMR (75 MHz, $CDCl_3$) δ 149.54, 148.81, 134.94, 132.91, 131.71, 131.41, 130.41, 130.04, 128.48, 128.28, 127.98, 127.92, 127.71, 127.54, 127.13, 126.92, 126.58, 125.90, 125.12, 124.61, 124.45, 124.30, 122.24, 121.96, 52.25, 52.10, 32.45, 32.18, 22.93, 14.11.

^{31}P NMR (162 MHz, $CDCl_3$) δ 145.86 (t, J = 11.2 Hz).

(S)-3-phenyl-2,2'-binaphtoyl-(R,R)-N,N-bis(1-phenylethyl)aminoylphosphine (L26)

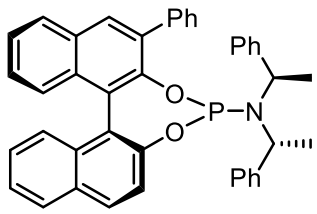

Following **General Procedure K**, (S)-3-phenyl-1,1'-binaphtyl (1.571 g, 4.8 mmol), (R,R)-N,N-bis(1-phenylethyl)amine (1.265 g, 4.8 mmol), PCl_3 (d=1.57 g/mL, 0.423 mL, 4.8 mmol) and Et_3N (d=0.726 g/mL, 4.0 mL, 28.7 mmol) in anhydrous CH_2Cl_2 (40 mL). The purification by flash chromatography column (silica gel, Hex/EtOAc 9:1) afforded the name compound (2.272 g, 76%).

R_f (Hex/EtOAc 8:2)= 0.46

^{1}H NMR (400 MHz, $CDCl_3$) δ 8.12 (s, 1H), 8.00 – 7.90 (m, 5H), 7.50 (q, J = 8.9, 8.2 Hz, 3H), 7.41 (dd, J = 8.0, 6.1 Hz, 3H), 7.33 (d, J = 8.5 Hz, 1H), 7.24 (m, 3H), 7.10 – 7.03 (m, 6H), 7.00 – 6.90 (m, 4H), 4.38 (s, broad, 2H), 1.08 (d, J = 7.2 Hz, 6H).

^{13}C NMR (75 MHz, $CDCl_3$) δ 149.84, 147.50, 147.41, 143.27, 138.25, 134.30, 133.07, 133.05, 132.62, 131.47, 130.74, 130.50, 130.33, 130.13, 128.43, 128.33, 128.25, 127.95, 127.73, 127.55, 127.14, 127.01, 126.59, 126.12, 126.07, 124.88, 124.77, 124.36, 124.30, 123.53, 123.49, 122.38, 51.86, 51.71.

^{31}P NMR (122 MHz, $CDCl_3$) δ 146.05 (d, J = 11.6 Hz).

(S)-3-mesithyl-2,2'-binaphtoyl-(R,R)-N,N-bis(1-phenylethyl)aminoylphosphine (L27)

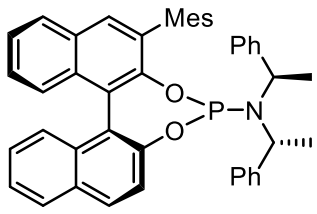

Following **General Procedure K**, (S)-3-mesityl-1,1'-binaphtyl (100 mg, 0.25 mmol), (R,R)-N,N-bis(1-phenylethyl)amine (65 mg, 0.25 mmol), PCl_3 (d=1.57 g/mL, 0.022 mL, 0.25 mmol) and Et_3N (d=0.726 g/mL, 0.207 mL, 1.48 mmol) in anhydrous CH_2Cl_2 (3 mL). The purification by flash chromatography column (silica gel, Hex/EtOAc 85:15) afforded the name compound (58 mg, 36%).

R_f (Hex/EtOAc 8:2)= 0.26

^{13}C NMR (75 MHz, $CDCl_3$) δ 151.10, 149.51, 136.80, 136.11, 135.95, 132.42, 132.22, 131.59, 130.16, 129.78, 128.58, 128.43, 128.34, 127.49, 127.38, 127.33, 127.22, 126.10, 126.06, 125.87, 125.70, 123.33, 123.23, 123.07, 122.68, 116.62, 111.53, 110.51, 54.12, 20.09, 19.54, 19.43.

1H NMR (400 MHz, $CDCl_3$) δ 7.98 (d, J = 8.9 Hz, 1H), 7.91 (d, J = 8.0 Hz, 2H), 7.80 (s, 1H), 7.54 (s, 1H), 7.49 – 7.30 (m, 13H), 7.23 (t, J = 9.5 Hz, 3H), 7.04 (s, 2H), 5.09 (s, 1H), 5.02 (s, 1H), 2.37 (s, 3H), 2.16 (d, J = 3.1 Hz, 6H), 1.58 (s, 6H).

^{31}P NMR (122 MHz, $CDCl_3$) δ 146.05 (d, J = 11.6 Hz).

6.3.4. Substrates Synthesis and Characterization

Dimethyl cyanomethylphosphonate

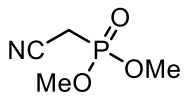

Following **General Procedure A**, bromoacetonitrile (12.000 g, 100.0 mmol) and trimethylphosphite (13.654 g, 110.0 mmol). The purification by flash chromatography column (silica gel, Hex/EtOAc 1:9) afforded the name compound (14.1 g, 93%).[50]

R_f (Hex/EtOAc 1:9)= 0.3

Dimethyl-α-cyano-β-phenylvinylphosphonate

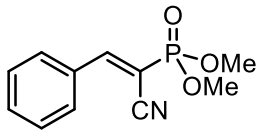

Following **General Procedure B**, benzaldehyde (d=1.044 g/mL, 0.35 mL, 3.35 mmol), dimethyl cyanomethylphosphonate (502 mg, 3.35 mmol), $ZnCl_2$ (457 mg, 3.35 mmol) and DIPEA (d=0.742 g/mL, 0.6 mL, 5.0 mmol) in dioxane (5 mL). The purification by flash chromatography column (silica gel, Hex/EtOAc 9:1 to 3:7) afforded the name compound (476 mg, 60%).[55]

R_f (Hex/EtOAc 3:7)= 0.24

Diethyl-α-cyano-β-phenylvinylphosphonate

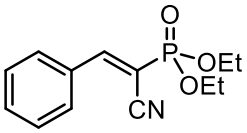

Following **General Procedure B**, benzaldehyde (d=1.044 g/mL, 3.5 mL, 34.4 mmol), diethyl cyanomethylphosphonate (d=1.095 g/mL, 5.5 mL, 34.0 mmol), $ZnCl_2$ (4.634 g, 34.0 mmol) and DIPEA (d=0.742 g/mL, 4.7 mL, 33.7 mmol) in dioxane (70 mL). The purification by flash chromatography column (silica gel, Hex/EtOAc 9:1 to 3:7) afforded the name compound (7.453 g, 83%).

R_f (Hex/EtOAc 3:7)= 0.38

^{1}H NMR (400 MHz, $CDCl_3$) δ 8.05 – 7.86 (m, 3H), 7.46 (dd, *J* = 14.8, 7.1 Hz, 3H), 4.19 (dq, *J* = 7.9, 7.4 Hz, 4H), 1.36 (t, *J* = 7.0 Hz, 6H).

^{13}C NMR (101 MHz, $CDCl_3$) δ 158.92 (d, *J* = 7.0 Hz), 133.08, 132.43 (d, *J* = 17.9 Hz), 130.47, 129.21, 115.38 (d, *J* = 10.2 Hz), 100.06 (d, *J* = 197.6 Hz), 63.62 (d, *J* = 5.9 Hz), 16.23 (d, *J* = 6.3 Hz).

^{31}P NMR (162 MHz, $CDCl_3$) δ 11.04 (dp, *J* = 21.9, 8.4 Hz).

Diethyl-α-cyano-β-cinnamylvinylphosphonate

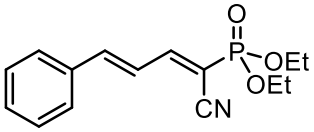

Following **General Procedure B**, cinnamaldehyde (d=1.050 g/mL, 0.78 mL, 6.2 mmol), diethyl cyanomethylphosphonate (1.006 g, 5.7 mmol), $ZnCl_2$ (769 mg, 5.6 mmol) and DIPEA (d=0.742 g/mL, 1.2 mL, 8.5 mmol) in dioxane (10 mL). The purification by flash chromatography column (silica gel, Hex/EtOAc 9:1 to 3:7) afforded the name compound (1.171 g, 71%).

R_f (Hex/EtOAc 3:7)= 0.45

^{1}H NMR (400 MHz, $CDCl_3$) δ 7.92 – 7.74 (m, 1H), 7.57 (d, *J* = 3.4 Hz, 2H), 7.42 (d, *J* = 3.2 Hz, 3H), 7.34 – 7.13 (m, 2H), 4.21 (hept, *J* = 7.5 Hz, 4H), 1.40 (t, *J* = 6.8 Hz, 6H).

^{13}C NMR (101 MHz, $CDCl_3$) δ 159.72 (d, *J* = 7.0 Hz), 147.66, 134.60 (d, *J* = 1.5 Hz), 131.02, 129.12, 128.42, 123.55 (d, *J* = 18.3 Hz), 114.62 (d, *J* = 11.3 Hz), 100.97 (d, *J* = 202.4 Hz), 63.43 (d, *J* = 5.8 Hz), 16.25 (d, *J* = 6.2 Hz).

^{31}P NMR (162 MHz, $CDCl_3$) δ 10.63 (dp, *J* = 16.7, 8.3 Hz).

Diethyl-α-cyano-β-(2-bromophenyl)vinylphosphonate

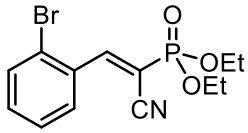

Following **General Procedure B**, 2-bromobenzaldehyde (d=1.585 g/mL, 1.9 mL, 16.3 mmol), diethyl cyanomethylphosphonate (d=1.095 g/mL, 2.6 mL, 16.3 mmol), $ZnCl_2$ (2.218 mg, 16.3 mmol) and DIPEA (d=0.742 g/mL, 3.4 mL, 24.4 mmol) in dioxane (35 mL). The purification by flash chromatography column (silica gel, Hex/EtOAc 9:1 to 3:7) afforded the name compound (2.8 g, 50%).

R_f (Hex/EtOAc 3:7)= 0.40

^{1}H NMR (400 MHz, $CDCl_3$) δ 8.33 (d, *J* = 20.8 Hz, 1H), 8.09 (d, *J* = 7.8 Hz, 1H), 7.67 (d, *J* = 7.9 Hz, 1H), 7.43 (t, *J* = 7.7 Hz, 1H), 7.35 (t, *J* = 7.7 Hz, 1H), 4.24 (dp, *J* = 9.4, 3.5 Hz, 4H), 1.41 (t, *J* = 7.0 Hz, 6H).

^{13}C NMR (101 MHz, $CDCl_3$) δ 157.52 (d, *J* = 8.0 Hz), 133.55, 133.39, 129.70 (d, *J* = 2.1 Hz), 127.99, 125.75, 114.66 (d, *J* = 10.6 Hz), 104.46 (d, *J* = 196.6 Hz), 63.86 (d, *J* = 5.9 Hz), 16.29 (d, *J* = 6.2 Hz).

^{31}P NMR (162 MHz, $CDCl_3$) δ 9.55 (dp, *J* = 21.3, 8.5 Hz).

Diethyl-α-cyano-β-(4-pyridyl)vinylphosphonate

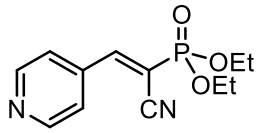

Following **General Procedure B**, pyridyl-4-carbaldehyde (d=1.122 g/mL, 2.7 mL, 28.28 mmol), diethyl cyanomethylphosphonate (d=1.095 g/mL, 4.6 mL, 28.28 mmol), $ZnCl_2$ (3.855 mg, 28.28 mmol) and DIPEA (d=0.742

g/mL, 5.9 mL, 42.42 mmol) in dioxane (45 mL). The purification by flash chromatography column (silica gel, Hex/EtOAc 9:1 to 3:7) afforded the name compound (658 g, 9%).

R_f (Hex/EtOAc 3:7)= 0.30

^{1}H NMR (400 MHz, $CDCl_3$) δ 8.81 – 8.74 (m, 2H), 7.94 (d, *J* = 20.9 Hz, 1H), 7.73 – 7.66 (m, 2H), 4.32 – 4.11 (m, 4H), 1.39 (t, *J* = 7.1 Hz, 6H).

^{13}C NMR (101 MHz, $CDCl_3$) δ 155.87 (d, *J* = 7.0 Hz), 151.13, 150.32, 138.85 (d, *J* = 18.1 Hz), 122.85, 121.09, 114.32 (d, *J* = 9.4 Hz), 106.65 (d, *J* = 194.1 Hz), 64.07 (d, *J* = 6.1 Hz), 16.26 (d, *J* = 6.2 Hz).

^{31}P NMR (162 MHz, $CDCl_3$) δ 8.70 (dp, *J* = 21.5, 8.7 Hz).

6.3.5. Products Synthesis and Characterization

1,3-diphenyl-2-cyano-1-pentene (36)

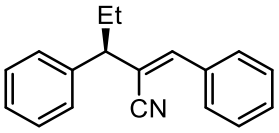

Following **General Procedure M**, diethyl-α-cyano-β-phenylvinylphosphonate (100 mg, 0.376mmol), CuTC (1.42 mg, 7.4 mmol), Et_2Zn (1 M in hexane, 0.56 mL, 0.56 mmol), **L26** (11.58 mg, 0.0188 mmol), benzaldehyde (d=1.044 g/mL, 0.057 mL, 0.564 mmol) in dry toluene (0.2 mL).
NMR yield = 79%

ee = 96%

^{1}H NMR (300 MHz, $CDCl_3$) δ 7.83 – 7.60 (m, 2H), 7.52 – 7.17 (m, 7H), 7.06 (s, 1H), 3.51 (t, *J* = 7.7 Hz, 1H), 2.17 (dq, *J* = 13.6, 7.5 Hz, 1H), 2.10 – 1.96 (m, 1H), 1.01 (t, *J* = 7.3 Hz, 3H).

^{13}C NMR (75 MHz, $CDCl_3$) δ 143.19, 141.05, 133.65, 130.05, 128.85, 128.79, 128.78, 127.69, 127.35, 118.04, 115.68, 53.49, 26.37, 12.32.

HPLC (Lux Cellulose 3, Hexane:*i*-PrOH 60:40, 1.0 mL/min, 295 nm) t_R: 6.4 min; 7.3 min (maj)

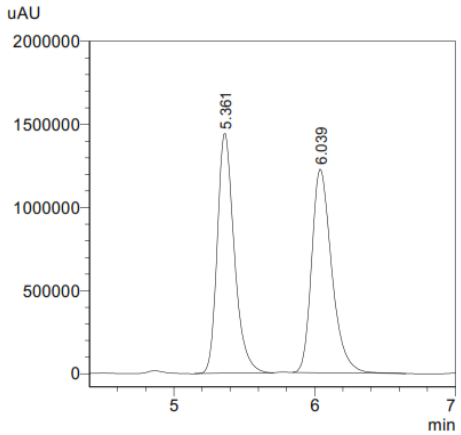

PDA Ch1 295nm

Peak#	Ret. Time	Area	Area%
1	5.361	12092760	49.896
2	6.039	12143396	50.104
Total		24236156	100.000

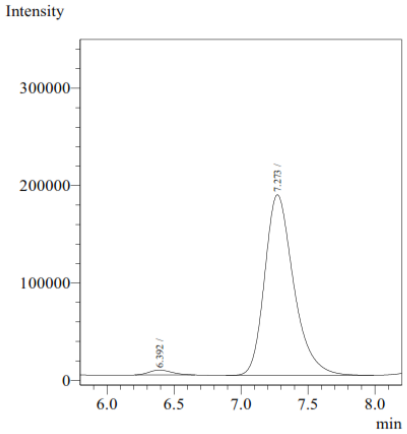

AD1

Peak#	Ret.Time	Area	Area%
1	6.392	59203	2.079
2	7.273	2788732	97.921
Total		2847935	100.000

1-(4'-methoxyphenyl)-3-phenyl-2-cyano-1-pentene (A1)

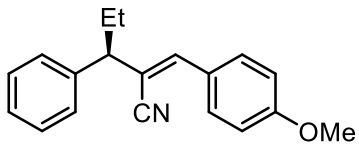

Following **General Procedure M**, diethyl-α-cyano-β-phenylvinylphosphonate (100 mg, 0.376mmol), CuTC (1.42 mg, 7.4 mmol), Et_2Zn (1 M in hexane, 0.56 mL, 0.56 mmol), **L26** (11.58 mg, 0.0188 mmol), 4-methoxybenzaldehyde (d=1.119 g/mL, 0.069 mL, 0.564 mmol) in dry toluene (0.2 mL).

NMR yield = 37%

ee = 96%

^{1}H NMR (400 MHz, $CDCl_3$) δ 7.63 (d, *J* = 8.9 Hz, 2H), 7.34 – 7.11 (m, 6H), 6.87 (s, 1H), 6.85 – 6.78 (m, 2H), 3.75 (s, 3H), 3.36 (t, *J* = 7.8 Hz, 1H), 2.11 – 1.97 (m, 1H), 1.96 – 1.85 (m, 1H), 0.89 (t, *J* = 7.3 Hz, 3H).

^{13}C NMR (101 MHz, $CDCl_3$) δ 160.96, 142.80, 141.45, 130.55, 128.80, 127.64, 127.23, 126.42, 118.57, 114.15, 112.63, 55.38, 53.43, 26.47, 12.35.

HPLC (Lux Cellulose 3, Hexane:*i*-PrOH 99:1, 1.0 mL/min, 300 nm) t_R: 33.4 min; 38.2 min (maj)

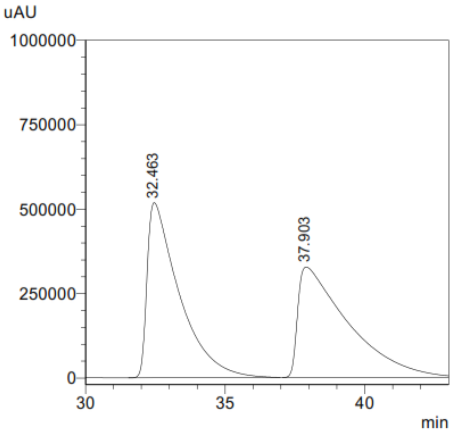

PDA Ch1 300nm

Peak#	Ret. Time	Area	Area%
1	32.463	41498027	50.375
2	37.903	40880072	49.625
Total		82378099	100.000

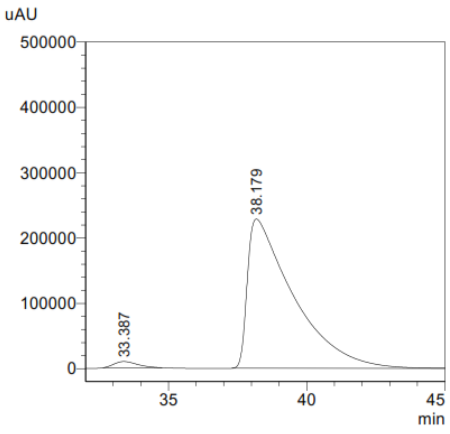

PDA Ch1 300nm

Peak#	Ret. Time	Area	Area%
1	33.387	552866	2.047
2	38.179	26457361	97.953
Total		27010227	100.000

1-(4'-trifluoromethylphenyl)-3-phenyl-2-cyano-1-pentene (A2)

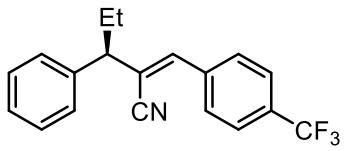

Following **General Procedure M**, diethyl-α-cyano-β-phenylvinylphosphonate (100 mg, 0.376mmol), CuTC (1.42 mg, 7.4 mmol), Et_2Zn (1 M in hexane, 0.56 mL, 0.56 mmol), **L26** (11.58 mg, 0.0188 mmol), 4-trifluoromethyl-benzaldehyde (98 mg, 0.564 mmol) in dry toluene (0.2 mL). NMR yield = 30%

ee = 96%

^{1}H NMR (400 MHz, $CDCl_3$) δ 7.73 (d, *J* = 8.2 Hz, 2H), 7.57 (d, *J* = 8.2 Hz, 2H), 7.32 – 7.18 (m, 5H), 3.43 (t, *J* = 7.7 Hz, 1H), 2.13 – 2.01 (m, 1H), 1.97 – 1.88 (m, 1H), 0.91 (t, *J* = 7.3 Hz, 3H).

^{13}C NMR (101 MHz, $CDCl_3$) δ 141.33, 140.42, 136.94, 131.69, 131.36, 128.97, 127.71, 127.58, 125.73 (q), 118.77, 117.43, 53.52, 26.34, 12.27.

^{19}F NMR (377 MHz, $CDCl_3$) δ -62.93.

HPLC (Lux Cellulose 1, Hexane:*i*-PrOH 99.5:0.5, 1.0 mL/min, 274 nm) t_R: 12.5 min; 13.9 min (maj)

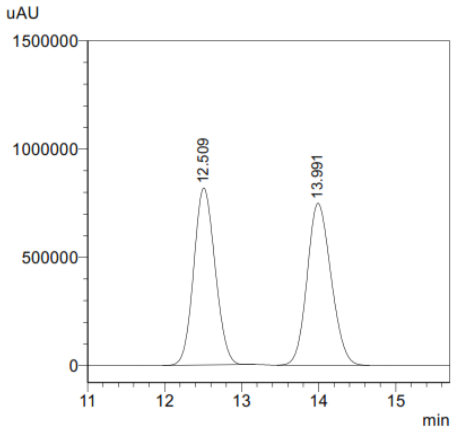

PDA Ch1 274nm

Peak#	Ret. Time	Area	Area%
1	12.509	15809610	49.469
2	13.991	16148993	50.531
Total		31958603	100.000

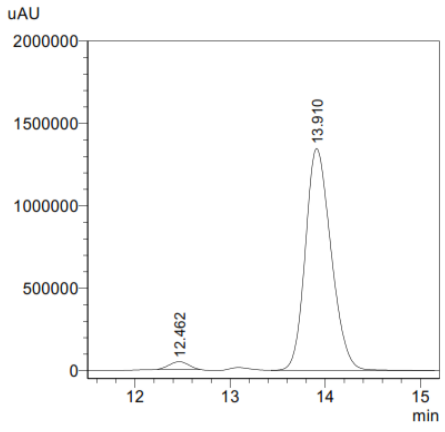

PDA Ch1 274nm

Peak#	Ret. Time	Area	Area%
1	12.462	637966	2.462
2	13.910	25273438	97.538
Total		25911404	100.000

1-(4'-bromophenyl)-3-phenyl-2-cyano-1-pentene (A3)

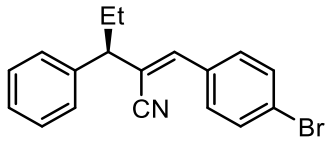

Following **General Procedure M**, diethyl-α-cyano-β-phenylvinylphosphonate (100 mg, 0.376mmol), CuTC (1.42 mg, 7.4 mmol), Et_2Zn (1 M in hexane, 0.56 mL, 0.56 mmol), **L26** (11.58 mg, 0.0188 mmol), 4-bromobenzaldehyde (104 mg, 0.564 mmol) in dry toluene (0.2 mL).

NMR yield = 93%

ee = 94%

^{1}H NMR (400 MHz, $CDCl_3$) δ 7.50 (d, *J* = 8.3 Hz, 2H), 7.44 (d, *J* = 8.5 Hz, 2H), 7.31 – 7.18 (m, 6H), 6.87 (s, 1H), 3.39 (t, *J* = 7.8 Hz, 1H), 2.05 (dp, *J* = 14.8, 7.4 Hz, 1H), 1.91 (dq, *J* = 14.6, 7.3 Hz, 1H), 0.89 (t, *J* = 7.3 Hz, 3H).

^{13}C NMR (101 MHz, $CDCl_3$) δ 141.78, 140.71, 132.50, 132.01, 130.22, 128.91, 127.68, 127.47, 124.28, 117.77, 116.61, 53.50, 26.36, 12.30.

HPLC (Lux Cellulose 5, Hexane:*i*-PrOH 99:1, 0.8 mL/min, 314 nm) t_R: 11.9 min; 13.0 min (maj)

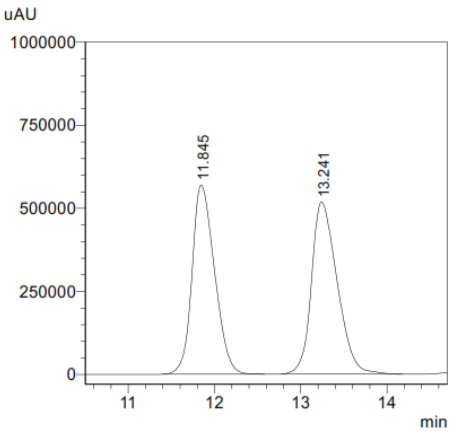

PDA Ch1 314nm

Peak#	Ret. Time	Area	Area%
1	11.845	10350745	49.075
2	13.241	10740768	50.925
Total		21091514	100.000

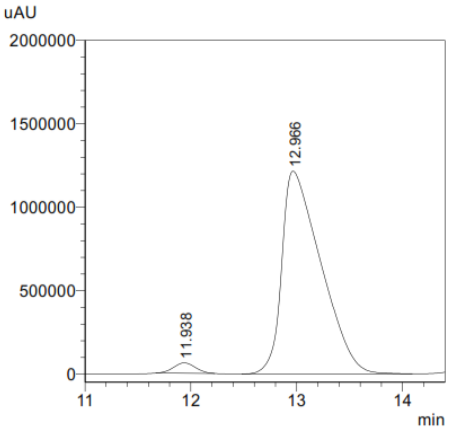

PDA Ch1 314nm

Peak#	Ret. Time	Area	Area%
1	11.938	899338	2.800
2	12.966	31217197	97.200
Total		32116535	100.000

1-(2'-pyridyl)-3-phenyl-2-cyano-1-pentene (A4)

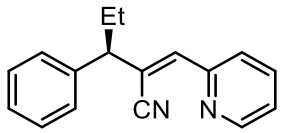

Following **General Procedure M**, diethyl-α-cyano-β-phenylvinylphosphonate (100 mg, 0.376mmol), CuTC (1.42 mg, 7.4 mmol), Et_2Zn (1 M in hexane, 0.56 mL, 0.56 mmol), **L26** (11.58 mg, 0.0188 mmol), 2-pyridynecarboxyaldehyde (d=1.126 g/mL, 0.054 mL, 0.564 mmol) in dry toluene (0.2 mL).

NMR yield = 61%

ee = 96%

^{1}H NMR (300 MHz, $CDCl_3$) δ 8.59 (d, *J* = 4.8 Hz, 1H), 7.76 (d, *J* = 7.9 Hz, 1H), 7.65 (td, *J* = 7.8, 1.8 Hz, 1H), 7.35 – 7.11 (m, 5H), 7.08 (s, 1H), 3.47 (t, *J* = 7.7 Hz, 1H), 2.11 (dq, *J* = 13.7, 7.4 Hz, 1H), 1.95 (dq, *J* = 13.7, 7.3 Hz, 1H), 0.91 (t, *J* = 7.3 Hz, 3H).

^{13}C NMR (101 MHz, $CDCl_3$) δ 152.16, 149.77, 142.49, 140.47, 136.75, 128.89, 127.82, 127.48, 124.03, 123.37, 119.36, 117.48, 53.53, 26.22, 12.30.

HPLC (Lux Cellulose 3, Hexane:*i*-PrOH 90:10, 1.0 mL/min, 254 nm) t_R: 11.7 min; 18.3 min (maj)

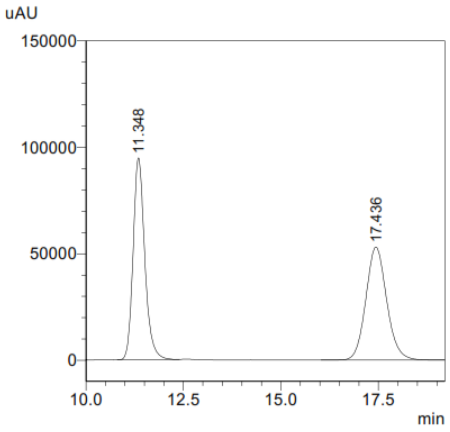

PDA Ch1 254nm

Peak#	Ret. Time	Area	Area%
1	11.348	1973191	49.929
2	17.436	1978813	50.071
Total		3952004	100.000

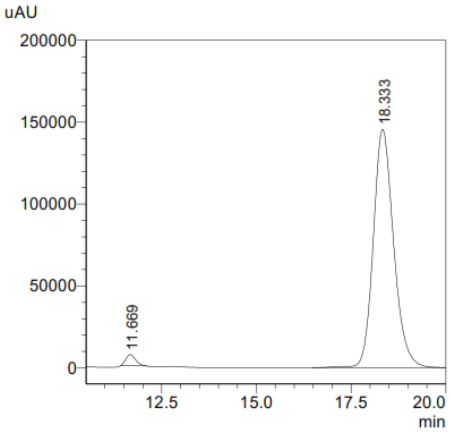

PDA Ch1 254nm

Peak#	Ret. Time	Area	Area%
1	11.669	125733	2.261
2	18.333	5435340	97.739
Total		5561073	100.000

1-(4'-Bpin)-3-phenyl-2-cyano-1-pentene (A5)

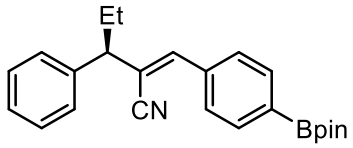

Following **General Procedure M**, diethyl-α-cyano-β-phenylvinylphosphonate (100 mg, 0.376mmol), CuTC (1.42 mg, 7.4 mmol), Et_2Zn (1 M in hexane, 0.56 mL, 0.56 mmol), **L26** (11.58 mg, 0.0188 mmol), 4-(4,4,5,5-tetramethyl-1,3,2-dioxaborolan-2-yl)benzaldehyde (131 mg, 0.564 mmol) in dry toluene (0.2 mL).

NMR yield = 96%

ee = 96%

^{1}H NMR (300 MHz, $CDCl_3$) δ 7.77 – 7.70 (m, 1H), 7.65 – 7.59 (m, 1H), 7.34 – 7.14 (m, 5H), 6.95 (s, 1H), 6.89 – 6.79 (m, 1H), 3.41 (t, *J* = 7.7 Hz, 1H), 2.13 – 2.00 (m, 1H), 1.99 – 1.87 (m, 1H), 1.49 (s, 12H), 0.90 (t, *J* = 7.3 Hz, 3H).

^{13}C NMR (101 MHz, $CDCl_3$) δ 143.10, 140.92, 136.09, 135.11, 128.87, 127.92, 127.73, 127.39, 117.89, 116.63, 84.04, 53.57, 26.40, 24.89, 24.88, 12.33.

HPLC (Lux Cellulose 4, Hexane:*i*-PrOH 99:1, 1.0 mL/min, 262 nm) t_R: 21.3 min (maj); 24.9 min

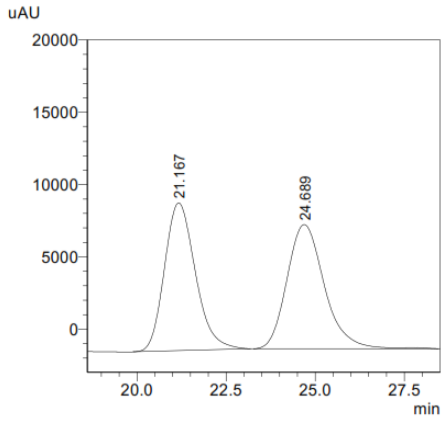

PDA Ch1 262nm

Peak#	Ret. Time	Area	Area%
1	21.167	615431	49.480
2	24.689	628364	50.520
Total		1243795	100.000

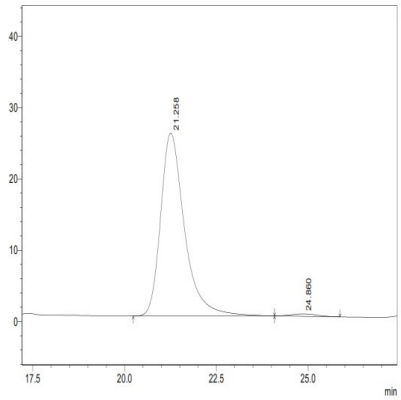

PDA Ch1 262 nm

Peak#	Ret. Time	Area	Area%
1	21.258	1160416	98.573
2	24.860	16795	1.427
Total		1177211	100

1,5-diphenyl-4-cyano-3-heptene (A6)

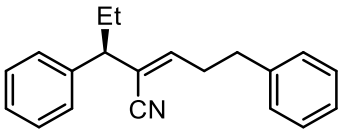

Following **General Procedure M**, diethyl-α-cyano-β-phenylvinylphosphonate (100 mg, 0.376mmol), CuTC (1.42 mg, 7.4 mmol), Et_2Zn (1 M in hexane, 0.56 mL, 0.56 mmol), **L26** (11.58 mg, 0.0188 mmol), dihydrocinnamic aldheyde (d=1.015 g/mL, 0.075 mL, 0.564 mmol) in dry toluene (0.2 mL).

NMR yield = 92%

ee = 92%

^{1}H NMR (400 MHz, $CDCl_3$) δ 7.30 – 7.16 (m, 5H), 7.16 – 7.02 (m, 5H), 6.12 (t, *J* = 7.1 Hz, 1H), 3.16 (t, *J* = 7.7 Hz, 1H), 2.73 – 2.52 (m, 4H), 1.86 (dq, *J* = 14.9, 7.4 Hz, 1H), 1.75 (dt, *J* = 13.8, 7.3 Hz, 1H), 0.77 (t, *J* = 7.3 Hz, 3H).

^{13}C NMR (101 MHz, $CDCl_3$) δ 146.24, 141.12, 140.11, 128.73, 128.54, 128.47, 127.57, 127.14, 126.31, 119.89, 116.80, 51.75, 34.78, 32.93, 26.34, 12.15.

HPLC (Lux Cellulose 3, Hexane:*i*-PrOH 99:1, 1.0 mL/min, 220 nm) t_R: 23.0 min (maj); 33.7 min

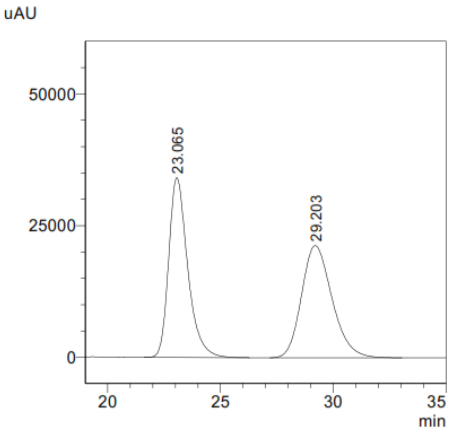

PDA Ch1 220nm

Peak#	Ret. Time	Area	Area%
1	23.065	2002148	49.928
2	29.203	2007895	50.072
Total		4010043	100.000

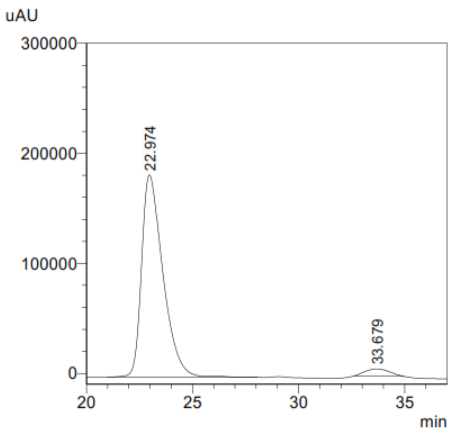

PDA Ch1 220nm

Peak#	Ret. Time	Area	Area%
1	22.974	12854605	96.165
2	33.679	512698	3.835
Total		13367303	100.000

1,5-diphenyl-4-cyano-hepta-1,3-diene (A7)

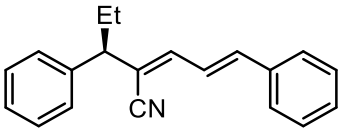

Following **General Procedure M**, diethyl-α-cyano-β-phenylvinylphosphonate (100 mg, 0.376mmol), CuTC (1.42 mg, 7.4 mmol), Et_2Zn (1 M in hexane, 0.56 mL, 0.56 mmol), **L26** (11.58 mg, 0.0188 mmol), cinnamic aldheyde (d=1.050 g/mL, 0.015 mL, 0.564 mmol) in dry toluene (0.2 mL).

NMR yield = 55%

ee = 96%

^{1}H NMR (400 MHz, $CDCl_3$) δ 7.42 – 7.36 (m, 2H), 7.30 – 7.17 (m, 8H), 7.09 (dd, *J* = 15.2, 11.3 Hz, 1H), 6.74 (d, *J* = 6.1 Hz, 1H), 6.71 (s, 1H), 3.31 (t, *J* = 7.7 Hz, 1H), 1.99 (dq, *J* = 14.8, 7.3 Hz, 1H), 1.88 (dq, *J* = 14.1, 7.3 Hz, 1H), 0.87 (t, *J* = 7.3 Hz, 3H).

^{13}C NMR (101 MHz, $CDCl_3$) δ 143.76, 141.13, 139.58, 135.79, 129.22, 128.86, 127.67, 127.29, 124.59, 117.56, 117.44, 51.85, 26.76, 12.30.

HPLC (Lux Cellulose 3, Hexane:*i*-PrOH 99.5:0.5, 1.0 mL/min, 308 nm) t_R: 26.2 min (maj); 32.9 min

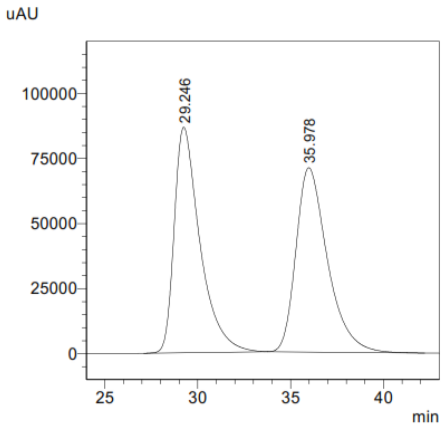

PDA Ch1 308nm

Peak#	Ret. Time	Area	Area%
1	29.246	8366985	50.008
2	35.978	8364229	49.992
Total		16731214	100.000

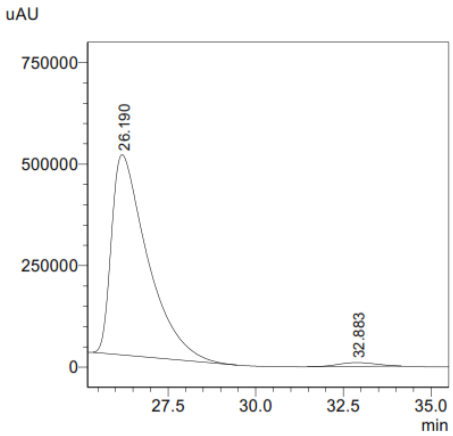

PDA Ch1 305nm

Peak#	Ret. Time	Area	Area%
1	26.190	35292374	97.990
2	32.883	723813	2.010
Total		36016188	100.000

1-(N-Boc-indole-3-)-3-phenyl-2-cyano-1-pentene (A8)

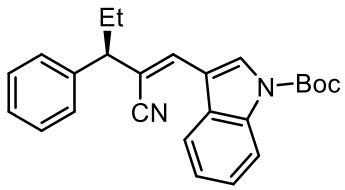

Following **General Procedure M**, diethyl-α-cyano-β-phenylvinylphosphonate (100 mg, 0.376 mmol), CuTC (1.42 mg, 7.4 mmol), Et_2Zn (1 M in hexane, 0.56 mL, 0.56 mmol), **L26** (11.58 mg, 0.0188 mmol), N-Boc-indole-3-carboxyaldehyde (136 mg, 0.564 mmol) in dry toluene (0.2 mL).

NMR yield = 54%

ee = 96%

^{1}H NMR (400 MHz, $CDCl_3$) δ 8.42 (s, 1H), 8.12 (d, *J* = 8.3 Hz, 1H), 7.50 (d, *J* = 7.8 Hz, 1H), 7.29 (m, 5H), 7.24 – 7.18 (m, 2H), 7.11 (s, 1H), 3.44 (t, *J* = 7.8 Hz, 1H), 2.15 – 2.01 (m, 1H), 2.01 – 1.88 (m, 1H), 1.59 (s, 9H), 0.92 (t, *J* = 7.3 Hz, 3H).

^{13}C NMR (101 MHz, $CDCl_3$) δ 149.15, 141.27, 135.00, 132.82, 129.21, 128.87, 127.67, 127.31, 126.01, 125.21, 123.16, 118.82, 117.99, 115.50, 114.44, 114.15, 84.63, 52.94, 28.10, 26.68, 12.35.

HPLC (Lux Cellulose 1, Hexane:*i*-PrOH 99.5:0.5, 1.0 mL/min, 352 nm) t_R: 14.5 min (maj); 15.9 min

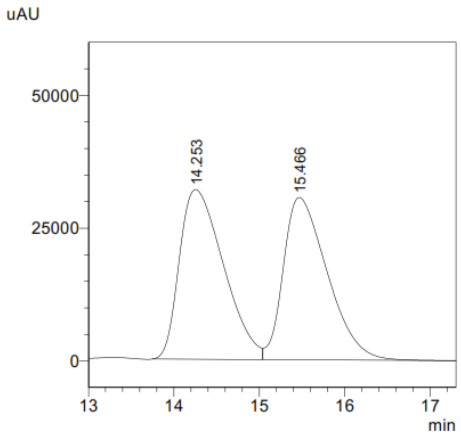

PDA Ch1 352nm

Peak#	Ret. Time	Area	Area%
1	14.253	1146388	51.132
2	15.466	1095616	48.868
Total		2242005	100.000

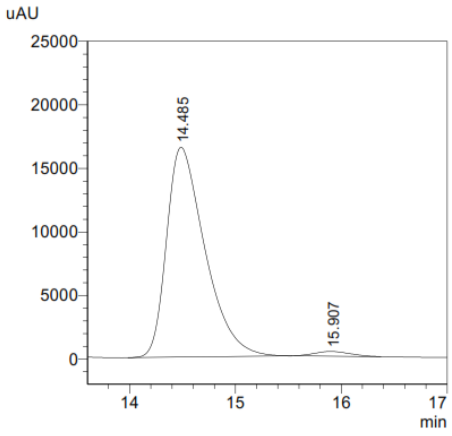

PDA Ch1 352nm

Peak#	Ret. Time	Area	Area%
1	14.485	417689	97.939
2	15.907	8789	2.061
Total		426478	100.000

N,N-diBoc-3-cyano-4-phenyl-hept-2-en-1-amine (A9)

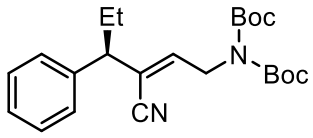

Following **General Procedure M**, diethyl-α-cyano-β-phenylvinylphosphonate (100 mg, 0.376 mmol), CuTC (1.42 mg, 7.4 mmol), Et_2Zn (1 M in hexane, 0.56 mL, 0.56 mmol), **L26** (11.58 mg, 0.0188 mmol), N,N-diBoc-glycinal (153 mg, 0.564 mmol) in dry toluene (0.2 mL).

NMR yield = 70%

ee = 94%

^{1}H NMR (400 MHz, $CDCl_3$) δ 7.26 (m, 2H), 7.21 – 7.11 (m, 3H), 6.09 (t, *J* = 6.3 Hz, 1H), 4.39 (qd, *J* = 16.4, 6.4 Hz, 2H), 3.23 (t, *J* = 7.7 Hz, 1H), 1.93 (dt, *J* = 13.5, 7.3 Hz, 1H), 1.88 – 1.75 (m, 1H), 1.39 (s, 18H), 0.84 (t, *J* = 7.3 Hz, 3H).

^{13}C NMR (101 MHz, $CDCl_3$) δ 151.71, 142.26, 140.49, 128.83, 127.61, 127.37, 120.50, 116.05, 83.23, 51.79, 46.46, 28.01, 26.14, 12.14.

HPLC (Lux Cellulose 1, Hexane:*i*-PrOH 99:1, 0.8 mL/min, 210 nm) t_R: 10.4 min (maj); 11.4 min

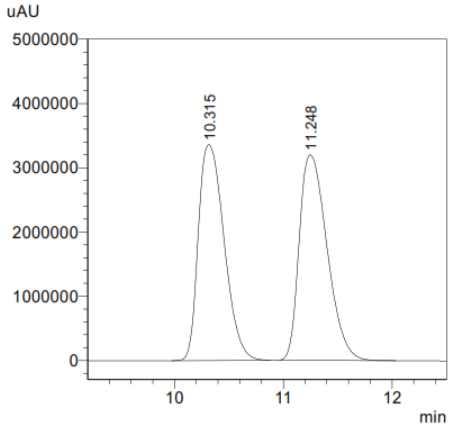

PDA Ch1 210nm

Peak#	Ret. Time	Area	Area%
1	10.315	55415765	49.343
2	11.248	56892508	50.657
Total		112308273	100.000

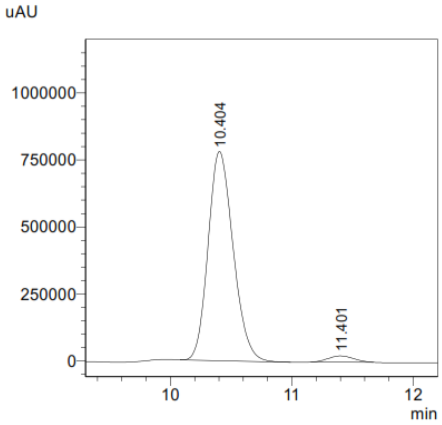

PDA Ch1 210nm

Peak#	Ret. Time	Area	Area%
1	10.404	11210268	97.030
2	11.401	343145	2.970
Total		11553413	100.000

2-methyl-4-cyano-5-phenyl-octa-2,4-dienoic ethyl ester (A10)

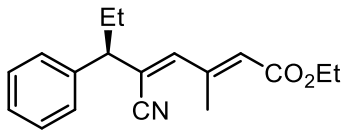

Following **General Procedure M**, diethyl-α-cyano-β-phenylvinylphosphonate (100 mg, 0.376 mmol), CuTC (1.42 mg, 7.4 mmol), Et_2Zn (1 M in hexane, 0.56 mL, 0.56 mmol), **L26** (11.58 mg, 0.0188 mmol), ethyl (*E*)-3-formyl-2-butenoate (d=1.044, 0.077 mL, 0.564 mmol) in dry toluene (0.2 mL).

NMR yield = 84%

ee = 98%

^{1}H NMR (400 MHz, $CDCl_3$) δ 7.32 – 7.24 (m, 2H), 7.22 (m, 3H), 6.49 (s, 1H), 5.92 (p, *J* = 1.2 Hz, 1H), 4.11 (q, *J* = 7.1 Hz, 2H), 3.32 (t, *J* = 7.7 Hz, 1H), 2.00 (dt, *J* = 13.7, 7.5 Hz, 1H), 1.88 (dt, *J* = 13.8, 7.3 Hz, 1H), 1.21 (t, *J* = 7.1 Hz, 3H), 0.86 (t, *J* = 7.3 Hz, 3H).

^{13}C NMR (101 MHz, $CDCl_3$) δ 165.94, 148.64, 145.45, 140.27, 128.93, 127.67, 127.57, 124.45, 119.97, 116.96, 60.32, 53.79, 26.15, 16.30, 14.22, 12.22.

HPLC (Lux Cellulose 3, Hexane:*i*-PrOH 99.5:0.5, 1.0 mL/min, 268 nm) t_R: 22.1 min; 23.2 min (maj)

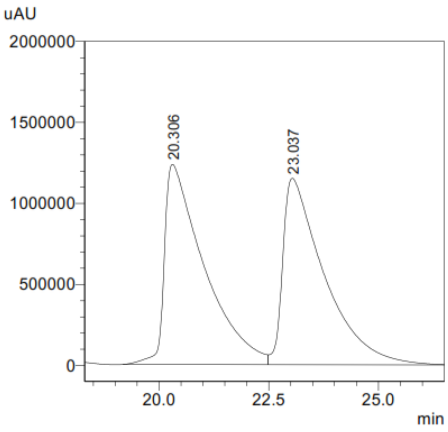

PDA Ch1 268nm

Peak#	Ret. Time	Area	Area%
1	20.306	78024104	50.688
2	23.037	75906121	49.312
Total		153930225	100.000

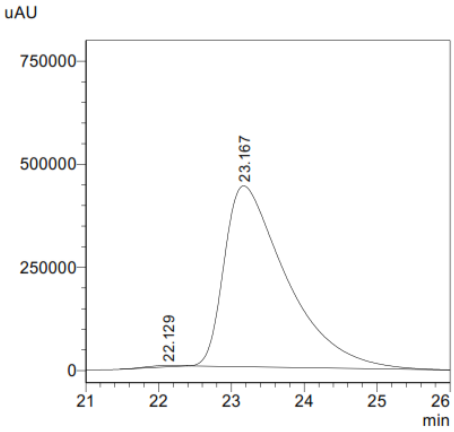

PDA Ch1 268nm

Peak#	Ret. Time	Area	Area%
1	22.129	114929	0.437
2	23.167	26156247	99.563
Total		26271175	100.000

1-phenyl-2-cyano-3-(4'-methoxyphenyl)-1-pentene (S1)

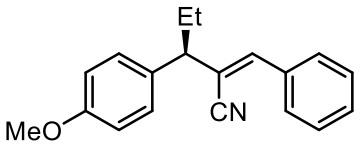

Following **General Procedure M**, diethyl-α-cyano-β-(4-methoxyphenyl)vinylphosphonate (111 mg, 0.376 mmol), CuTC (1.42 mg, 7.4 mmol), Et_2Zn (1 M in hexane, 0.56 mL, 0.56 mmol), **L26** (11.58 mg, 0.0188 mmol), benzaldehyde (d=1.044 g/mL, 0.057 mL, 0.564 mmol) in dry toluene (0.2 mL).

NMR yield = 34%

ee = 20%

^{1}H NMR (400 MHz, $CDCl_3$) δ 7.74 (dd, *J* = 7.7, 1.9 Hz, 2H), 7.44 – 7.38 (m, 3H), 7.28 (m, 2H), 7.03 (s, 1H), 6.95 – 6.90 (m, 2H), 3.83 (s, 3H), 3.47 (t, *J* = 7.8 Hz, 1H), 2.21 – 2.08 (m, 1H), 2.05 – 1.93 (m, 1H), 1.00 (t, *J* = 7.3 Hz, 3H).

^{13}C NMR (101 MHz, $CDCl_3$) δ 158.81, 142.74, 133.71, 132.99, 129.99, 128.77, 128.71, 128.36, 118.11, 116.11, 114.22, 55.29, 52.72, 26.42, 12.32.

HPLC (Lux Cellulose 3, Hexane:*i*-PrOH 99:1, 0.8 mL/min, 312 nm) t_R: 22.0 min (maj); 24.9 min

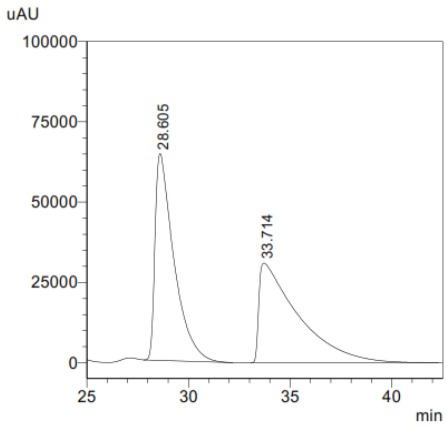

PDA Ch1 312nm

Peak#	Ret. Time	Area	Area%
1	28.605	4154430	50.012
2	33.714	4152438	49.988
Total		8306868	100.000

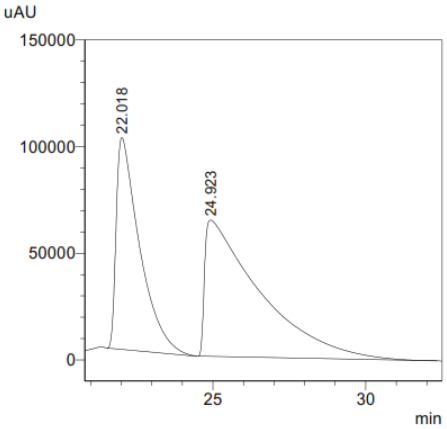

PDA Ch1 312nm

Peak#	Ret. Time	Area	Area%
1	22.018	5281925	39.727
2	24.923	8013735	60.273
Total		13295660	100.000

1-phenyl-2-cyano-3-(3'-methylphenyl)-1-pentene (S2)

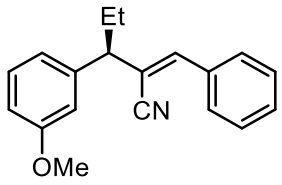

Following **General Procedure M**, diethyl-α-cyano-β-(3-methoxyphenyl)vinylphosphonate (111 mg, 0.376 mmol), CuTC (1.42 mg, 7.4 mmol), Et_2Zn (1 M in hexane, 0.56 mL, 0.56 mmol), **L26** (11.58 mg, 0.0188 mmol), benzaldehyde (d=1.044 g/mL, 0.057 mL, 0.564 mmol) in dry toluene (0.2 mL).

NMR yield = 48%

ee = 88%

^{1}H NMR (400 MHz, $CDCl_3$) δ 7.74 (dd, *J* = 7.5, 2.3 Hz, 2H), 7.41 (m, 3H), 7.30 (t, *J* = 8.0 Hz, 1H), 7.05 (s, 1H), 6.96 (d, *J* = 7.7 Hz, 1H), 6.91 (s, 1H), 6.84 (dd, *J* = 8.2, 2.6 Hz, 1H), 3.84 (s, 3H), 3.47 (t, *J* = 7.8 Hz, 1H), 2.19 – 2.08 (m, 1H), 2.02 (dp, *J* = 14.6, 7.4 Hz, 1H), 1.01 (t, *J* = 7.3 Hz, 3H).

^{13}C NMR (101 MHz, $CDCl_3$) δ 159.91, 143.29, 142.69, 133.64, 130.06, 129.83, 128.81, 128.78, 120.01, 118.06, 115.51, 113.66, 112.41, 55.24, 53.46, 26.39, 12.31.

HPLC (Lux Cellulose 3, Hexane:*i*-PrOH 94:6, 1.0 mL/min, 275 nm) t_R: 10.9 min (maj); 13.4 min

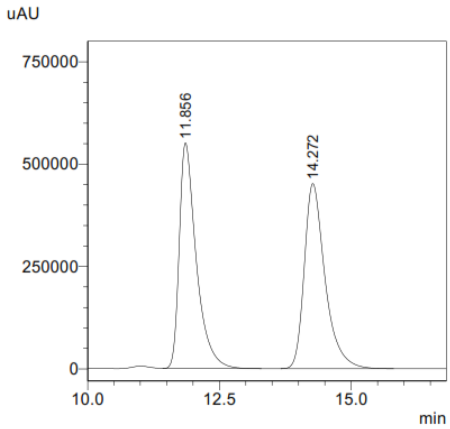

PDA Ch1 275nm

Peak#	Ret. Time	Area	Area%
1	11.856	12349840	49.892
2	14.272	12403436	50.108
Total		24753275	100.000

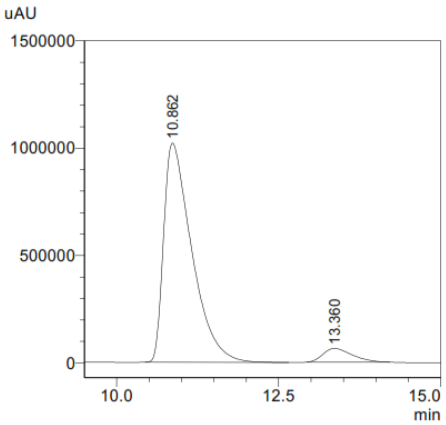

PDA Ch1 275nm

Peak#	Ret. Time	Area	Area%
1	10.862	30856187	93.904
2	13.360	2003201	6.096
Total		32859388	100.000

1-phenyl-2-cyano-3-(2'-methoxyphenyl)-1-pentene (S3)

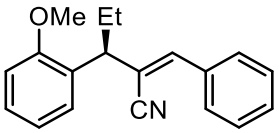

Following **General Procedure M**, diethyl-α-cyano-β-(2-methoxyphenyl)vinylphosphonate (111 mg, 0.376 mmol), CuTC (1.42 mg, 7.4 mmol), Et_2Zn (1 M in hexane, 0.56 mL, 0.56 mmol), **L26** (11.58 mg, 0.0188 mmol), benzaldehyde (d=1.044 g/mL, 0.057 mL, 0.564 mmol) in dry toluene (0.2 mL). NMR yield = 66%

ee = 54%

^{1}H NMR (300 MHz, $CDCl_3$) δ 7.80 – 7.66 (m, 2H), 7.52 – 7.31 (m, 4H), 7.27 (td, *J* = 8.1, 7.5, 1.8 Hz, 1H), 7.08 (s, 1H), 7.02 (td, *J* = 7.5, 1.2 Hz, 1H), 6.90 (dd, *J* = 8.3, 1.2 Hz, 1H), 4.02 (t, *J* = 7.8 Hz, 1H), 3.86 (s, 3H), 2.19 – 2.04 (m, 1H), 1.97 (dq, *J* = 13.9, 7.2 Hz, 1H), 1.01 (t, *J* = 7.3 Hz, 3H).

^{13}C NMR (101 MHz, $CDCl_3$) δ 156.01, 142.38, 132.97, 128.74, 128.24, 127.70, 127.67, 127.12, 126.38, 119.83, 117.18, 113.94, 109.60, 54.39, 44.04, 24.42, 11.26.

HPLC (Lux Cellulose 4, Hexane:*i*-PrOH 99:1, 1.0 mL/min, 254 nm) t_R: 8.6 min; 9.7 min (maj)

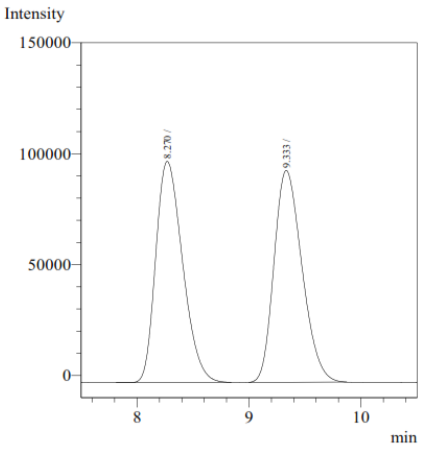

AD1

Peak#	Ret.Time	Area	Area%
1	8.270	1665845	50.068
2	9.333	1661334	49.932
Total		3327178	100.000

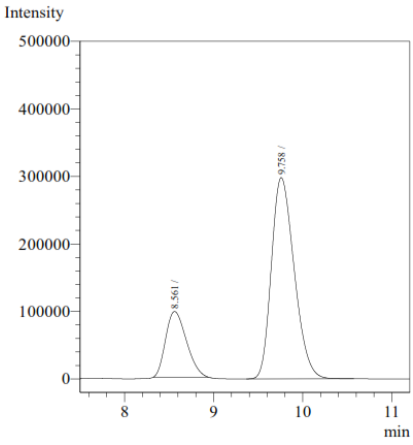

AD1

Peak#	Ret.Time	Area	Area%
1	8.561	1572108	22.823
2	9.758	5316124	77.177
Total		6888232	100.000

1-phenyl-2-cyano-3-(4'-methylphenyl)-1-pentene (S4)

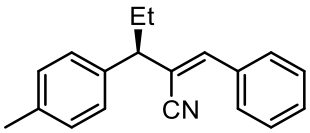

Following **General Procedure M**, diethyl-α-cyano-β-(4-methylphenyl)vinylphosphonate (106 mg, 0.376 mmol), CuTC (1.42 mg, 7.4 mmol), Et_2Zn (1 M in hexane, 0.56 mL, 0.56 mmol), **L26** (11.58 mg, 0.0188 mmol), benzaldehyde (d=1.044 g/mL, 0.057 mL, 0.564 mmol) in dry toluene (0.2 mL).

NMR yield = 91%

ee = 94%

^{1}H NMR (400 MHz, $CDCl_3$) δ 7.74 (dd, *J* = 7.7, 2.0 Hz, 2H), 7.46 – 7.35 (m, 3H), 7.30 – 7.22 (m, 2H), 7.22 – 7.15 (m, 2H), 7.04 (s, 1H), 3.47 (t, *J* = 7.7 Hz, 1H), 2.37 (s, 3H), 2.21 – 2.08 (m, 1H), 2.08 – 1.94 (m, 1H), 1.00 (t, *J* = 7.3 Hz, 3H).

^{13}C NMR (101 MHz, $CDCl_3$) δ 142.94, 137.99, 136.98, 133.71, 129.98, 129.53, 128.78, 128.76, 127.56, 118.10, 115.96, 53.14, 26.37, 21.08, 12.33.

HPLC (Lux Cellulose 3, Hexane:*i*-PrOH 90:10, 1.0 mL/min, 302 nm) t_R: 9.6 min; 11.9 min (maj)

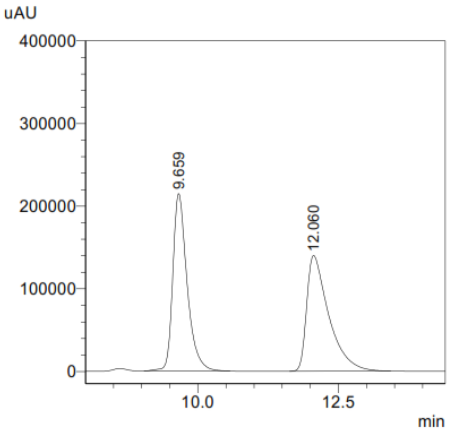

PDA Ch1 302nm

Peak#	Ret. Time	Area	Area%
1	9.659	3811575	49.971
2	12.060	3815982	50.029
Total		7627557	100.000

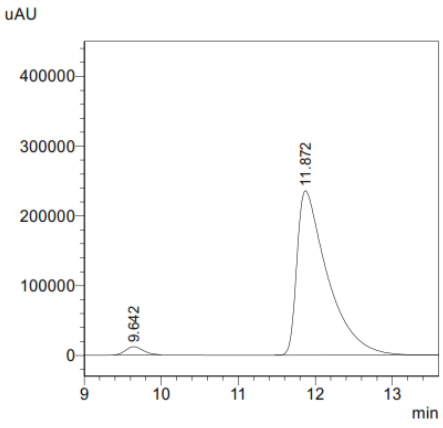

PDA Ch1 302nm

Peak#	Ret. Time	Area	Area%
1	9.642	184720	2.750
2	11.872	6532394	97.250
Total		6717114	100.000

1-phenyl-2-cyano-3-(3'-methylphenyl)-1-pentene (S5)

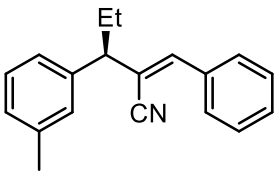

Following **General Procedure M**, diethyl-α-cyano-β-(3-methylphenyl)vinylphosphonate (106 mg, 0.376 mmol), CuTC (1.42 mg, 7.4 mmol), Et_2Zn (1 M in hexane, 0.56 mL, 0.56 mmol), **L26** (11.58 mg, 0.0188 mmol), benzaldehyde (d=1.044 g/mL, 0.057 mL, 0.564 mmol) in dry toluene (0.2 mL).

NMR yield = 74%

ee = 92%

^{1}H NMR (300 MHz, $CDCl_3$) δ 7.83 – 7.64 (m, 2H), 7.51 – 7.33 (m, 3H), 7.32 – 7.23 (m, 1H), 7.23 – 7.06 (m, 3H), 7.04 (s, 1H), 3.46 (t, *J* = 7.7 Hz, 1H), 2.39 (s, 3H), 2.19 – 2.08 (m, 1H), 2.08 – 1.94 (m, 1H), 1.00 (t, *J* = 7.3 Hz, 3H).

^{13}C NMR (101 MHz, $CDCl_3$) δ 143.12, 141.02, 138.45, 133.70, 130.01, 128.80, 128.77, 128.71, 128.44, 128.10, 124.64, 118.08, 115.78, 53.45, 26.38, 21.53, 12.35.

HPLC (Lux Cellulose 3, Hexane:*i*-PrOH 99:1, 1.0 mL/min, 299 nm) t_R: 9.0 min; 9.7 min (maj)

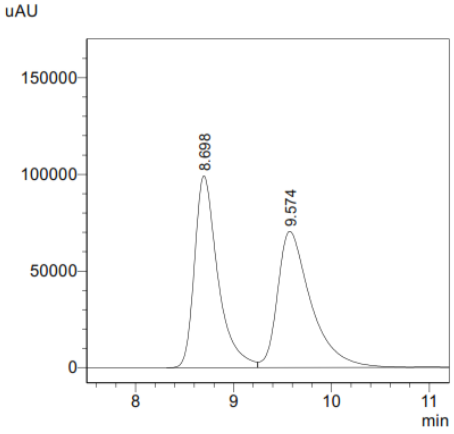

PDA Ch1 299nm

Peak#	Ret. Time	Area	Area%
1	8.698	1648234	49.625
2	9.574	1673148	50.375
Total		3321381	100.000

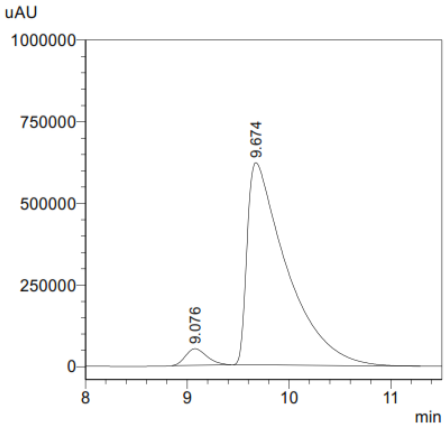

PDA Ch1 299nm

Peak#	Ret. Time	Area	Area%
1	9.076	740419	4.228
2	9.674	16772749	95.772
Total		17513168	100.000

1-phenyl-2-cyano-3-(2'-methylphenyl)-1-pentene (S6)

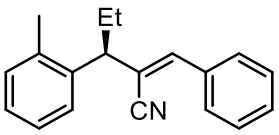

Following **General Procedure M**, diethyl-α-cyano-β-(2-methylphenyl)vinylphosphonate (106 mg, 0.376 mmol), CuTC (1.42 mg, 7.4 mmol), Et_2Zn (1 M in hexane, 0.56 mL, 0.56 mmol), **L26** (11.58 mg, 0.0188 mmol), benzaldehyde (d=1.044 g/mL, 0.057 mL, 0.564 mmol) in dry toluene (0.2 mL). NMR yield = 87%

ee = 88%

^{1}H NMR (400 MHz, $CDCl_3$) δ 7.65 – 7.59 (m, 2H), 7.34 – 7.27 (m, 4H), 7.19 (h, *J* = 4.2 Hz, 1H), 7.13 – 7.09 (m, 2H), 6.86 (s, 1H), 3.67 (d, *J* = 7.6 Hz, 1H), 2.30 (s, 3H), 2.16 – 2.02 (m, 1H), 1.97 – 1.83 (m, 1H), 0.91 (t, *J* = 7.3 Hz, 3H).

^{13}C NMR (101 MHz, $CDCl_3$) δ 143.13, 138.60, 136.31, 133.64, 130.74, 130.02, 128.78, 128.76, 127.10, 126.63, 126.61, 118.25, 115.05, 48.46, 26.62, 19.82, 12.32.

HPLC (Lux Cellulose 3, Hexane:*i*-PrOH 99:1, 1.0 mL/min, 295 nm) t_R: 9.1 min; 10.0 min (maj)

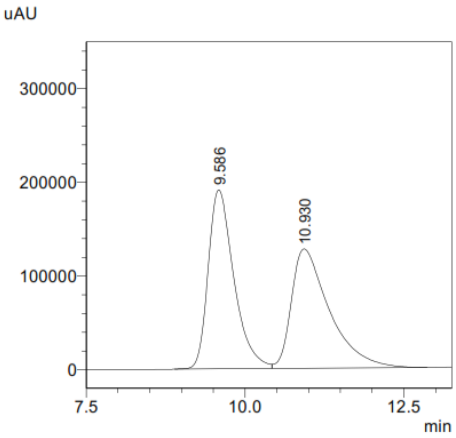

PDA Ch1 295nm

Peak#	Ret. Time	Area	Area%
1	9.586	5373586	50.317
2	10.930	5305797	49.683
Total		10679382	100.000

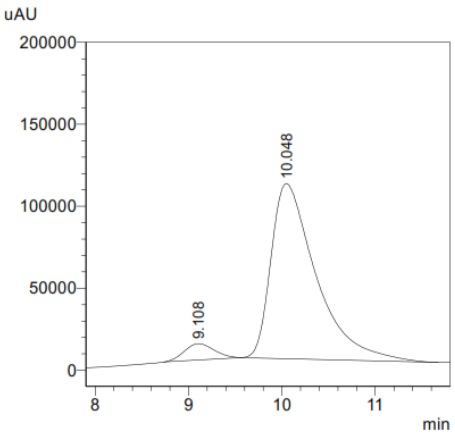

PDA Ch1 295nm

Peak#	Ret. Time	Area	Area%
1	9.108	222069	5.826
2	10.048	3589385	94.174
Total		3811454	100.000

1-phenyl-2-cyano-3-(4'-chlorophenyl)-1-pentene (S7)

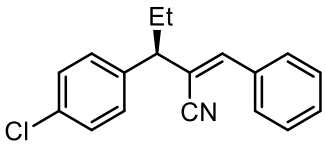

Following **General Procedure M**, diethyl-α-cyano-β-(4-chlorophenyl)vinylphosphonate (106 mg, 0.376 mmol), CuTC (1.42 mg, 7.4 mmol), Et_2Zn (1 M in hexane, 0.56 mL, 0.56 mmol), **L26** (11.58 mg, 0.0188 mmol), benzaldehyde (d=1.044 g/mL, 0.057 mL, 0.564 mmol) in dry toluene (0.2 mL).

NMR yield = 74%

ee = 82%

^{1}H NMR (300 MHz, $CDCl_3$) δ 7.83 – 7.66 (m, 2H), 7.57 – 7.15 (m, 7H), 7.05 (s, 1H), 3.49 (t, *J* = 7.7 Hz, 1H), 2.21 – 1.92 (m, 2H), 1.00 (t, *J* = 7.3 Hz, 3H).

^{13}C NMR (101 MHz, $CDCl_3$) δ 143.41, 139.50, 133.45, 133.18, 130.25, 129.04, 129.02, 128.85, 128.82, 117.83, 115.11, 52.84, 26.31, 12.22.

HPLC (Lux Cellulose 3, Hexane:*i*-PrOH 99:1, 1.0 mL/min, 275 nm) t_R: 12.9 min; 18.4 min (maj)

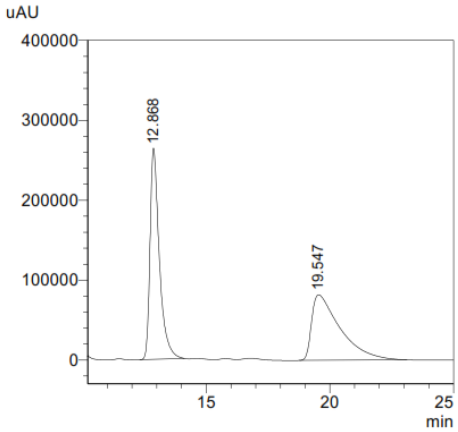

PDA Ch1 275nm

Peak#	Ret. Time	Area	Area%
1	12.868	6906292	51.328
2	19.547	6548827	48.672
Total		13455119	100.000

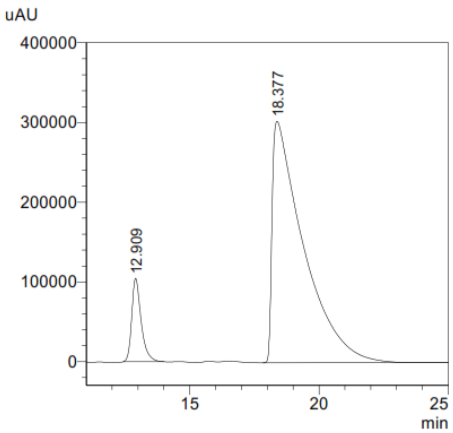

PDA Ch1 275nm

Peak#	Ret. Time	Area	Area%
1	12.909	2650768	9.416
2	18.377	25500385	90.584
Total		28151153	100.000

1-phenyl-2-cyano-3-(2'-bromophenyl)-1-pentene (S8)

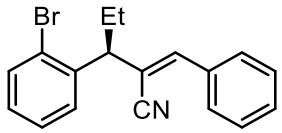

Following **General Procedure M**, diethyl-α-cyano-β-(2-bromophenyl)vinylphosphonate (130 mg, 0.376 mmol), CuTC (1.42 mg, 7.4 mmol), Et_2Zn (1 M in hexane, 0.56 mL, 0.56 mmol), **L26** (11.58 mg, 0.0188 mmol), benzaldehyde (d=1.044 g/mL, 0.057 mL, 0.564 mmol) in dry toluene (0.2 mL). NMR yield = 84%

ee = 90%

^{1}H NMR (400 MHz, $CDCl_3$) δ 7.65 (d, *J* = 8.7 Hz, 2H), 7.51 (d, *J* = 8.1 Hz, 1H), 7.43 (d, *J* = 7.8 Hz, 1H), 7.36 – 7.25 (m, 4H), 7.10 (s, 1H), 7.06 (t, *J* = 7.7 Hz, 1H), 4.00 (t, *J* = 7.7 Hz, 1H), 2.05 (dq, *J* = 15.0, 7.4 Hz, 1H), 1.91 (dp, *J* = 14.5, 7.3 Hz, 1H), 0.93 (t, *J* = 7.3 Hz, 3H).

^{13}C NMR (101 MHz, $CDCl_3$) δ 144.69, 139.72, 133.56, 133.24, 130.18, 128.87, 128.80, 128.76, 128.37, 128.06, 125.29, 117.75, 113.59, 51.10, 26.36, 12.10.

HPLC (Lux Cellulose 4, Hexane:*i*-PrOH 99:1, 1.0 mL/min, 254 nm) t_R: 10.7 min; 12.3 min (maj)

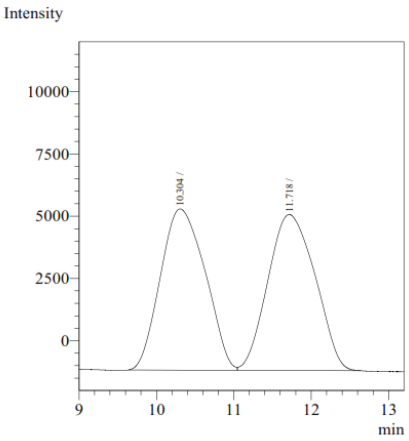

AD1

Peak#	Ret.Time	Area	Area%
1	10.304	261077	49.517
2	11.718	266174	50.483
Total		527251	100.000

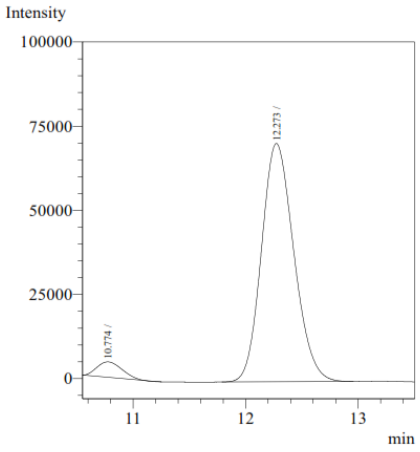

AD1

Peak#	Ret.Time	Area	Area%
1	10.774	70195	4.718
2	12.273	1417686	95.282
Total		1487881	100.000

1-phenyl-2-cyano-3-(4'-pyridyl)-1-pentene (S9)

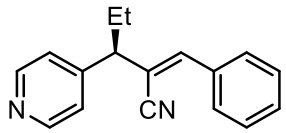

Following **General Procedure M**, diethyl-α-cyano-β-(4-pyridyl)vinylphosphonate (100 mg, 0.376 mmol), CuTC (1.42 mg, 7.4 mmol), Et_2Zn (1 M in hexane, 0.56 mL, 0.56 mmol), **L26** (11.58 mg, 0.0188 mmol), benzaldehyde (d=1.044 g/mL, 0.057 mL, 0.564 mmol) in dry toluene (0.2 mL). NMR yield = 50%

ee = 60%

^{1}H NMR (400 MHz, $CDCl_3$) δ 8.53 (s, 2H), 7.66 (dd, *J* = 6.7, 2.9 Hz, 2H), 7.34 (dd, *J* = 5.1, 2.1 Hz, 3H), 7.24 (m, 3H), 7.01 (s, 1H), 3.40 (t, *J* = 7.8 Hz, 1H), 2.04 (dq, *J* = 15.1, 7.0 Hz, 1H), 1.94 (dp, *J* = 14.4, 7.4 Hz, 1H), 0.93 (t, *J* = 7.3 Hz, 3H).

^{13}C NMR (101 MHz, $CDCl_3$) δ 150.50, 149.85, 144.56, 133.11, 130.57, 129.15, 128.92, 128.89, 117.47, 113.44, 52.82, 25.88, 12.10.

HPLC (Lux Cellulose 2, Hexane:*i*-PrOH 80:20, 1.0 mL/min, 254 nm) t_R: 12.5 min; 14.0 min (maj)

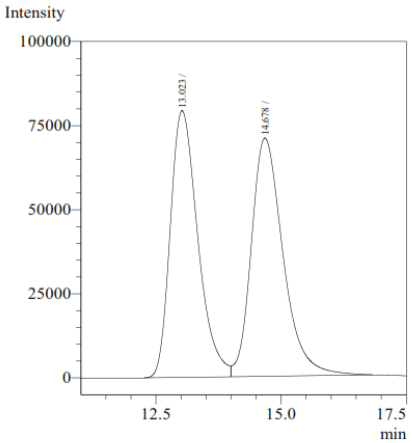

AD1

Peak#	Ret.Time	Area	Area%
1	13.023	3031786	49.193
2	14.678	3131206	50.807
Total		6162993	100.000

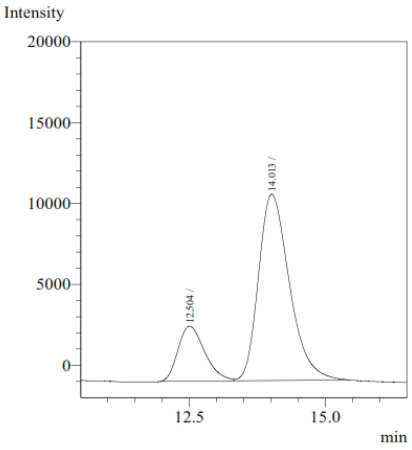

AD1

Peak#	Ret.Time	Area	Area%
1	12.504	116185	20.293
2	14.013	456351	79.707
Total		572536	100.000

1-phenyl-2-cyano-3-(2'-naphtyl)-1-pentene (S10)

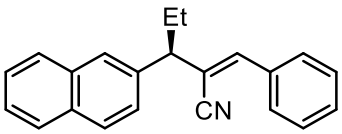

Following **General Procedure M**, diethyl-α-cyano-β-(2-naphtyl)vinylphosphonate (118 mg, 0.376 mmol), CuTC (1.42 mg, 7.4 mmol), Et_2Zn (1 M in hexane, 0.56 mL, 0.56 mmol), **L26** (11.58 mg, 0.0188 mmol), benzaldehyde (d=1.044 g/mL, 0.057 mL, 0.564 mmol) in dry toluene (0.2 mL). NMR yield = 98%

ee = 72%

^{1}H NMR (400 MHz, $CDCl_3$) δ 7.92 – 7.81 (m, 3H), 7.79 (s, 1H), 7.76 – 7.69 (m, 2H), 7.53 – 7.43 (m, 3H), 7.39 (d, *J* = 6.9 Hz, 3H), 7.08 (s, 1H), 3.66 (t, *J* = 7.7 Hz, 1H), 2.25 (dp, *J* = 14.8, 7.4 Hz, 1H), 2.13 (dp, *J* = 14.7, 7.4 Hz, 1H), 1.02 (t, *J* = 7.3 Hz, 3H).

^{13}C NMR (101 MHz, $CDCl_3$) δ 143.41, 138.39, 133.63, 133.57, 132.73, 130.10, 128.82, 128.80, 128.63, 127.93, 127.67, 126.49, 126.26, 125.94, 125.81, 118.12, 115.60, 53.48, 26.35, 12.37.

HPLC (Lux Cellulose 3, Hexane:*i*-PrOH 99:1, 1.0 mL/min, 220 nm) t_R: 25.1 min; 35.3 min (maj)

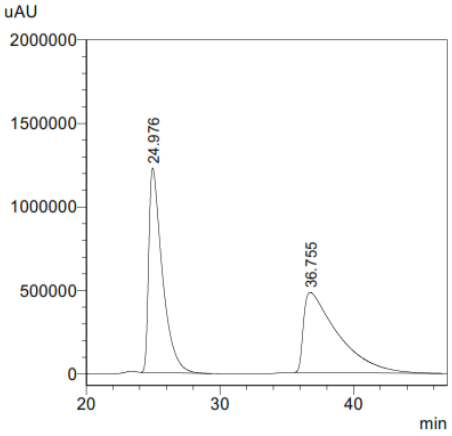

PDA Ch1 220nm

Peak#	Ret. Time	Area	Area%
1	24.976	86489629	50.242
2	36.755	85655196	49.758
Total		172144825	100.000

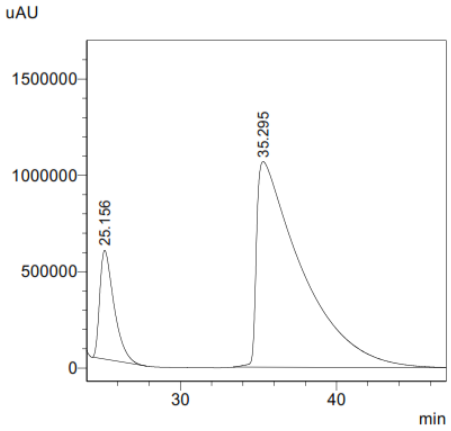

PDA Ch1 220nm

Peak#	Ret. Time	Area	Area%
1	25.156	36002399	14.357
2	35.295	214764329	85.643
Total		250766728	100.000

1-phenyl-2-cyano-3-(3'-thiophenyl)-1-pentene (S11)

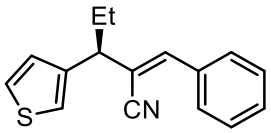

Following **General Procedure M**, diethyl-α-cyano-β-(3-thiophenyl)vinylphosphonate (102 mg, 0.376 mmol), CuTC (1.42 mg, 7.4 mmol), Et_2Zn (1 M in hexane, 0.56 mL, 0.56 mmol), **L26** (11.58 mg, 0.0188 mmol), benzaldehyde (d=1.044 g/mL, 0.057 mL, 0.564 mmol) in dry toluene (0.2 mL).

NMR yield = 76%

ee = 56%

^{1}H NMR (400 MHz, $CDCl_3$) δ 7.76 (dd, *J* = 7.4, 2.2 Hz, 2H), 7.42 (dd, *J* = 5.0, 2.9 Hz, 3H), 7.34 (dd, *J* = 5.0, 2.9 Hz, 1H), 7.21 (s, 1H), 7.09 (dd, *J* = 5.0, 1.4 Hz, 1H), 7.03 (s, 1H), 3.62 (t, *J* = 7.7 Hz, 1H), 2.07 (tp, *J* = 21.2, 7.2 Hz, 2H), 1.02 (t, *J* = 7.4 Hz, 3H).

^{13}C NMR (101 MHz, $CDCl_3$) δ 143.31, 141.79, 133.57, 130.12, 128.82, 128.79, 126.93, 126.16, 121.44, 117.89, 115.09, 49.13, 26.78, 12.25.

HPLC (Lux Cellulose 3, Hexane:*i*-PrOH 99:1, 1.0 mL/min, 275 nm) t_R: 13.9 min (maj); 16.7 min

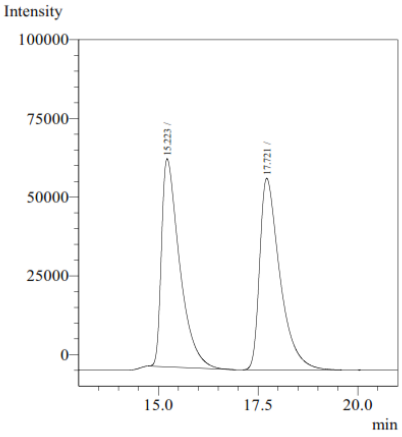

AD1

Peak#	Ret.Time	Area	Area%
1	15.223	2085760	49.269
2	17.721	2147671	50.731
Total		4233430	100.000

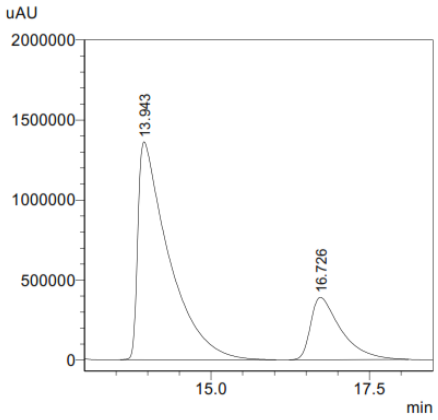

PDA Ch1 275nm

Peak#	Ret. Time	Area	Area%
1	13.943	46121501	78.095
2	16.726	12936417	21.905
Total		59057918	100.000

1-phenyl-2-cyano-3-(2'-furyl)-1-pentene (S12)

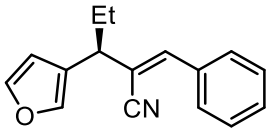

Following **General Procedure M**, diethyl-α-cyano-β-(3-furyl)vinylphosphonate (100 mg, 0.376 mmol), CuTC (1.42 mg, 7.4 mmol), Et_2Zn (1 M in hexane, 0.56 mL, 0.56 mmol), **L26** (11.58 mg, 0.0188 mmol), benzaldehyde (d=1.044 g/mL, 0.057 mL, 0.564 mmol) in dry toluene (0.2 mL).

NMR yield = 50% (*Z*/*E* = 85:15)

ee = 34%

Z-isomer:

^{1}H NMR (400 MHz, $CDCl_3$) δ 7.77 (dd, *J* = 7.5, 2.2 Hz, 2H), 7.47 – 7.37 (m, 4H), 7.04 (s, 1H), 6.38 (dd, *J* = 3.3, 1.9 Hz, 1H), 6.28 (d, *J* = 3.3 Hz, 1H), 3.61 (t, *J* = 7.7 Hz, 1H), 2.14 – 2.01 (m, 2H), 1.04 (t, *J* = 7.4 Hz, 3H).

^{13}C NMR (101 MHz, $CDCl_3$) δ 153.94, 144.22, 142.05, 133.46, 130.23, 128.87, 128.82, 117.52, 112.79, 110.45, 106.60, 47.17, 24.94, 11.94.

HPLC (Lux Cellulose 3, Hexane:*i*-PrOH 99:1, 1.0 mL/min, 273 nm) t_R: 10.3 min (maj); 13.8 min

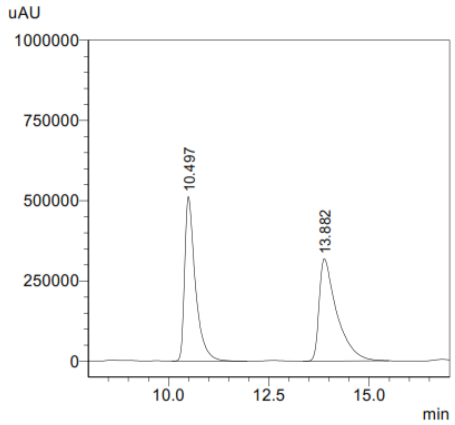

PDA Ch1 273nm

Peak#	Ret. Time	Area	Area%
1	10.497	9506727	49.343
2	13.882	9760072	50.657
Total		19266799	100.000

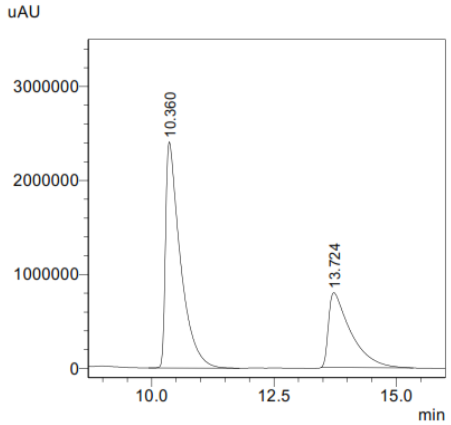

PDA Ch1 273nm

Peak#	Ret. Time	Area	Area%
1	10.360	50766806	66.840
2	13.724	25186436	33.160
Total		75953242	100.000

1,5-diphenyl-2-cyano-3-ethyl-1-pentene (S13)

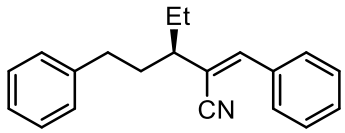

Following **General Procedure M**, diethyl-α-cyano-β-(dihydrocinnamyl)vinylphosphonate (110 mg, 0.376 mmol), CuTC (1.42 mg, 7.4 mmol), Et_2Zn (1 M in hexane, 0.56 mL, 0.56 mmol), **L26** (11.58 mg, 0.0188 mmol), benzaldehyde (d=1.044 g/mL, 0.057 mL, 0.564 mmol) in dry toluene (0.2 mL).

NMR yield = 60%

ee = 8%

^{1}H NMR (400 MHz, $CDCl_3$) δ 7.75 (d, *J* = 7.3 Hz, 2H), 7.45 – 7.28 (m, 5H), 7.19 (m, 3H), 6.88 (s, 1H), 2.86 – 2.66 (m, 1H), 2.63 – 2.42 (m, 1H), 1.99 – 1.83 (m, 2H), 1.63 (p, *J* = 7.5 Hz, 3H), 0.91 (t, *J* = 7.3 Hz, 3H).

^{13}C NMR (75 MHz, $CDCl_3$) δ 144.23, 141.47, 133.69, 129.98, 128.83, 128.70, 128.45, 128.43, 125.98, 117.38, 114.98, 48.05, 35.12, 33.45, 26.98, 11.82.

HPLC (Lux Cellulose 3, Hexane:*i*-PrOH 90:10, 1.0 mL/min, 242 nm) t_R: 6.3 min (maj); 7.1 min

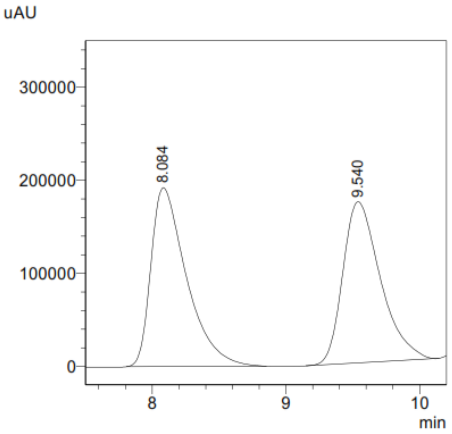

PDA Ch1 242nm

Peak#	Ret. Time	Area	Area%
1	8.084	3557245	51.220
2	9.540	3387803	48.780
Total		6945047	100.000

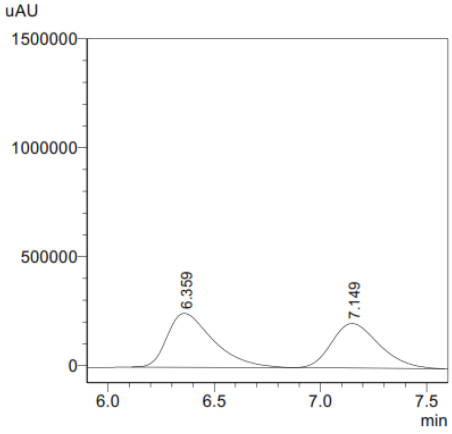

PDA Ch1 242nm

Peak#	Ret. Time	Area	Area%
1	6.359	3702936	53.829
2	7.149	3176129	46.171
Total		6879065	100.000

1,5-diphenyl-3-ethyl-4-cyano-penta-1,4-diene (S14)

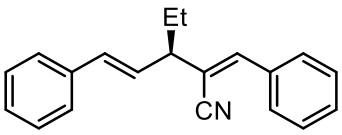

Following **General Procedure M**, diethyl-α-cyano-β-cinnamylvinylphosphonate (110 mg, 0.376 mmol), CuTC (1.42 mg, 7.4 mmol), Et_2Zn (1 M in hexane, 0.56 mL, 0.56 mmol), **L26** (11.58 mg, 0.0188 mmol), benzaldehyde (d=1.044 g/mL, 0.057 mL, 0.564 mmol) in dry toluene (0.2 mL).

NMR yield = 16%

ee = 16%

^{1}H NMR (400 MHz, $CDCl_3$) δ 7.79 – 7.70 (m, 2H), 7.43 – 7.36 (m, 5H), 7.32 (t, *J* = 7.6 Hz, 3H), 7.01 (s, 1H), 6.53 (d, *J* = 15.9 Hz, 1H), 6.23 (dd, *J* = 15.8, 8.1 Hz, 1H), 3.08 (q, *J* = 7.7 Hz, 1H), 1.89 (dq, *J* = 14.6, 7.3 Hz, 1H), 1.79 (dq, *J* = 14.0, 7.2 Hz, 1H), 1.01 (t, *J* = 7.4 Hz, 3H).

^{13}C NMR (101 MHz, $CDCl_3$) δ 143.20, 136.80, 133.69, 131.97, 130.07, 129.35, 128.82, 128.76, 128.65, 128.61, 127.69, 126.41, 114.56, 51.23, 26.76, 11.84.

HPLC (Lux Cellulose 1, Hexane:*i*-PrOH 99:1, 1.0 mL/min, 268 nm) t_R: 22.3 min (maj); 30.2 min

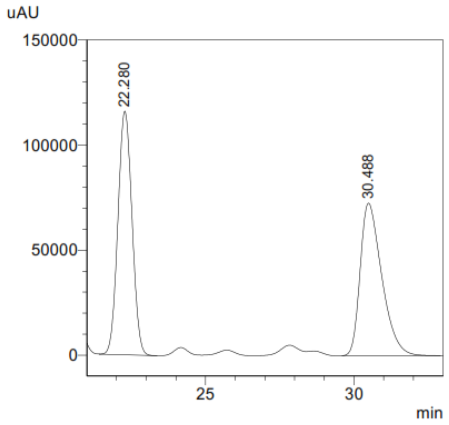

PDA Ch1 268nm

Peak#	Ret. Time	Area	Area%
1	22.280	3826736	51.042
2	30.488	3670544	48.958
Total		7497280	100.000

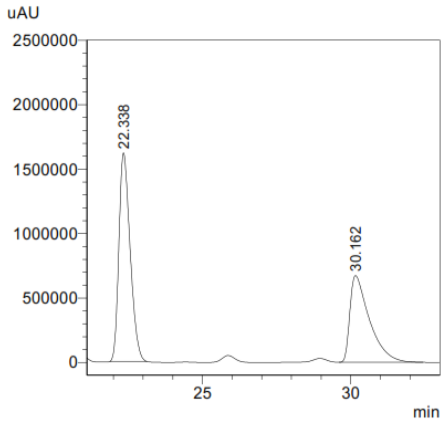

PDA Ch1 268nm

Peak#	Ret. Time	Area	Area%
1	22.338	42582474	57.995
2	30.162	30841298	42.005
Total		73423771	100.000

1,5-diphenyl-2-methyl-3-ethyl-4-cyano-penta-1,4-diene (S15)

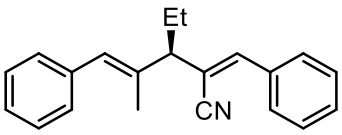

Following **General Procedure M**, diethyl-α-cyano-β-(1-methyl-cinnamyl)vinylphosphonate (110 mg, 0.376 mmol), CuTC (1.42 mg, 7.4 mmol), Et_2Zn (1 M in hexane, 0.56 mL, 0.56 mmol), **L26** (11.58 mg, 0.0188 mmol), benzaldehyde (d=1.044 g/mL, 0.057 mL, 0.564 mmol) in dry toluene (0.2 mL).

NMR yield = 99%

ee = 14%

^{1}H NMR (300 MHz, $CDCl_3$) δ 7.70 (dd, *J* = 7.7, 2.0 Hz, 2H), 7.50 – 7.03 (m, 8H), 6.96 (s, 1H), 6.46 (s, 1H), 2.90 (t, *J* = 7.6 Hz, 1H), 1.90 – 1.81 (m, 2H), 1.79 (d, *J* = 1.4 Hz, 3H), 0.95 (t, *J* = 7.3 Hz, 3H).

^{13}C NMR (101 MHz, $CDCl_3$) δ 143.72, 137.72, 137.01, 133.74, 130.06, 129.05, 128.82, 128.12, 128.04, 127.90, 126.50, 118.11, 114.32, 56.39, 23.97, 15.72, 12.15.

HPLC (Lux Cellulose 1, Hexane:*i*-PrOH 99:1, 1.0 mL/min, 254 nm) t_R: 18.0 min (maj); 18.7 min

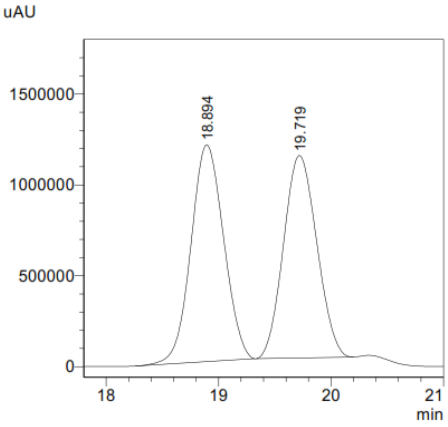

PDA Ch1 254nm

Peak#	Ret. Time	Area	Area%
1	18.894	24167477	51.278
2	19.719	22963134	48.722
Total		47130610	100.000

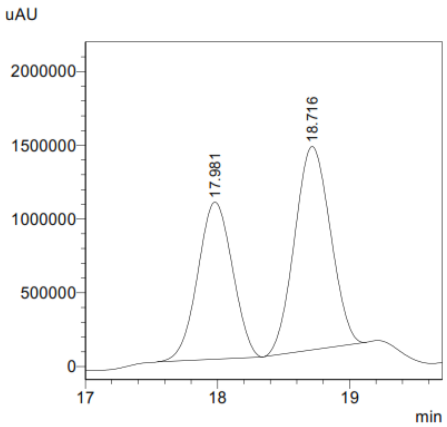

PDA Ch1 254nm

Peak#	Ret. Time	Area	Area%
1	17.981	19508966	42.874
2	18.716	25993585	57.126
Total		45502551	100.000

1,5-diphenyl-3-ethyl-4-cyano-pent-4-en-1-yne (S16)

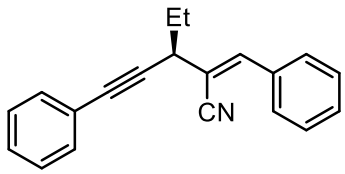

Following **General Procedure M**, diethyl-α-cyano-β-(3-phenylpropargyl)vinylphosphonate (108 mg, 0.376 mmol), CuTC (1.42 mg, 7.4 mmol), Et_2Zn (1 M in hexane, 0.56 mL, 0.56 mmol), **L26** (11.58 mg, 0.0188 mmol), benzaldehyde (d=1.044 g/mL, 0.057 mL, 0.564 mmol) in dry toluene (0.2 mL).

NMR yield = 11%

ee = 8%

^{1}H NMR (400 MHz, $CDCl_3$) δ 7.70 (m, 2H), 7.41 (m, 2H), 7.35 (m, 2H), 7.29 – 7.25 (m, 4H), 7.18 (s, 1H), 3.51 (t, J=7.3 Hz, 1H), 1.94 (dq, *J* = 13.4, 7.3, Hz, 1H), 1.85 (dq, *J* = 14.0, 7.4 Hz, 1H), 1.06 (t, *J* = 7.4 Hz, 3H).

^{13}C NMR (101 MHz, $CDCl_3$) δ 144.04, 133.35, 131.75, 130.30, 128.92, 128.86, 128.38, 128.35, 122.86, 117.85, 111.78, 86.96, 86.52, 39.95, 27.94, 11.25.

HPLC (Lux Cellulose 3, Hexane:*i*-PrOH 99:1, 1.0 mL/min, 201 nm) t_R: 12.7 min (maj); 14.5 min

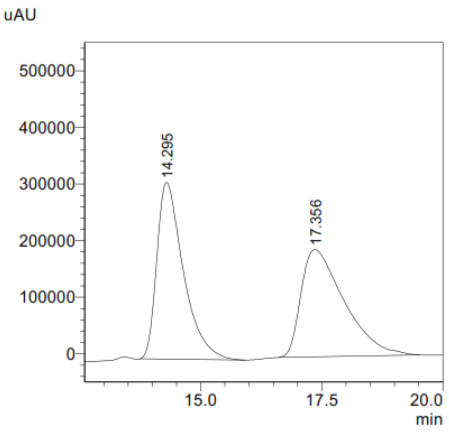

PDA Ch1 201nm

Peak#	Ret. Time	Area	Area%
1	14.295	11914734	50.440
2	17.356	11706653	49.560
Total		23621386	100.000

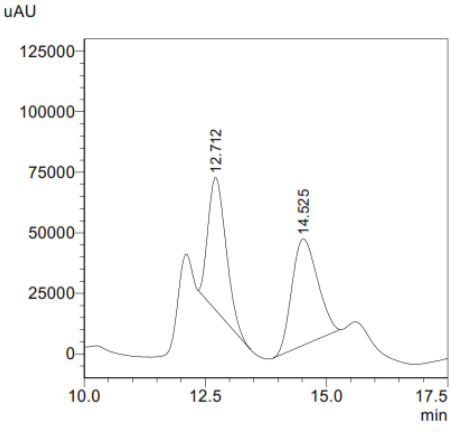

PDA Ch1 201nm

Peak#	Ret. Time	Area	Area%
1	12.712	1407614	46.447
2	14.525	1622945	53.553
Total		3030559	100.000

Methyl 2-(1-phenyl-propyl)-cinnamate (S17)

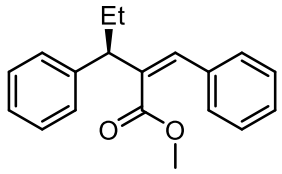

Following **General Procedure M**, diethyl-α-methoxycarbonyl-β-phenylvinylphosphonate (112 mg, 0.376 mmol), CuTC (1.42 mg, 7.4 mmol), Et_2Zn (1 M in hexane, 0.56 mL, 0.56 mmol), **L26** (11.58 mg, 0.0188 mmol), benzaldehyde (d=1.044 g/mL, 0.057 mL, 0.564 mmol) in dry toluene (0.2 mL).

NMR yield = 10%

ee = 90%

^{1}H NMR (400 MHz, $CDCl_3$) δ 7.35 – 7.19 (m, 10H), 6.62 (s, 1H), 3.66 (t, J = 8.5 Hz, 1H), 3.49 (s, 3H), 2.05 (dp, *J* = 14.0, 7.2 Hz, 1H), 1.90 (dq, *J* = 14.5, 7.3 Hz, 1H), 0.93 (t, *J* = 7.3 Hz, 3H).

^{13}C NMR (101 MHz, $CDCl_3$) δ 170.43, 141.60, 138.33, 136.22, 131.53, 128.42, 128.30, 128.21, 127.98, 127.73, 126.68, 51.83, 51.54, 26.64, 12.46.

HPLC (Lux Cellulose 1, Hexane:*i*-PrOH 99:1, 1.0 mL/min, 254 nm) t_R: 6.4 min; 7.0 min (maj)

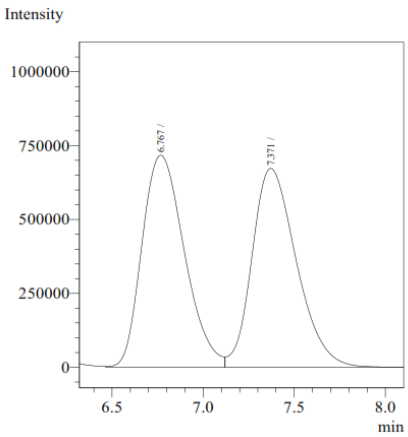

AD1

Peak#	Ret.Time	Area	Area%
1	6.767	11644386	50.471
2	7.371	11427167	49.529
Total		23071554	100.000

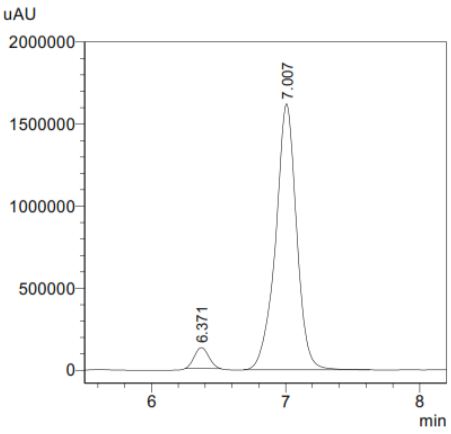

PDA Ch1 254nm

Peak#	Ret. Time	Area	Area%
1	6.371	954817	5.131
2	7.007	17655272	94.869
Total		18610089	100.000

1,3-diphenyl-2-cyano-1-butene (Z1)

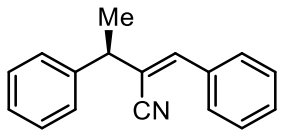

Following **General Procedure M**, diethyl-α-cyano-β-phenylvinylphosphonate (100 mg, 0.376mmol), CuTC (1.42 mg, 7.4 mmol), Me_2Zn (1 M in heptane, 0.56 mL, 0.56 mmol), **L26** (11.58 mg, 0.0188 mmol), benzaldehyde (d=1.044 g/mL, 0.057 mL, 0.564 mmol) in dry toluene (0.2 mL).

NMR yield = 51%

ee = 96%

^{1}H NMR (400 MHz, $CDCl_3$) δ 7.76 (dd, *J* = 7.7, 2.0 Hz, 2H), 7.46 – 7.28 (m, 8H), 7.03 (s, 1H), 3.87 (q, *J* = 7.1 Hz, 1H), 1.69 (d, *J* = 7.1 Hz, 3H).

^{13}C NMR (101 MHz, $CDCl_3$) δ 142.40, 141.92, 133.63, 130.08, 128.87, 128.81, 128.80, 127.41, 127.37, 118.15, 116.77, 45.29, 19.61.

HPLC (Lux Cellulose 3, Hexane:*i*-PrOH 60:40, 1.0 mL/min, 275 nm) t_R: 7.3 min; 8.4 min (maj)

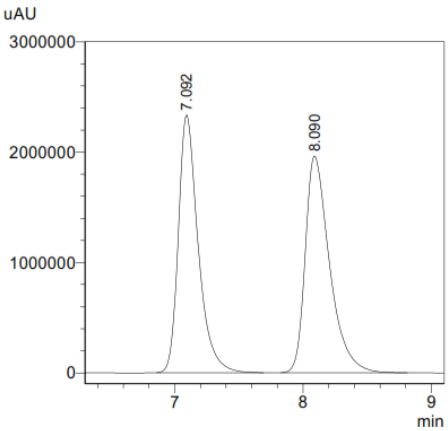

PDA Ch1 275nm

Peak#	Ret. Time	Area	Area%
1	7.092	25045109	49.173
2	8.090	25887827	50.827
Total		50932936	100.000

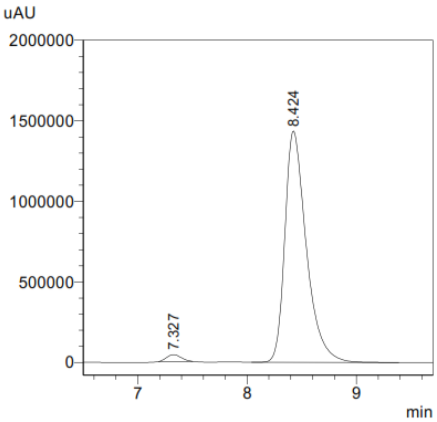

PDA Ch1 275nm

Peak#	Ret. Time	Area	Area%
1	7.327	389194	1.949
2	8.424	19575398	98.051
Total		19964592	100.000

1,3-diphenyl-2-cyano-1-heptene (Z2)

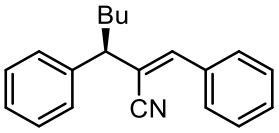

Following **General Procedure M**, diethyl-α-cyano-β-phenylvinylphosphonate (100 mg, 0.376mmol), CuTC (1.42 mg, 7.4 mmol), Bu_2Zn (1 M in hexane, 0.56 mL, 0.56 mmol), **L26** (11.58 mg, 0.0188 mmol), benzaldehyde (d=1.044 g/mL, 0.057 mL, 0.564 mmol) in dry toluene (0.2 mL).

NMR yield = 75%

ee = 70%

^{1}H NMR (400 MHz, $CDCl_3$) δ 7.83 – 7.69 (m, 2H), 7.45 – 7.35 (m, 7H), 7.31 (m, 1H), 7.05 (s, 1H), 3.60 (t, *J* = 7.8 Hz, 1H), 2.22 – 2.08 (m, 1H), 2.01 (dqt, *J* = 13.5, 8.4, 6.2 Hz, 1H), 1.46 – 1.27 (m, 4H), 0.94 (t, *J* = 7.0 Hz, 3H).

^{13}C NMR (101 MHz, $CDCl_3$) δ 143.00, 141.26, 133.67, 130.05, 128.86, 128.80, 128.79, 127.66, 127.33, 118.09, 115.92, 51.71, 33.00, 29.82, 22.52, 13.98.

HPLC (Lux Cellulose 3, Hexane:*i*-PrOH 99.5:0.5, 1.0 mL/min, 254 nm) t_R: 19.5 min; 20.9 min (maj)

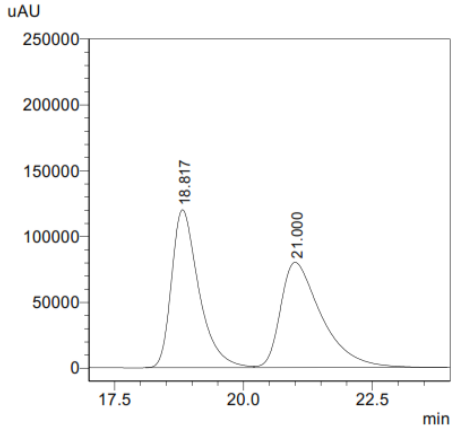

PDA Ch1 254nm

Peak#	Ret. Time	Area	Area%
1	18.817	4429697	49.989
2	21.000	4431678	50.011
Total		8861375	100.000

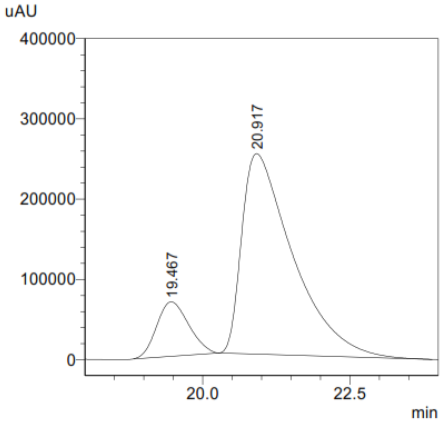

PDA Ch1 254nm

Peak#	Ret. Time	Area	Area%
1	19.467	2569764	14.564
2	20.917	15075081	85.436
Total		17644844	100.000

1-pyridyl-2-cyano-3-phenyl-1-butene (Z3)

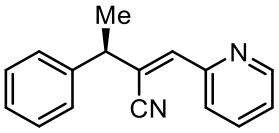

Following **General Procedure M**, diethyl-α-cyano-β-phenylvinylphosphonate (100 mg, 0.376mmol), CuTC (1.42 mg, 7.4 mmol), Me_2Zn (1 M in heptane, 0.56 mL, 0.56 mmol), **L26** (11.58 mg, 0.0188 mmol), 2-pyridynecarboxyaldehyde (d=1.126 g/mL, 0.054 mL, 0.564 mmol) in dry toluene (0.2 mL).

NMR yield = 64%

ee = 96%

^{1}H NMR (300 MHz, $CDCl_3$) δ 8.66 (s, 1H), 7.66 (t, *J* = 7.6 Hz, 1H), 7.45 – 7.31 (m, 2H), 7.31 – 7.03 (m, 4H), 6.98 (s, 1H), 5.63 (q, *J* = 7.1 Hz, 1H), 1.54 (d, *J* = 7.1 Hz, 3H).

^{13}C NMR (101 MHz, $CDCl_3$) δ 153.41, 149.69, 142.45, 140.03, 136.67, 128.60, 127.34, 127.00, 125.06, 123.73, 119.09, 36.23, 18.86.

HPLC (Lux Cellulose 3, Hexane:*i*-PrOH 90:10, 1.0 mL/min, 248 nm) t_R: 13.2 min (maj); 20.4 min

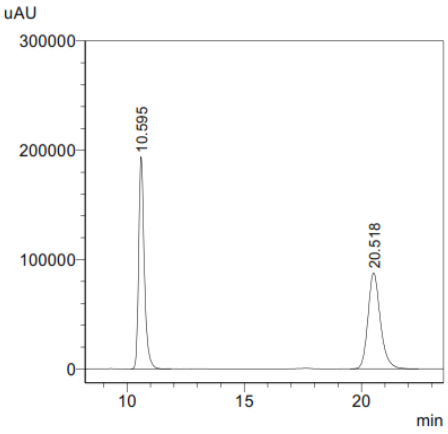

PDA Ch1 248nm

Peak#	Ret. Time	Area	Area%
1	10.595	3217937	49.972
2	20.518	3221543	50.028
Total		6439480	100.000

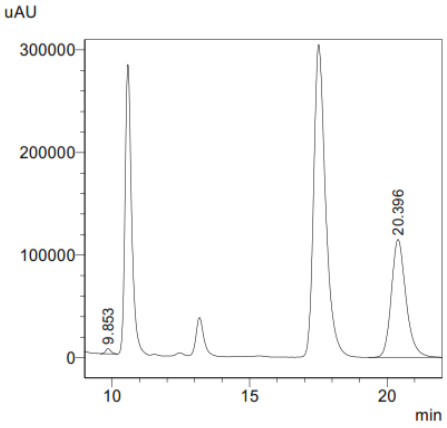

PDA Ch1 248nm

Peak#	Ret. Time	Area	Area%
1	9.853	65413	1.519
2	20.396	4240770	98.481
Total		4306183	100.000

2,5-diphenyl-3-cyano-3-exene (Z4)

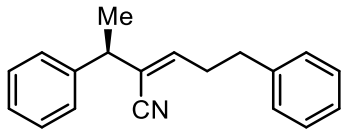

Following **General Procedure M**, diethyl-α-cyano-β-phenylvinylphosphonate (100 mg, 0.376mmol), CuTC (1.42 mg, 7.4 mmol), Me_2Zn (1 M in heptane, 0.56 mL, 0.56 mmol), **L26** (11.58 mg, 0.0188 mmol), dihydrocinnamic aldheyde (d=1.015 g/mL, 0.075 mL, 0.564 mmol) in dry toluene (0.2 mL).

NMR yield = 90%

ee = 92%

^{1}H NMR (400 MHz, $CDCl_3$) δ 7.37 – 7.23 (m, 6H), 7.19 (d, *J* = 7.8 Hz, 4H), 6.19 (t, *J* = 7.2 Hz, 1H), 3.62 (q, *J* = 7.2 Hz, 1H), 2.83 – 2.69 (m, 4H), 1.50 (d, *J* = 7.1 Hz, 3H).

^{13}C NMR (101 MHz, $CDCl_3$) δ 145.36, 141.96, 140.13, 128.74, 128.55, 128.51, 127.26, 127.15, 126.33, 120.95, 116.90, 43.56, 34.76, 32.92, 19.63.

HPLC (Lux Cellulose 3, Hexane:*i*-PrOH 99:1, 1.0 mL/min, 203 nm) t_R: 32.5 min; 49.3 min (maj)

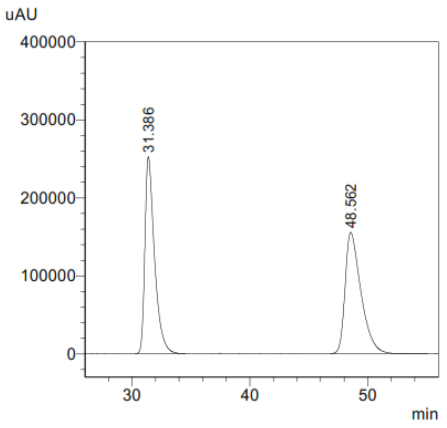

PDA Ch1 203nm

Peak#	Ret. Time	Area	Area%
1	31.386	14327742	49.742
2	48.562	14476584	50.258
Total		28804326	100.000

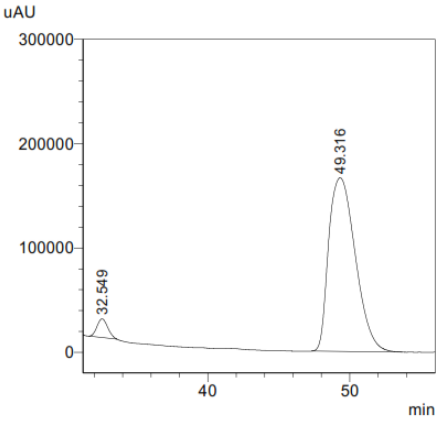

PDA Ch1 203nm

Peak#	Ret. Time	Area	Area%
1	32.549	945242	4.162
2	49.316	21763302	95.838
Total		22708543	100.000

1-phenyl-2-cyano-3-(3'-methoxyphenyl)-1-butene (Z5)

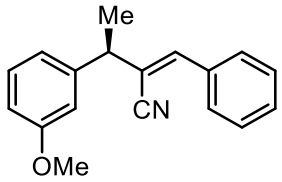

Following **General Procedure M**, diethyl-α-cyano-β-(3-methoxyphenyl)vinylphosphonate (111 mg, 0.376 mmol), CuTC (1.42 mg, 7.4 mmol), Me_2Zn (1 M in heptane, 0.56 mL, 0.56 mmol), **L26** (11.58 mg, 0.0188 mmol), benzaldehyde (d=1.044 g/mL, 0.057 mL, 0.564 mmol) in dry toluene (0.2 mL).

NMR yield = 50%

ee = 94%

^{1}H NMR (400 MHz, $CDCl_3$) δ 7.64 (dd, *J* = 7.7, 2.0 Hz, 2H), 7.39 – 7.27 (m, 3H), 7.23 – 7.18 (m, 1H), 6.91 (s, 1H), 6.85 (d, *J* = 7.7 Hz, 1H), 6.80 (t, *J* = 2.1 Hz, 1H), 6.75 (ddd, *J* = 8.2, 2.6, 1.0 Hz, 1H), 3.74 (s, 3H), 3.73 (q, J = 7.1 Hz, 1H)1.56 (d, *J* = 7.1 Hz, 3H).

^{13}C NMR (101 MHz, $CDCl_3$) δ 159.92, 143.54, 142.47, 133.60, 130.06, 129.84, 128.79, 119.73, 118.13, 116.57, 113.46, 112.37, 55.25, 45.24, 19.58.

HPLC (Lux Cellulose 3, Hexane:*i*-PrOH 94:6, 1.0 mL/min, 274 nm) t_R: 13.7 min (maj); 17.1 min

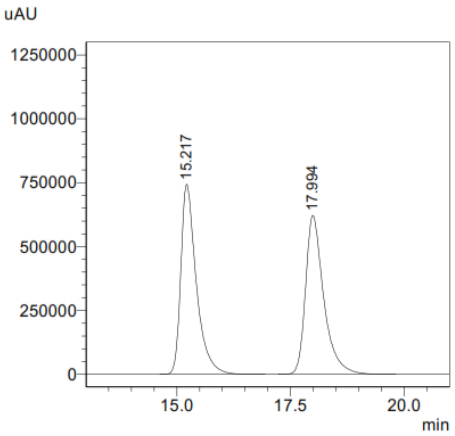

PDA Ch1 274nm

Peak#	Ret. Time	Area	Area%
1	15.217	17585571	50.398
2	17.994	17308089	49.602
Total		34893660	100.000

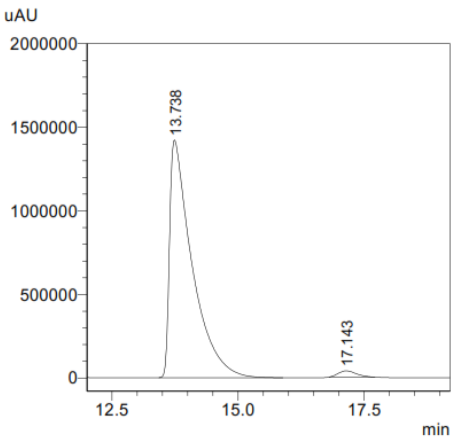

PDA Ch1 274nm

Peak#	Ret. Time	Area	Area%
1	13.738	44107729	97.923
2	17.143	935692	2.077
Total		45043422	100.000

1-phenyl-2-cyano-3-(2'-bromophenyl)-1-butene (Z6)

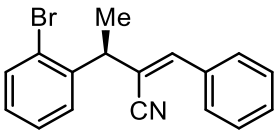

Following **General Procedure M**, diethyl-α-cyano-β-(2-bromophenyl)vinylphosphonate (130 mg, 0.376 mmol), CuTC (1.42 mg, 7.4 mmol), Me_2Zn (1 M in heptane, 0.56 mL, 0.56 mmol), **L26** (11.58 mg, 0.0188 mmol), benzaldehyde (d=1.044 g/mL, 0.057 mL, 0.564 mmol) in dry toluene (0.2 mL).

NMR yield = 80%

ee = 82%

^{1}H NMR (400 MHz, $CDCl_3$) δ 7.75 (dd, *J* = 7.4, 2.3 Hz, 2H), 7.63 (dd, *J* = 8.0, 1.4 Hz, 1H), 7.50 (dd, *J* = 7.9, 1.7 Hz, 1H), 7.45 – 7.37 (m, 4H), 7.18 (td, *J* = 7.7, 1.7 Hz, 1H), 7.11 (s, 1H), 4.38 (q, *J* = 7.1 Hz, 1H), 1.66 (d, *J* = 7.1 Hz, 3H).

^{13}C NMR (101 MHz, $CDCl_3$) δ 143.58, 140.70, 133.56, 133.30, 130.18, 128.90, 128.83, 128.82, 128.28, 128.08, 124.82, 117.97, 114.89, 43.73, 19.38.

HPLC (Lux Cellulose 3, Hexane:*i*-PrOH 99.5:0.5 1.0 mL/min, 199 nm) t_R: 9.6 min; 10.1 min (maj)

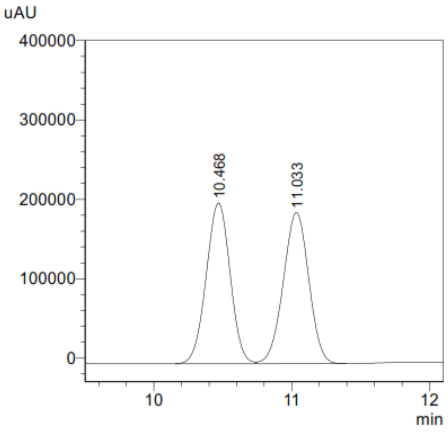

PDA Ch1 199nm

Peak#	Ret. Time	Area	Area%
1	10.468	2448084	49.940
2	11.033	2453966	50.060
Total		4902050	100.000

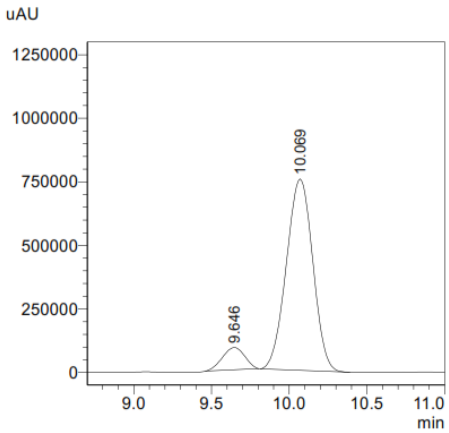

PDA Ch1 199nm

Peak#	Ret. Time	Area	Area%
1	9.646	876491	8.957
2	10.069	8909415	91.043
Total		9785906	100.000

7. NMR Spectra

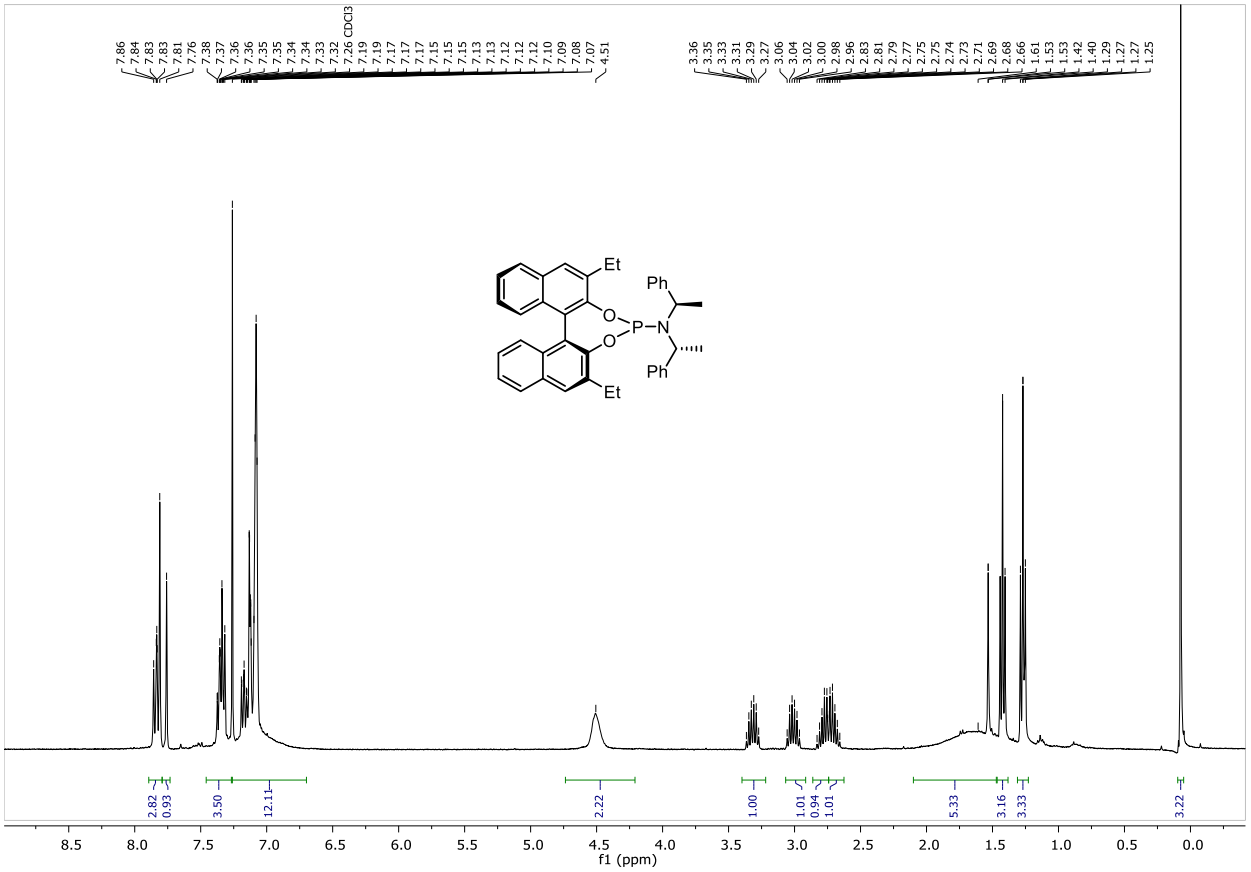

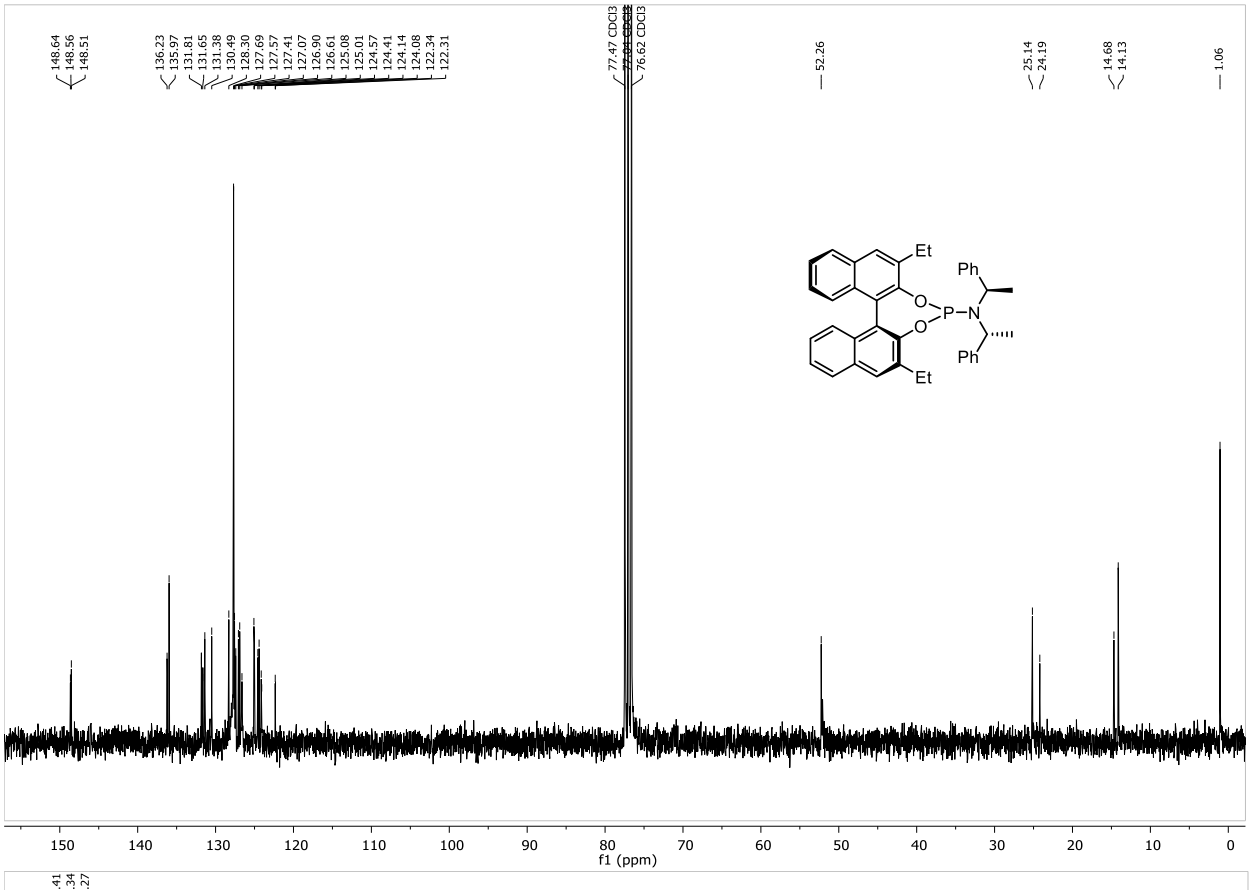
148.64
148.56
148.51
136.23
135.97
131.81
131.65
131.38
130.49
128.30
127.69
127.57
127.41
127.07
126.90
126.61
125.08
125.01
124.57
124.41
124.14
124.08
122.34
122.31
77.47 CDCl3
77.04 CDCl3
76.62 CDCl3
52.26
25.14
24.19
14.68
14.13
1.06
Et
Ph
O
P
N
O
Ph
Et
150
140
130
120
110
100
90
80
70
60
50
40
30
20
10
0
f1 (ppm)

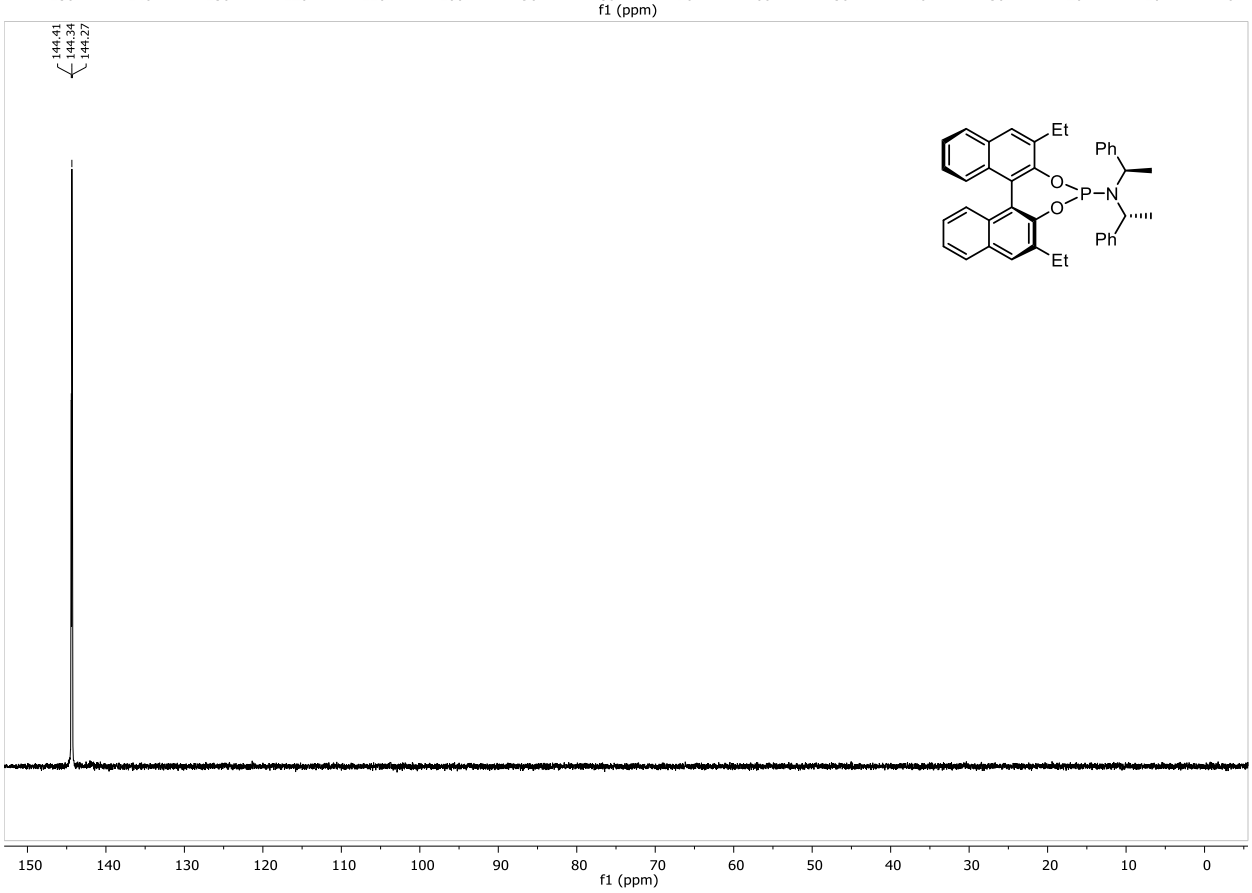
144.41
144.34
144.27
Et
Ph
O
P
N
O
Ph
Et
150
140
130
120
110
100
90
80
70
60
50
40
30
20
10
0
f1 (ppm)

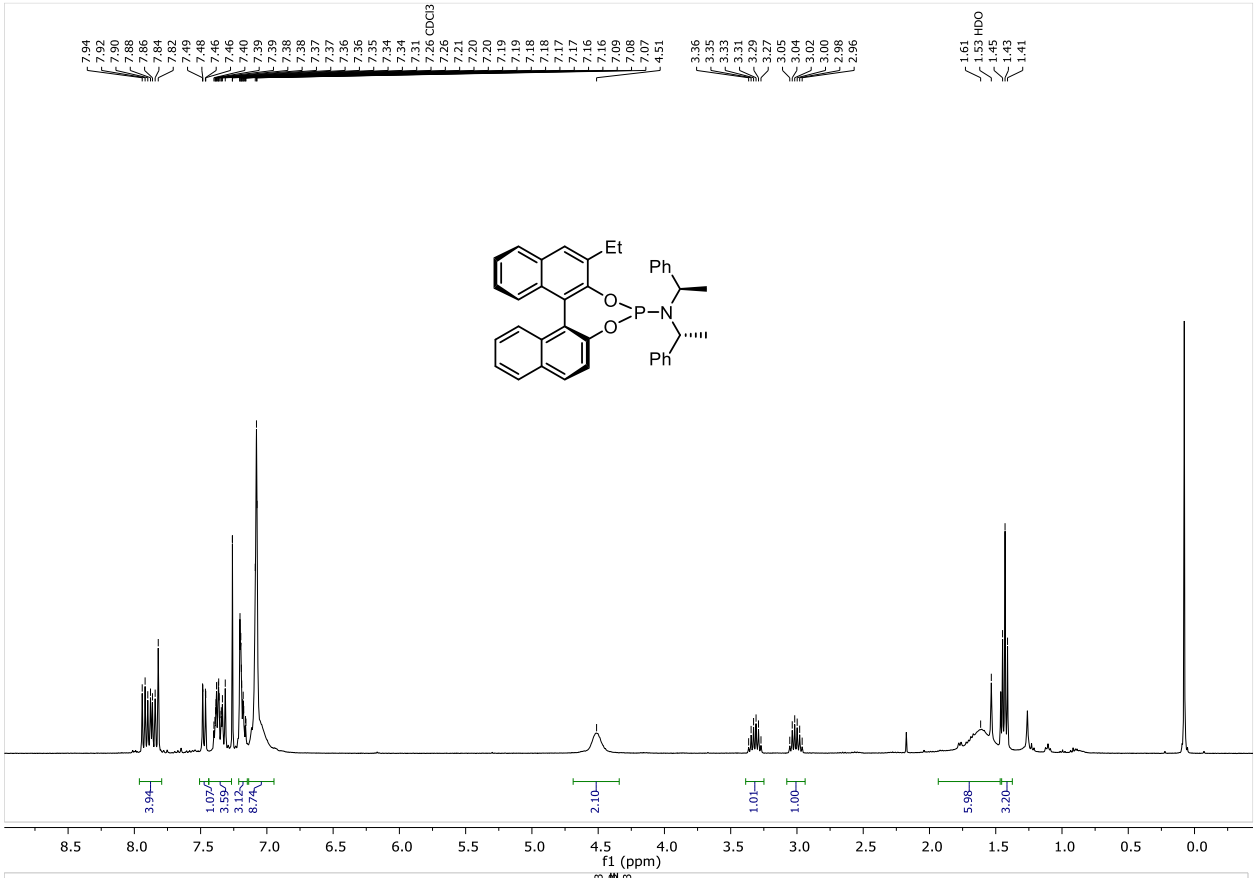
7.94 7.92 7.90 7.88 7.86 7.84 7.82 7.49 7.48 7.46 7.46 7.40 7.39 7.39 7.38 7.38 7.37 7.37 7.36 7.36 7.35 7.34 7.34 7.31 7.26 CDCl3 7.26 7.21 7.20 7.20 7.19 7.19 7.18 7.18 7.17 7.17 7.16 7.16 7.09 7.08 7.07 4.51
3.36 3.35 3.33 3.31 3.29 3.27 3.05 3.04 3.02 3.00 2.98 2.96
1.61 1.53 HDO 1.45 1.43 1.41
Et
Ph
O
P
N
O
Ph
3.94 1.02 3.59 3.12 8.74 2.10 1.01 1.00 5.98 3.20
8.5 8.0 7.5 7.0 6.5 6.0 5.5 5.0 4.5 4.0 3.5 3.0 2.5 2.0 1.5 1.0 0.5 0.0
f1 (ppm)

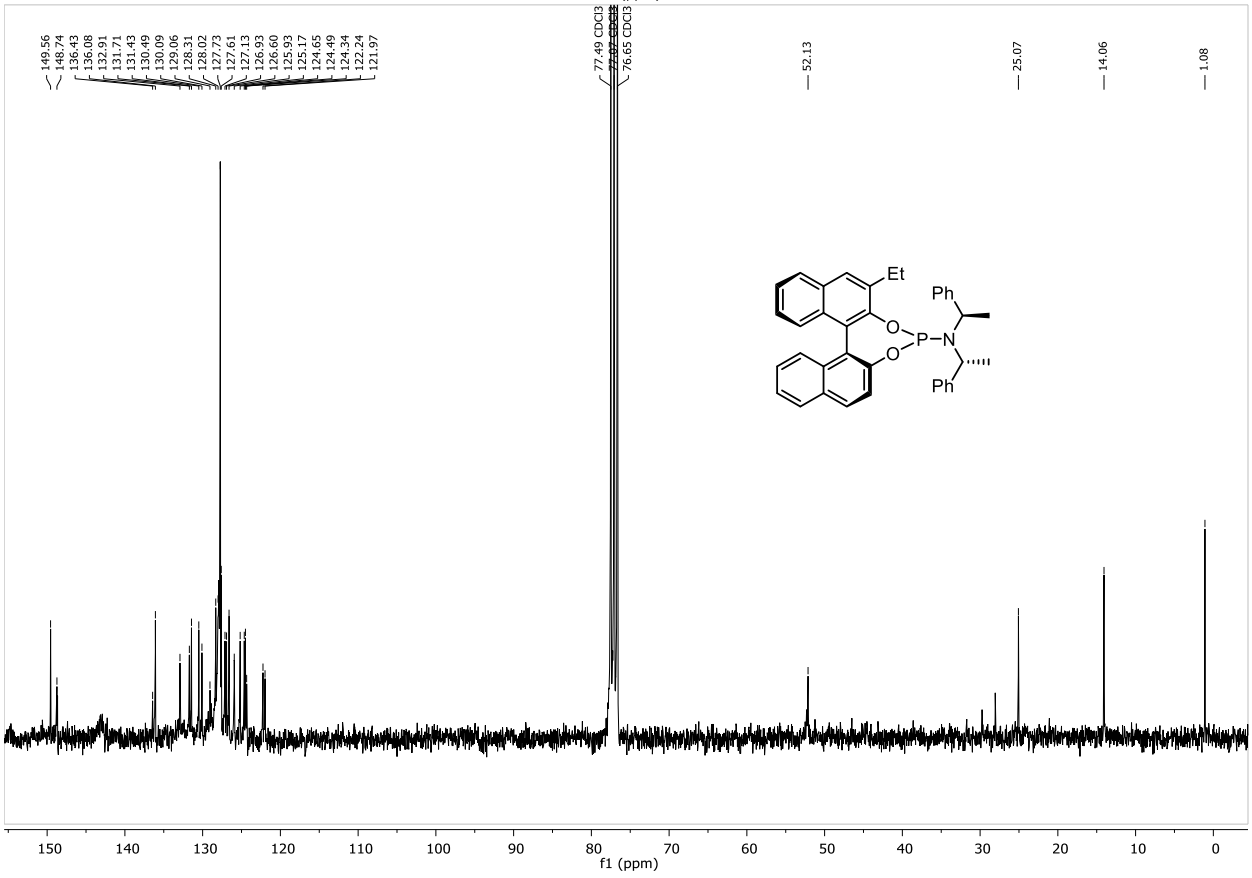
149.56 148.74 136.43 136.08 132.91 131.71 131.43 130.49 130.09 129.06 128.31 128.02 127.73 127.61 127.13 126.93 126.60 125.93 125.17 124.65 124.49 124.34 122.24 121.97
77.49 CDCl3 77.07 CDCl3 76.65 CDCl3
52.13
25.07
14.06
1.08
Et
Ph
O
P
N
O
Ph
150 140 130 120 110 100 90 80 70 60 50 40 30 20 10 0
f1 (ppm)

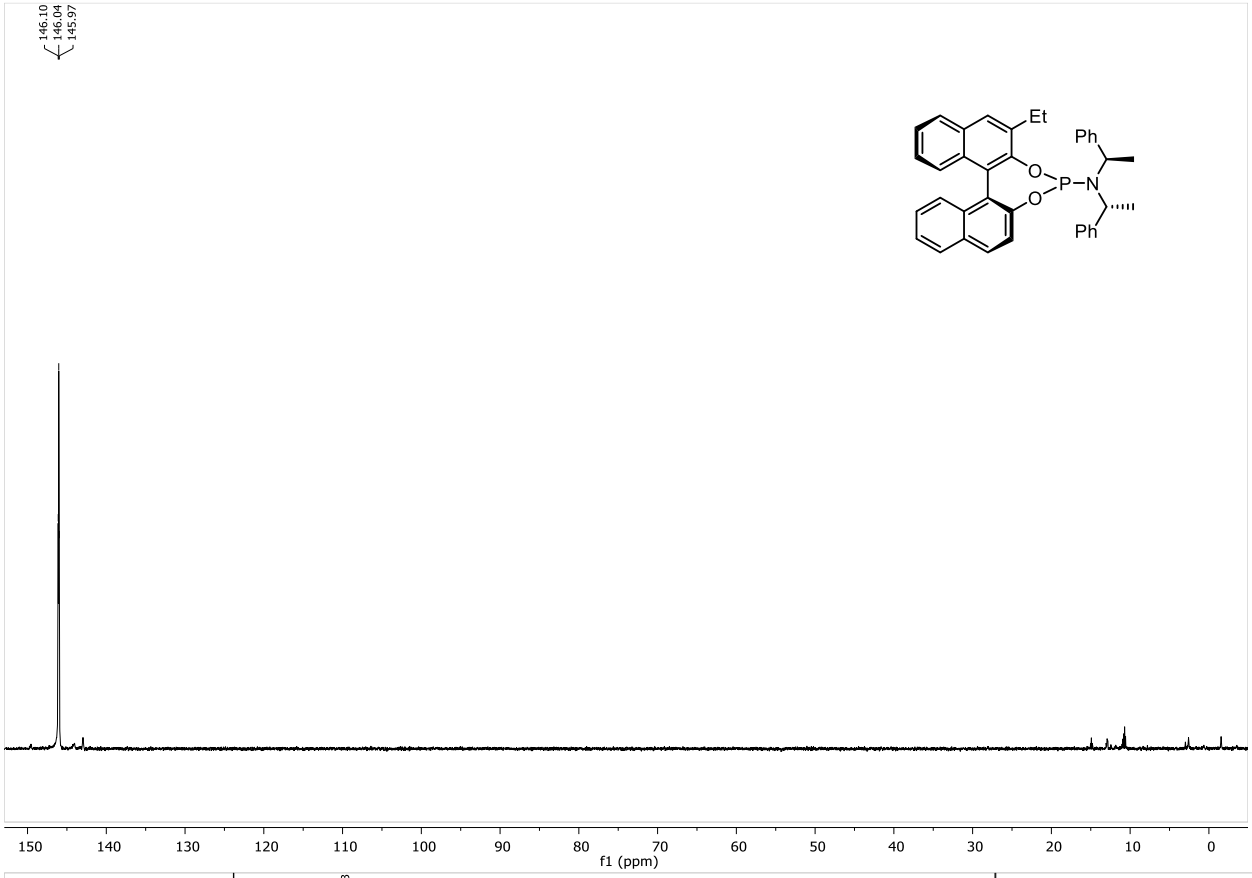
146.10
146.04
145.97
Et
Ph
O
P
N
O
Ph
150
140
130
120
110
100
90
80
70
60
50
40
30
20
10
0
f1 (ppm)

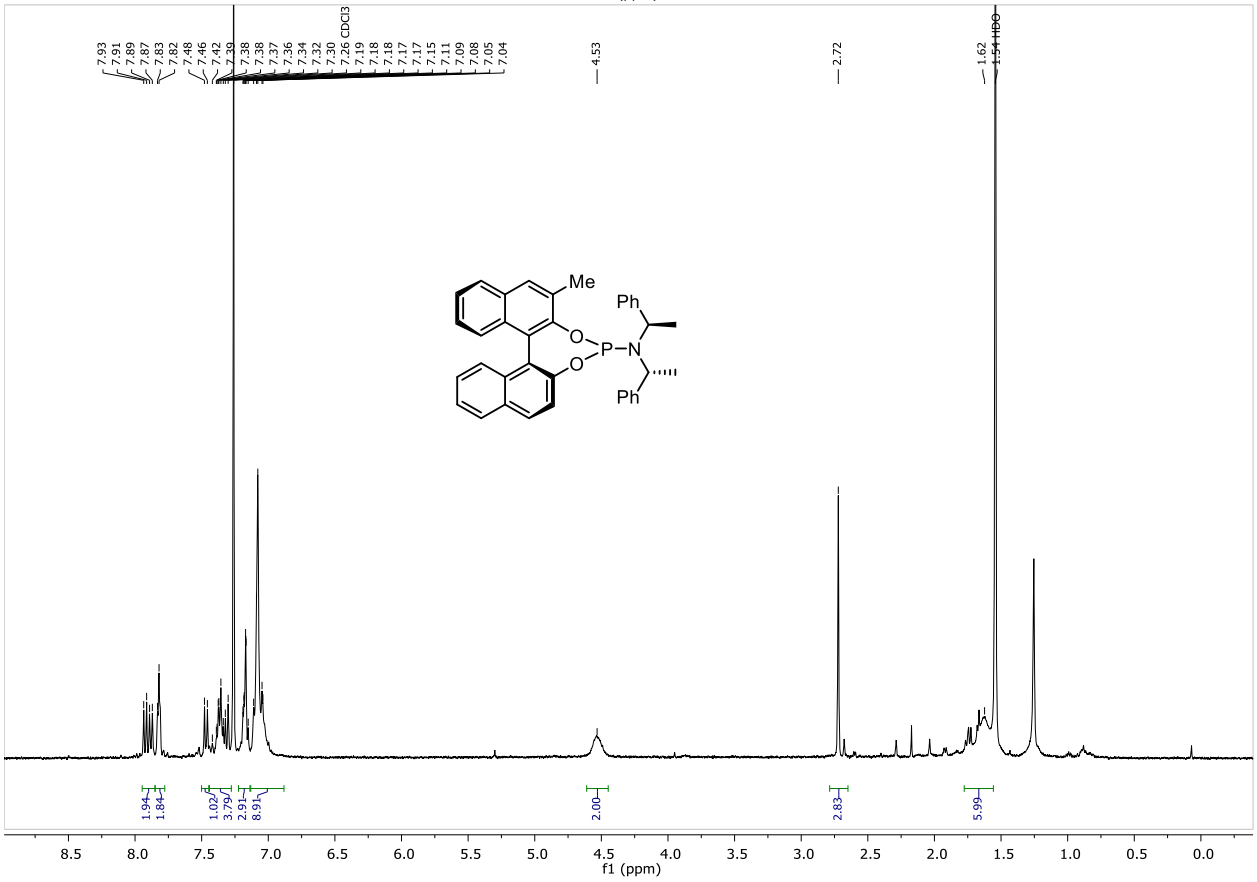
7.93
7.91
7.89
7.87
7.83
7.82
7.48
7.46
7.42
7.39
7.38
7.38
7.37
7.36
7.34
7.32
7.30
7.26 CDCl3
7.19
7.18
7.18
7.17
7.17
7.15
7.11
7.09
7.08
7.05
7.04
4.53
2.72
1.62
1.54 H2O
Me
Ph
O
P
N
O
Ph
1.94
1.84
1.02
3.79
2.91
8.91
2.00
2.83
5.99
8.5
8.0
7.5
7.0
6.5
6.0
5.5
5.0
4.5
4.0
3.5
3.0
2.5
2.0
1.5
1.0
0.5
0.0
f1 (ppm)

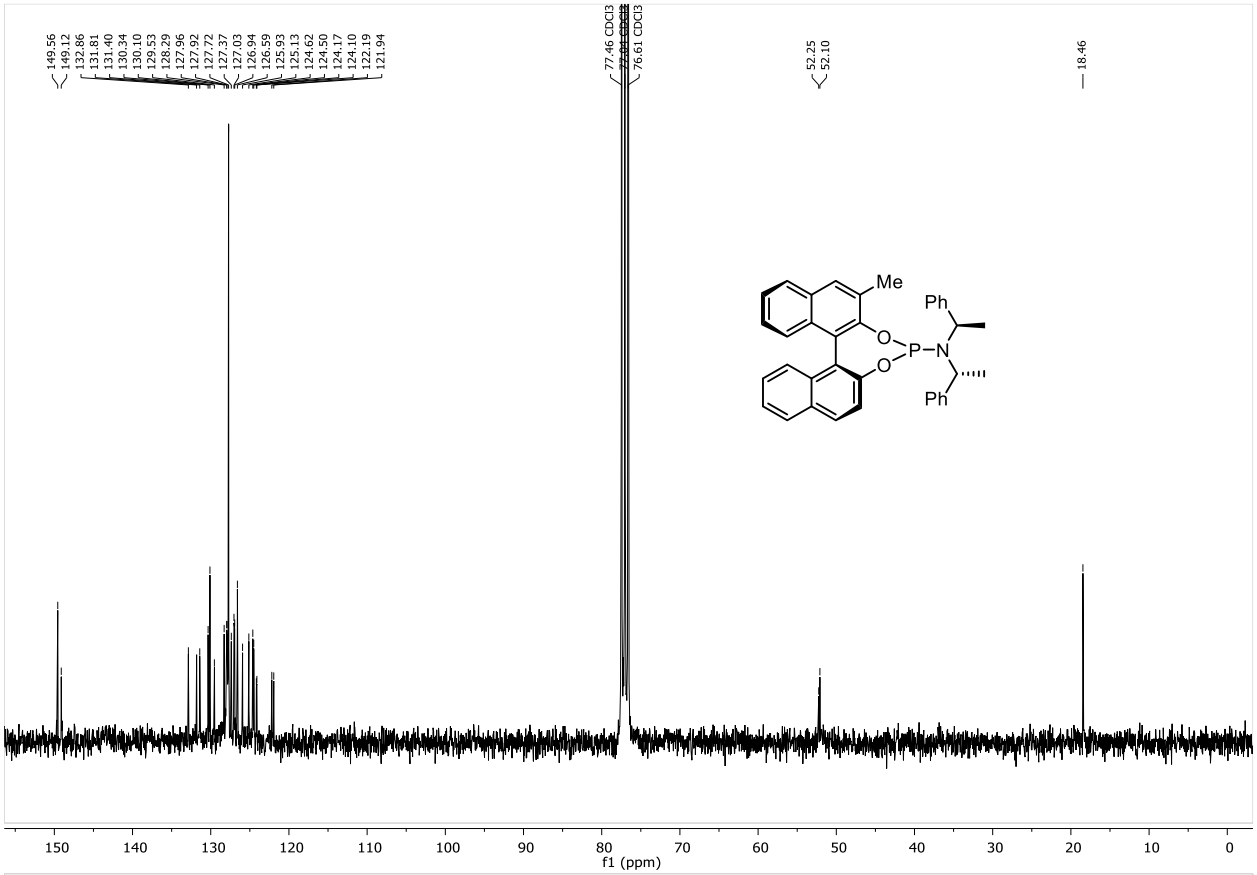
149.56
149.12
132.86
131.81
131.40
130.34
130.10
129.53
128.29
127.96
127.92
127.72
127.37
127.03
126.94
126.59
125.93
125.13
124.62
124.50
124.17
124.10
122.19
121.94
77.46 CDCl3
76.61 CDCl3
52.25
52.10
18.46
Me
Ph
O
P
N
O
Ph
150
140
130
120
110
100
90
80
70
60
50
40
30
20
10
0
f1 (ppm)

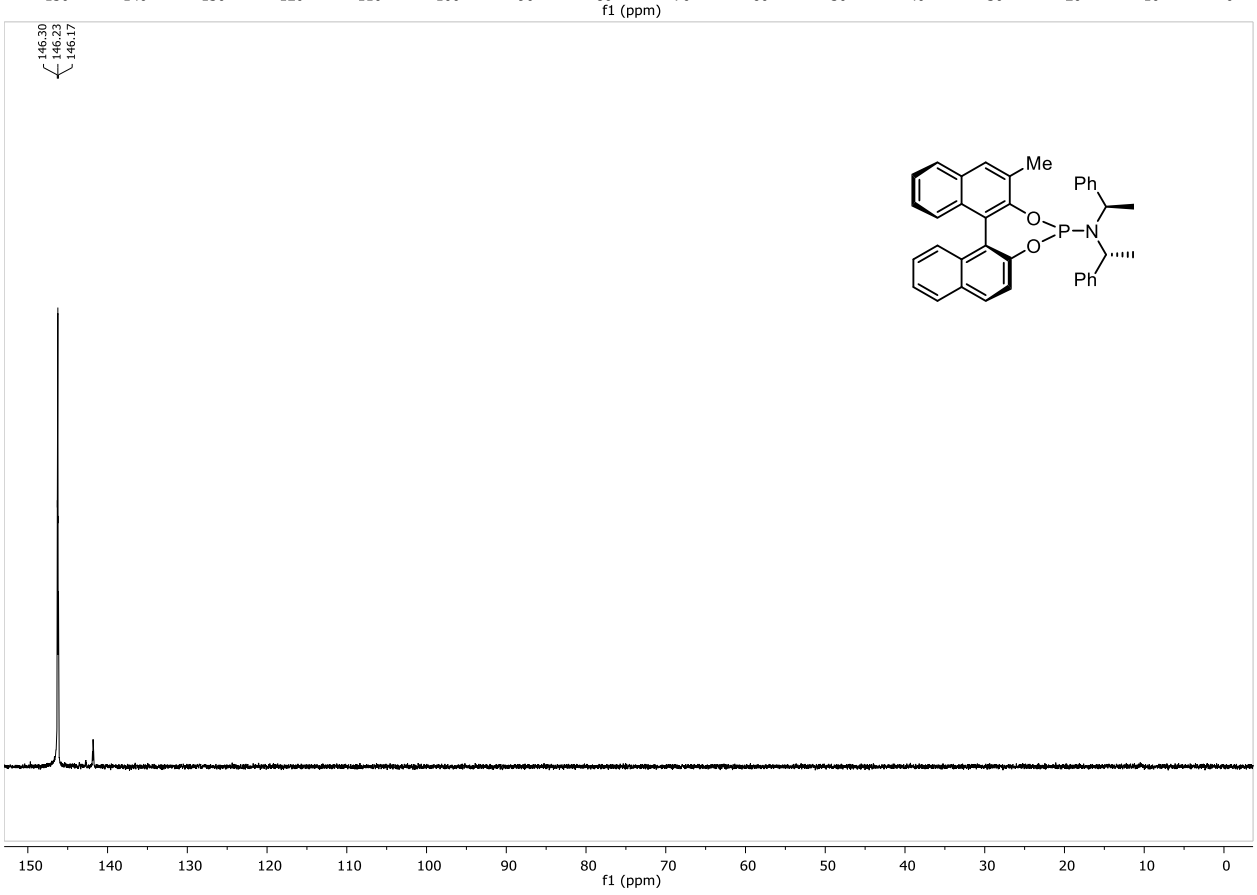
146.30
146.23
146.17
Me
Ph
O
P
N
O
Ph
150
140
130
120
110
100
90
80
70
60
50
40
30
20
10
0
f1 (ppm)

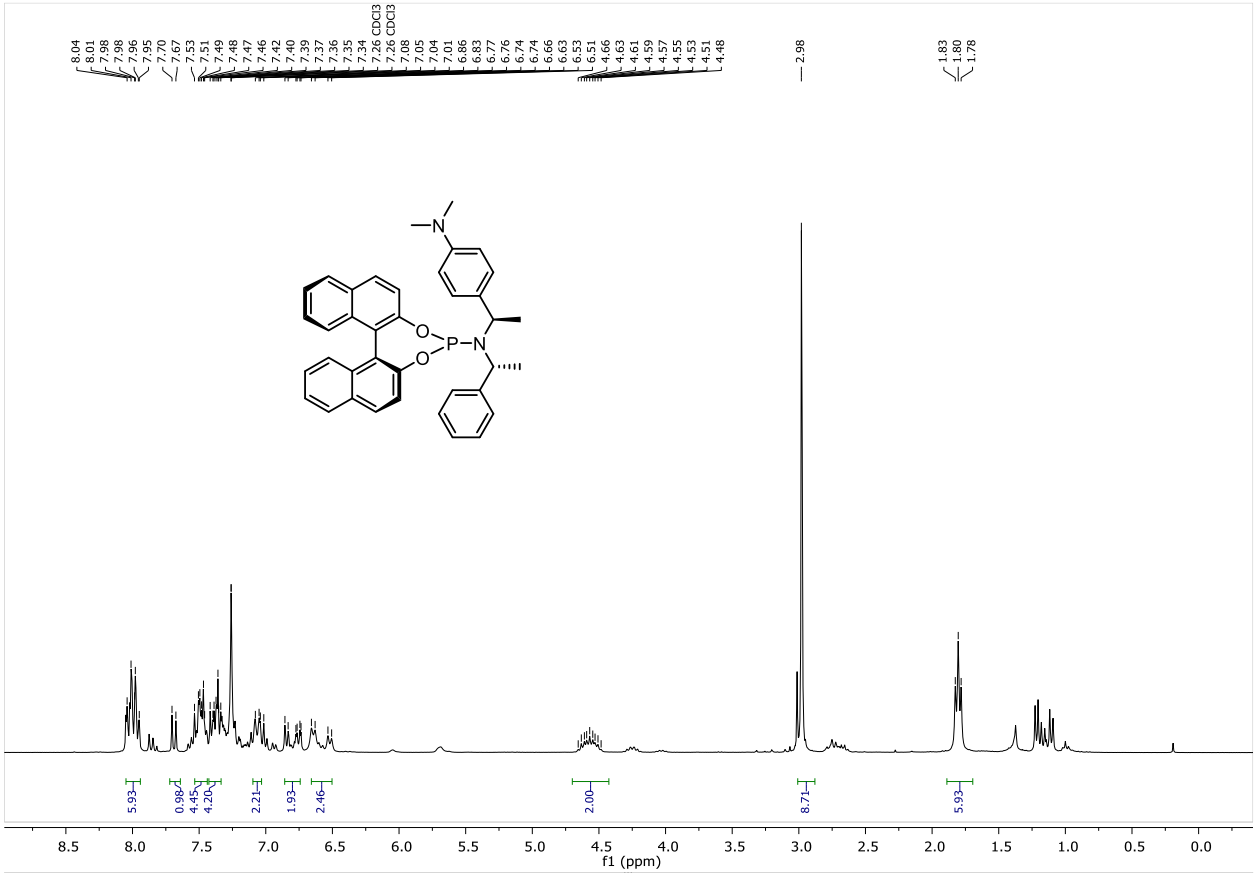
8.04
8.01
7.98
7.98
7.96
7.95
7.70
7.67
7.53
7.51
7.49
7.48
7.47
7.46
7.42
7.40
7.39
7.37
7.36
7.35
7.34
7.26 CDCl3
7.26 CDCl3
7.08
7.05
7.04
7.01
6.86
6.83
6.77
6.76
6.74
6.74
6.66
6.63
6.53
6.51
4.66
4.63
4.61
4.59
4.57
4.55
4.53
4.51
4.48
2.98
1.83
1.80
1.78
5.93
0.98
4.45
4.20
2.21
1.93
2.46
2.00
8.71
5.93
f1 (ppm)

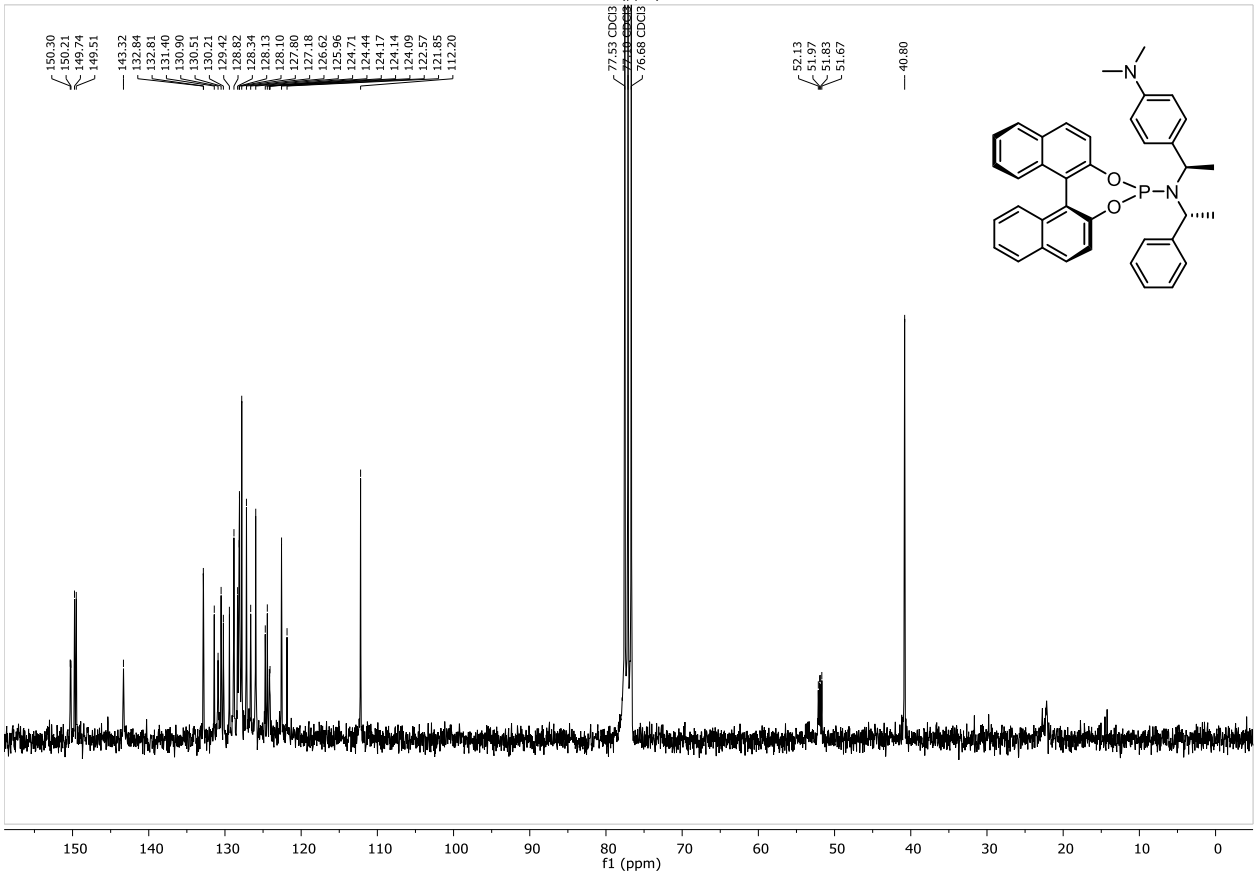
150.30
150.21
149.74
149.51
143.32
132.84
132.81
131.40
130.90
130.51
130.21
129.42
128.82
128.34
128.13
128.10
127.80
127.18
126.62
125.96
124.71
124.44
124.17
124.14
124.09
122.57
121.85
112.20
77.53 CDCl3
77.10 CDCl3
76.68 CDCl3
52.13
51.97
51.83
51.67
40.80
f1 (ppm)

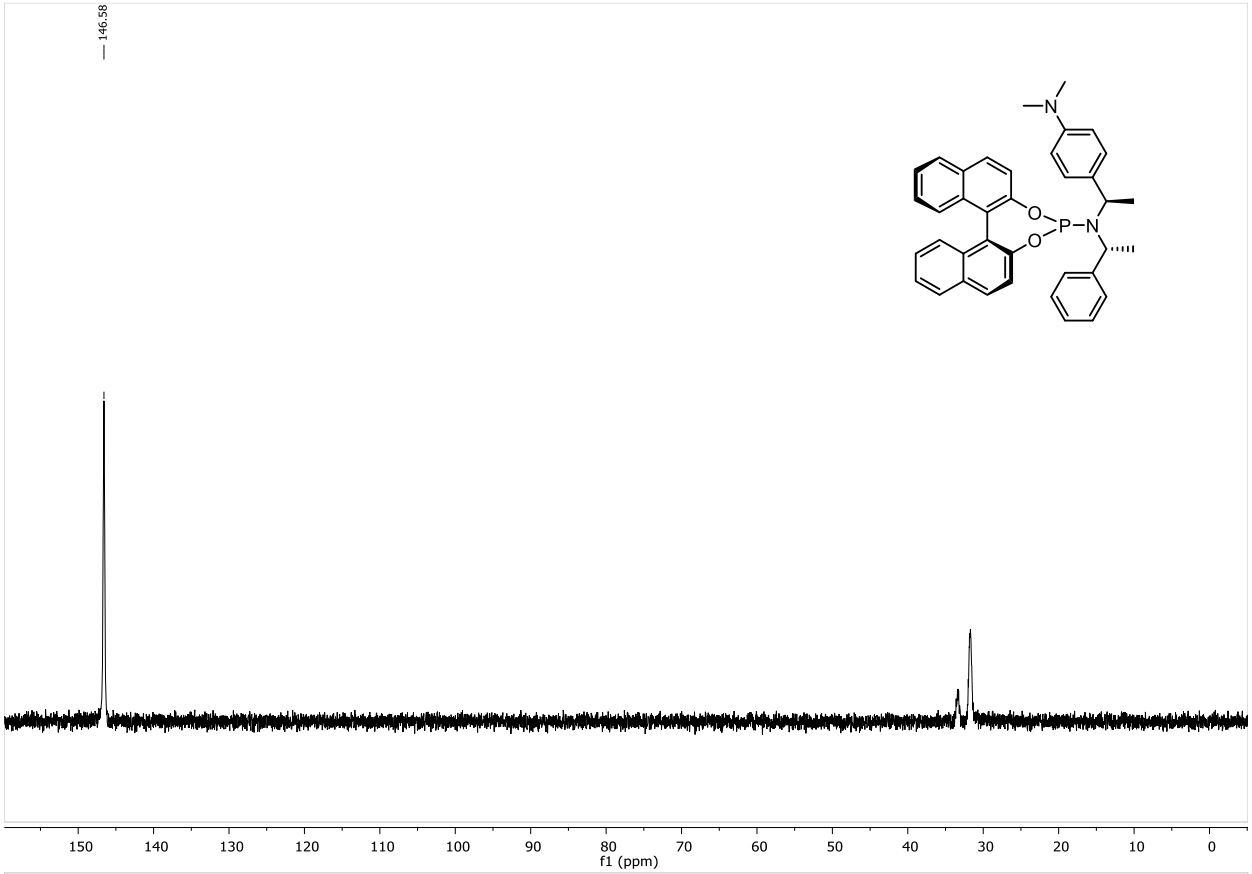
146.58
N
O
P
N
O
150
140
130
120
110
100
90
80
70
60
50
40
30
20
10
0
f1 (ppm)

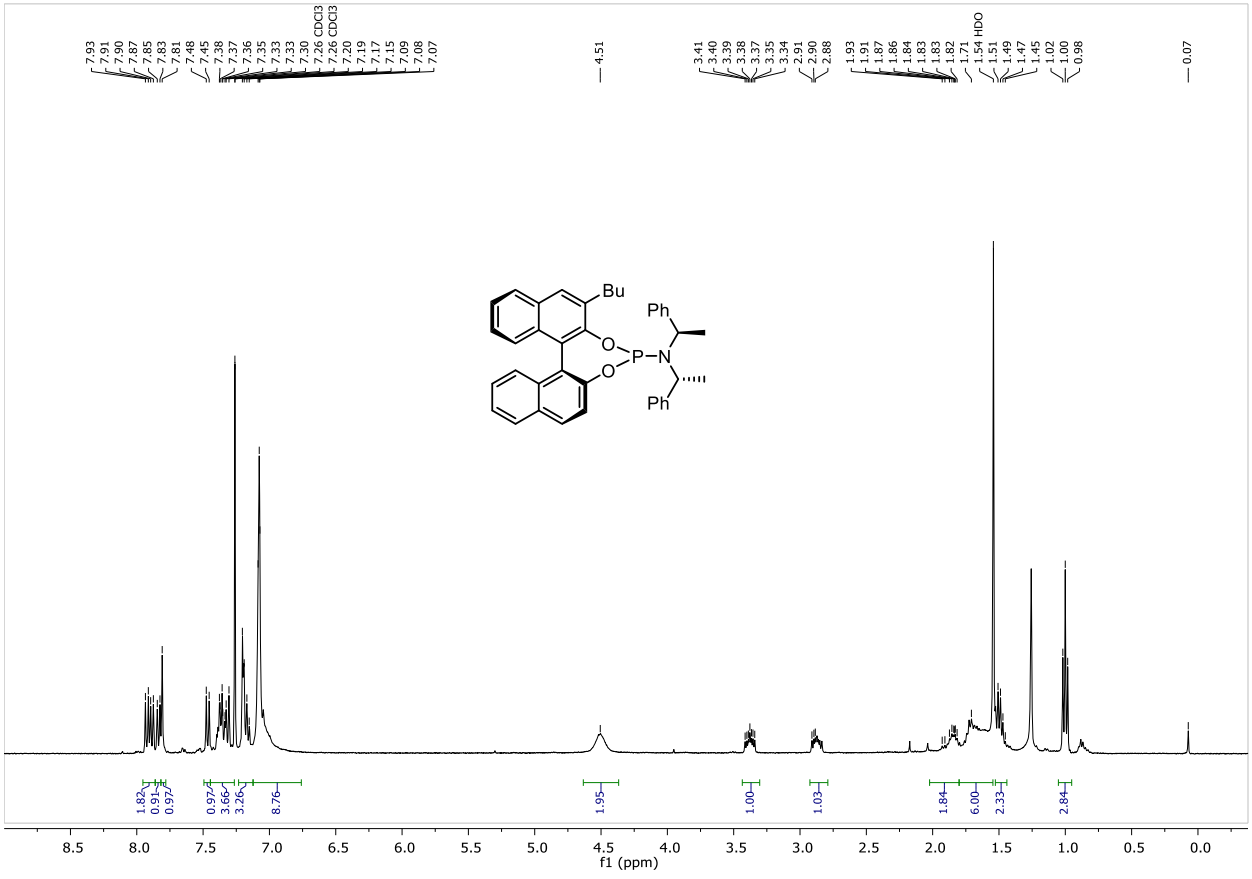
7.93
7.91
7.90
7.87
7.85
7.83
7.81
7.48
7.45
7.38
7.37
7.36
7.35
7.33
7.30
7.26 CDCl3
7.26 CDCl3
7.20
7.19
7.17
7.15
7.09
7.08
7.07
4.51
3.41
3.40
3.39
3.38
3.37
3.35
3.34
2.91
2.90
2.88
1.93
1.91
1.87
1.86
1.84
1.83
1.82
1.71
1.54 HDO
1.51
1.49
1.47
1.45
1.02
1.00
0.98
0.07
Bu
Ph
O
P
N
O
Ph
1.82
0.91
0.97
0.97
3.66
3.26
8.76
1.95
1.00
1.03
1.84
6.00
2.33
2.84
8.5
8.0
7.5
7.0
6.5
6.0
5.5
5.0
4.5
4.0
3.5
3.0
2.5
2.0
1.5
1.0
0.5
0.0
f1 (ppm)

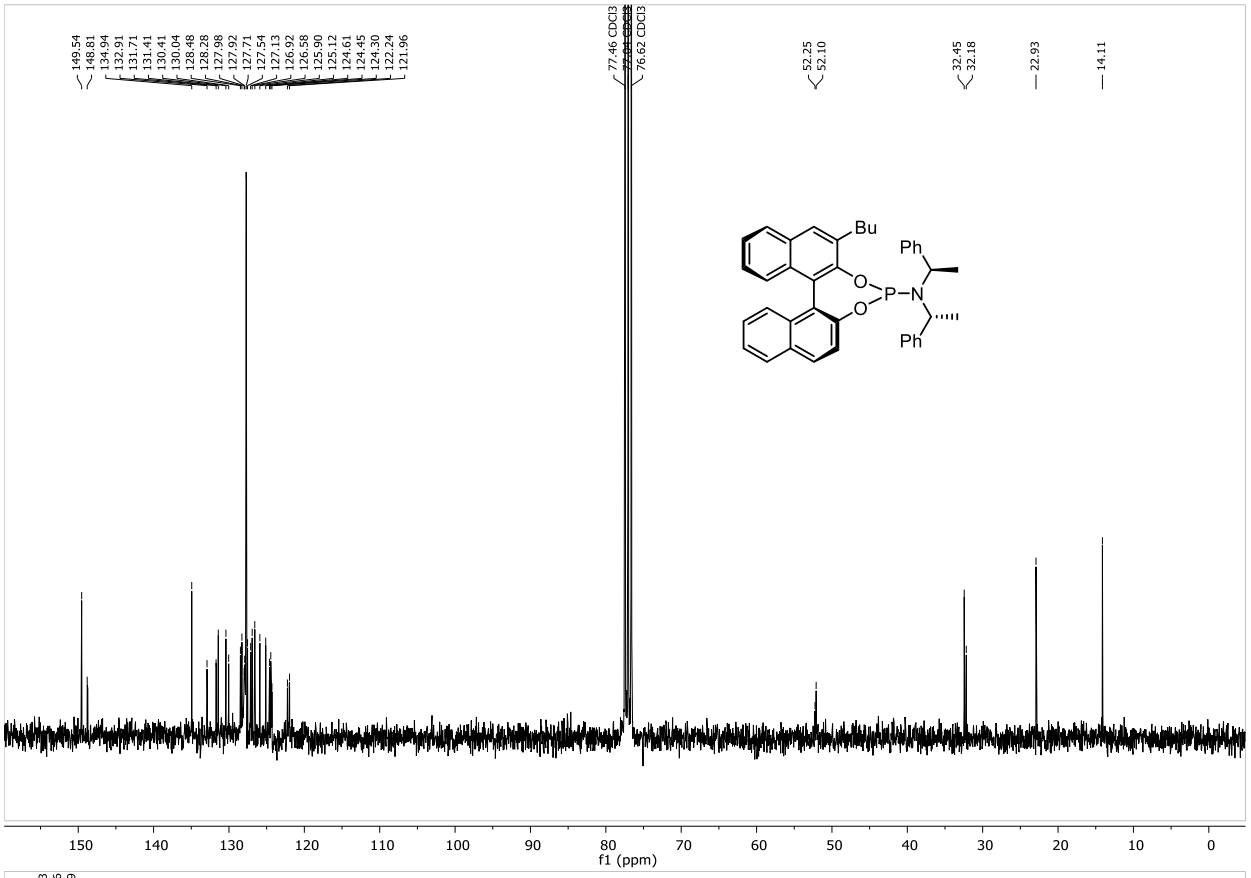
149.54
148.81
134.94
132.91
131.71
131.41
130.41
130.04
128.48
128.28
127.98
127.92
127.71
127.54
127.13
126.92
126.58
125.90
125.12
124.61
124.45
124.30
122.24
121.96
77.46 CDCl3
76.62 CDCl3
52.25
52.10
32.45
32.18
22.93
14.11
Bu
Ph
O
P
N
O
Ph
150
140
130
120
110
100
90
80
70
60
50
40
30
20
10
0
f1 (ppm)

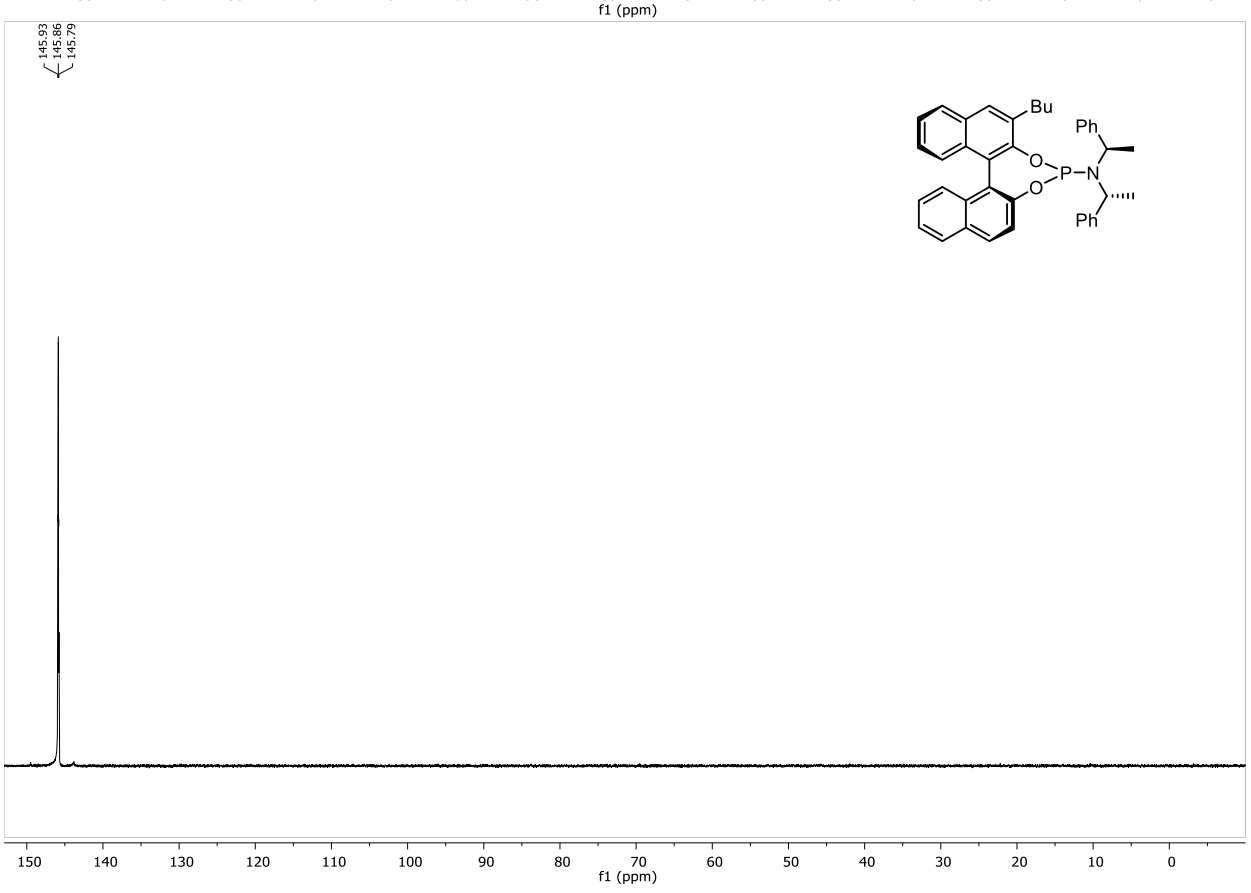
145.93
145.86
145.79
Bu
Ph
O
P
N
O
Ph
150
140
130
120
110
100
90
80
70
60
50
40
30
20
10
0
f1 (ppm)

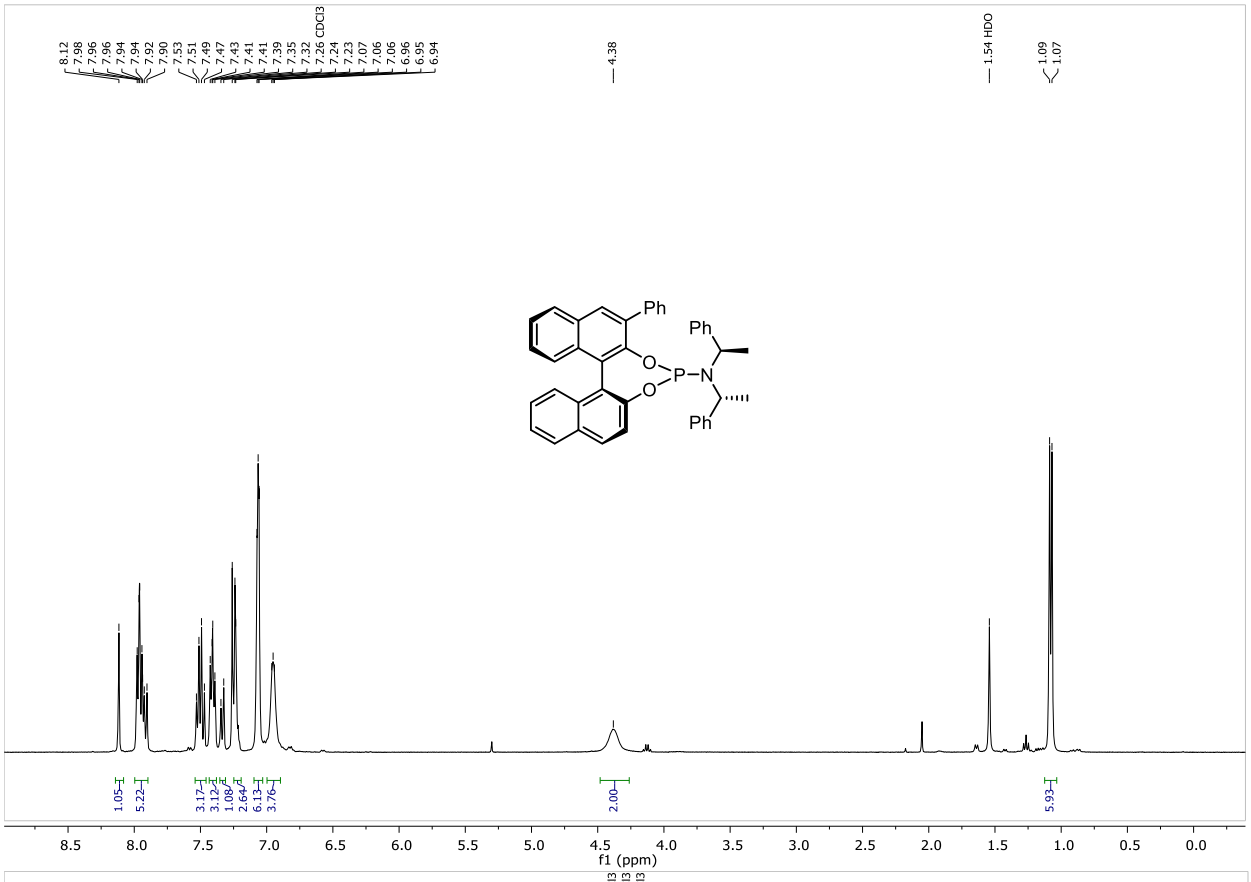
8.12
7.98
7.96
7.96
7.94
7.94
7.92
7.90
7.53
7.51
7.49
7.47
7.43
7.41
7.41
7.39
7.35
7.32
7.26 CDCl3
7.24
7.23
7.07
7.06
7.06
6.96
6.95
6.94
4.38
1.54 HDO
1.09
1.07
Ph
Ph
O
P
N
O
Ph
1.05
5.22
3.17
3.12
1.08
2.64
6.13
3.76
2.00
5.93
8.5
8.0
7.5
7.0
6.5
6.0
5.5
5.0
4.5
4.0
3.5
3.0
2.5
2.0
1.5
1.0
0.5
0.0
f1 (ppm)

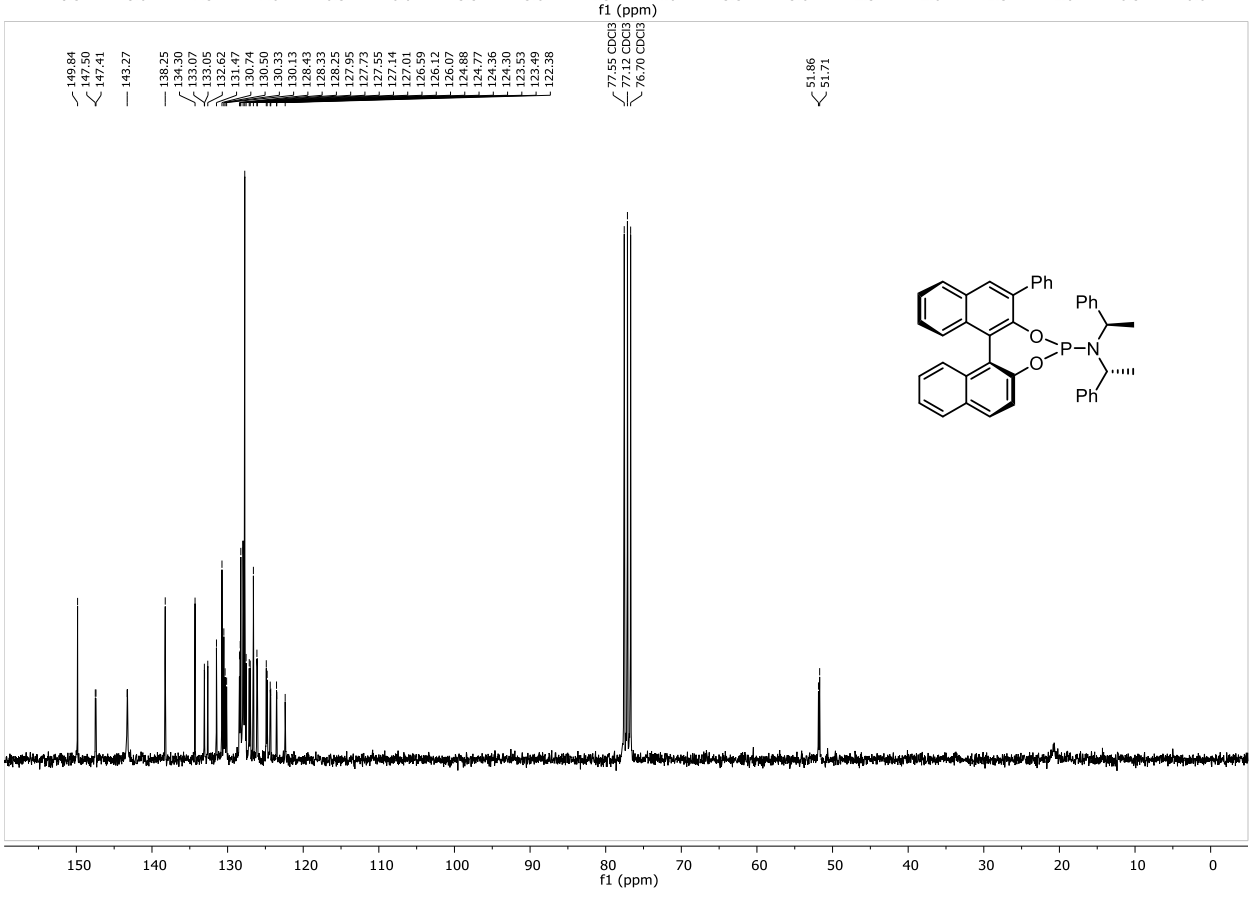
149.84
147.50
147.41
143.27
138.25
134.30
133.07
133.05
132.62
131.47
130.74
130.50
130.33
130.13
128.43
128.33
128.25
127.95
127.73
127.55
127.14
127.01
126.99
126.12
126.07
124.88
124.77
124.36
124.30
123.53
123.49
122.38
77.55 CDCl3
77.12 CDCl3
76.70 CDCl3
51.86
51.71
Ph
Ph
O
P
N
O
Ph
150
140
130
120
110
100
90
80
70
60
50
40
30
20
10
0
f1 (ppm)

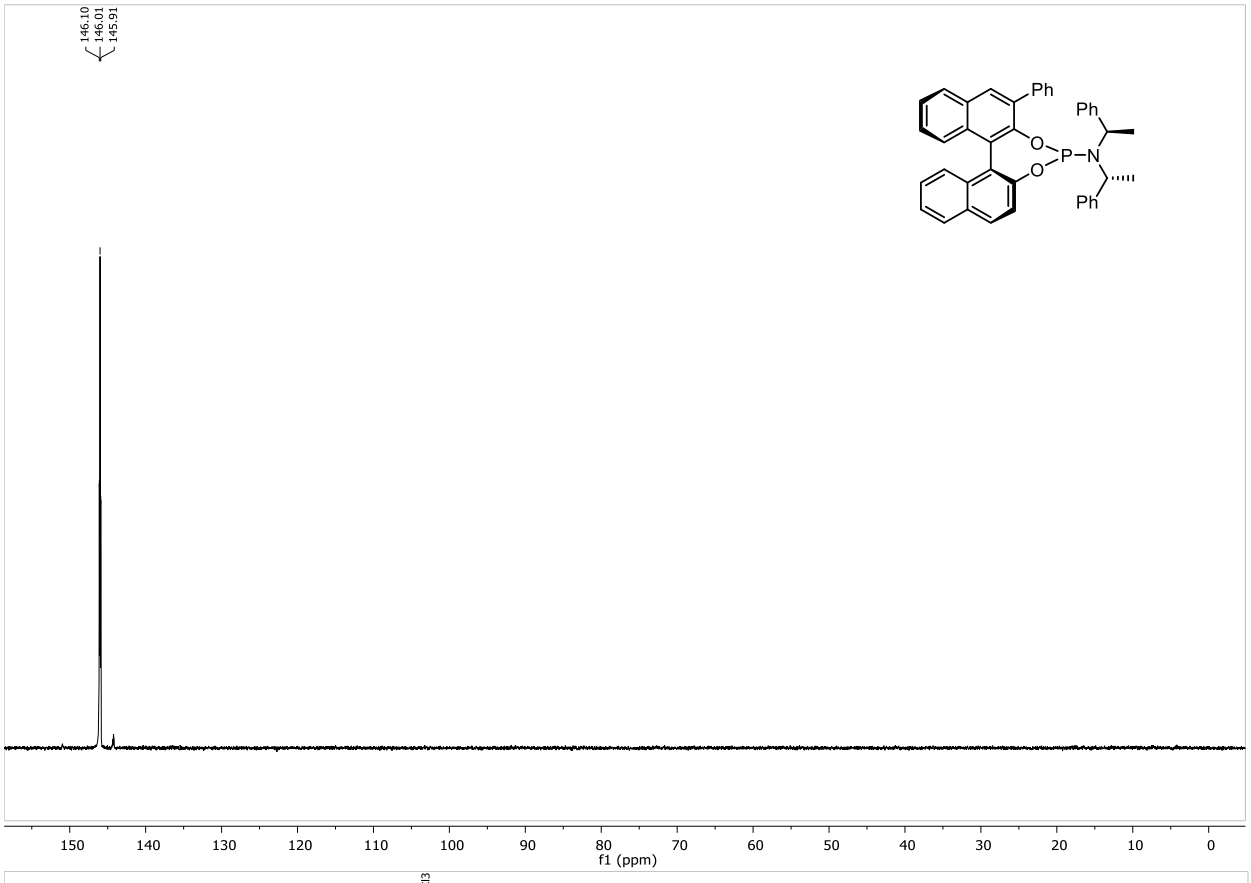
146.10
146.01
145.91
Ph
Ph
O
P–N
O
Ph
150 140 130 120 110 100 90 80 70 60 50 40 30 20 10 0
f1 (ppm)

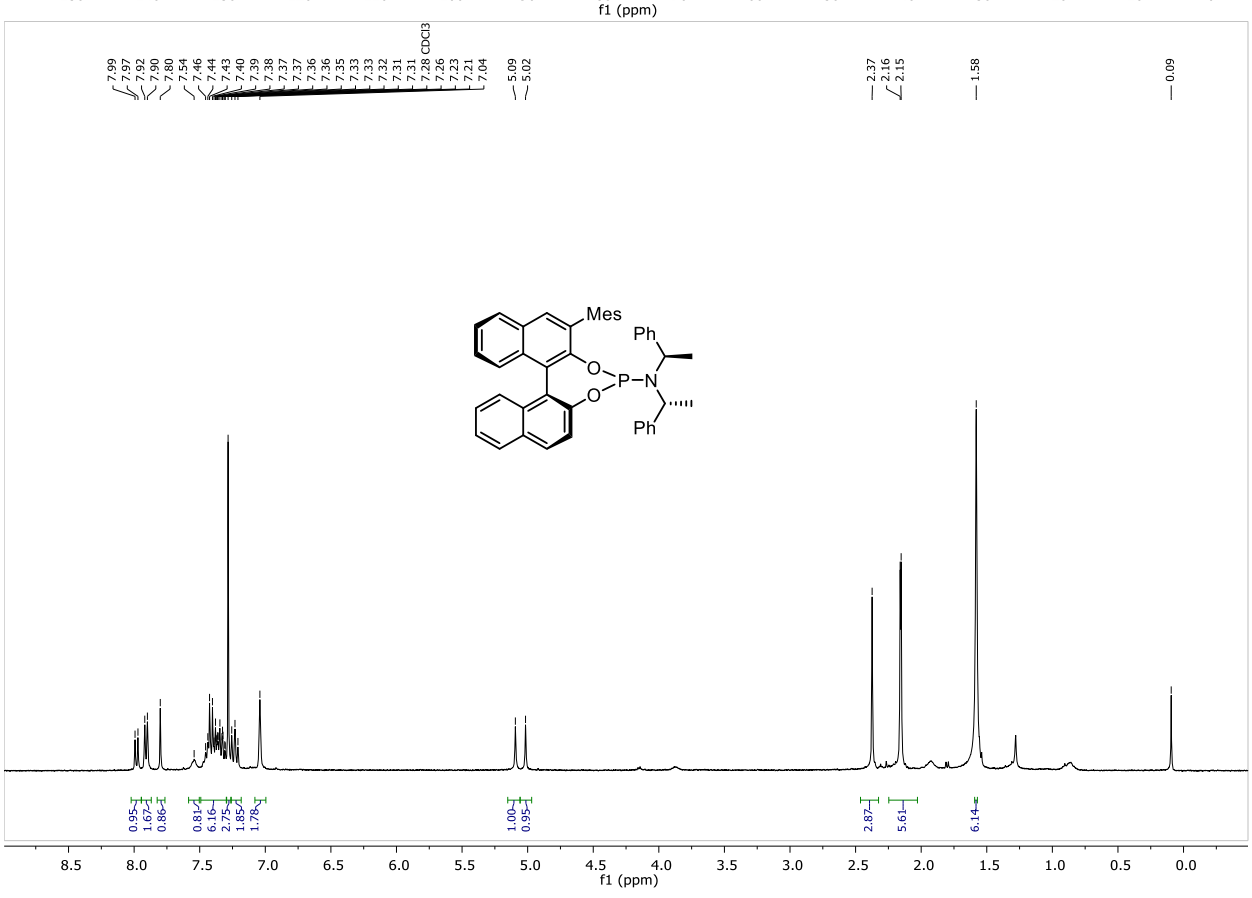
7.99
7.97
7.92
7.90
7.80
7.54
7.46
7.44
7.43
7.40
7.39
7.38
7.37
7.37
7.36
7.36
7.35
7.33
7.33
7.32
7.31
7.31
7.28 CDCl3
7.26
7.23
7.21
7.04
5.09
5.02
2.37
2.16
2.15
1.58
0.09
Mes
Ph
O
P–N
O
Ph
0.95
1.67
0.86
0.81
6.16
2.75
1.85
1.78
1.00
0.95
2.87
5.61
6.14
8.5 8.0 7.5 7.0 6.5 6.0 5.5 5.0 4.5 4.0 3.5 3.0 2.5 2.0 1.5 1.0 0.5 0.0
f1 (ppm)

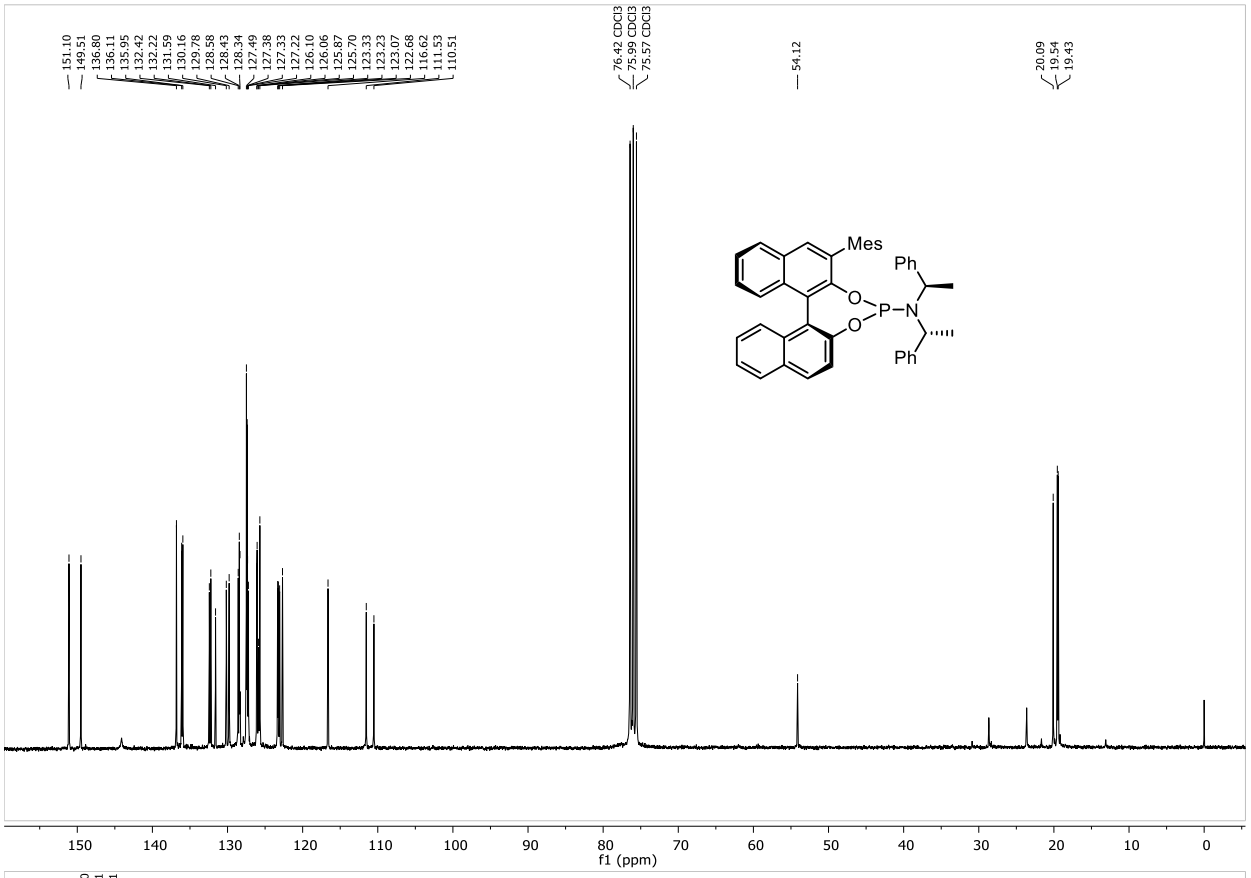
151.10
149.51
136.80
136.11
135.95
132.42
132.22
131.59
130.16
129.78
128.58
128.43
128.34
127.49
127.38
127.33
127.22
126.10
126.06
125.87
125.70
123.33
123.23
123.07
122.68
116.62
111.53
110.51
76.42 CDCl3
75.99 CDCl3
75.57 CDCl3
54.12
20.09
19.54
19.43
Mes
Ph
O
P
N
O
Ph
150
140
130
120
110
100
90
80
70
60
50
40
30
20
10
0
f1 (ppm)

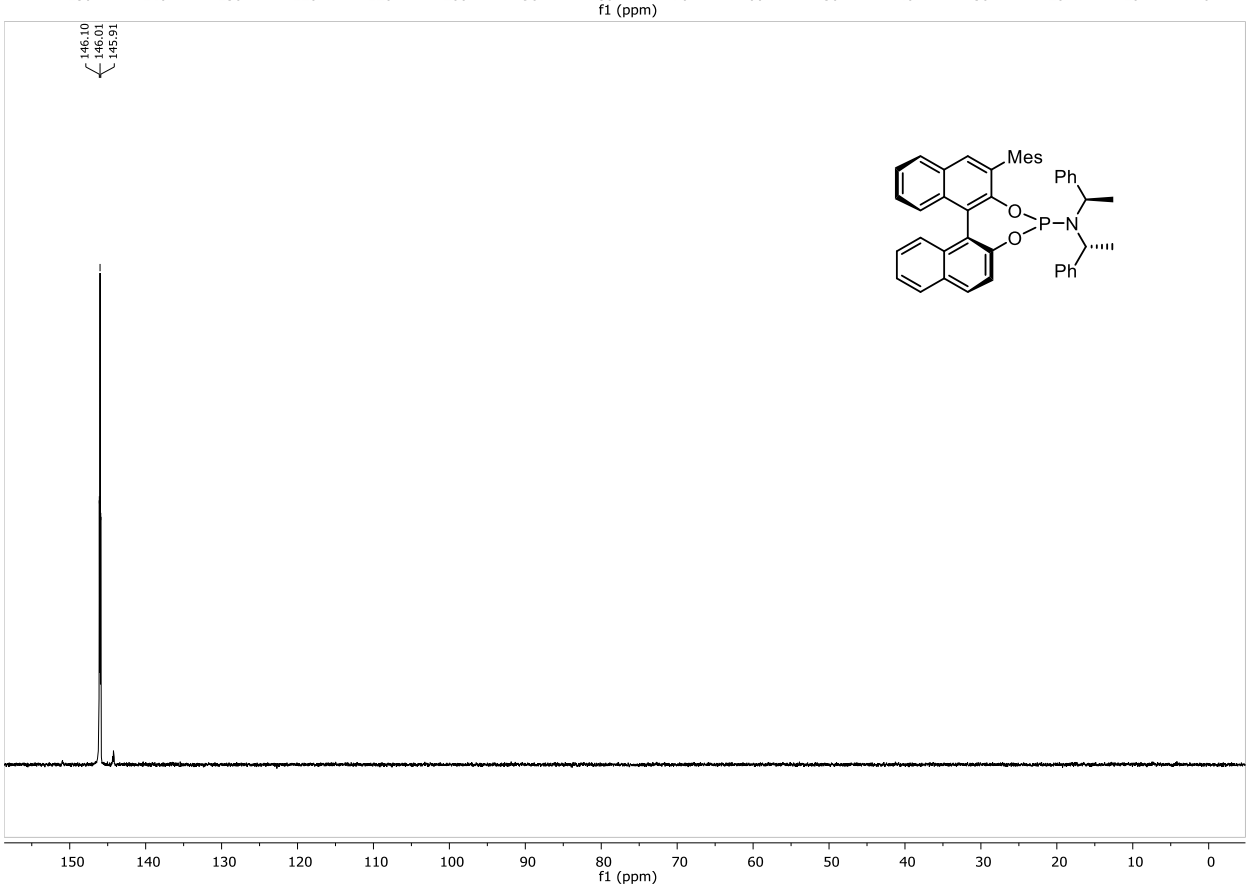
146.10
146.01
145.91
Mes
Ph
O
P
N
O
Ph
150
140
130
120
110
100
90
80
70
60
50
40
30
20
10
0
f1 (ppm)

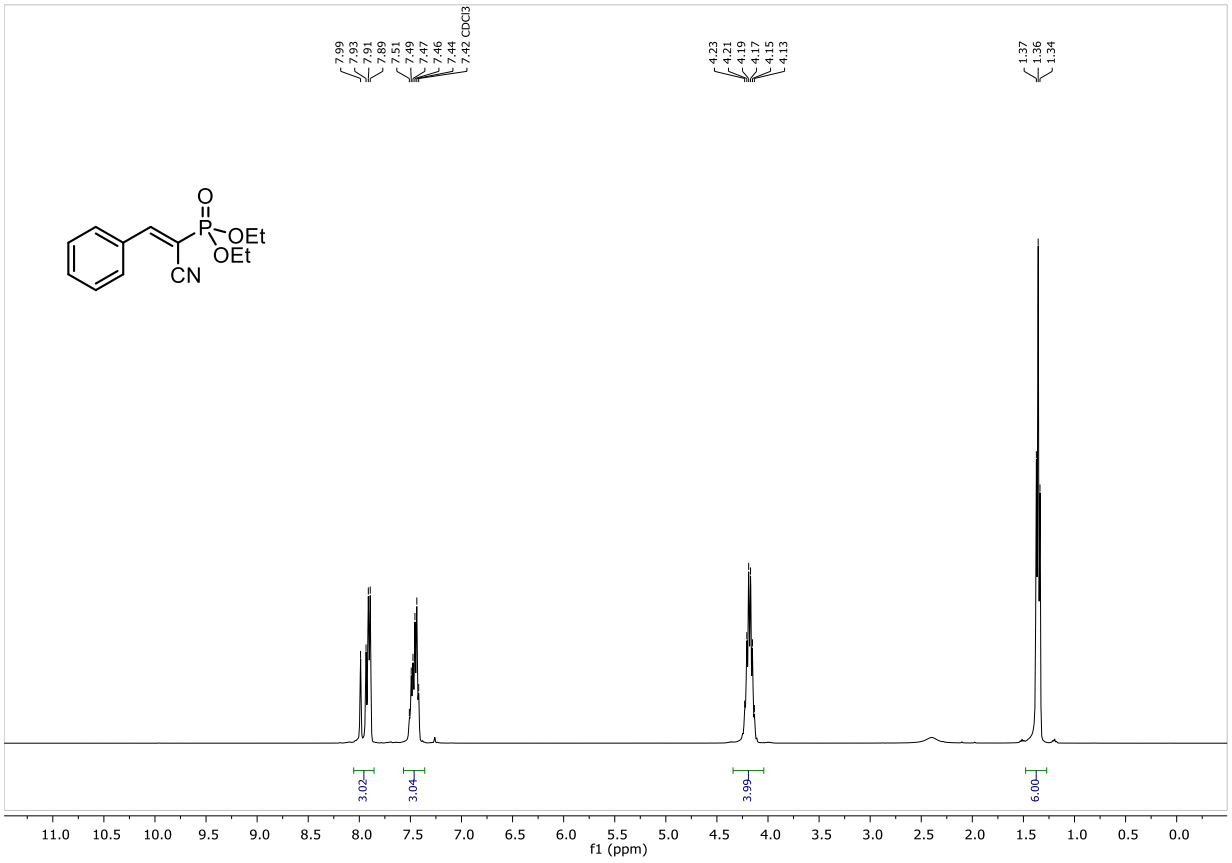
7.99
7.93
7.91
7.89
7.51
7.49
7.47
7.46
7.44
7.42 CDCl3
4.23
4.21
4.19
4.17
4.15
4.13
1.37
1.36
1.34
O
P
OEt
OEt
CN
3.02
3.04
3.99
6.00
11.0 10.5 10.0 9.5 9.0 8.5 8.0 7.5 7.0 6.5 6.0 5.5 5.0 4.5 4.0 3.5 3.0 2.5 2.0 1.5 1.0 0.5 0.0
f1 (ppm)

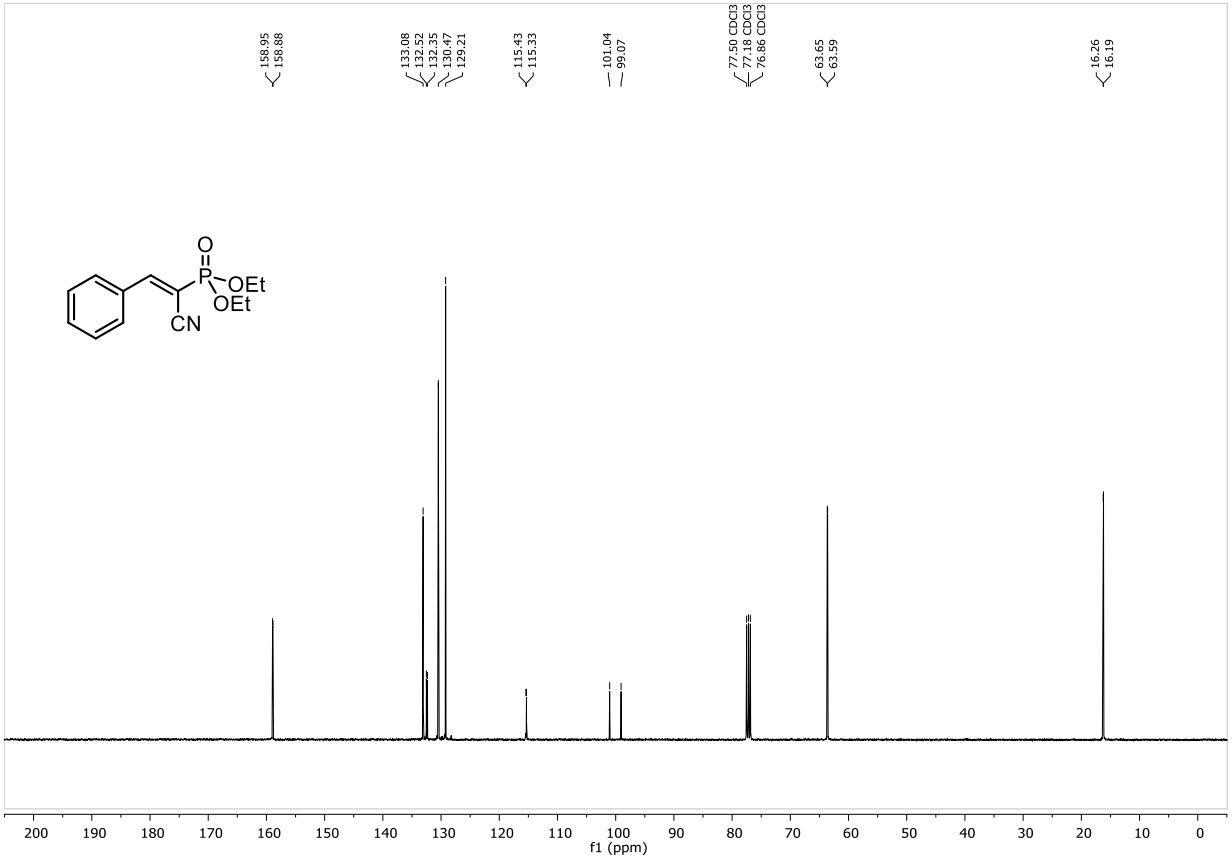
158.95
158.88
133.08
132.52
132.35
130.47
129.21
115.43
115.33
101.04
99.07
77.50 CDCl3
77.18 CDCl3
76.86 CDCl3
63.65
63.59
16.26
16.19
O
P
OEt
OEt
CN
200 190 180 170 160 150 140 130 120 110 100 90 80 70 60 50 40 30 20 10 0
f1 (ppm)

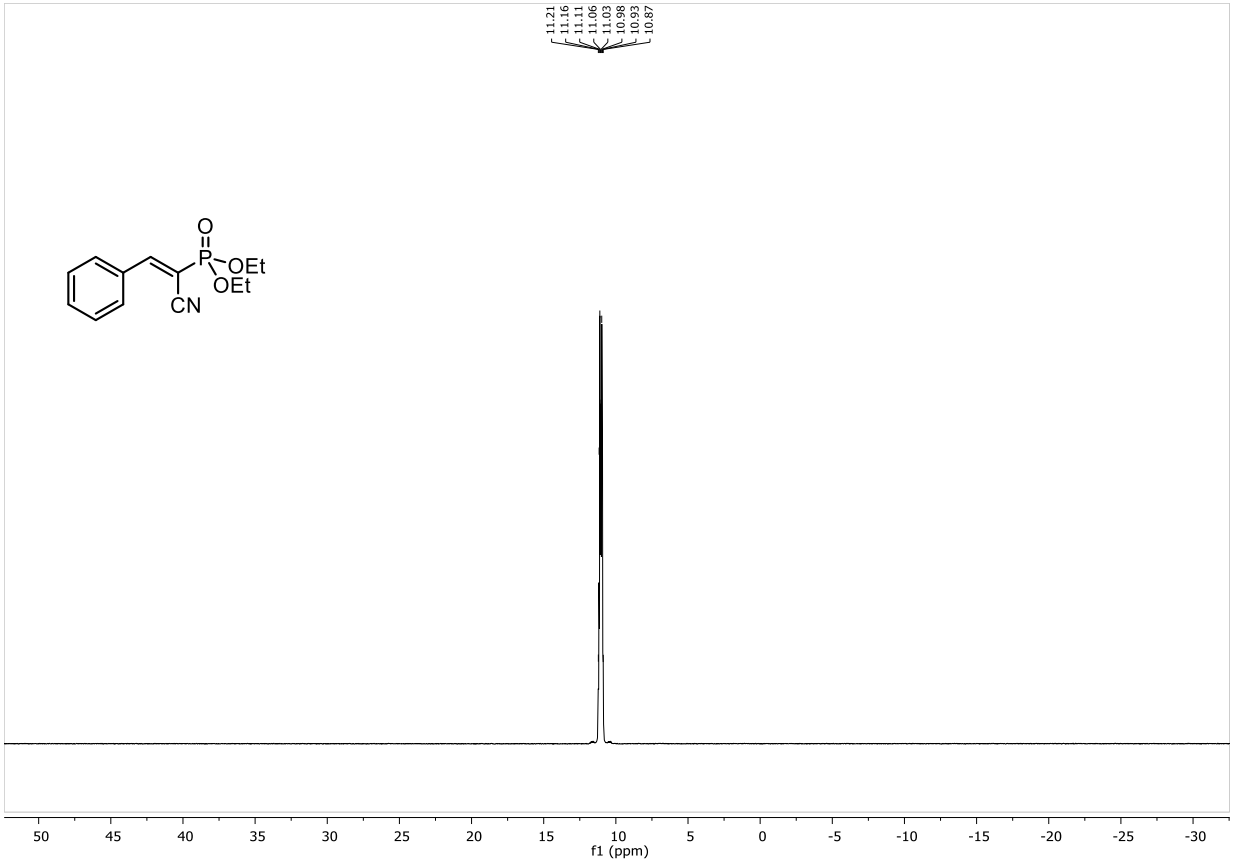
11.21
11.16
11.11
11.06
11.03
10.98
10.93
10.87
O
P
OEt
OEt
CN
50 45 40 35 30 25 20 15 10 5 0 -5 -10 -15 -20 -25 -30
f1 (ppm)

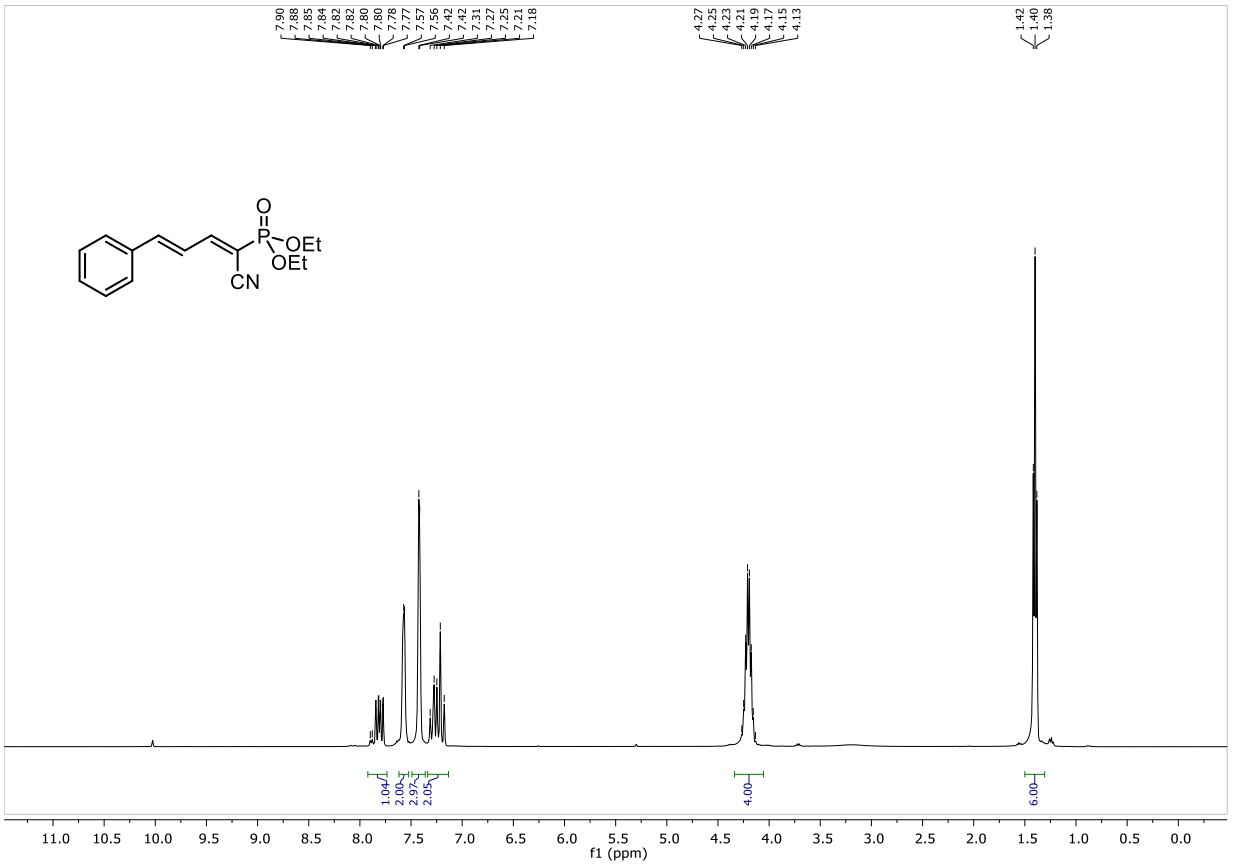
7.90
7.88
7.85
7.84
7.82
7.82
7.80
7.80
7.78
7.77
7.57
7.56
7.42
7.42
7.31
7.27
7.25
7.21
7.18
4.27
4.25
4.23
4.21
4.19
4.17
4.15
4.13
1.42
1.40
1.38
O
P
OEt
OEt
CN
1.04
2.00
2.97
2.05
4.00
6.00
11.0 10.5 10.0 9.5 9.0 8.5 8.0 7.5 7.0 6.5 6.0 5.5 5.0 4.5 4.0 3.5 3.0 2.5 2.0 1.5 1.0 0.5 0.0
f1 (ppm)

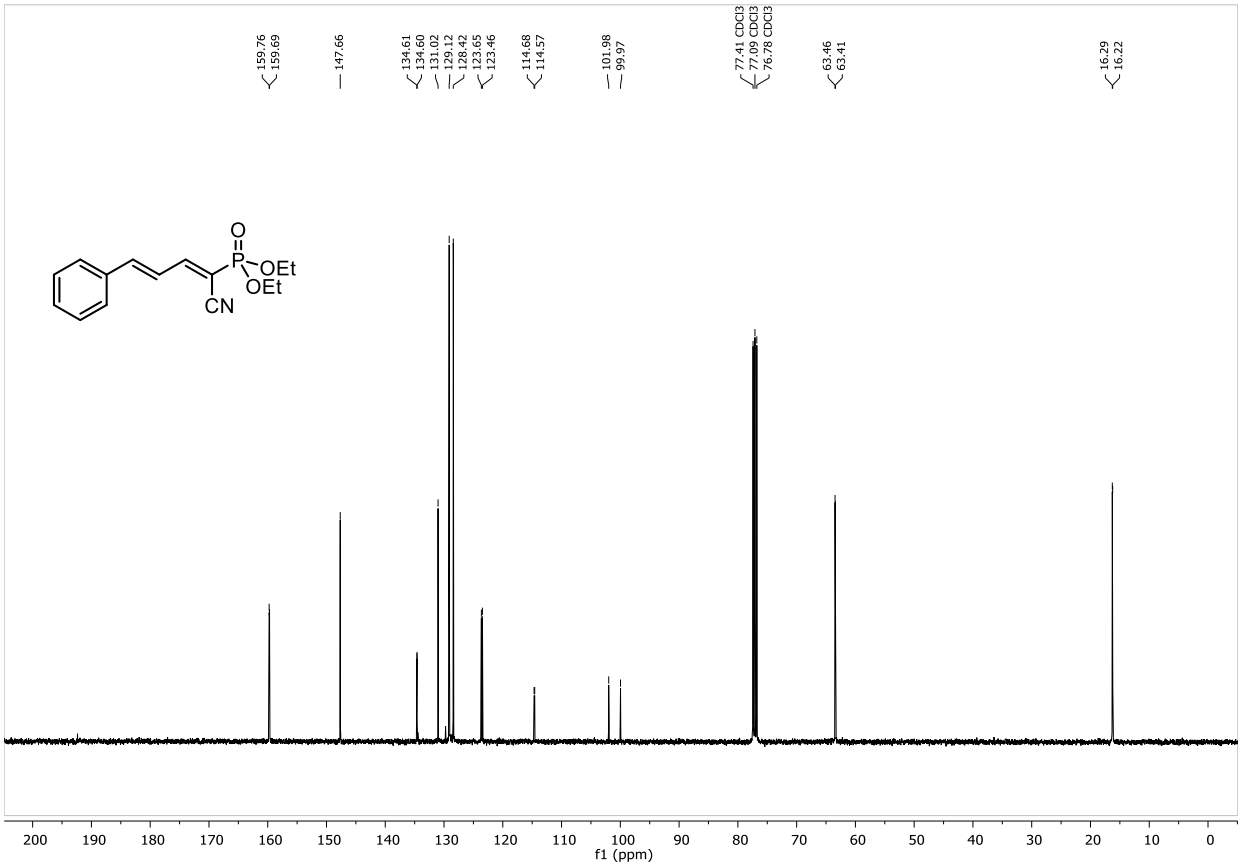
159.76
159.69
147.66
134.61
134.60
131.02
129.12
128.42
123.65
123.46
114.68
114.57
101.98
99.97
77.41 CDCl3
77.09 CDCl3
76.78 CDCl3
63.46
63.41
16.29
16.22
O
P
OEt
OEt
CN
200 190 180 170 160 150 140 130 120 110 100 90 80 70 60 50 40 30 20 10 0
f1 (ppm)

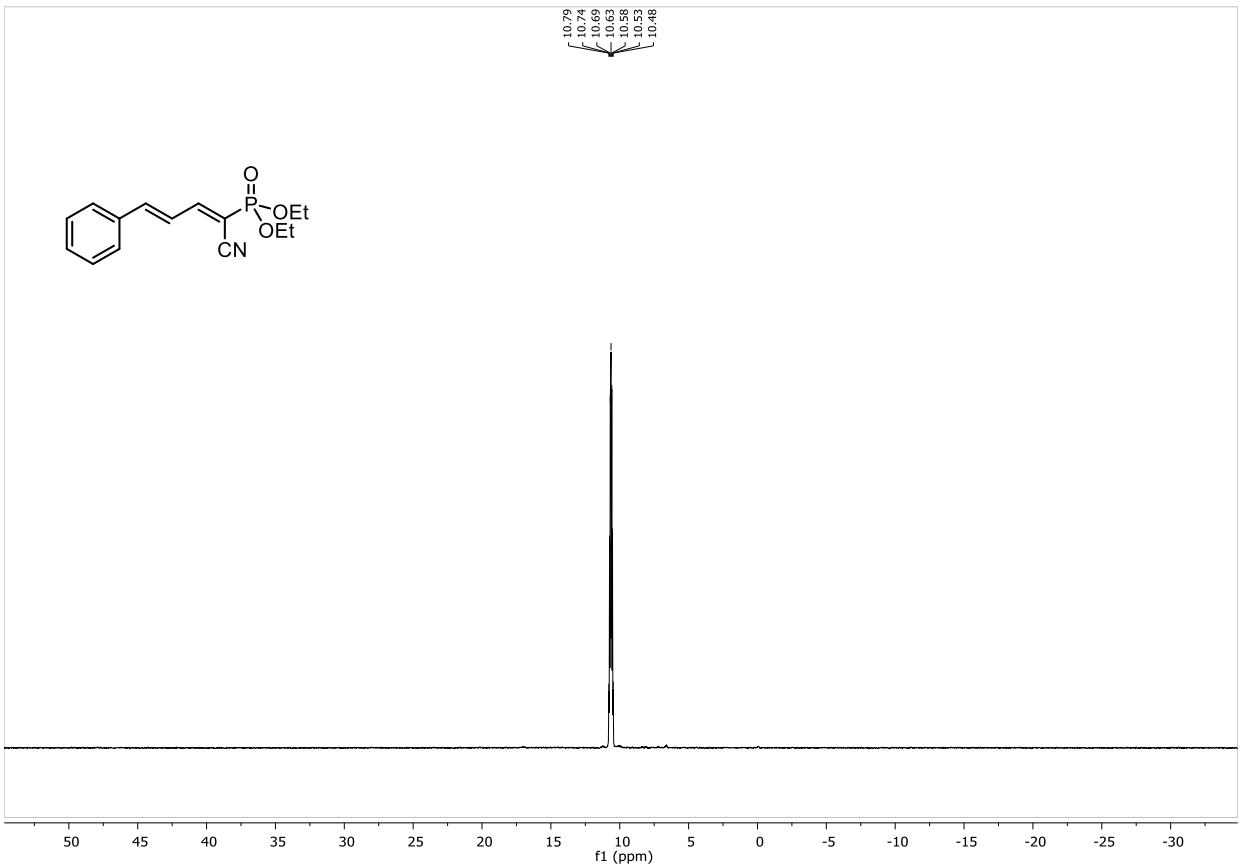
10.79
10.74
10.69
10.63
10.58
10.53
10.48
O
P
OEt
OEt
CN
50 45 40 35 30 25 20 15 10 5 0 -5 -10 -15 -20 -25 -30
f1 (ppm)

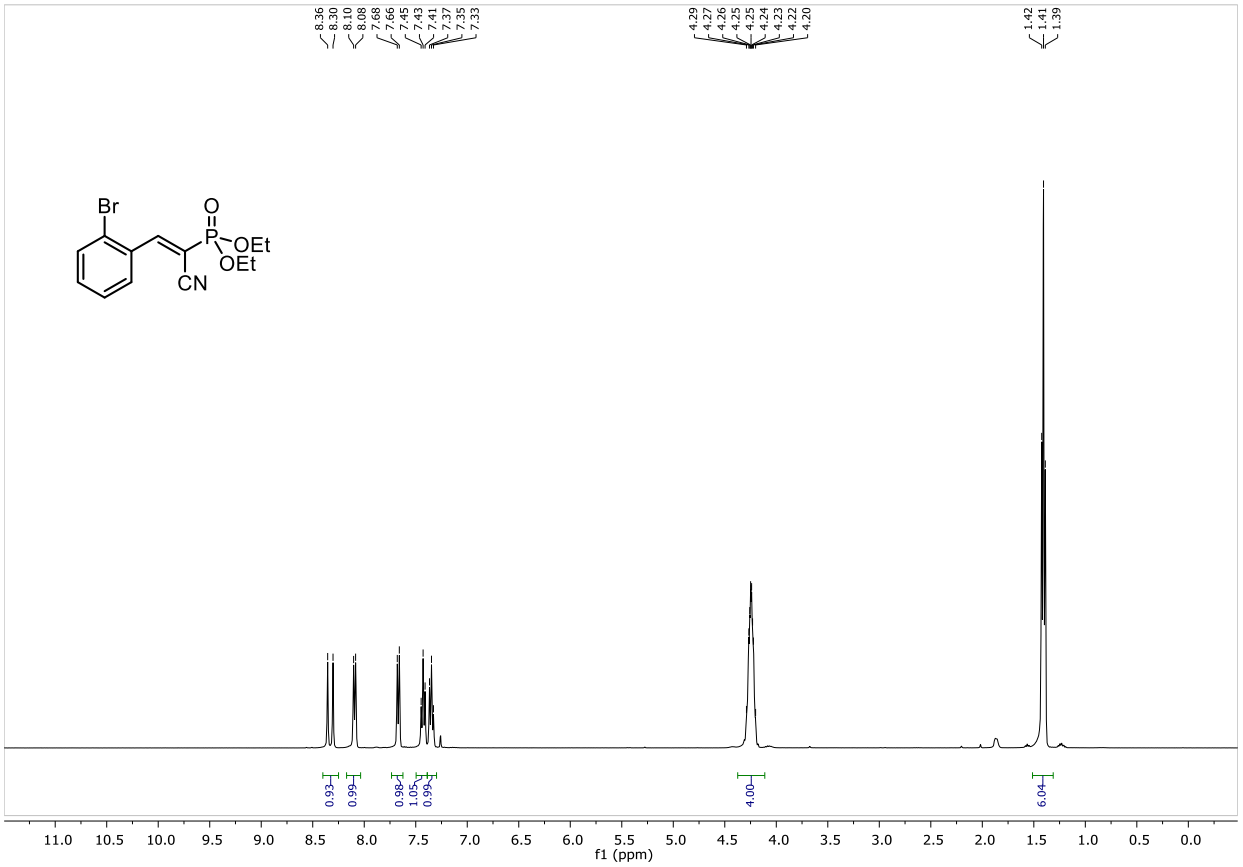
8.36
8.30
8.10
8.08
7.68
7.66
7.45
7.43
7.41
7.37
7.35
7.33
4.29
4.27
4.26
4.25
4.25
4.24
4.23
4.22
4.20
1.42
1.41
1.39
Br
O
P
OEt
OEt
CN
0.93
0.99
0.98
1.05
0.99
4.00
6.04
11.0 10.5 10.0 9.5 9.0 8.5 8.0 7.5 7.0 6.5 6.0 5.5 5.0 4.5 4.0 3.5 3.0 2.5 2.0 1.5 1.0 0.5 0.0
f1 (ppm)

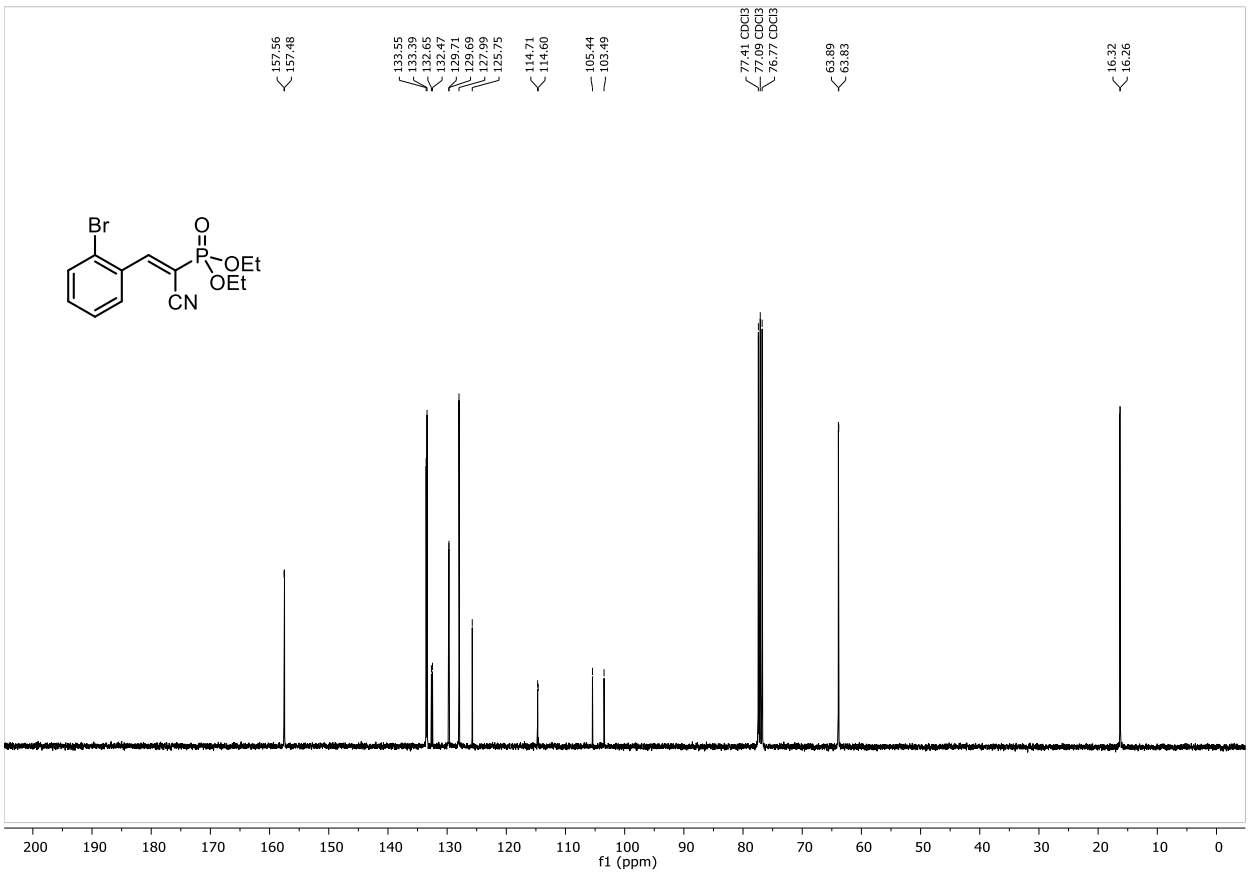
157.56
157.48
133.55
133.39
132.65
132.47
129.71
129.69
127.99
125.75
114.71
114.60
105.44
103.49
77.41 CDCl3
77.09 CDCl3
76.77 CDCl3
63.89
63.83
16.32
16.26
Br
O
P
OEt
OEt
CN
200 190 180 170 160 150 140 130 120 110 100 90 80 70 60 50 40 30 20 10 0
f1 (ppm)

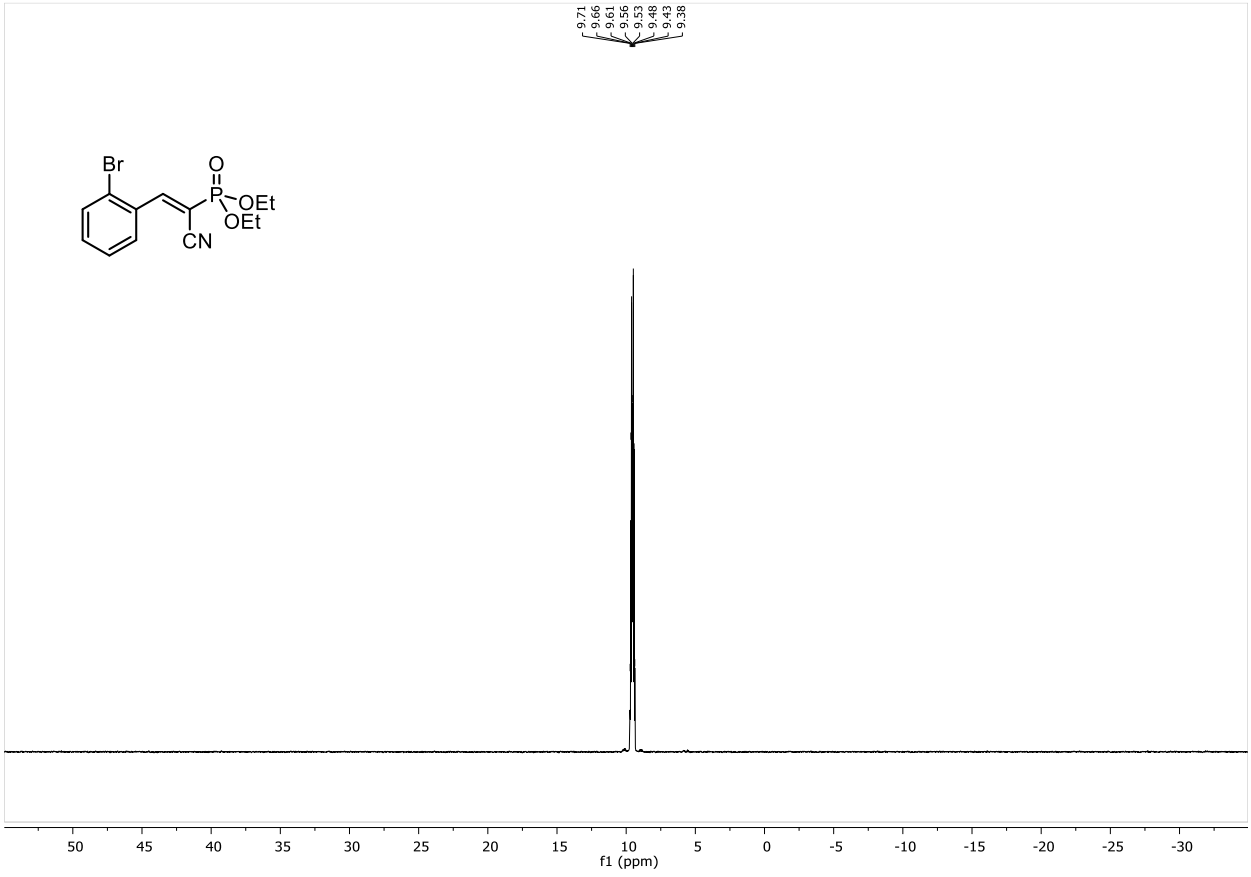
9.71
9.66
9.61
9.56
9.53
9.48
9.43
9.38
Br
O
P
OEt
OEt
CN
50 45 40 35 30 25 20 15 10 5 0 -5 -10 -15 -20 -25 -30
f1 (ppm)

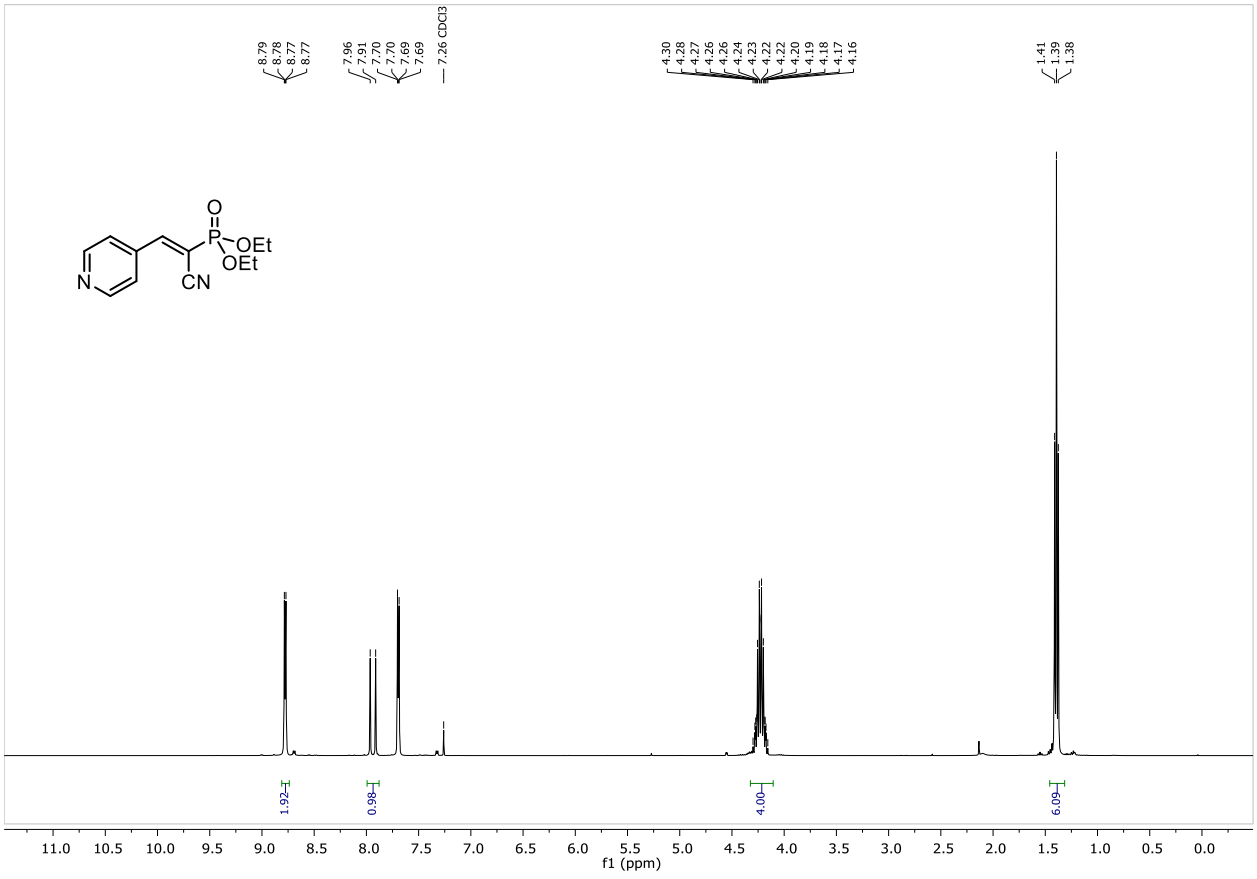
8.79
8.78
8.77
8.77
7.96
7.91
7.70
7.70
7.69
7.69
7.26 CDCl3
4.30
4.28
4.27
4.26
4.26
4.24
4.23
4.22
4.22
4.20
4.19
4.18
4.17
4.16
1.41
1.39
1.38
O
P
OEt
OEt
N
CN
1.92
0.98
4.00
6.09
11.0 10.5 10.0 9.5 9.0 8.5 8.0 7.5 7.0 6.5 6.0 5.5 5.0 4.5 4.0 3.5 3.0 2.5 2.0 1.5 1.0 0.5 0.0
f1 (ppm)

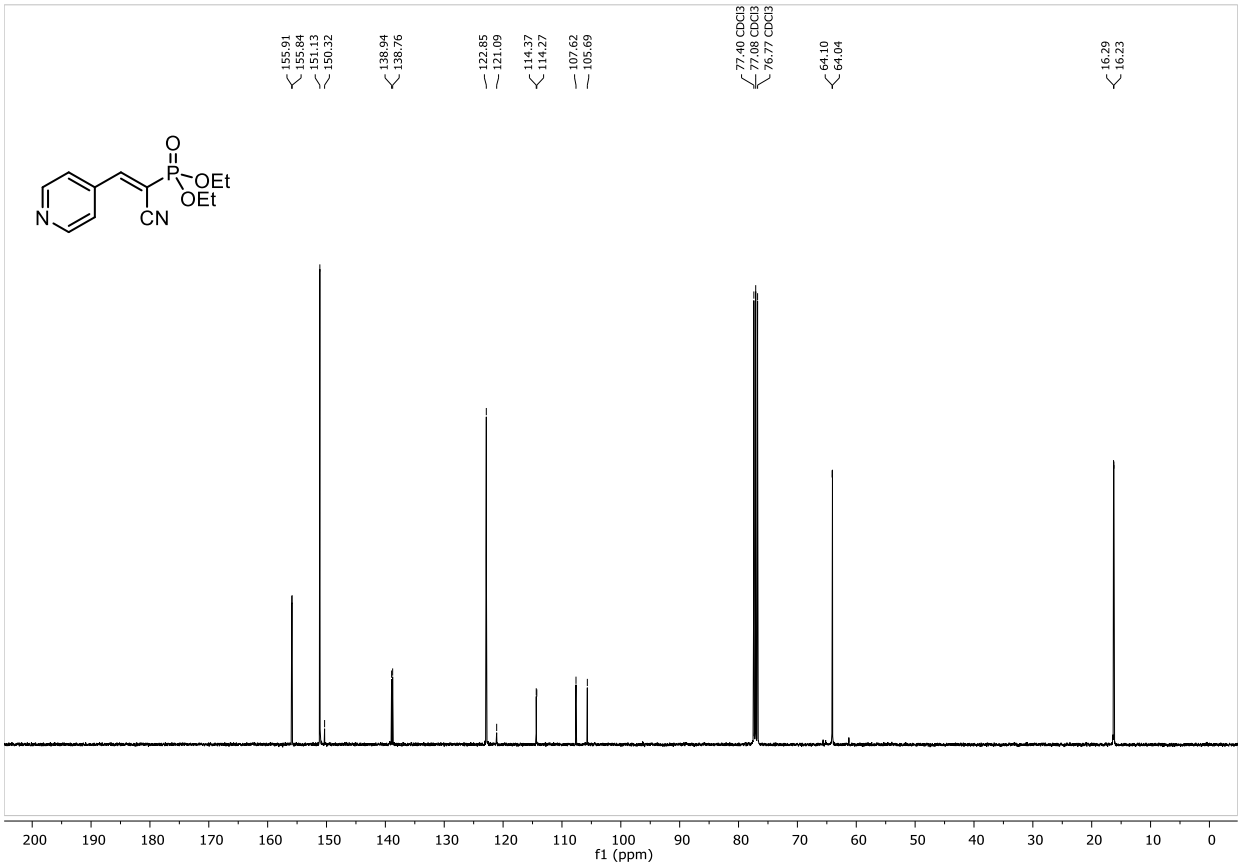
155.91
155.84
151.13
150.32
138.94
138.76
122.85
121.09
114.37
114.27
107.62
105.69
77.40 CDCl3
77.08 CDCl3
76.77 CDCl3
64.10
64.04
16.29
16.23
O
P
OEt
OEt
N
CN
200 190 180 170 160 150 140 130 120 110 100 90 80 70 60 50 40 30 20 10 0
f1 (ppm)

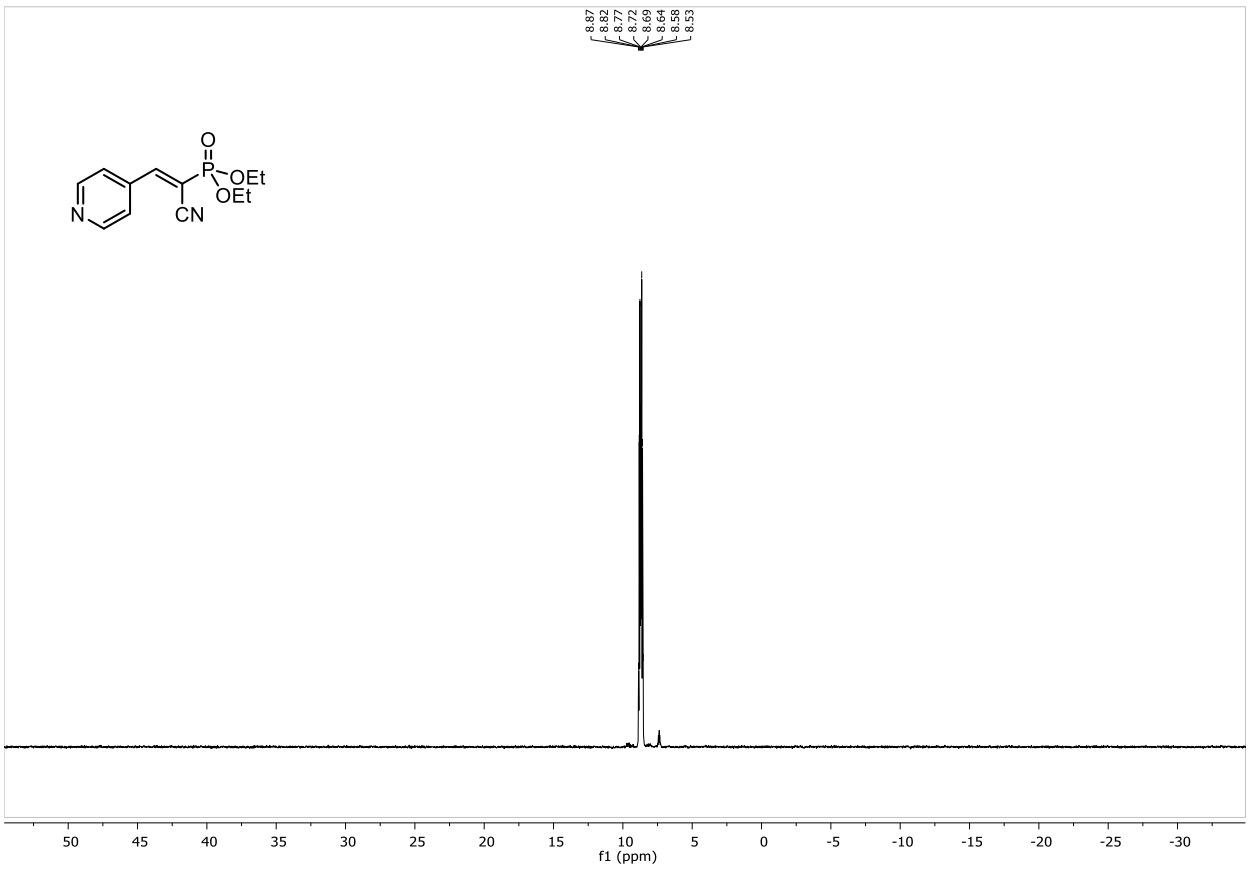
8.87
8.82
8.77
8.72
8.69
8.64
8.58
8.53
O
P
OEt
OEt
N
CN
50 45 40 35 30 25 20 15 10 5 0 -5 -10 -15 -20 -25 -30
f1 (ppm)

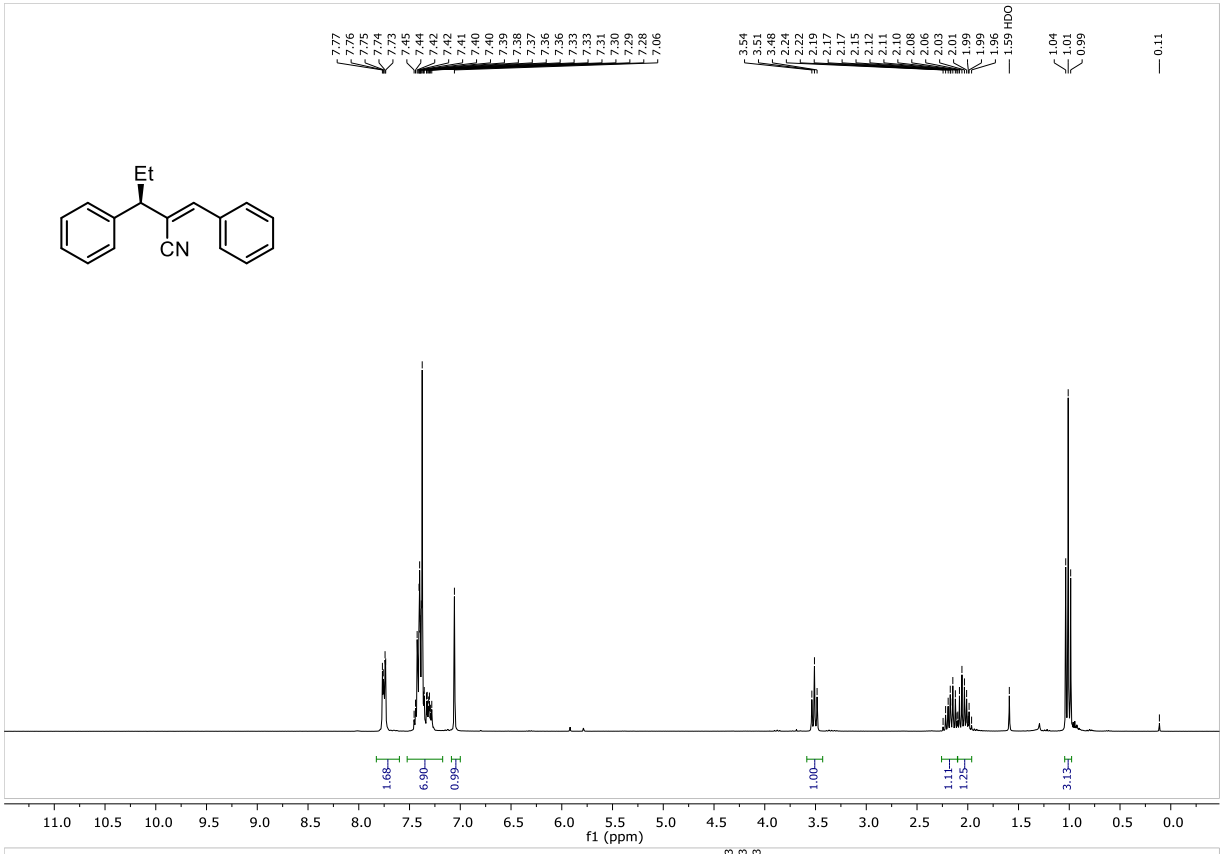
7.77
7.76
7.75
7.74
7.73
7.45
7.44
7.42
7.42
7.41
7.40
7.40
7.39
7.38
7.37
7.36
7.36
7.33
7.33
7.31
7.30
7.29
7.28
7.06
3.54
3.51
3.48
2.24
2.22
2.19
2.17
2.17
2.15
2.12
2.11
2.10
2.08
2.06
2.03
2.01
1.99
1.99
1.96
1.59 HDO
1.04
1.01
0.99
0.11
Et
CN
1.68
6.90
0.99
1.00
1.11
1.25
3.13
11.0 10.5 10.0 9.5 9.0 8.5 8.0 7.5 7.0 6.5 6.0 5.5 5.0 4.5 4.0 3.5 3.0 2.5 2.0 1.5 1.0 0.5 0.0
f1 (ppm)

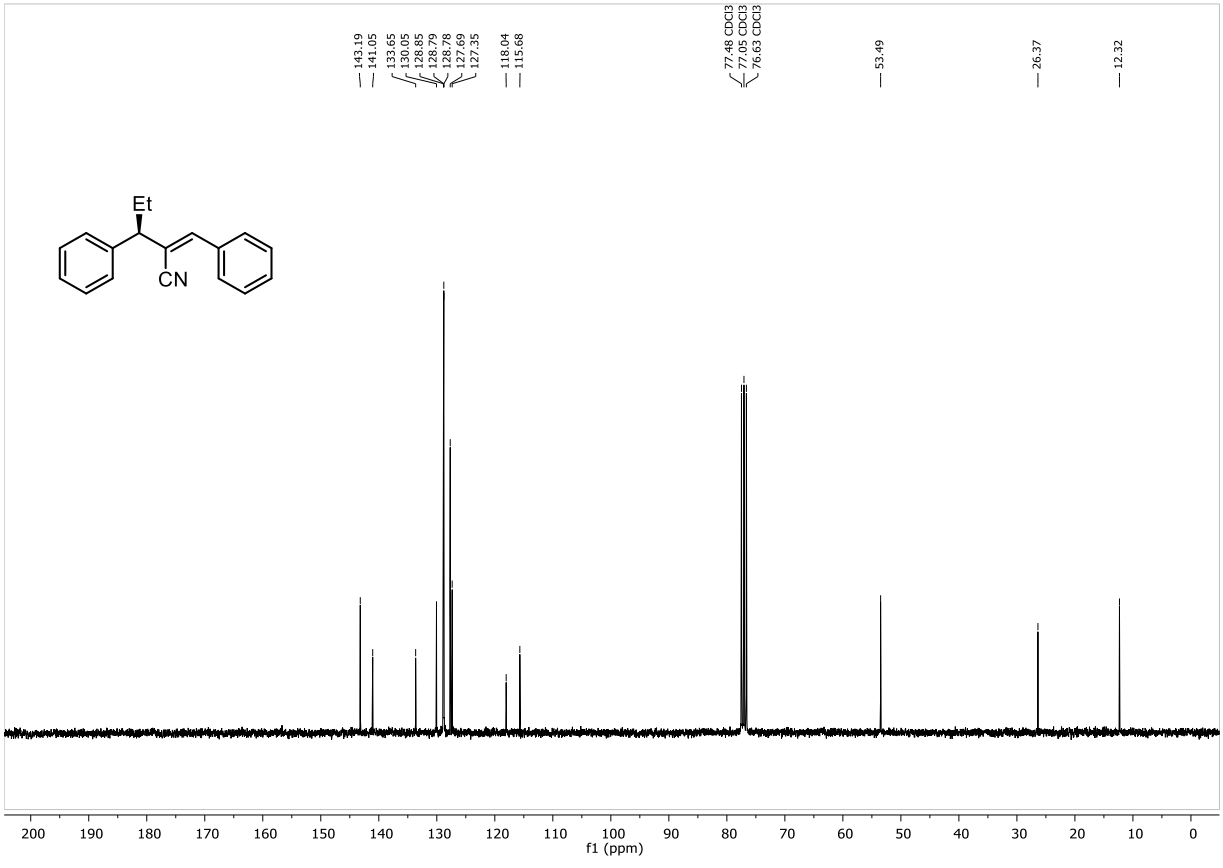
143.19
141.05
133.65
130.05
128.85
128.79
128.78
127.69
127.35
118.04
115.68
77.48 CDCl3
77.05 CDCl3
76.63 CDCl3
53.49
26.37
12.32
Et
CN
200 190 180 170 160 150 140 130 120 110 100 90 80 70 60 50 40 30 20 10 0
f1 (ppm)

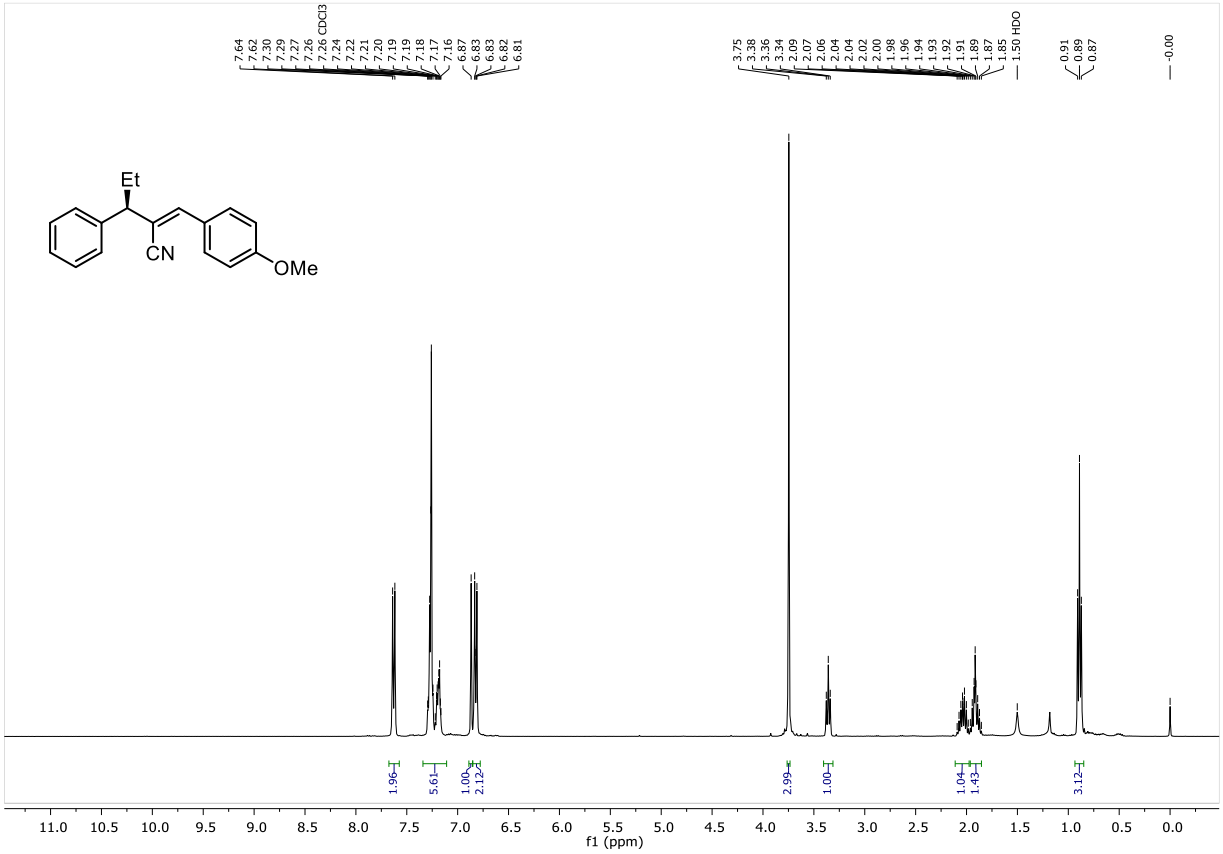
7.64
7.62
7.30
7.29
7.27
7.26 CDCl3
7.24
7.22
7.21
7.20
7.19
7.18
7.17
7.16
6.87
6.83
6.83
6.82
6.81
3.75
3.38
3.36
3.34
2.09
2.07
2.06
2.04
2.04
2.02
2.00
1.98
1.96
1.94
1.93
1.92
1.91
1.89
1.87
1.85
1.50 HDO
0.91
0.89
0.87
-0.00
Et
CN
OMe
1.96
5.61
1.00
2.12
2.99
1.00
1.04
1.43
3.12
11.0 10.5 10.0 9.5 9.0 8.5 8.0 7.5 7.0 6.5 6.0 5.5 5.0 4.5 4.0 3.5 3.0 2.5 2.0 1.5 1.0 0.5 0.0
f1 (ppm)

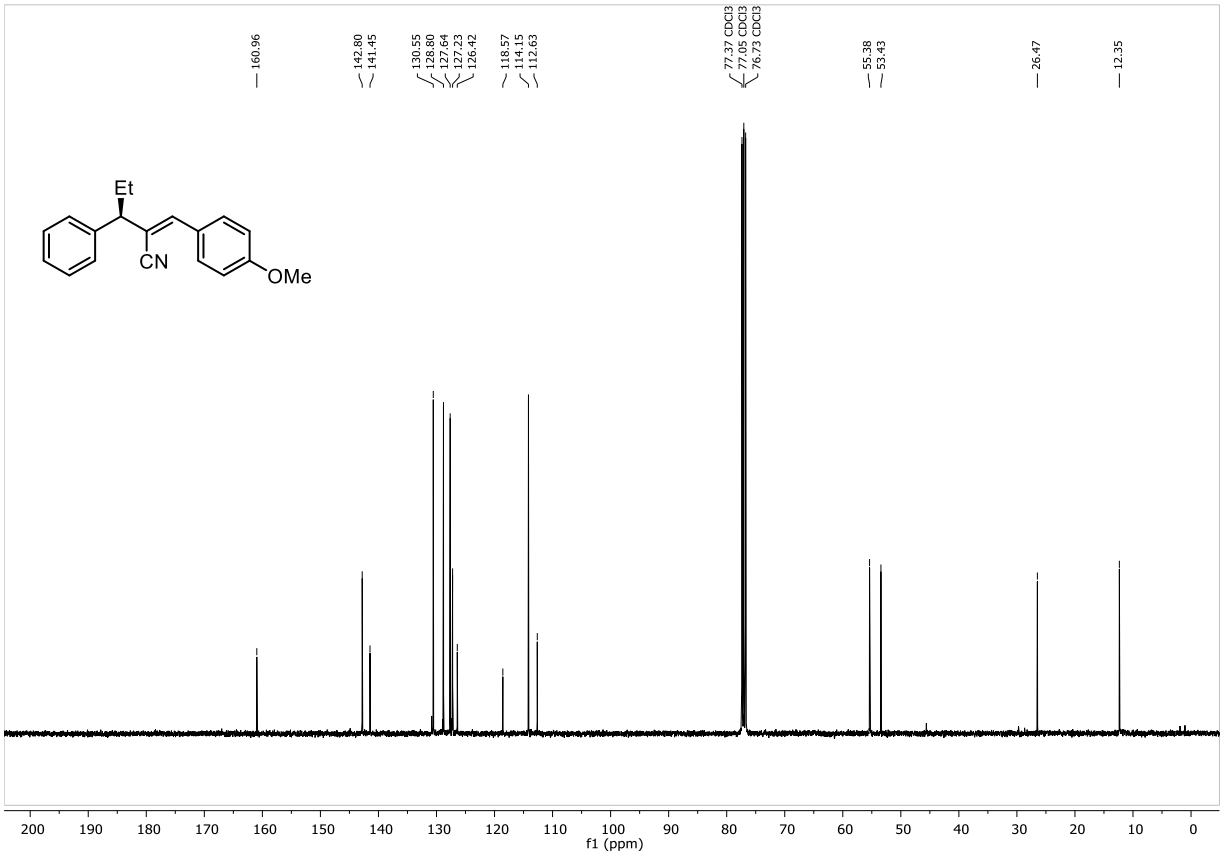
160.96
142.80
141.45
130.55
128.80
127.64
127.23
126.42
118.57
114.15
112.63
77.37 CDCl3
77.05 CDCl3
76.73 CDCl3
55.38
53.43
26.47
12.35
Et
CN
OMe
200 190 180 170 160 150 140 130 120 110 100 90 80 70 60 50 40 30 20 10 0
f1 (ppm)

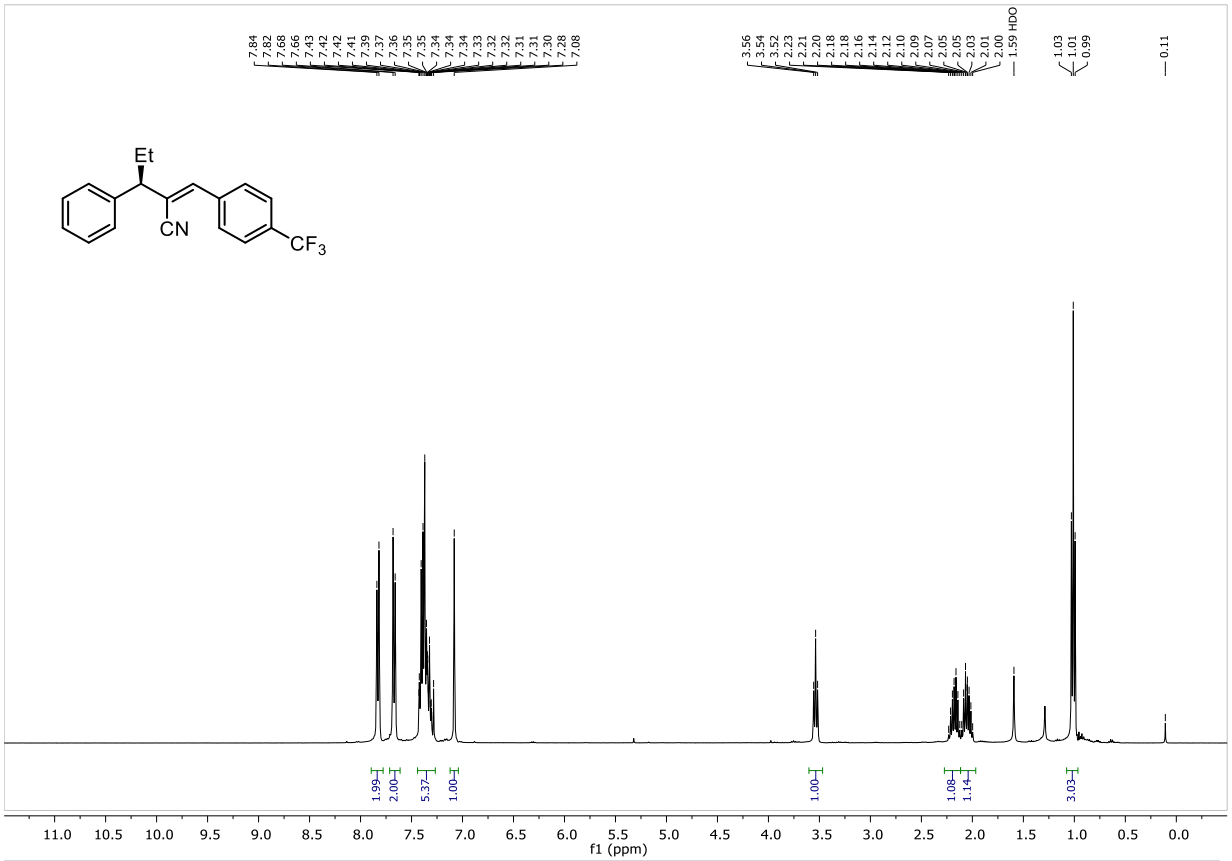
Et
CN
CF3
f1 (ppm)

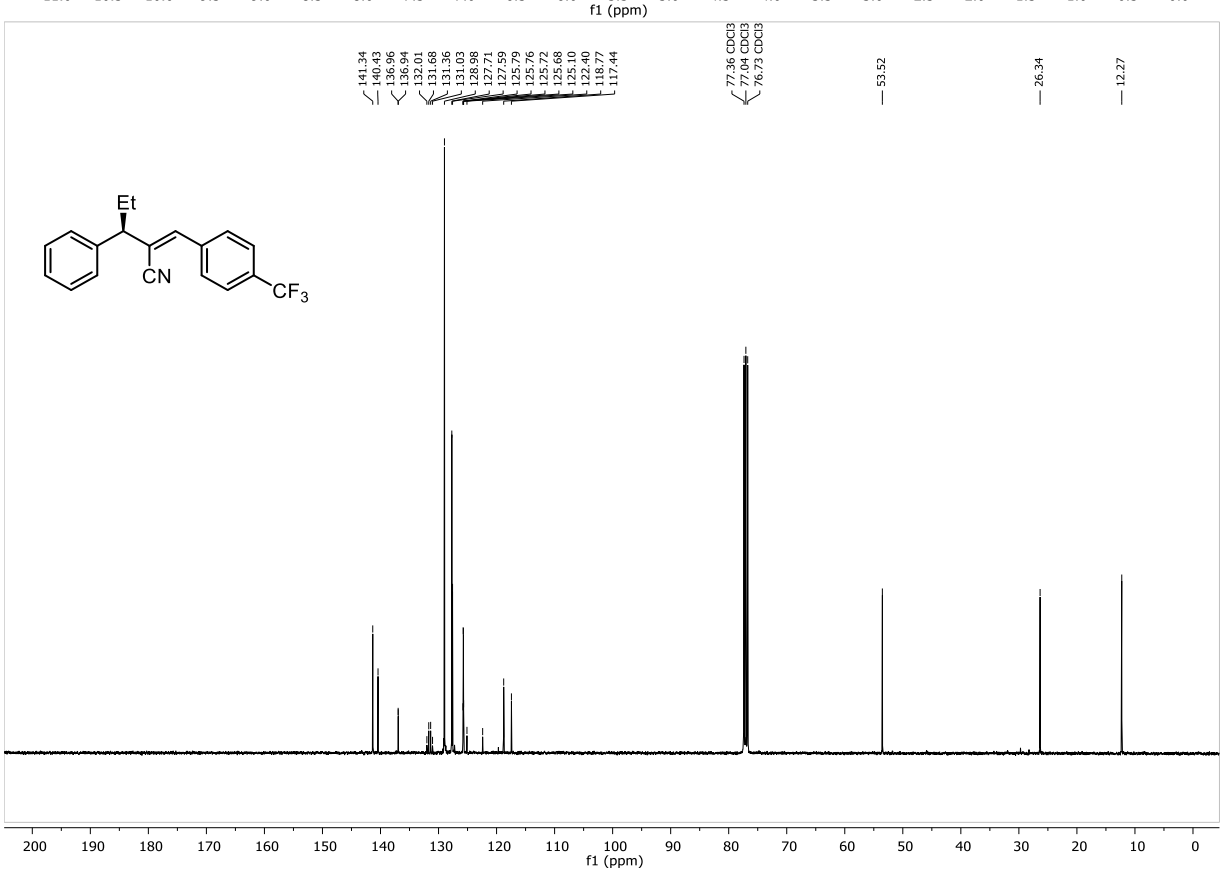
Et
CN
CF3
f1 (ppm)

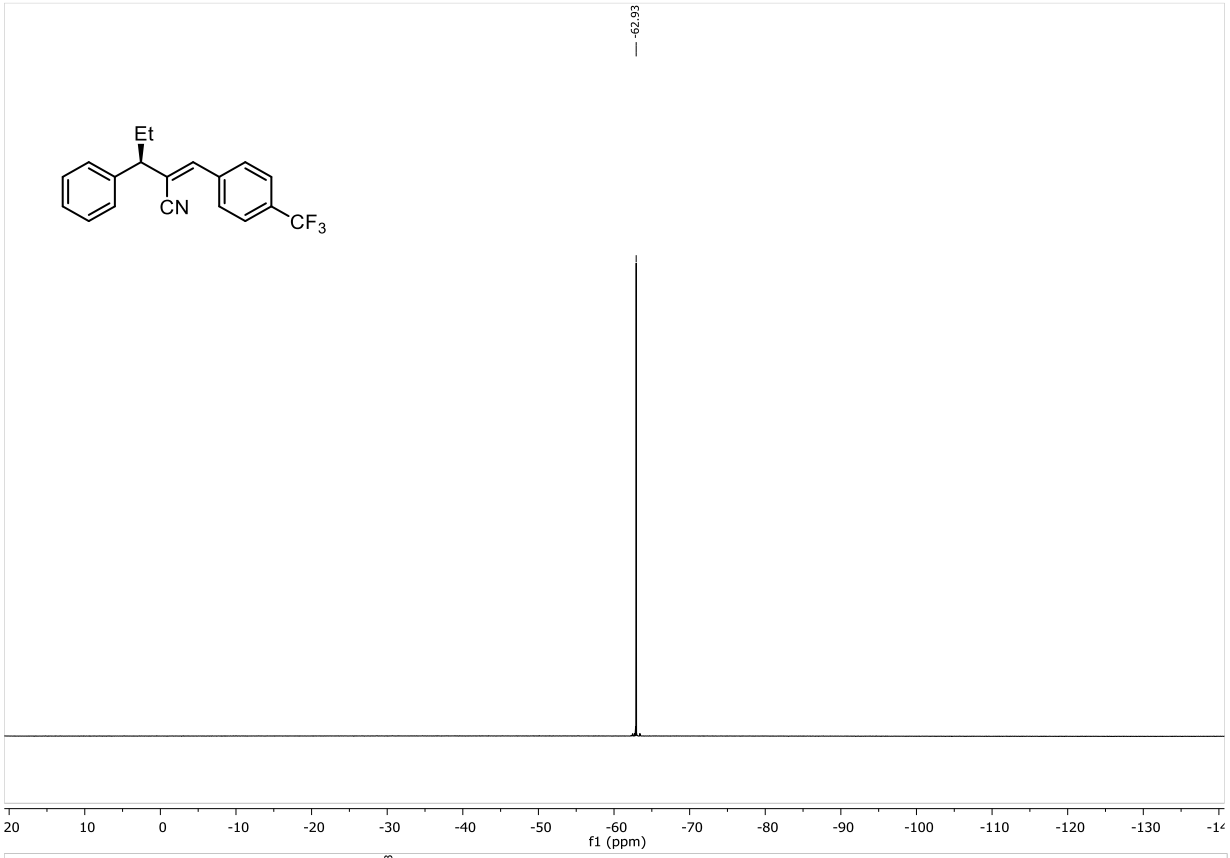
-62.93
Et
CN
CF3
f1 (ppm)

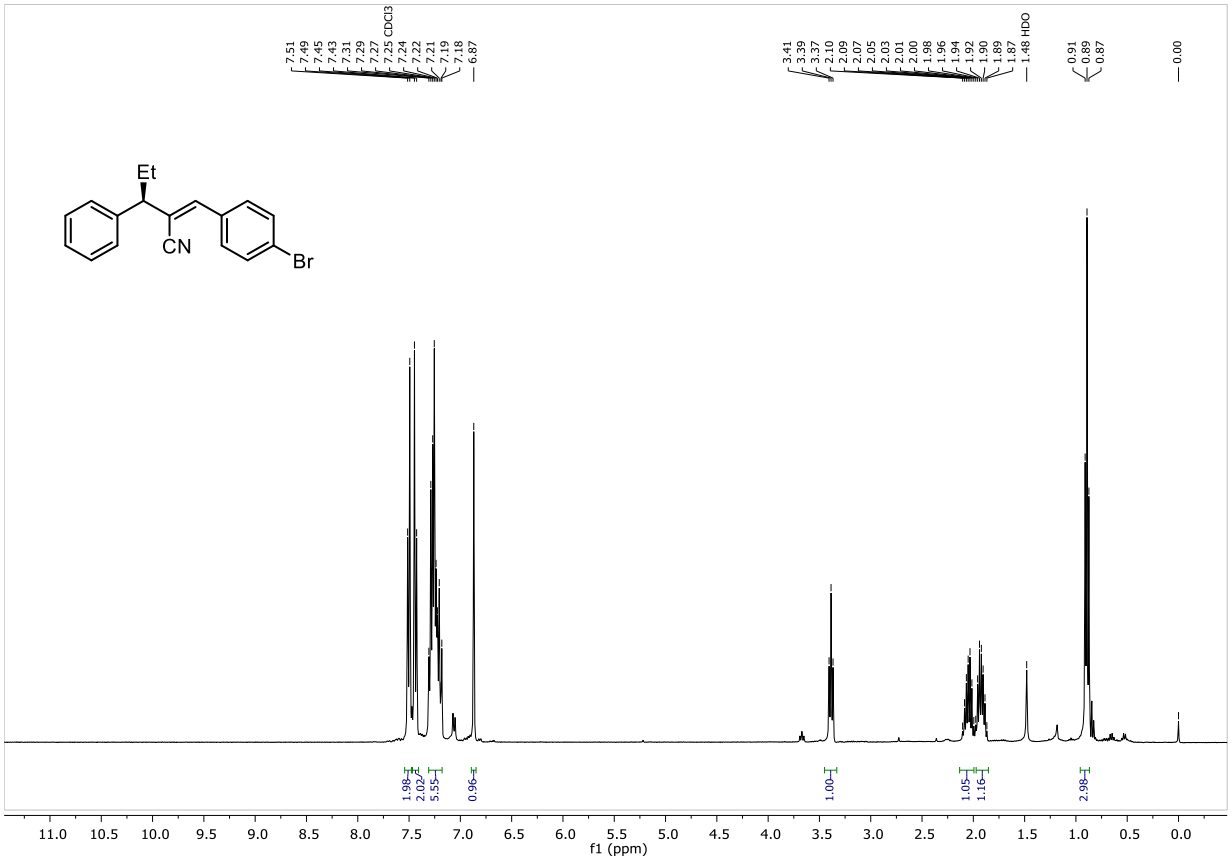
7.51
7.49
7.45
7.43
7.31
7.29
7.27
7.25 CDCl3
7.24
7.22
7.21
7.19
7.18
6.87
3.41
3.39
3.37
2.10
2.09
2.07
2.05
2.03
2.01
2.00
1.98
1.96
1.94
1.92
1.90
1.89
1.87
1.48 HDO
0.91
0.89
0.87
0.00
Et
CN
Br
1.98
2.02
5.55
0.96
1.00
1.05
1.16
2.98
f1 (ppm)

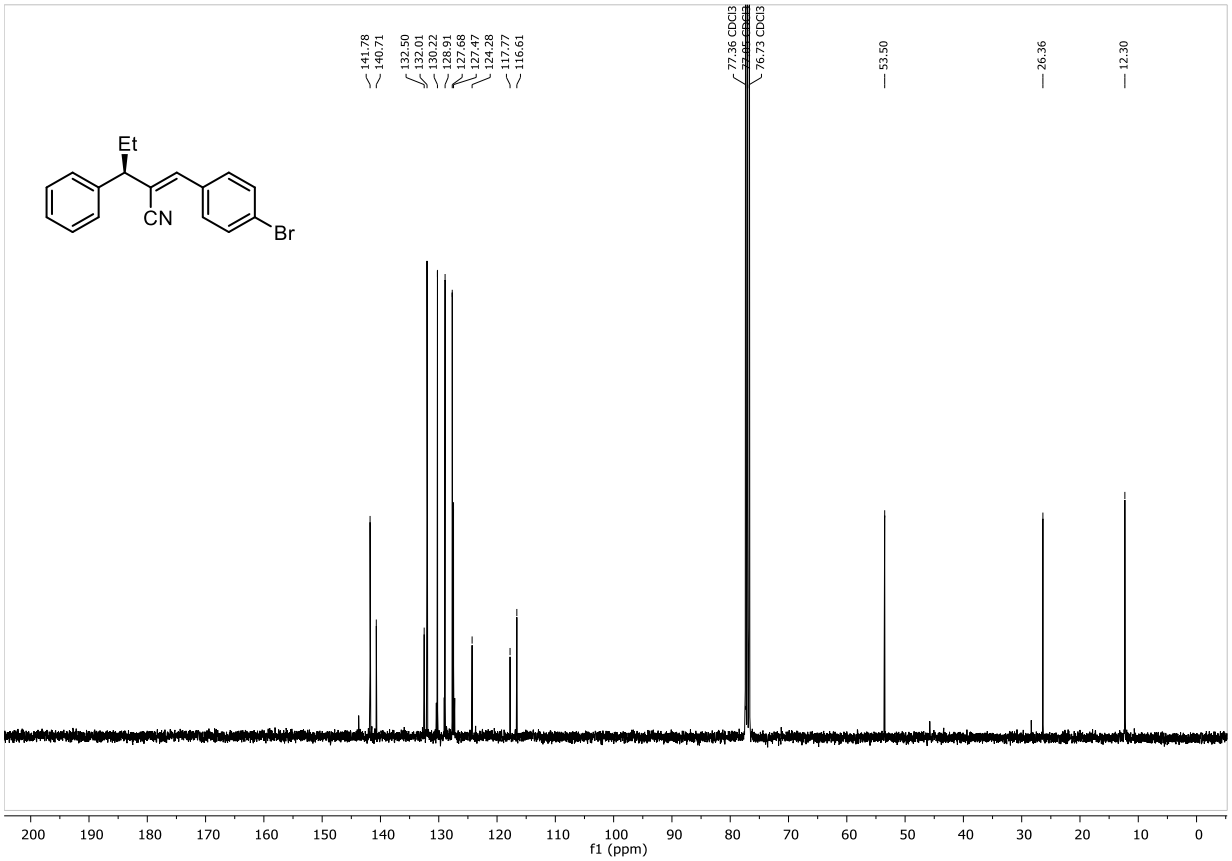
141.78
140.71
132.50
132.01
130.22
128.91
127.68
127.47
124.28
117.77
116.61
77.36 CDCl3
76.73 CDCl3
53.50
26.36
12.30
Et
CN
Br
f1 (ppm)

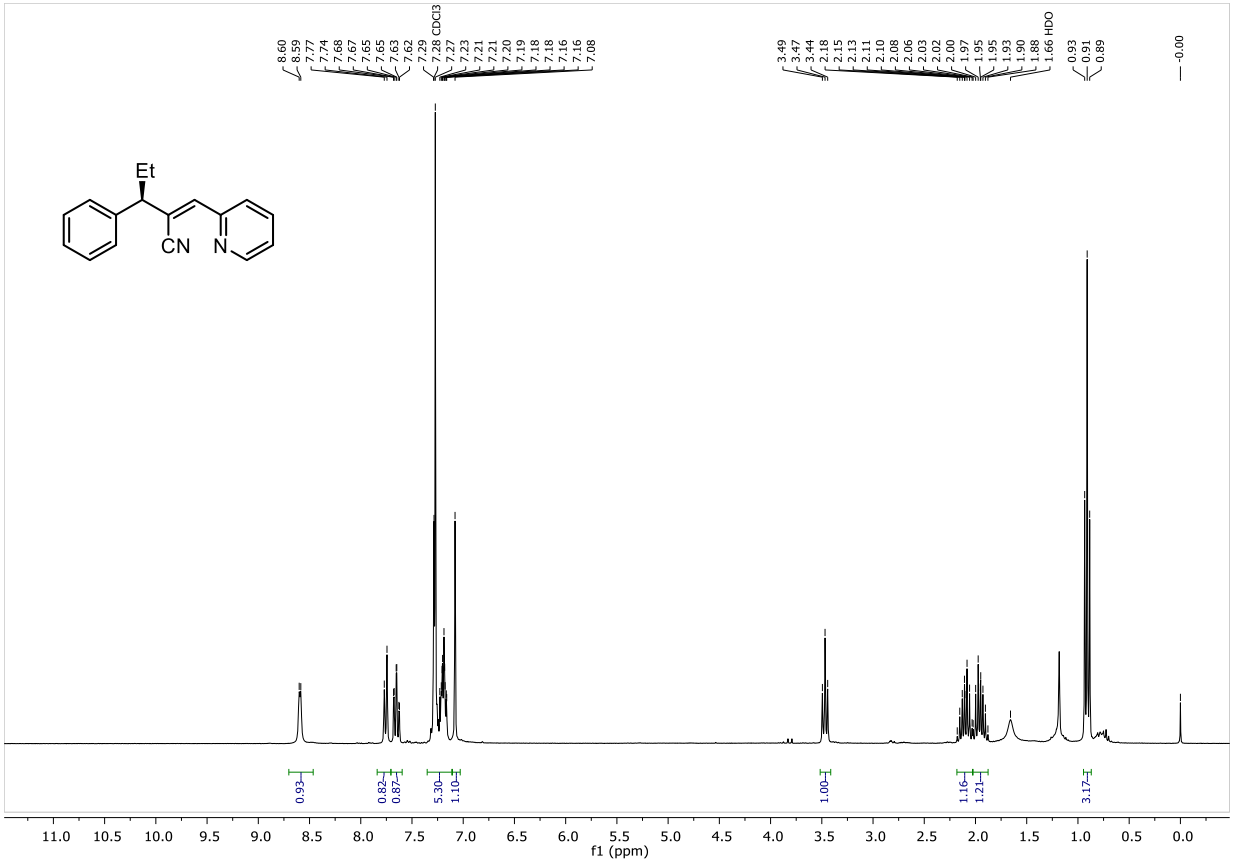
8.60
8.59
7.77
7.74
7.68
7.67
7.65
7.65
7.63
7.62
7.29
7.28 CDCl3
7.27
7.23
7.21
7.21
7.20
7.19
7.18
7.18
7.16
7.16
7.08
3.49
3.47
3.44
2.18
2.15
2.13
2.11
2.10
2.08
2.06
2.03
2.02
2.00
1.97
1.95
1.95
1.93
1.90
1.88
1.66 HDO
0.93
0.91
0.89
-0.00
Et
CN
N
0.93
0.82
0.87
5.30
1.10
1.00
1.16
1.21
3.17
f1 (ppm)

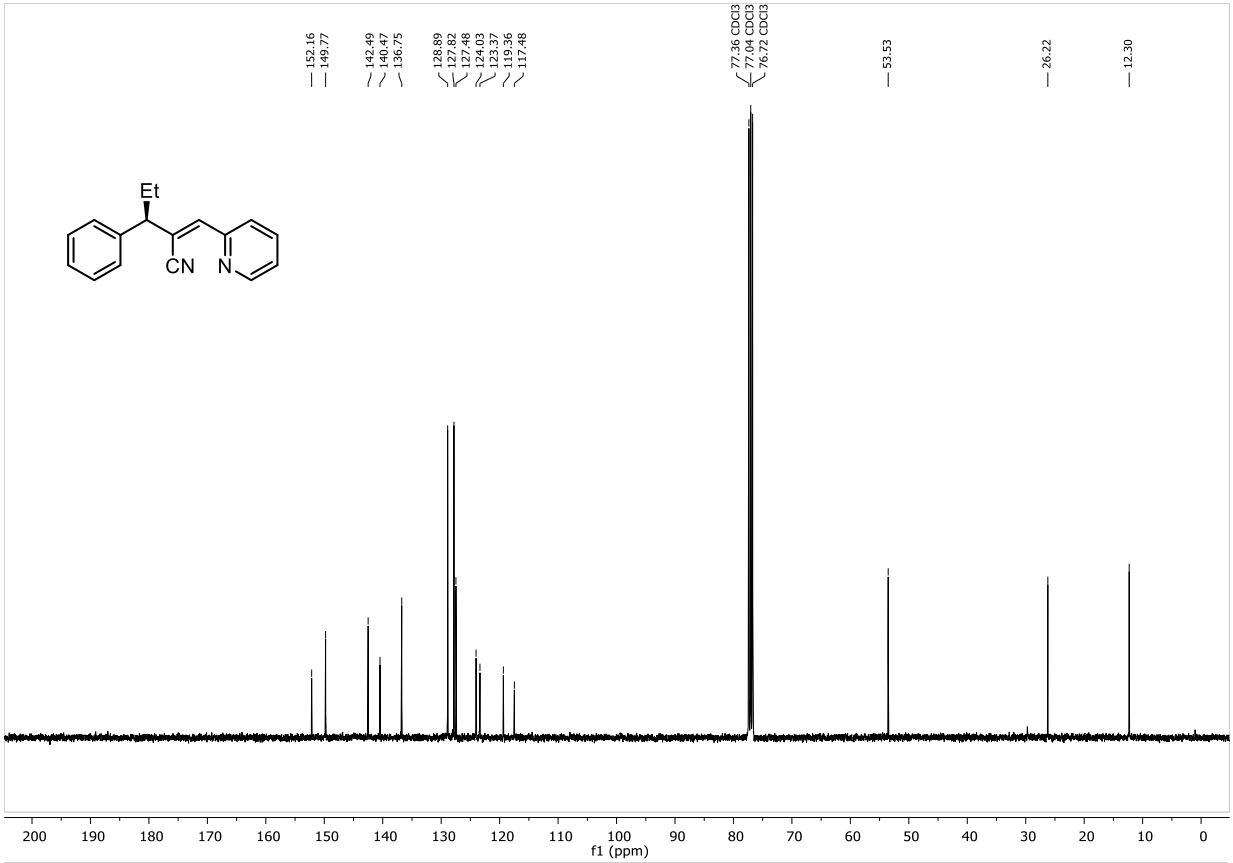
152.16
149.77
142.49
140.47
136.75
128.89
127.82
127.48
124.03
123.37
119.36
117.48
77.36 CDCl3
77.04 CDCl3
76.72 CDCl3
53.53
26.22
12.30
Et
CN
N
f1 (ppm)

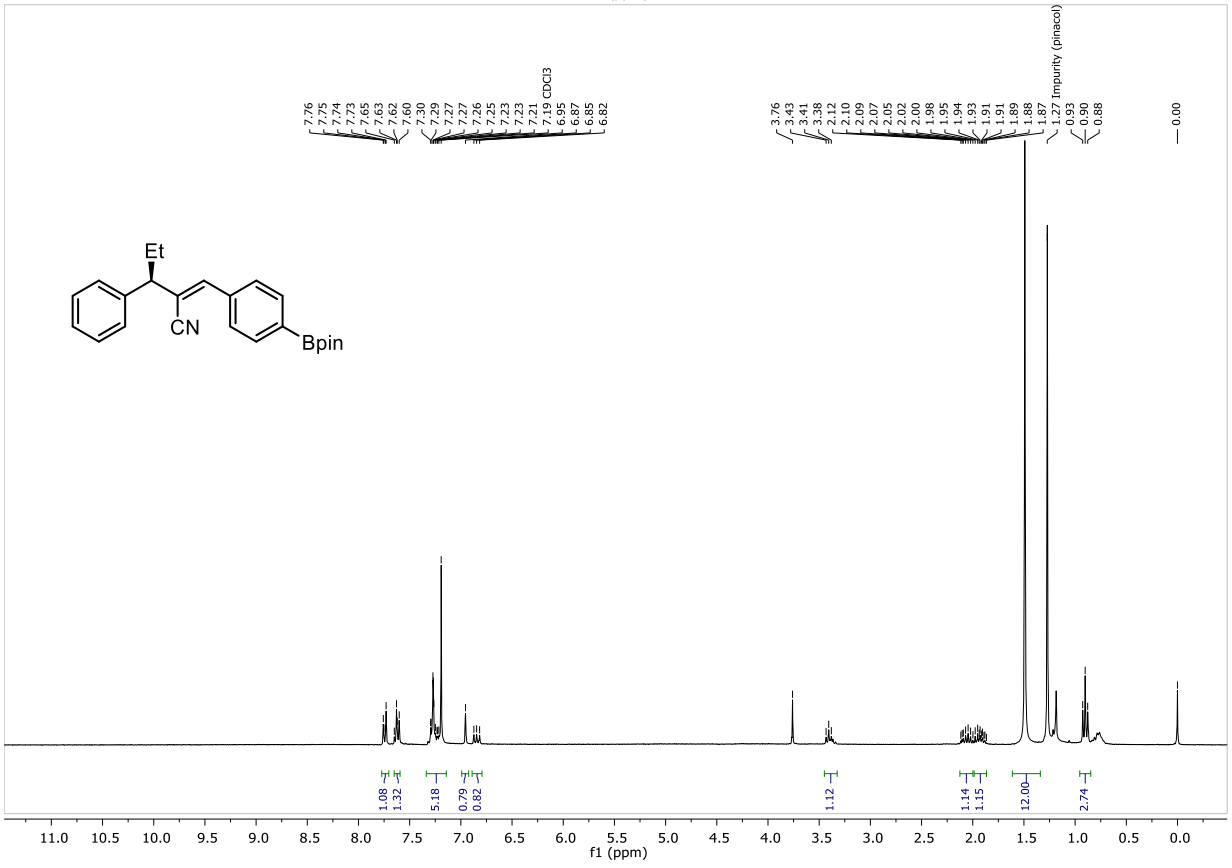
7.76
7.75
7.74
7.73
7.65
7.63
7.62
7.60
7.30
7.29
7.27
7.27
7.26
7.25
7.23
7.23
7.21
7.19 CDCl3
6.95
6.87
6.85
6.82
3.76
3.43
3.41
3.38
2.12
2.10
2.09
2.07
2.05
2.02
2.00
1.98
1.95
1.94
1.93
1.91
1.91
1.89
1.88
1.87
1.27 Impurity (pinacol)
0.93
0.90
0.88
0.00
Et
CN
Bpin
1.08
1.32
5.18
0.79
0.82
1.12
1.14
1.15
12.00
2.74
f1 (ppm)

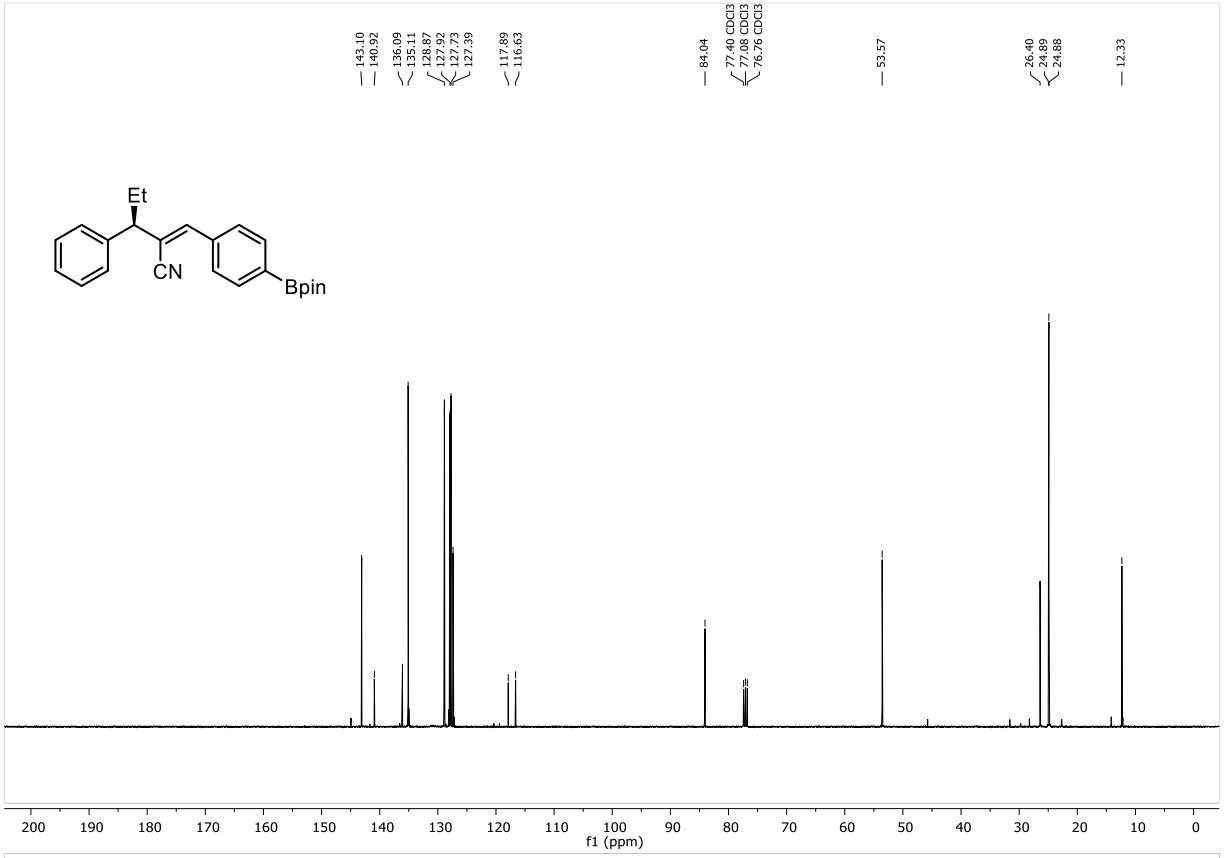
143.10
140.92
136.09
135.11
128.87
127.92
127.73
127.39
117.89
116.63
84.04
77.40 CDCl3
77.08 CDCl3
76.76 CDCl3
53.57
26.40
24.89
24.88
12.33
Et
CN
Bpin
f1 (ppm)

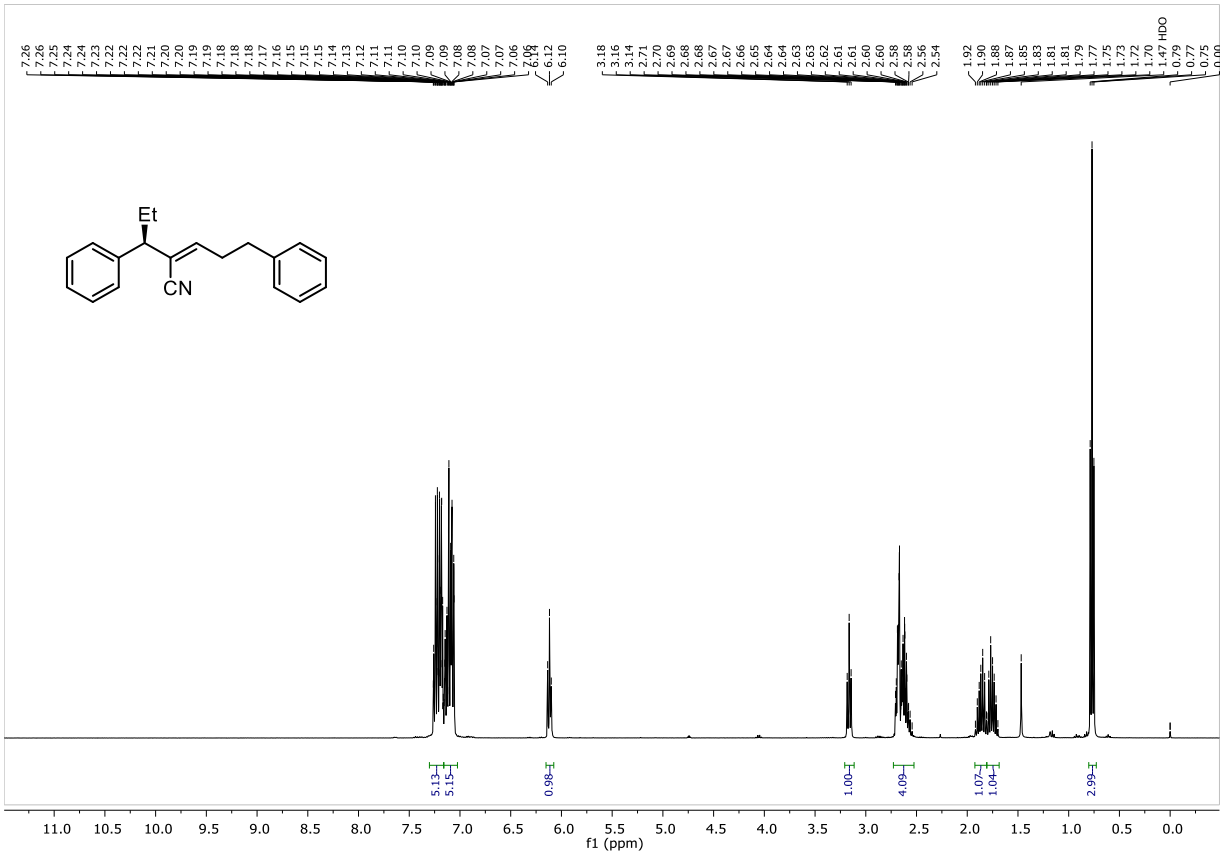
HDO
Et
CN
5.13
5.15
0.98
1.00
4.09
1.07
1.04
2.99
f1 (ppm)

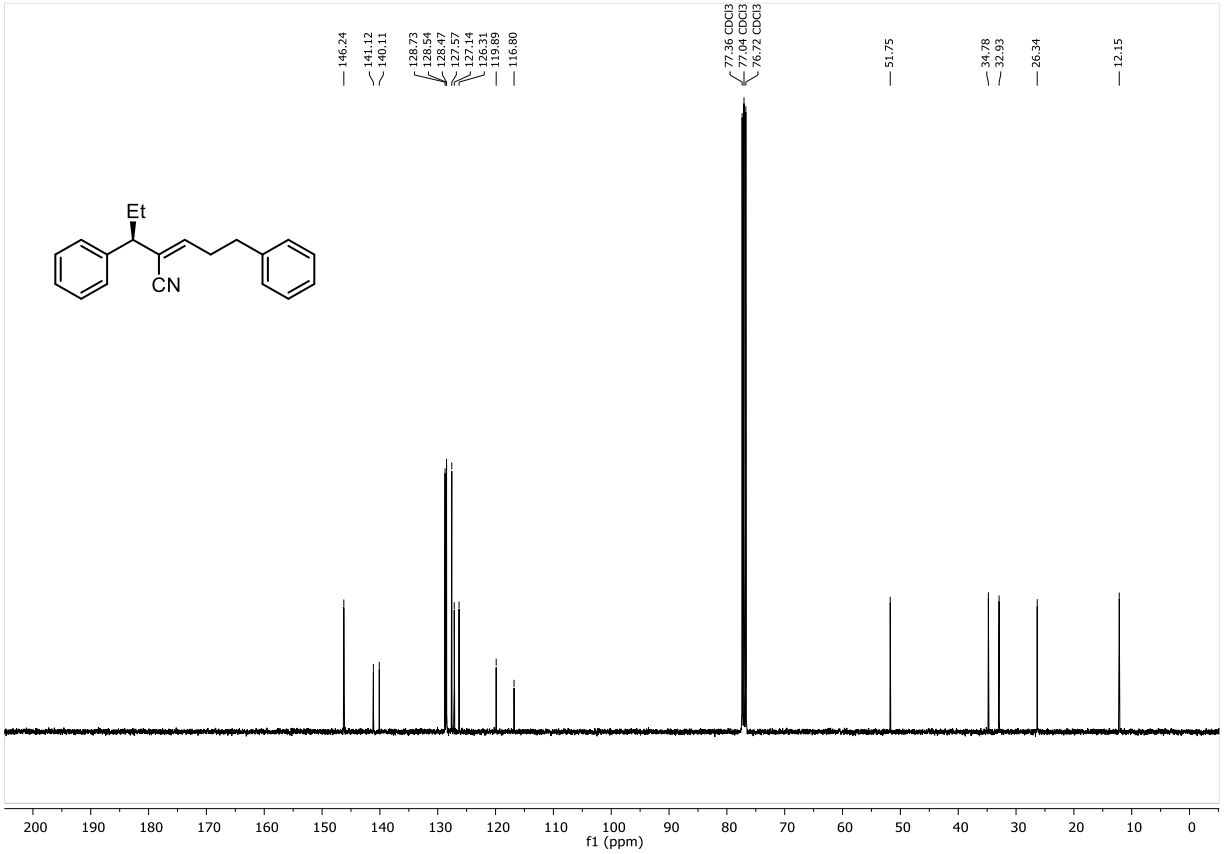
146.24
141.12
140.11
128.73
128.54
128.47
127.57
127.14
126.31
119.89
116.80
77.36 CDCl3
77.04 CDCl3
76.72 CDCl3
51.75
34.78
32.93
26.34
12.15
Et
CN
f1 (ppm)

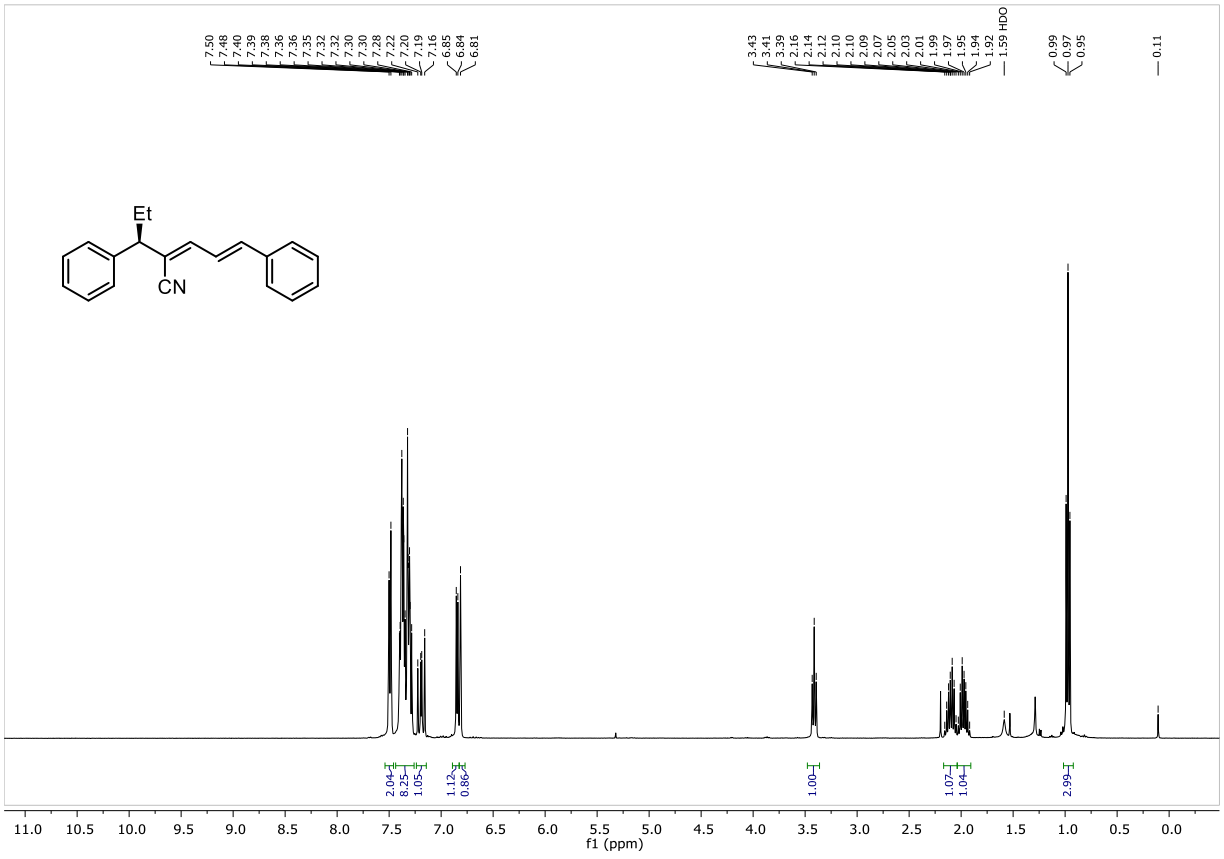
7.50
7.48
7.40
7.39
7.38
7.36
7.36
7.35
7.32
7.32
7.30
7.30
7.28
7.22
7.20
7.19
7.16
6.85
6.84
6.81
3.43
3.41
3.39
2.16
2.14
2.12
2.10
2.10
2.09
2.07
2.05
2.03
2.01
1.99
1.97
1.95
1.94
1.92
1.59 HDO
0.99
0.97
0.95
0.11
Et
CN
2.04
8.25
1.05
1.12
0.86
1.00
1.07
1.04
2.99
f1 (ppm)

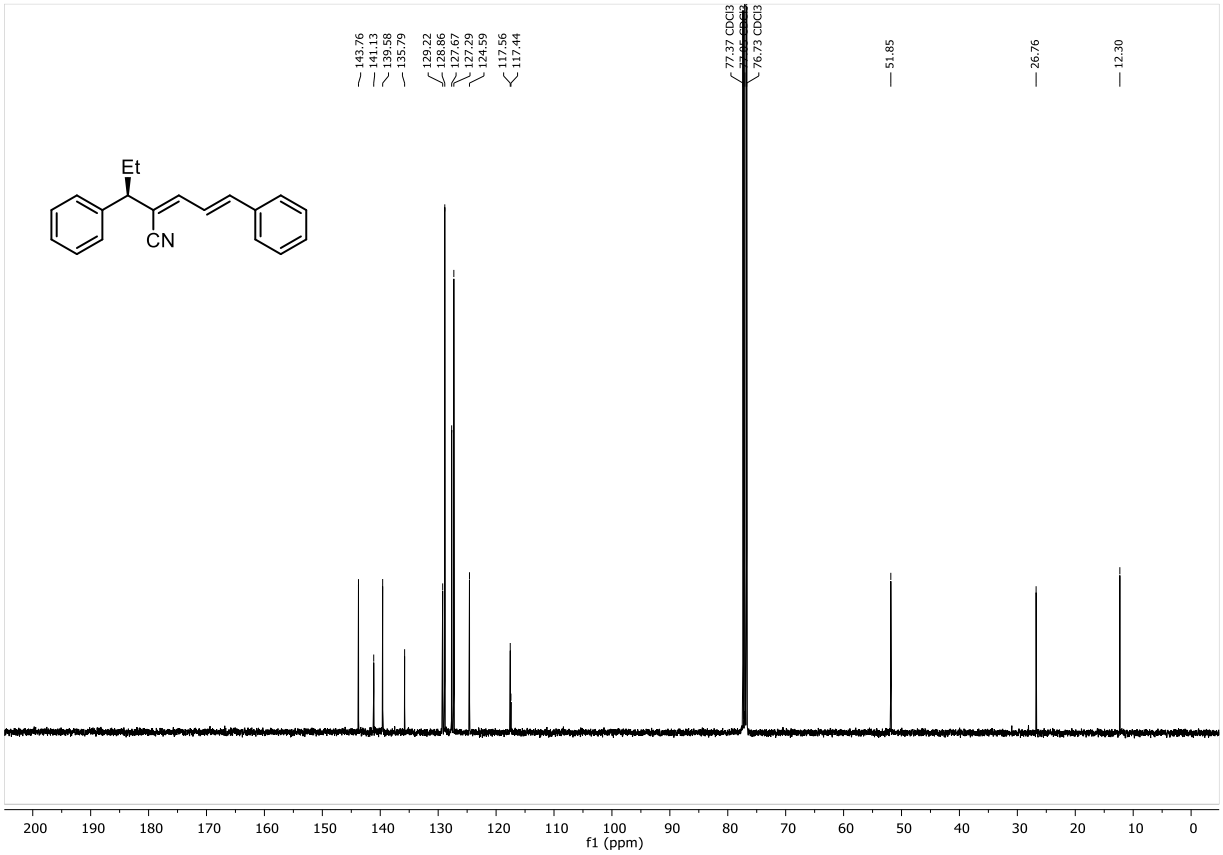
143.76
141.13
139.58
135.79
129.22
128.86
127.67
127.29
124.59
117.56
117.44
77.37 CDCl3
76.73 CDCl3
51.85
26.76
12.30
Et
CN
f1 (ppm)

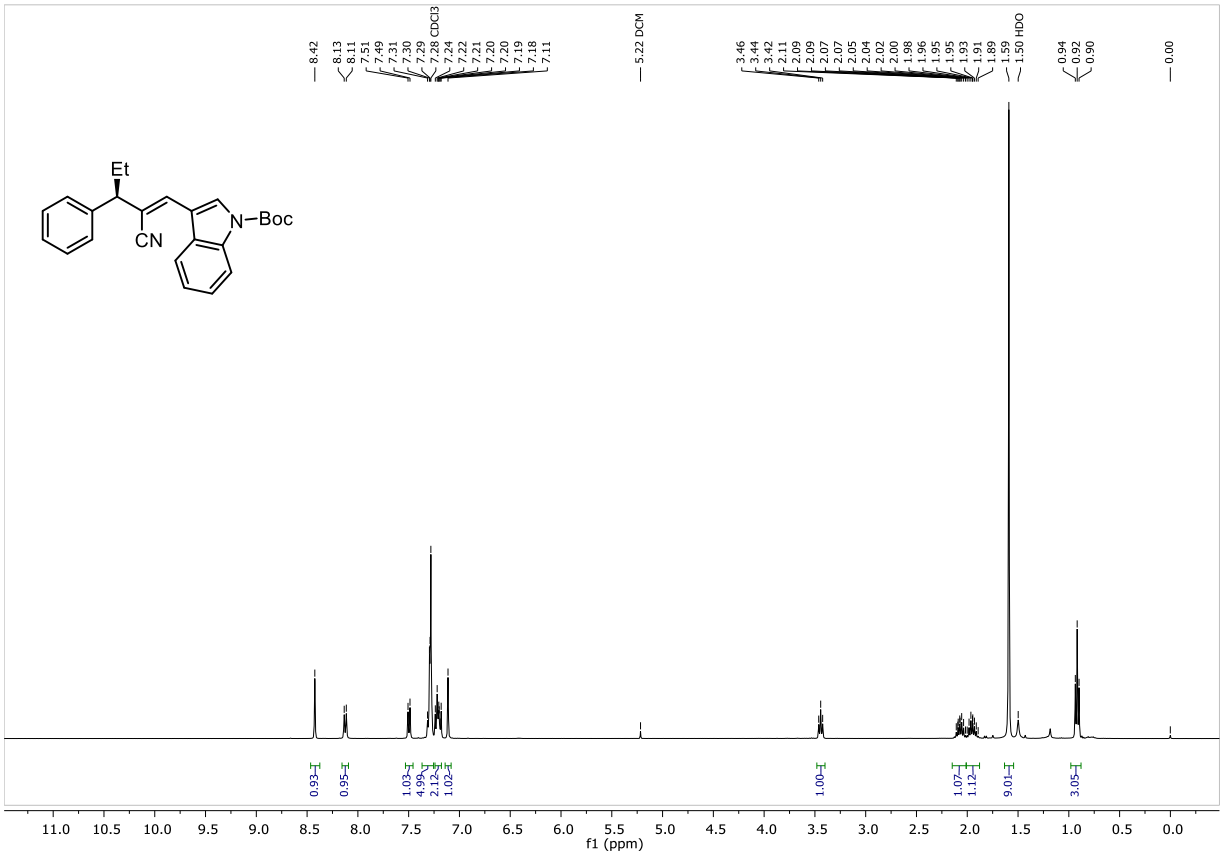
8.42
8.13
8.11
7.51
7.49
7.31
7.30
7.28 CDCl3
7.24
7.22
7.21
7.20
7.19
7.18
7.11
5.22 DCM
3.46
3.44
3.42
2.11
2.09
2.09
2.07
2.07
2.05
2.04
2.02
2.00
1.98
1.96
1.95
1.95
1.93
1.91
1.89
1.59
1.50 HDO
0.94
0.92
0.90
0.00
Et
CN
N–Boc
0.93
0.95
1.03
4.99
2.12
1.02
1.00
1.07
1.12
9.01
3.05
f1 (ppm)

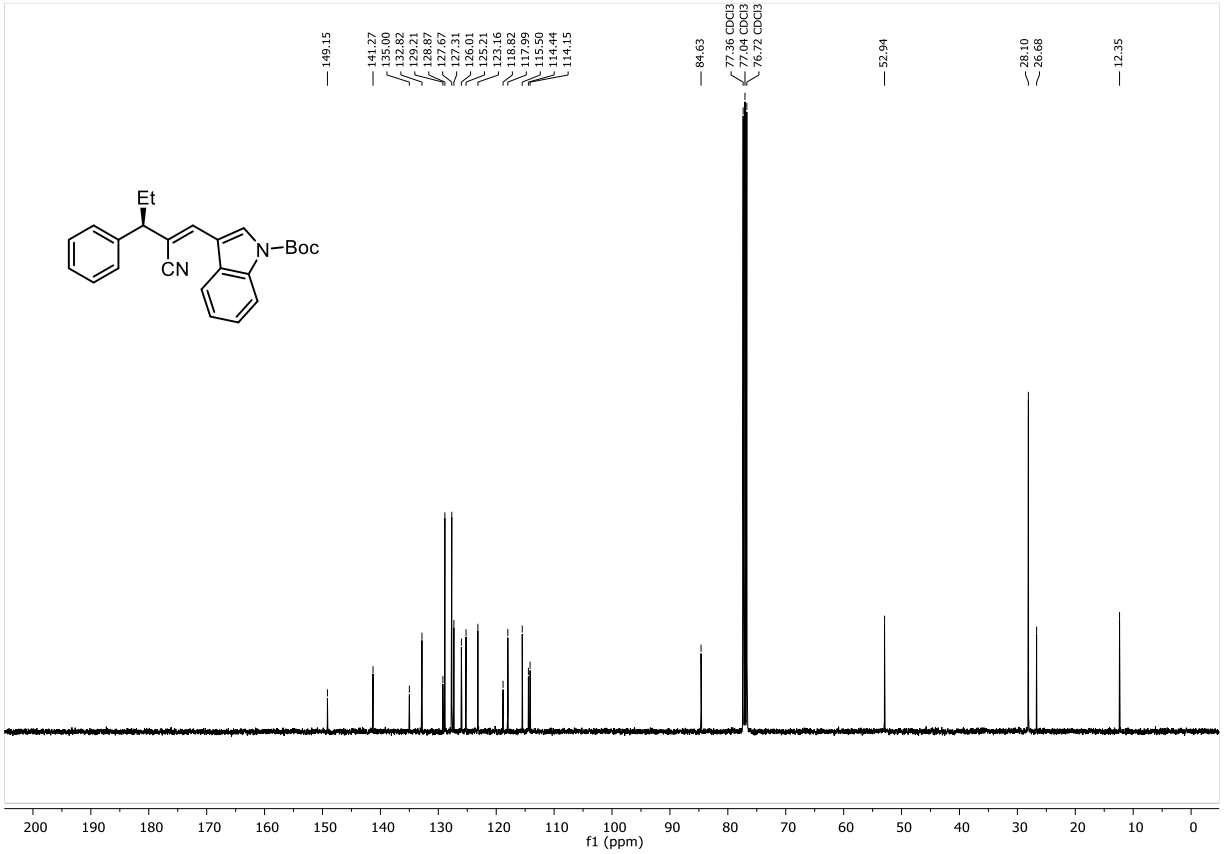
149.15
141.27
135.00
132.82
129.21
128.87
127.67
127.31
126.01
125.21
123.16
118.82
117.99
115.50
114.44
114.15
84.63
77.36 CDCl3
77.04 CDCl3
76.72 CDCl3
52.94
28.10
26.68
12.35
Et
CN
N–Boc
f1 (ppm)

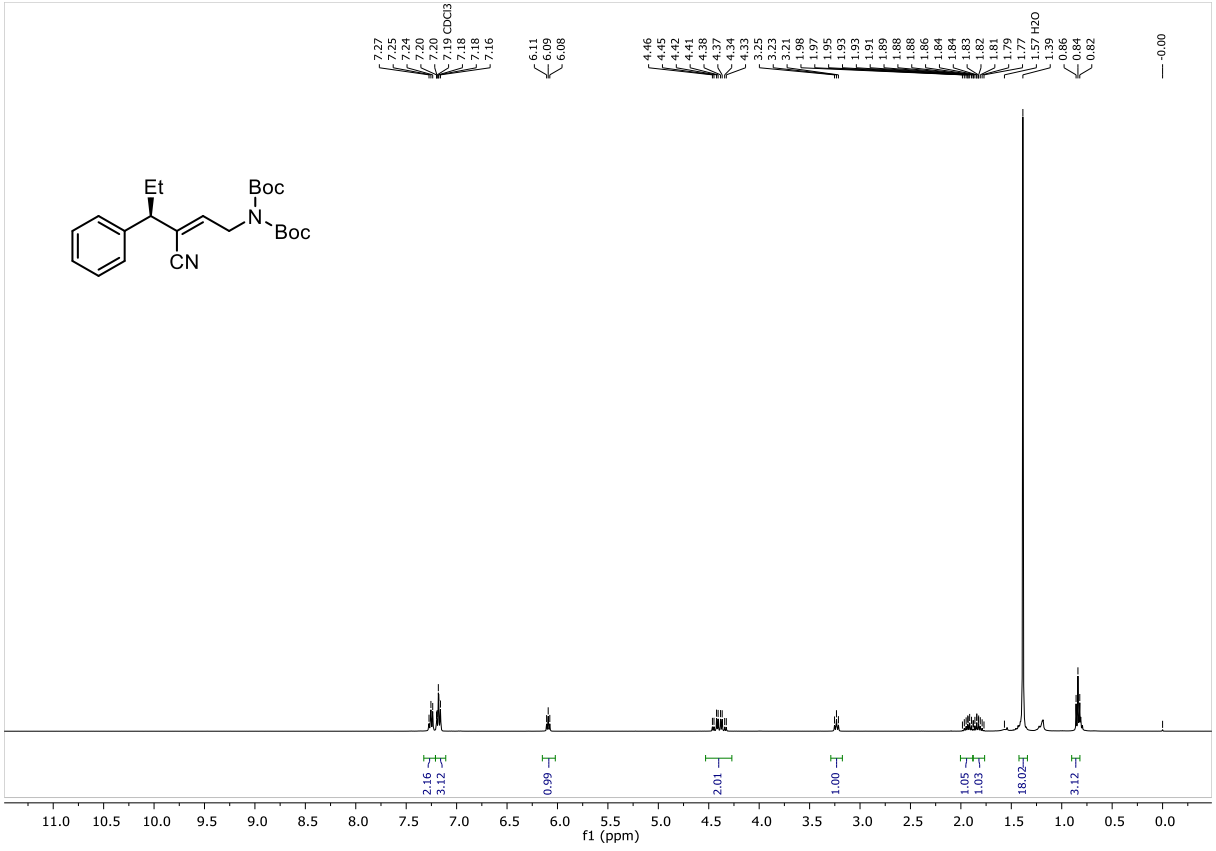
7.27
7.25
7.24
7.20
CDCl3
7.19
7.18
7.18
7.16
6.11
6.09
6.08
4.46
4.45
4.42
4.41
4.38
4.37
4.34
4.33
3.25
3.23
3.21
1.98
1.97
1.95
1.93
1.93
1.91
1.89
1.88
1.88
1.86
1.84
1.84
1.83
1.82
1.81
1.79
1.77
1.57 H2O
1.39
0.86
0.84
0.82
-0.00
Et
Boc
N
Boc
CN
2.16
3.12
0.99
2.01
1.00
1.05
1.03
18.02
3.12
f1 (ppm)

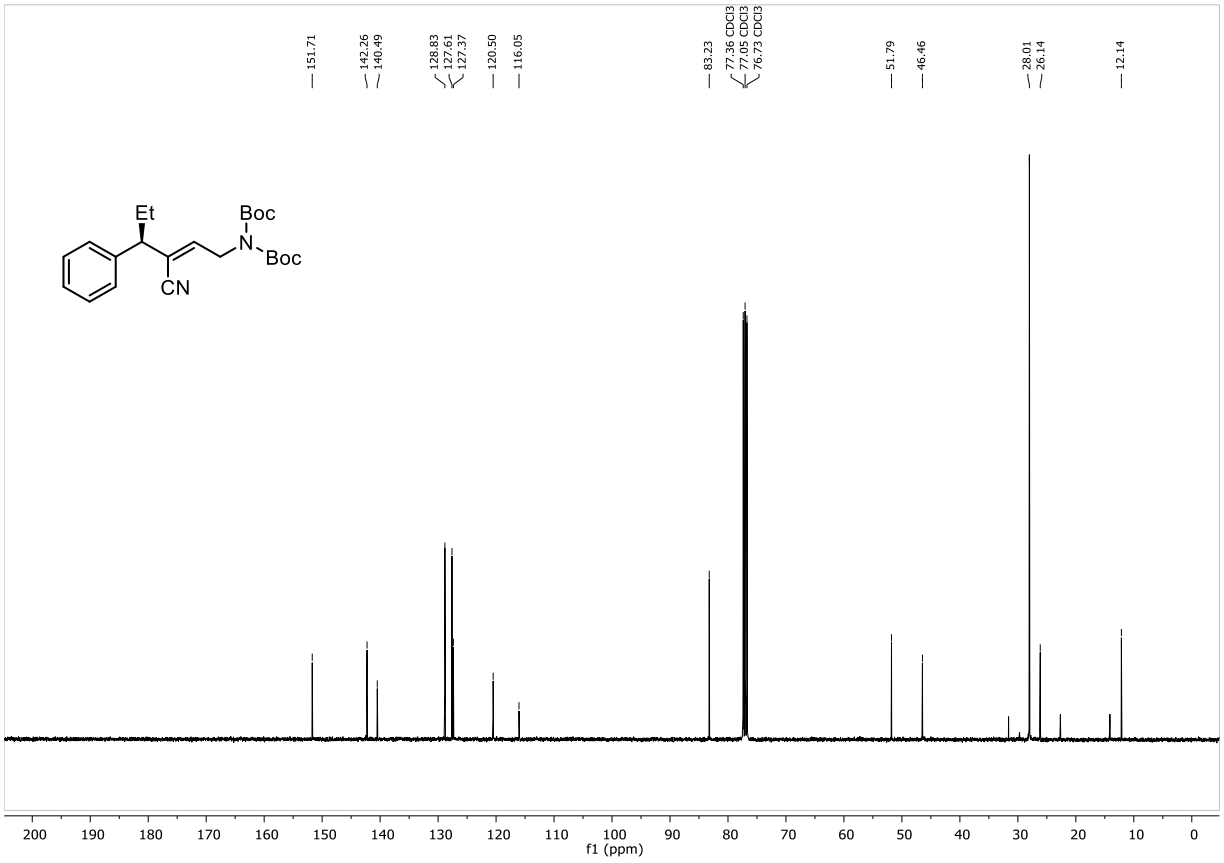
151.71
142.26
140.49
128.83
127.61
127.37
120.50
116.05
83.23
77.36 CDCl3
77.05 CDCl3
76.73 CDCl3
51.79
46.46
28.01
26.14
12.14
Et
Boc
N
Boc
CN
f1 (ppm)

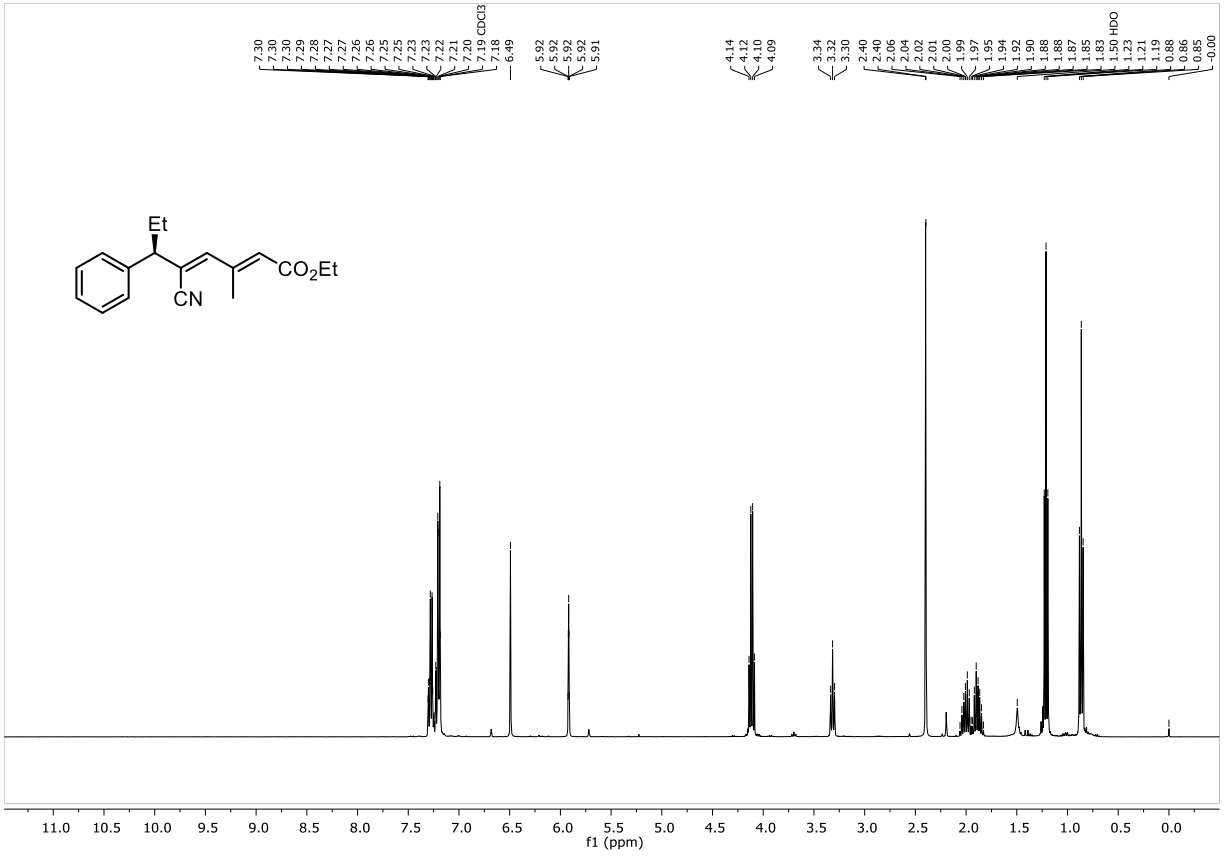
7.30
7.30
7.30
7.29
7.28
7.27
7.27
7.26
7.26
7.25
7.25
7.23
7.22
7.21
7.20
7.19 CDCl3
7.18
6.49
5.92
5.92
5.92
5.92
5.91
4.14
4.12
4.10
4.09
3.34
3.32
3.30
2.40
2.40
2.06
2.04
2.02
2.01
2.00
1.99
1.97
1.95
1.94
1.92
1.90
1.88
1.88
1.87
1.85
1.83
1.50 HDO
1.23
1.21
1.19
0.88
0.86
0.85
0.00
Et
CO2Et
CN
f1 (ppm)

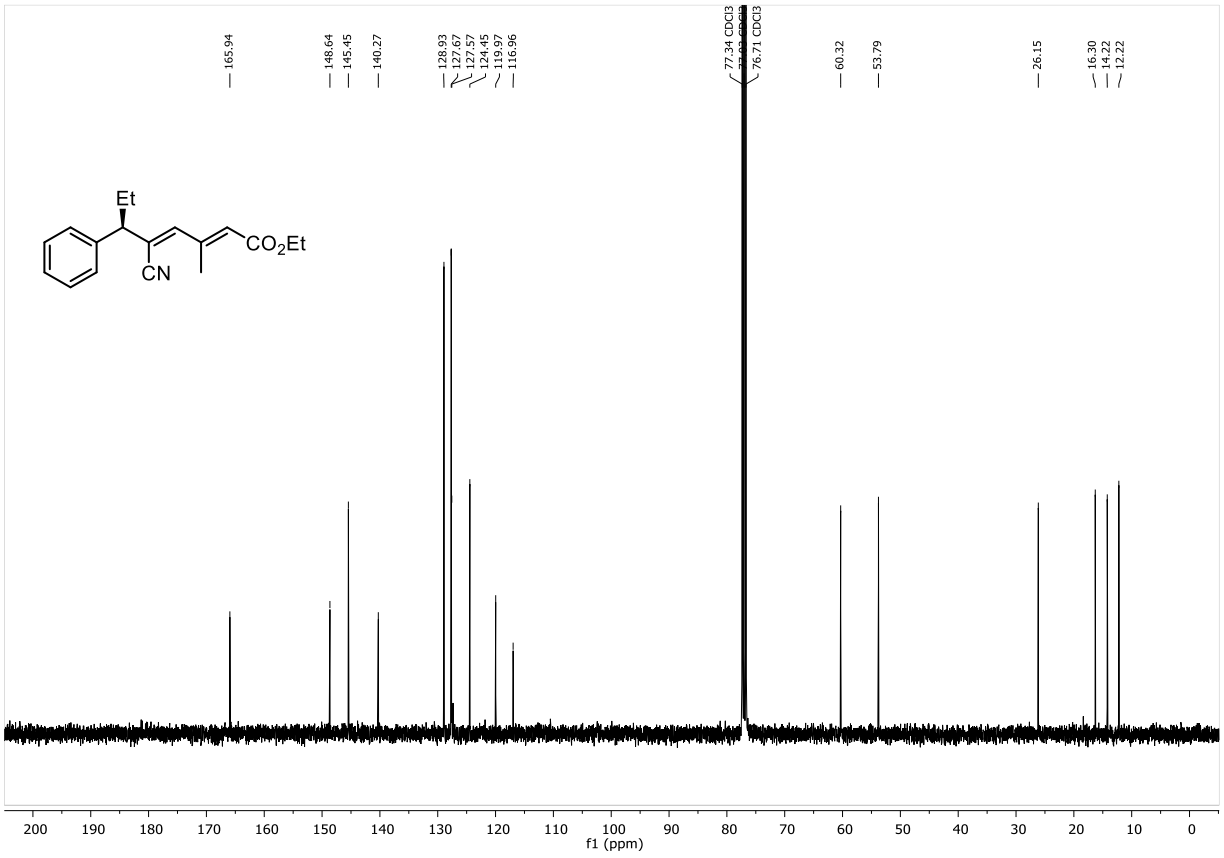
165.94
148.64
145.45
140.27
128.93
127.67
127.57
124.45
119.97
116.96
77.34 CDCl3
77.03 CDCl3
76.71 CDCl3
60.32
53.79
26.15
16.30
14.22
12.22
Et
CN
CO2Et
f1 (ppm)

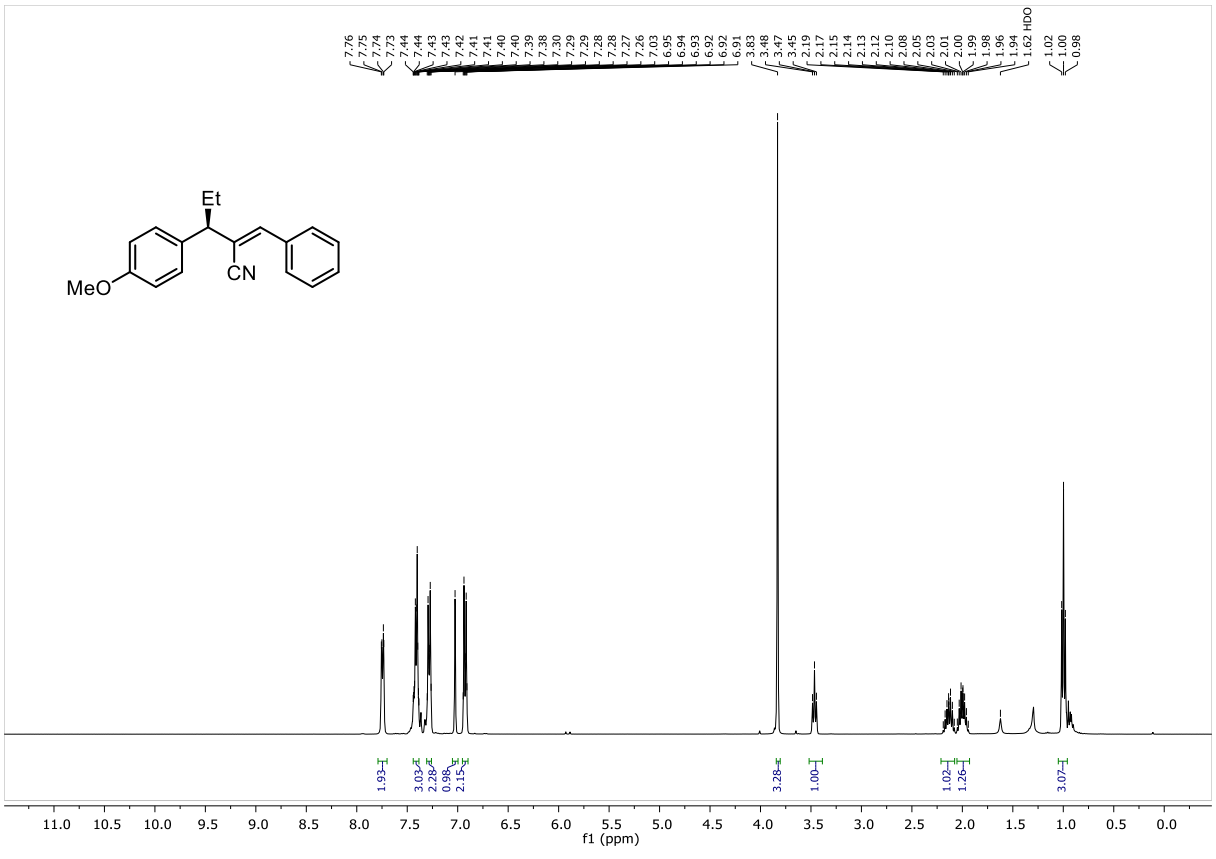
7.76
7.75
7.74
7.73
7.44
7.44
7.43
7.43
7.42
7.41
7.41
7.40
7.40
7.39
7.38
7.30
7.29
7.29
7.28
7.28
7.27
7.26
7.03
6.95
6.94
6.93
6.92
6.92
6.91
3.83
3.48
3.47
3.45
2.19
2.17
2.15
2.14
2.13
2.12
2.10
2.08
2.05
2.03
2.01
2.00
1.99
1.98
1.96
1.94
1.62 HDO
1.02
1.00
0.98
Et
CN
MeO
1.93
3.03
2.28
0.98
2.15
3.28
1.00
1.02
1.26
3.07
f1 (ppm)

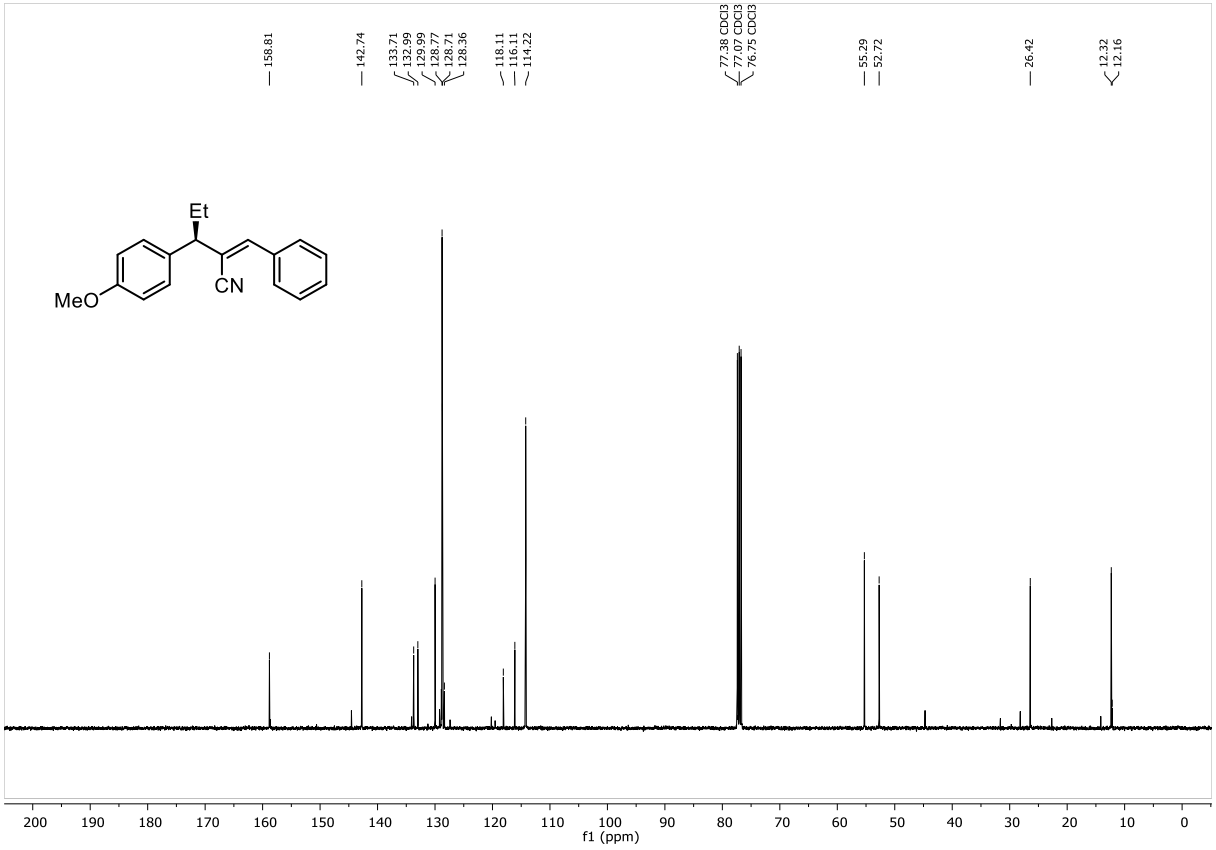
158.81
142.74
133.71
132.99
129.99
128.77
128.71
128.36
118.11
116.11
114.22
77.38 CDCl3
77.07 CDCl3
76.75 CDCl3
55.29
52.72
26.42
12.32
12.16
Et
CN
MeO
f1 (ppm)

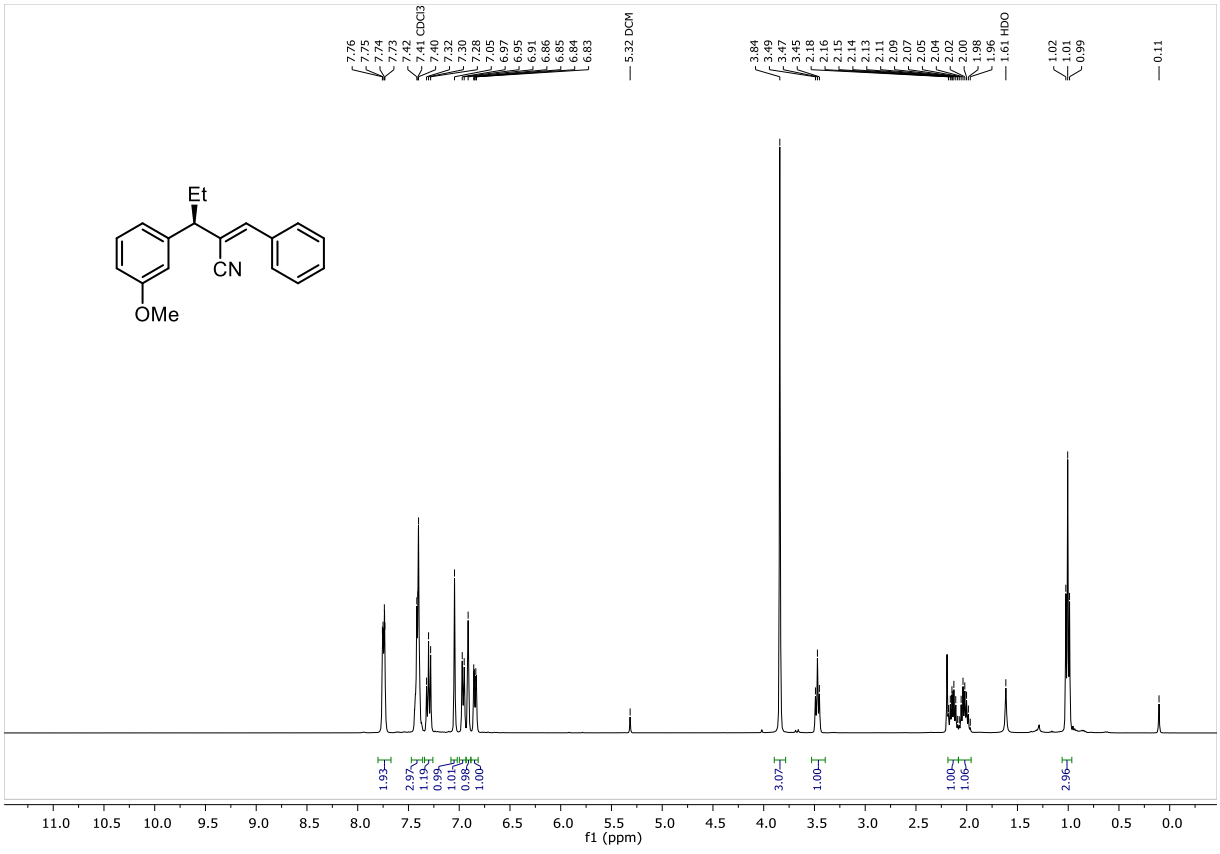
7.76
7.75
7.74
7.73
7.42
7.41 CDCl3
7.40
7.32
7.30
7.28
7.05
6.97
6.95
6.91
6.86
6.85
6.84
6.83
5.32 DCM
3.84
3.49
3.47
3.45
2.18
2.16
2.15
2.14
2.13
2.11
2.09
2.07
2.05
2.04
2.02
2.00
1.98
1.96
1.61 HDO
1.02
1.01
0.99
0.11
Et
CN
OMe
1.93
2.97
1.19
0.99
1.01
0.98
1.00
3.07
1.00
1.00
1.06
2.96
f1 (ppm)

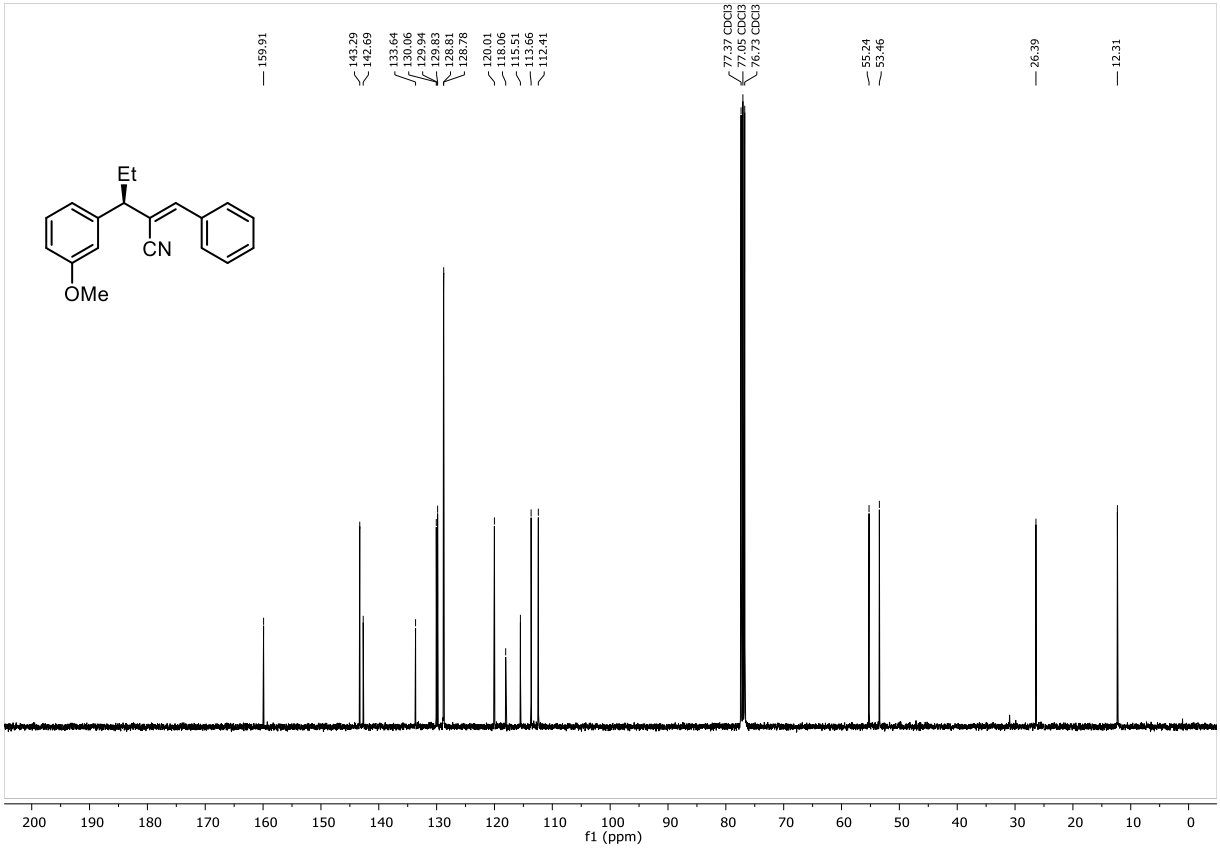
159.91
143.29
142.69
133.64
130.06
129.94
129.83
128.81
128.78
120.01
118.06
115.51
113.66
112.41
77.37 CDCl3
77.05 CDCl3
76.73 CDCl3
55.24
53.46
26.39
12.31
Et
CN
OMe
f1 (ppm)

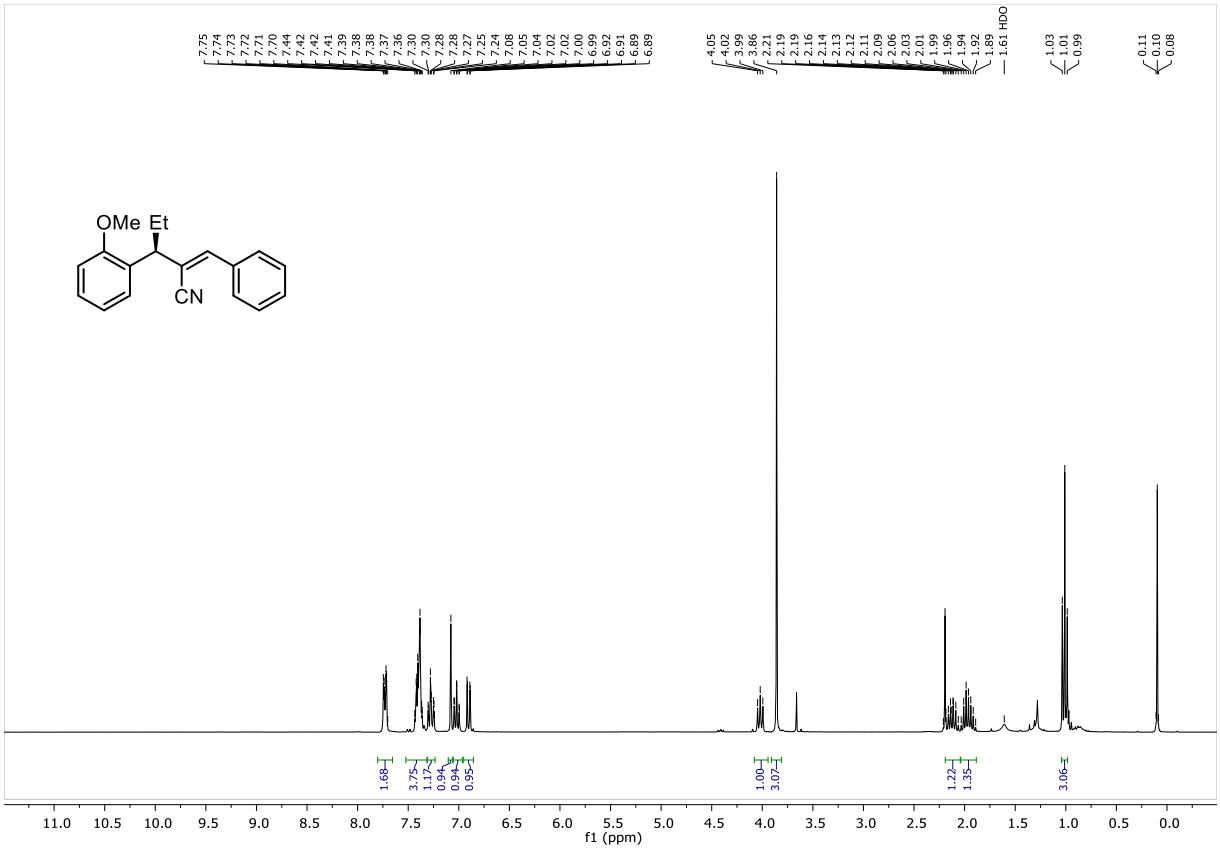
7.75
7.74
7.73
7.72
7.71
7.70
7.44
7.42
7.42
7.41
7.39
7.38
7.38
7.37
7.36
7.30
7.30
7.28
7.28
7.27
7.25
7.24
7.08
7.05
7.04
7.02
7.02
7.00
6.99
6.92
6.91
6.89
6.89
4.05
4.02
3.99
3.86
2.21
2.19
2.19
2.16
2.14
2.13
2.12
2.11
2.09
2.06
2.03
2.01
1.99
1.96
1.94
1.92
1.89
1.61 HDO
1.03
1.01
0.99
0.11
0.10
0.08
OMe Et
CN
1.68
3.75
1.17
0.94
0.94
0.95
1.00
3.07
1.22
1.35
3.06
f1 (ppm)

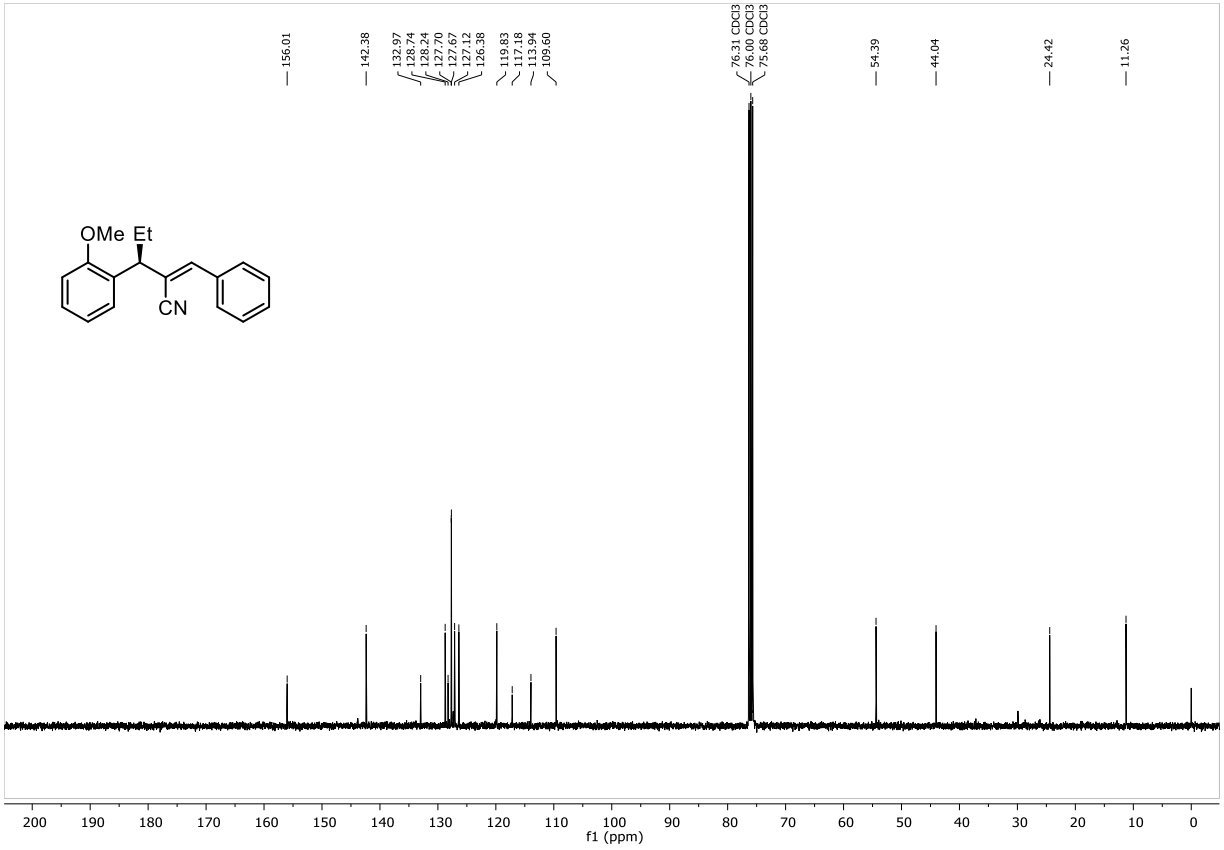
156.01
142.38
132.97
128.74
128.24
127.70
127.67
127.12
126.38
119.83
117.18
113.94
109.60
76.31 CDCl3
76.00 CDCl3
75.68 CDCl3
54.39
44.04
24.42
11.26
OMe Et
CN
f1 (ppm)

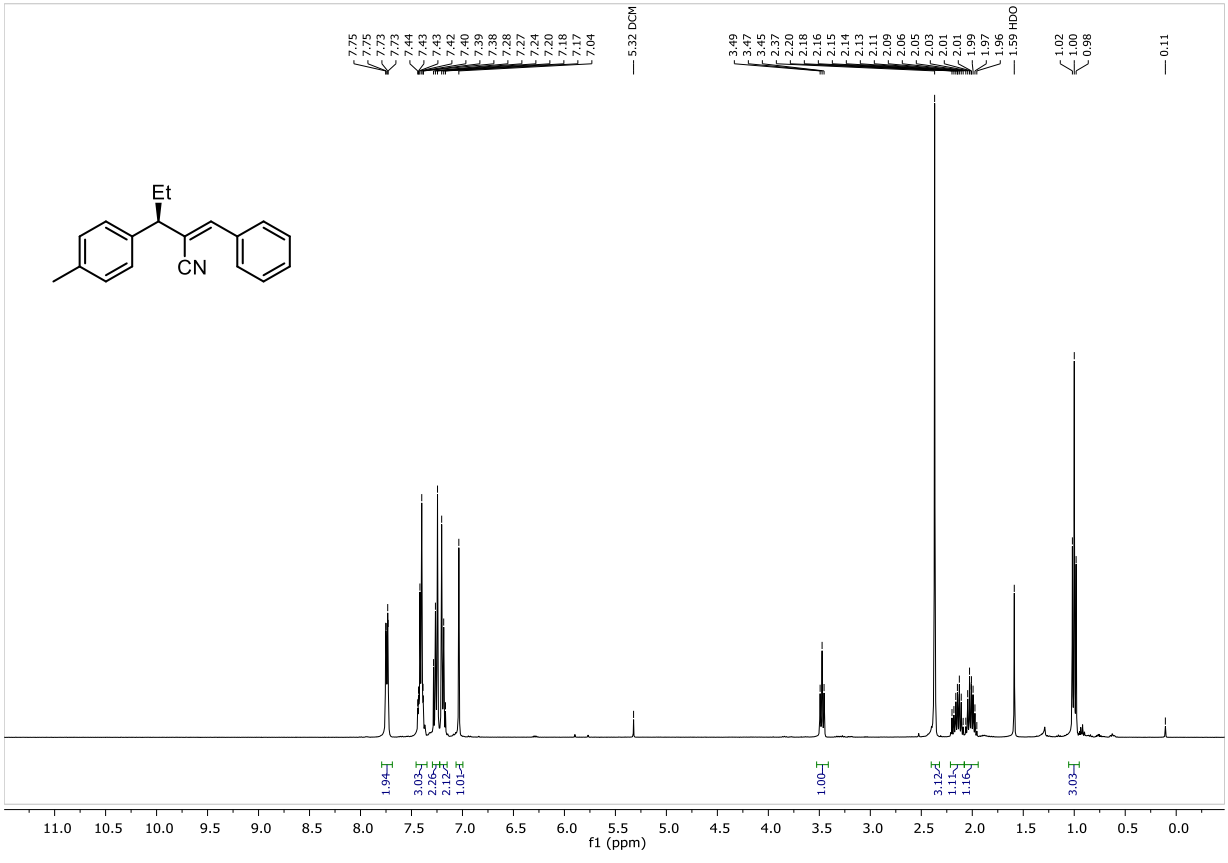
7.75
7.75
7.73
7.73
7.44
7.43
7.43
7.42
7.40
7.39
7.38
7.28
7.27
7.24
7.20
7.18
7.17
7.04
5.32 DCM
3.49
3.47
3.45
2.37
2.20
2.18
2.16
2.15
2.14
2.13
2.11
2.09
2.06
2.05
2.03
2.01
2.01
1.99
1.97
1.96
1.59 HDO
1.02
1.00
0.98
0.11
Et
CN
1.94
3.03
2.26
2.12
1.01
1.00
3.12
1.11
1.16
3.03
f1 (ppm)

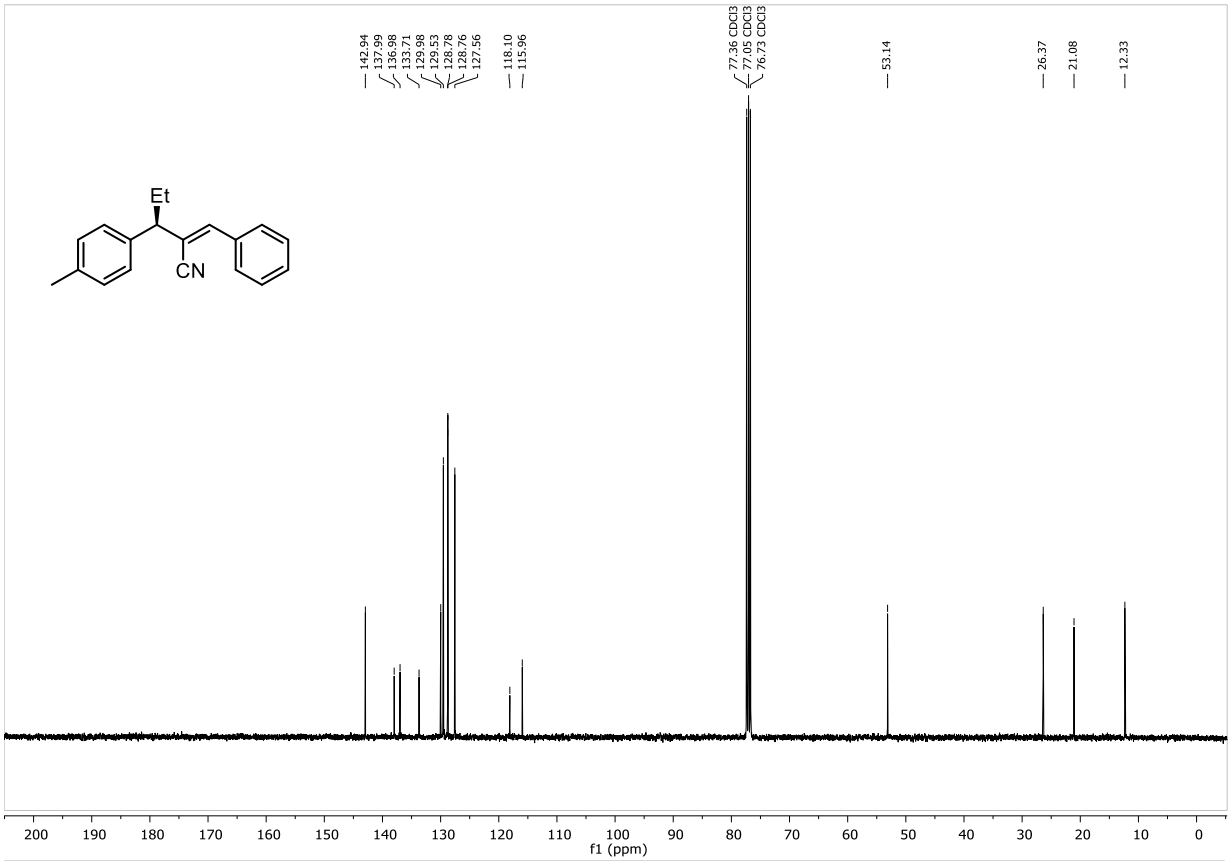
142.94
137.99
136.98
133.71
129.98
129.53
128.78
128.76
127.56
118.10
115.96
77.36 CDCl3
77.05 CDCl3
76.73 CDCl3
53.14
26.37
21.08
12.33
Et
CN
f1 (ppm)

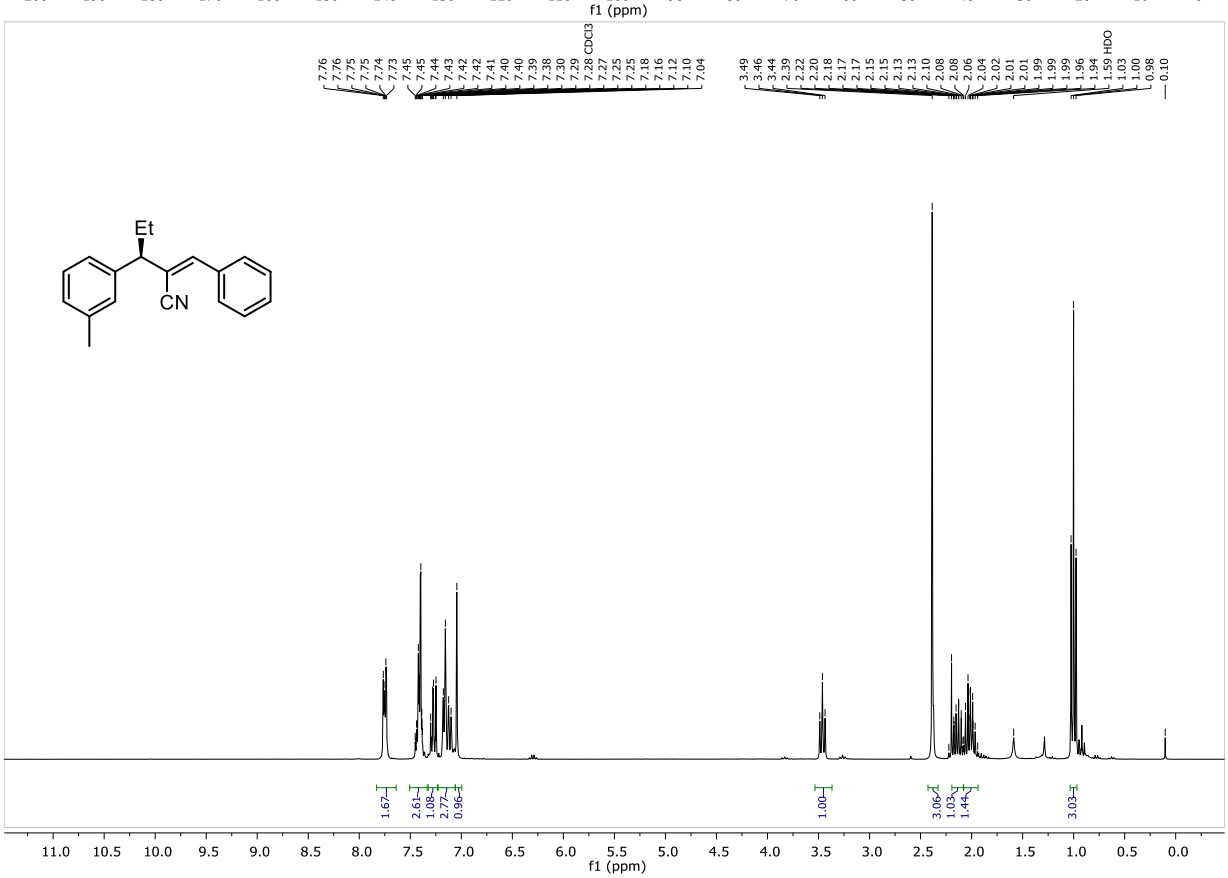
7.76
7.76
7.75
7.75
7.74
7.73
7.45
7.45
7.44
7.43
7.42
7.42
7.41
7.40
7.40
7.39
7.38
7.30
7.29
CDCl3
7.27
7.25
7.25
7.18
7.16
7.12
7.10
7.04
3.49
3.46
3.44
2.39
2.22
2.20
2.18
2.17
2.17
2.15
2.15
2.13
2.13
2.10
2.08
2.08
2.06
2.04
2.02
2.01
2.01
1.99
1.99
1.99
1.96
1.94
1.59
HDO
1.03
1.00
0.98
0.10
Et
CN
1.67
2.61
1.08
2.77
0.96
1.00
3.06
1.03
1.44
3.03
f1 (ppm)

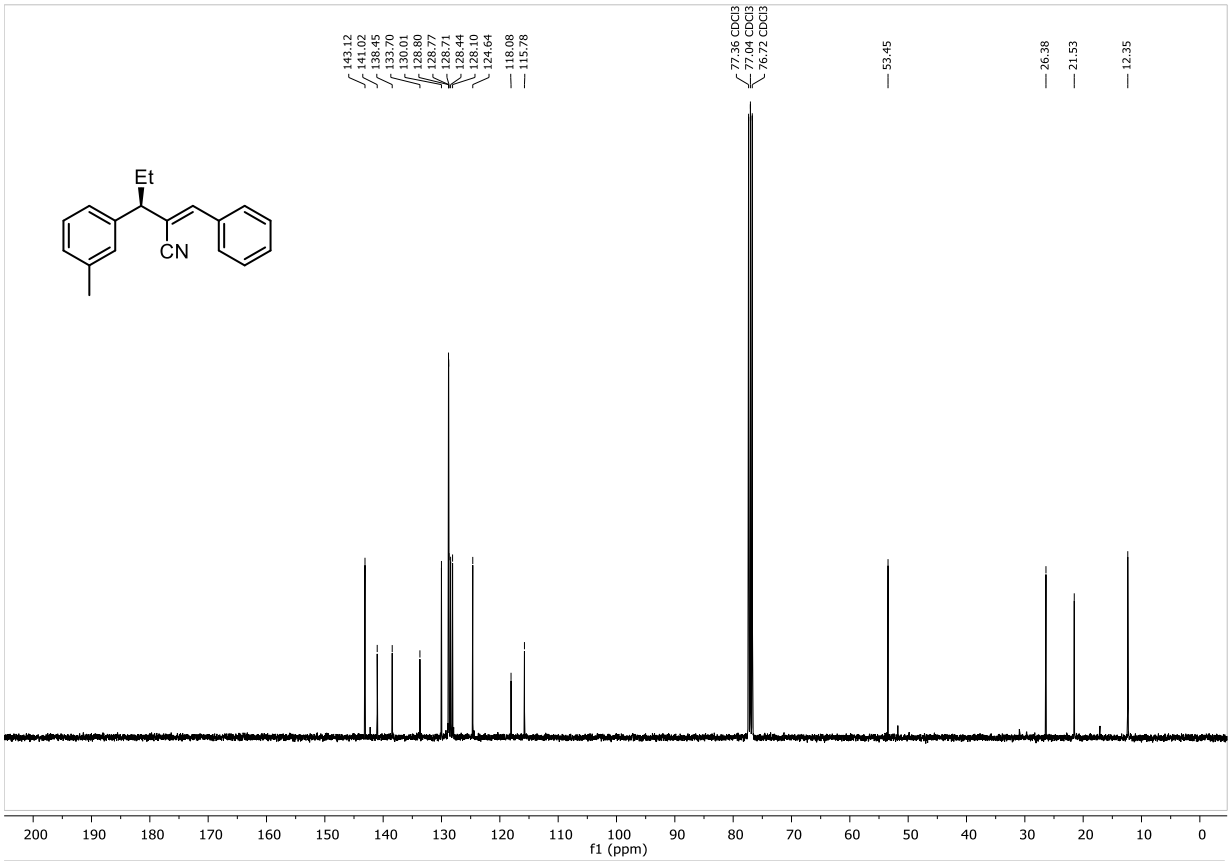
143.12
141.02
138.45
133.70
130.01
128.80
128.77
128.71
128.44
128.10
124.64
118.08
115.78
77.36 CDCl3
77.04 CDCl3
76.72 CDCl3
53.45
26.38
21.53
12.35
Et
CN
f1 (ppm)

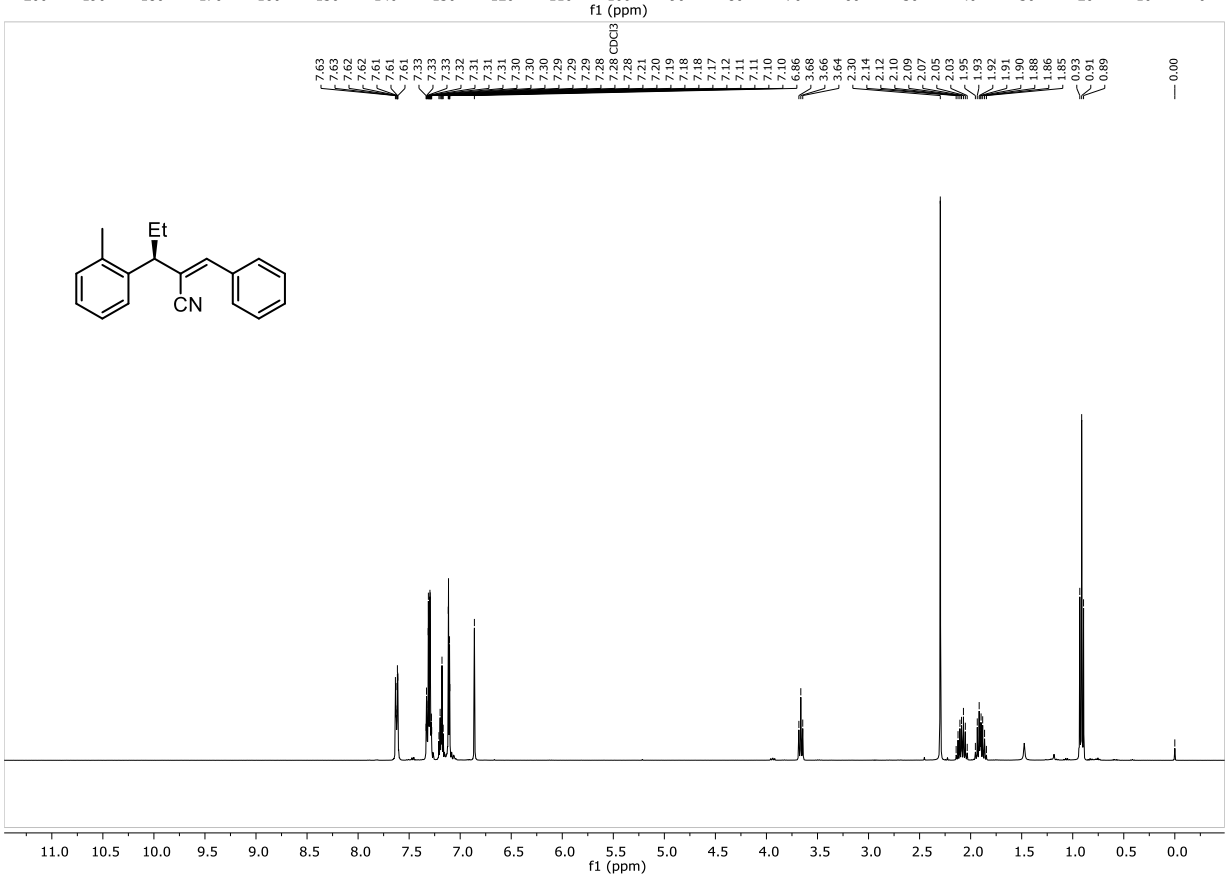
7.63
7.63
7.62
7.62
7.61
7.61
7.61
7.33
7.33
7.33
7.32
7.31
7.31
7.31
7.30
7.30
7.30
7.29
7.29
7.29
7.28 CDCl3
7.28
7.28
7.21
7.20
7.19
7.18
7.18
7.17
7.12
7.11
7.11
7.10
7.10
6.86
3.68
3.66
3.64
2.30
2.14
2.12
2.10
2.09
2.07
2.05
2.03
1.95
1.93
1.92
1.91
1.90
1.88
1.86
1.85
0.93
0.91
0.89
0.00
Et
CN
f1 (ppm)

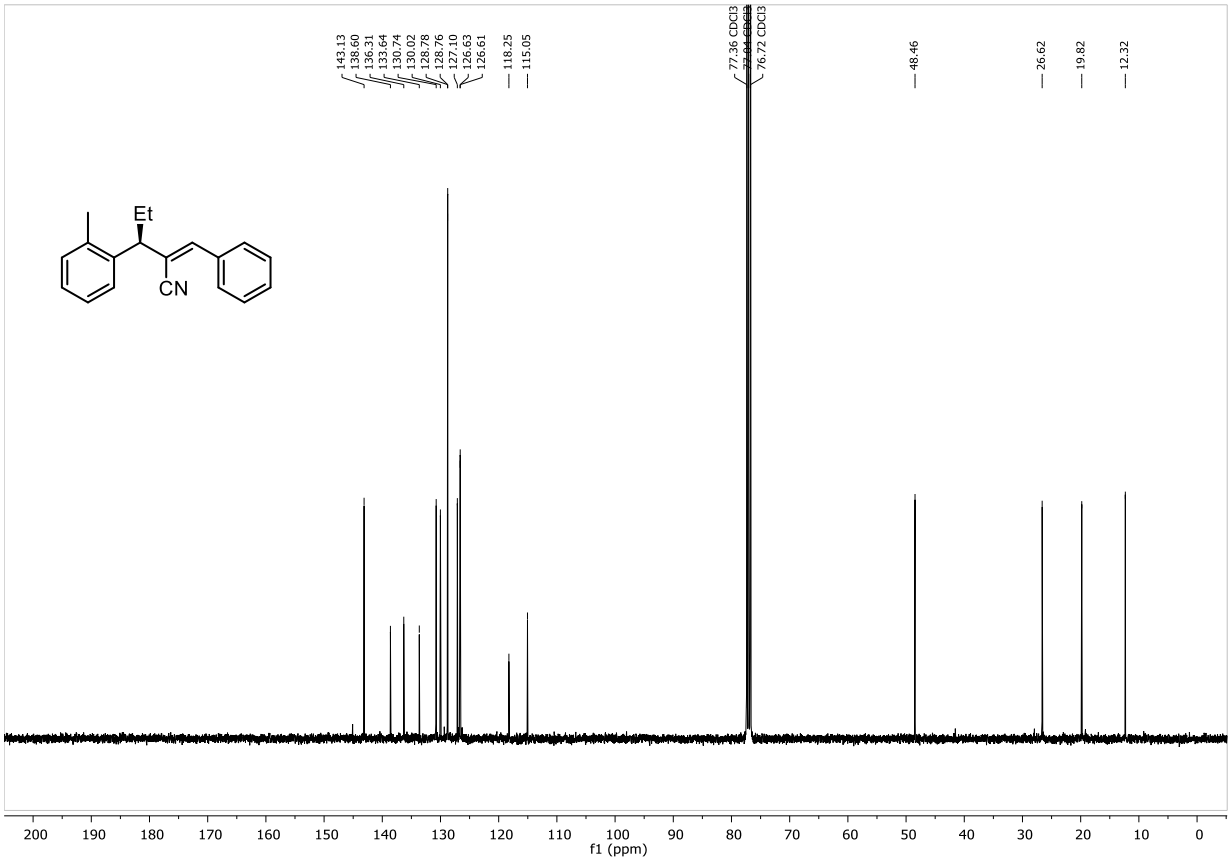
143.13
138.60
136.31
133.64
130.74
130.02
128.78
128.76
127.10
126.63
126.61
118.25
115.05
77.36 CDCl3
76.72 CDCl3
48.46
26.62
19.82
12.32
Et
CN
f1 (ppm)

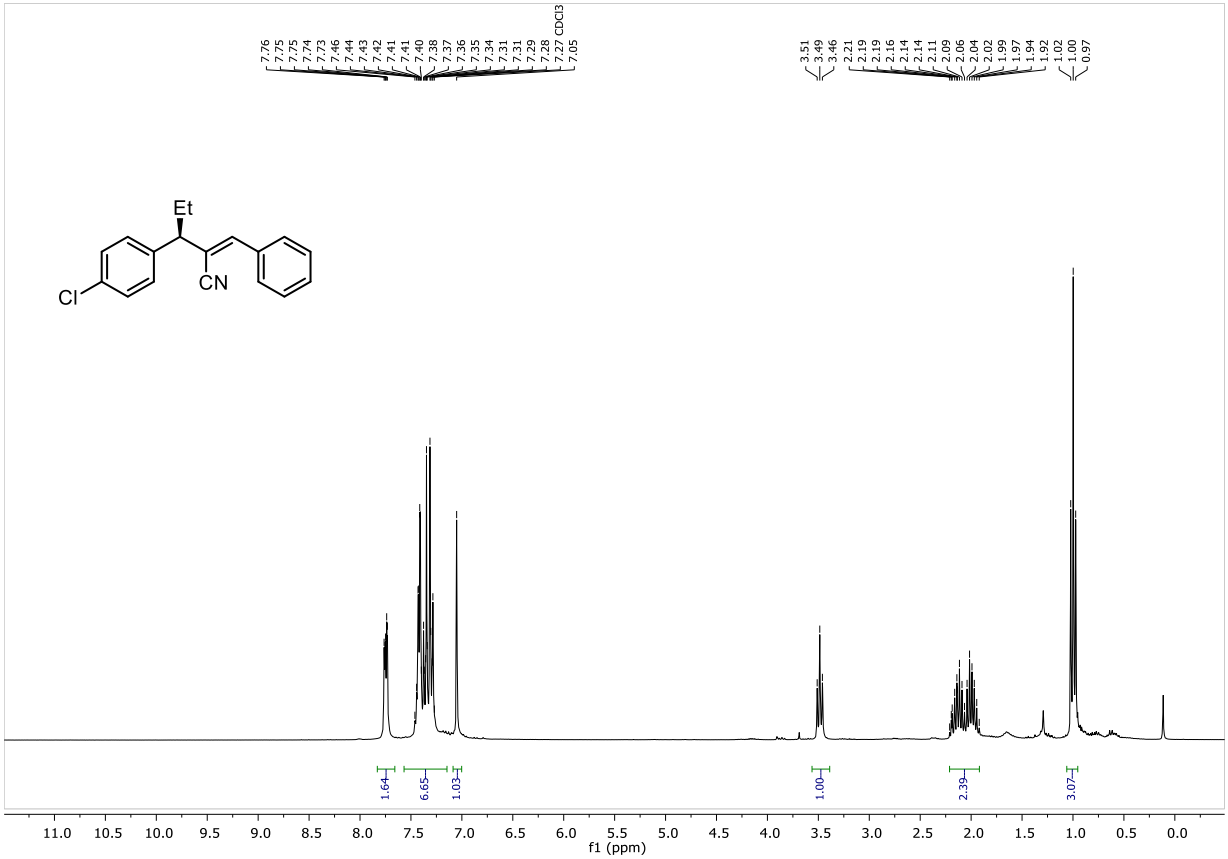
7.76
7.75
7.75
7.74
7.73
7.46
7.44
7.43
7.42
7.41
7.41
7.40
7.38
7.37
7.36
7.35
7.34
7.31
7.29
7.28
7.27 CDCl3
7.05
3.51
3.49
3.46
2.21
2.19
2.19
2.16
2.14
2.14
2.11
2.09
2.06
2.04
2.02
1.99
1.97
1.94
1.92
1.02
1.00
0.97
Et
Cl
CN
1.64
6.65
1.03
1.00
2.39
3.07
f1 (ppm)

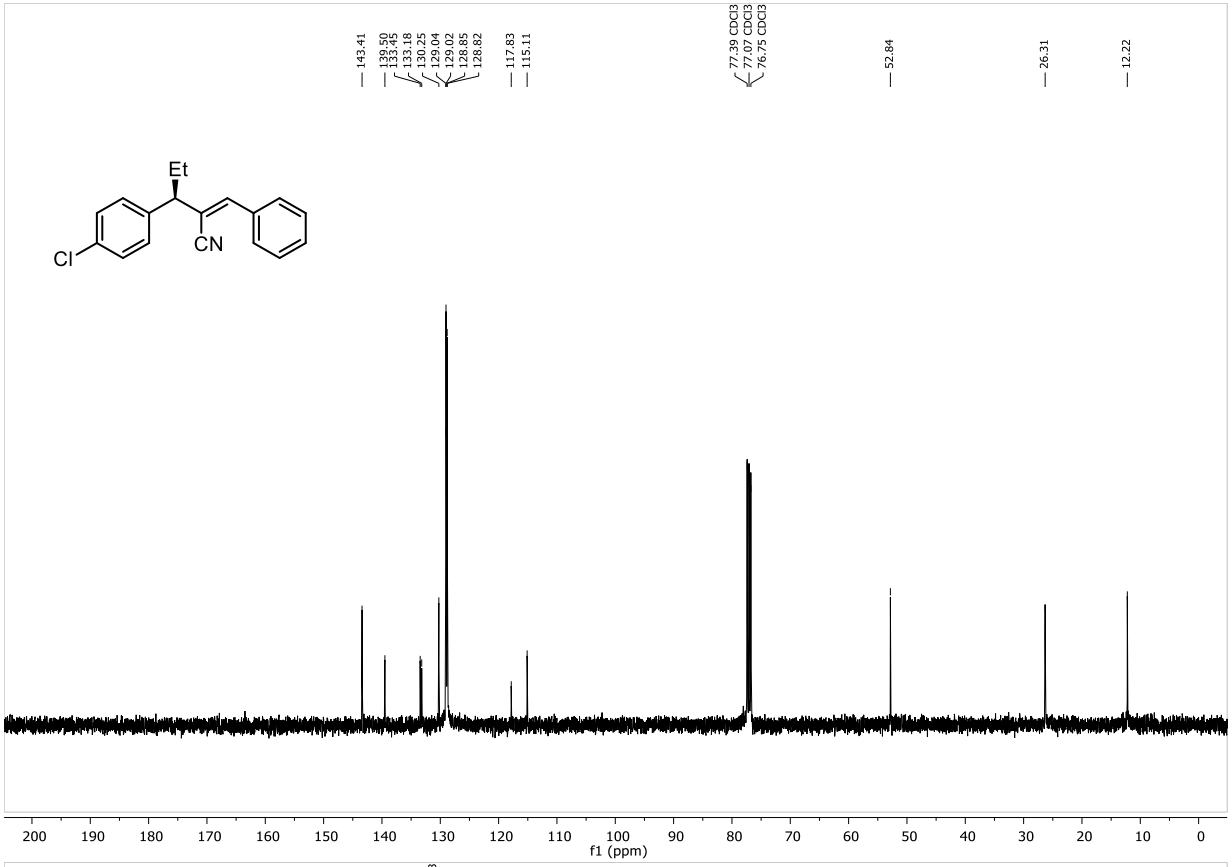
143.41
139.50
133.45
133.18
130.25
129.04
129.02
128.85
128.82
117.83
115.11
77.39 CDCl3
77.07 CDCl3
76.75 CDCl3
52.84
26.31
12.22
Et
Cl
CN
f1 (ppm)

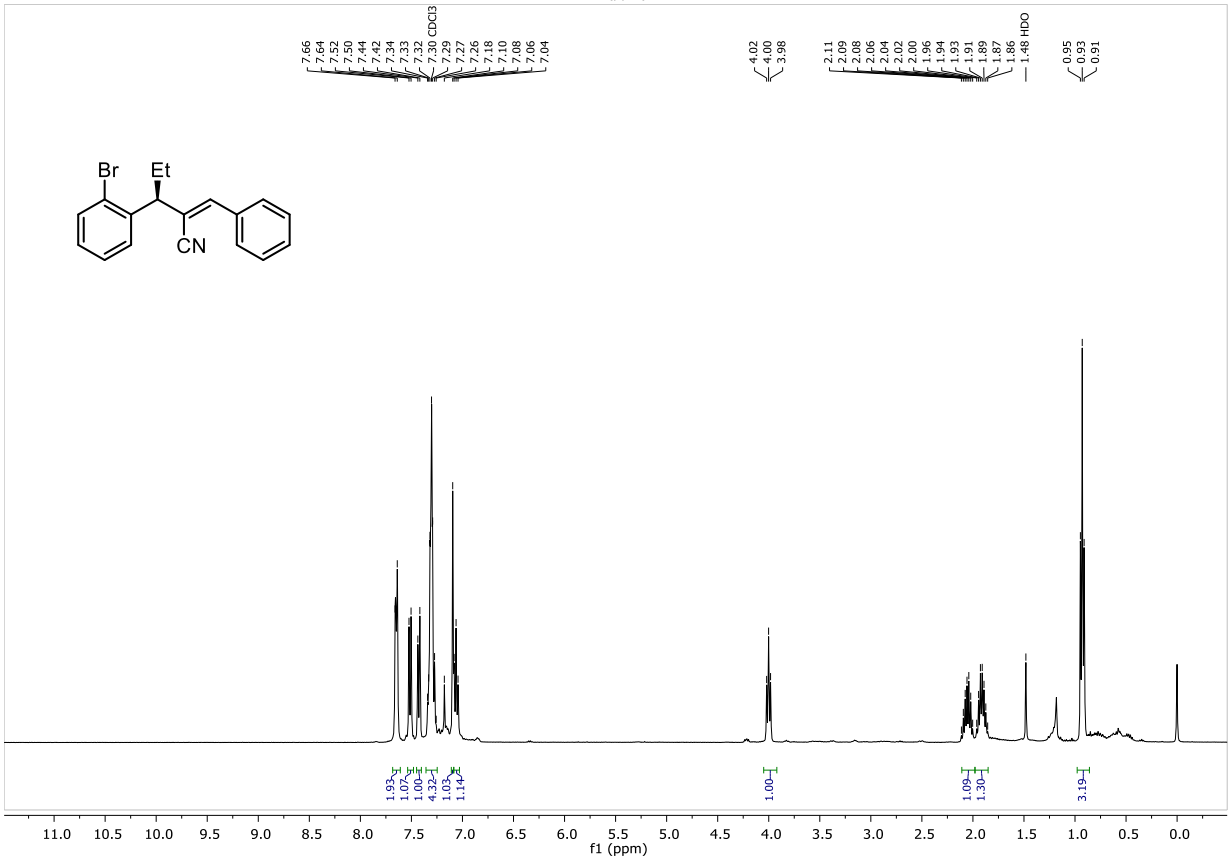
7.66
7.64
7.52
7.50
7.44
7.42
7.34
7.33
7.32
7.30 CDCl3
7.29
7.27
7.26
7.18
7.10
7.08
7.06
7.04
4.02
4.00
3.98
2.11
2.09
2.08
2.06
2.04
2.02
2.00
1.96
1.94
1.93
1.91
1.89
1.87
1.86
1.48 HDO
0.95
0.93
0.91
Br
Et
CN
1.93
1.07
1.00
4.32
1.03
1.14
1.00
1.09
1.30
3.19
f1 (ppm)

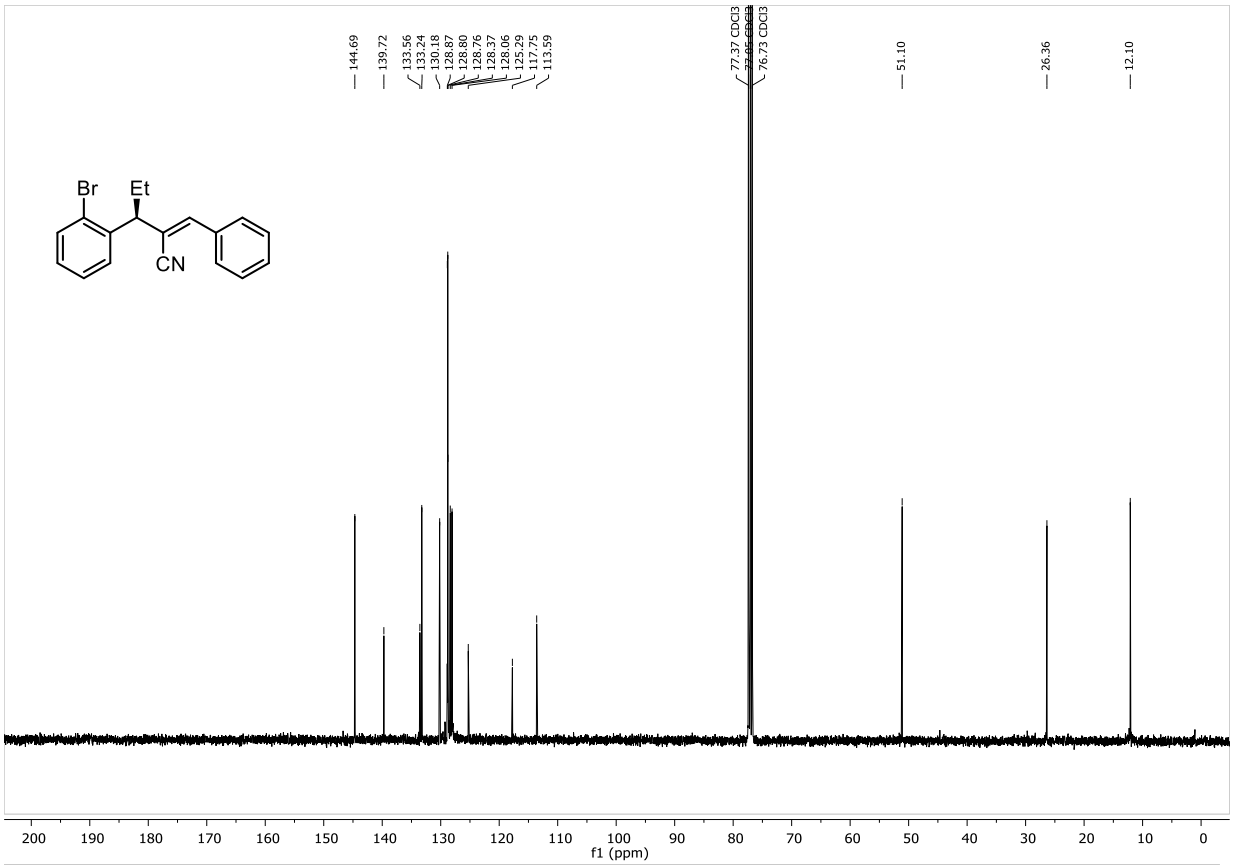
144.69
139.72
133.56
133.24
130.18
128.87
128.80
128.76
128.37
128.06
125.29
117.75
113.59
77.37 CDCl3
76.73 CDCl3
51.10
26.36
12.10
Br
Et
CN
f1 (ppm)

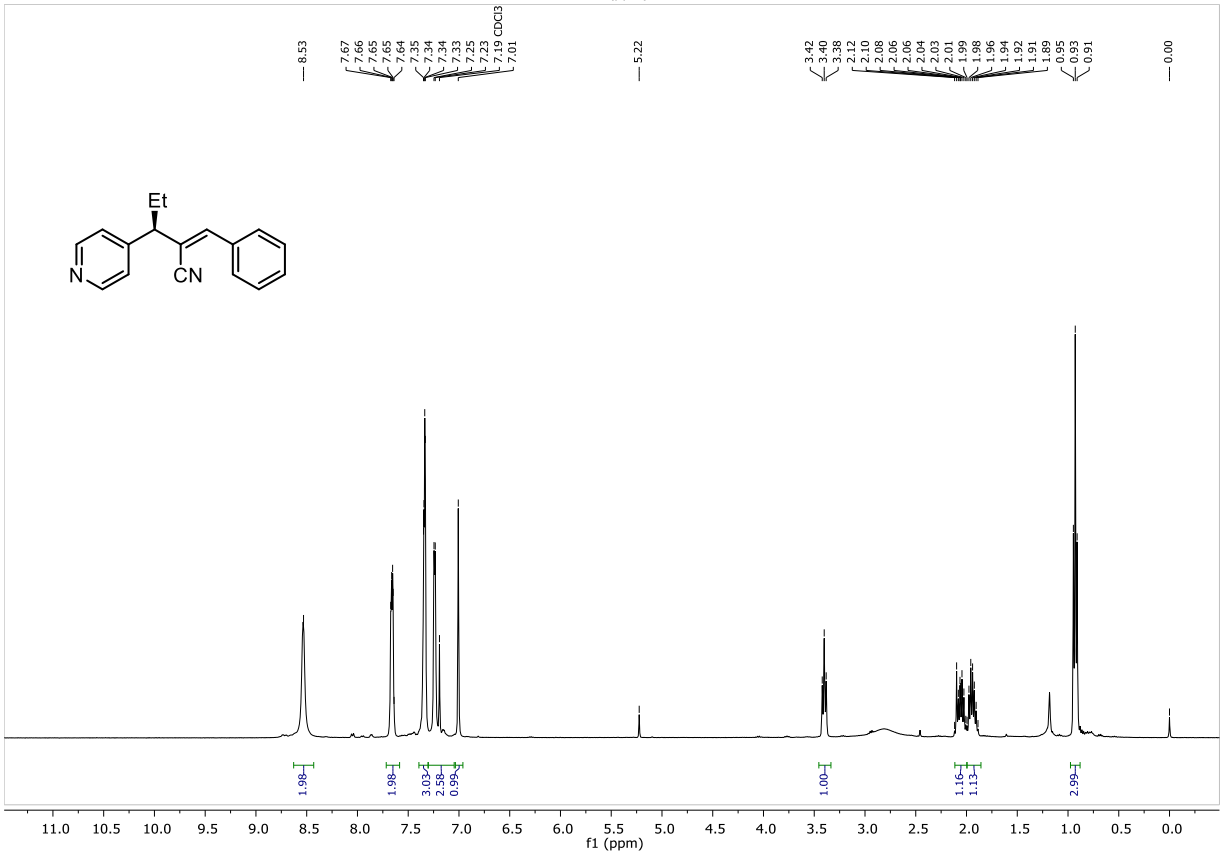
8.53
7.67
7.66
7.65
7.65
7.64
7.35
7.34
7.34
7.33
7.25
7.23
7.19 CDCl3
7.01
5.22
3.42
3.40
3.38
2.12
2.10
2.08
2.06
2.06
2.04
2.03
2.01
1.99
1.98
1.96
1.94
1.92
1.91
1.89
0.95
0.93
0.91
0.00
Et
N
CN
1.98
1.98
3.03
2.58
0.99
1.00
1.16
1.13
2.99
f1 (ppm)

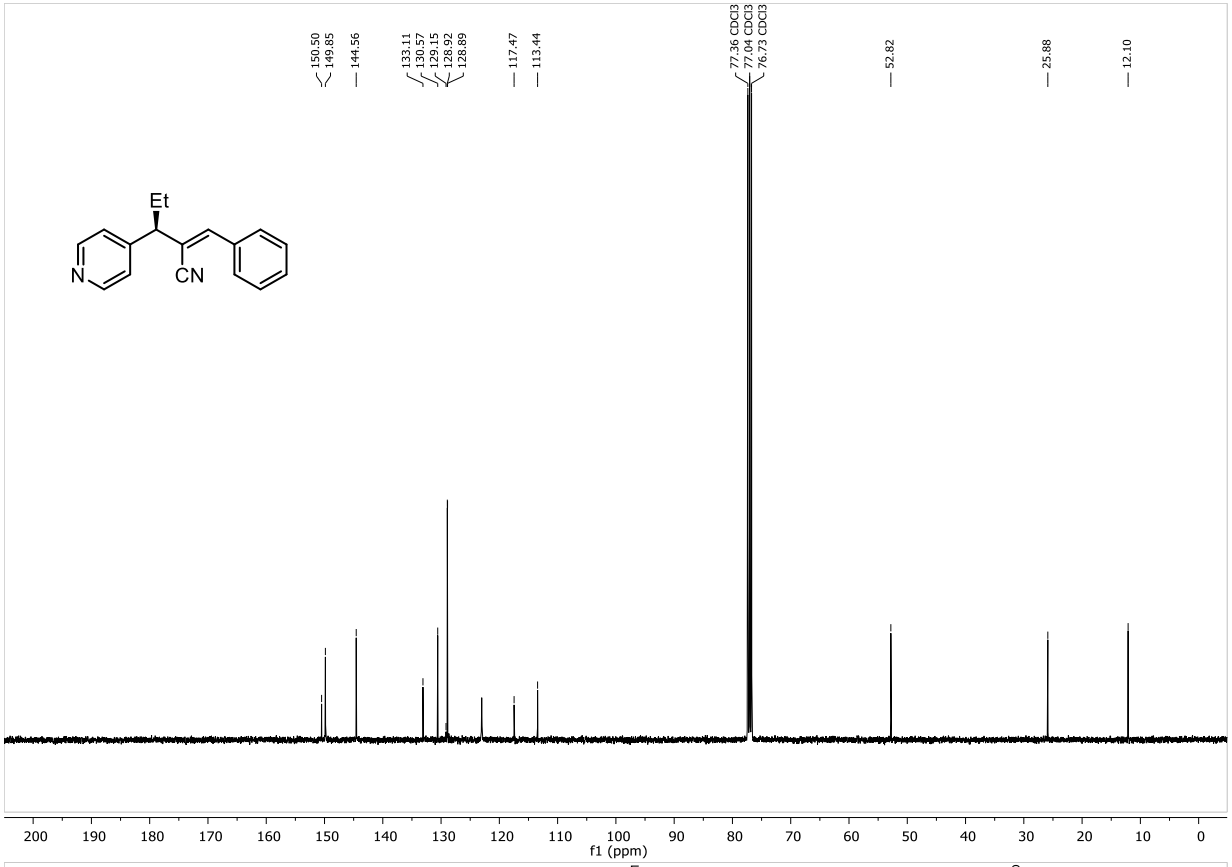
150.50
149.85
144.56
133.11
130.57
129.15
128.92
128.89
117.47
113.44
77.36 CDCl3
77.04 CDCl3
76.73 CDCl3
52.82
25.88
12.10
Et
N
CN
f1 (ppm)

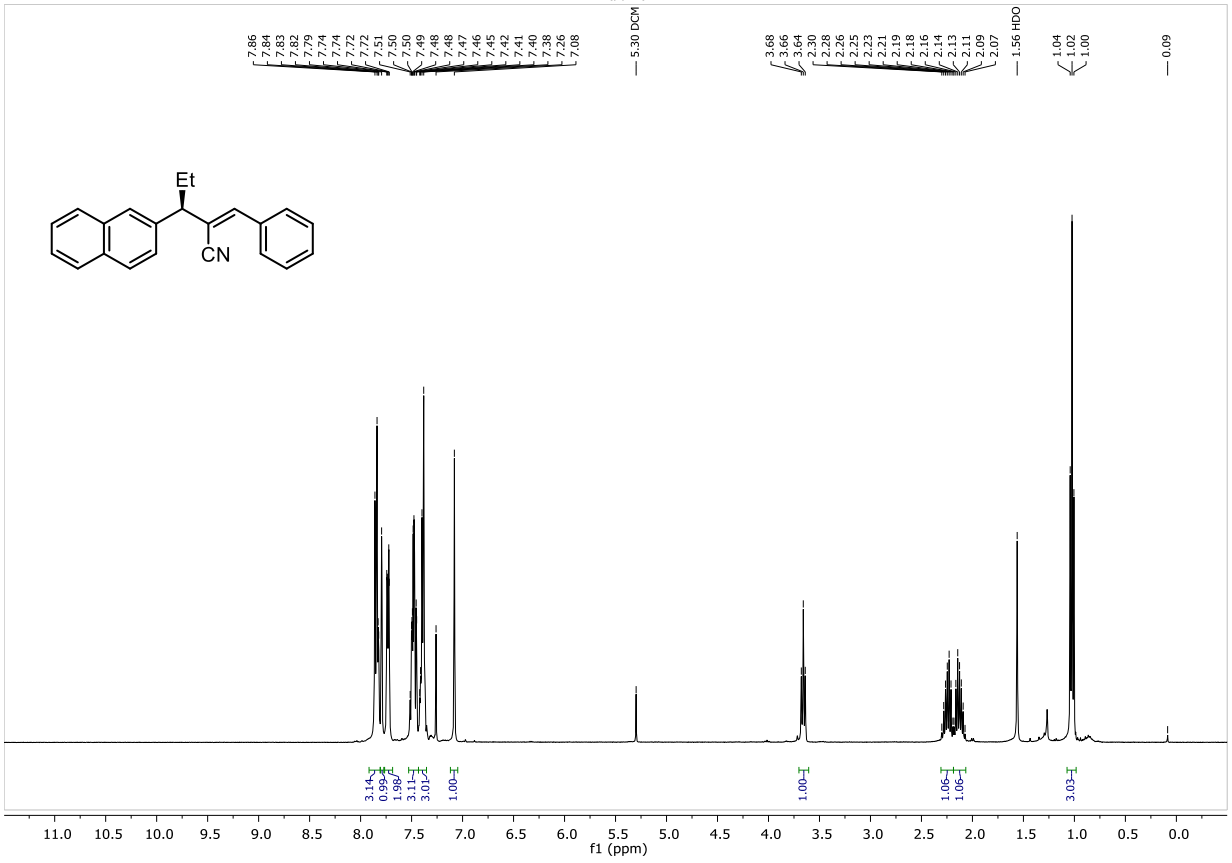
7.86
7.84
7.83
7.82
7.79
7.74
7.74
7.72
7.72
7.51
7.50
7.50
7.49
7.48
7.48
7.47
7.46
7.45
7.42
7.41
7.40
7.38
7.26
7.08
5.30 DCM
3.68
3.66
3.64
2.30
2.28
2.26
2.25
2.23
2.21
2.19
2.18
2.16
2.14
2.13
2.11
2.09
2.07
1.56 HDO
1.04
1.02
1.00
0.09
Et
CN
3.14
0.99
1.98
3.11
3.01
1.00
1.00
1.06
1.06
3.03
f1 (ppm)

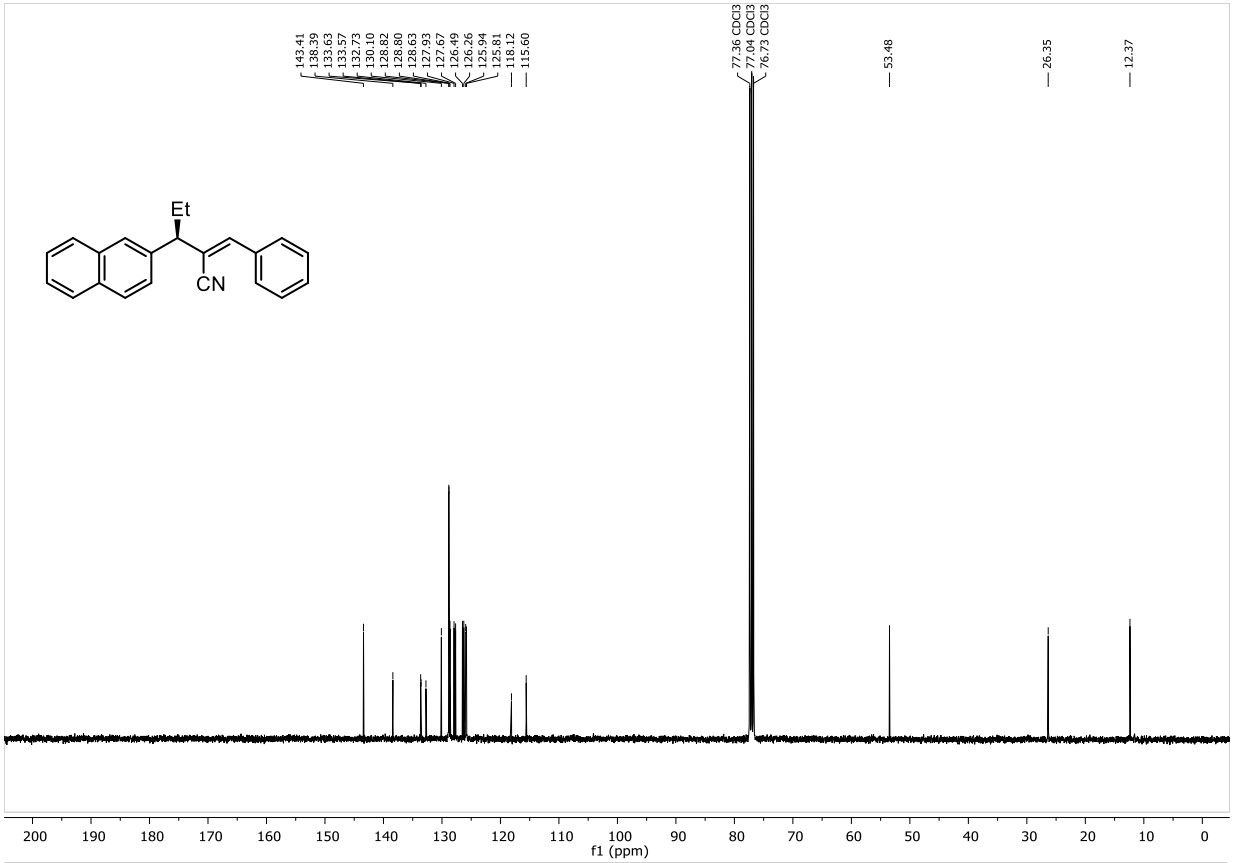
143.41
138.39
133.63
133.57
132.73
130.10
128.82
128.80
128.63
127.93
127.67
126.49
126.26
125.94
125.81
118.12
115.60
77.36 CDCl3
77.04 CDCl3
76.73 CDCl3
53.48
26.35
12.37
Et
CN
f1 (ppm)

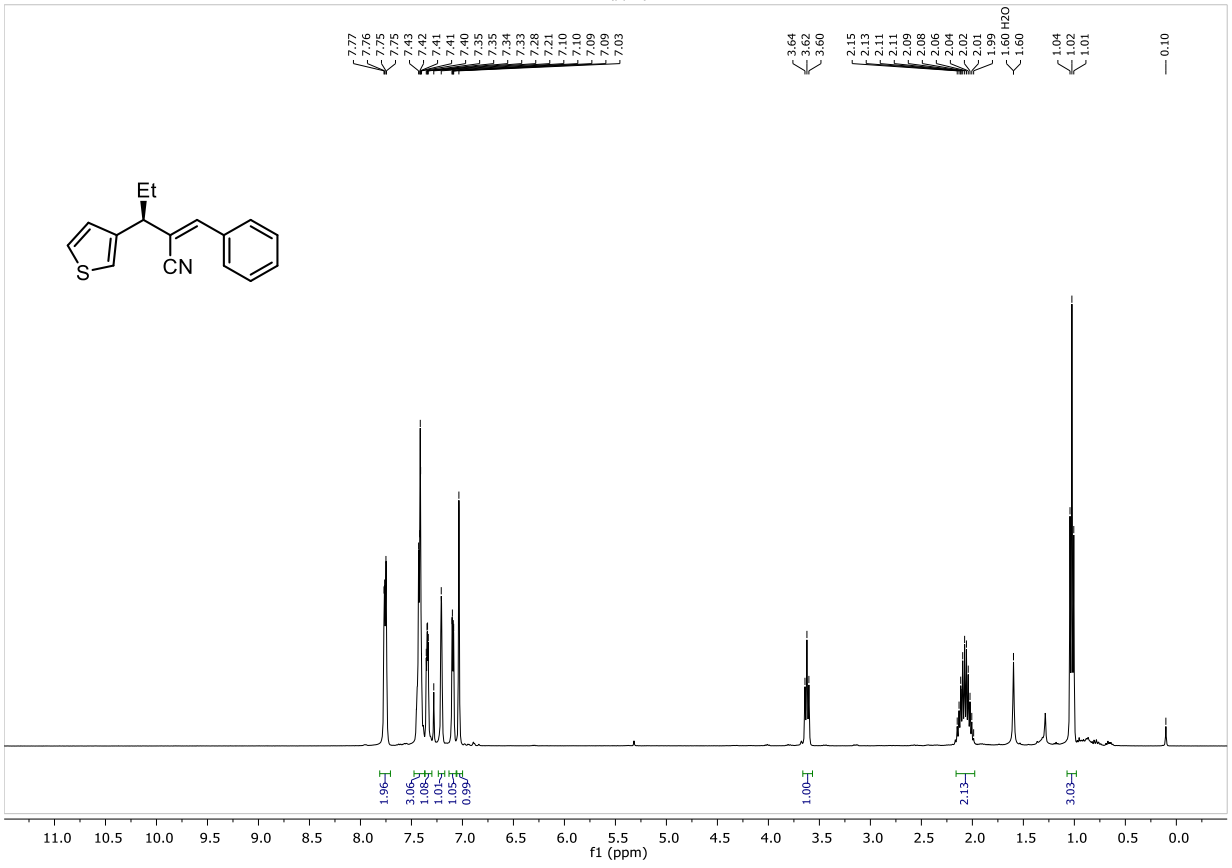
7.77
7.76
7.75
7.75
7.43
7.42
7.41
7.41
7.40
7.35
7.35
7.34
7.33
7.28
7.21
7.10
7.10
7.09
7.09
7.03
3.64
3.62
3.60
2.15
2.13
2.11
2.11
2.09
2.08
2.06
2.04
2.02
2.01
1.99
1.60 H2O
1.60
1.04
1.02
1.01
0.10
Et
S
CN
1.96
3.06
1.08
1.01
1.05
0.99
1.00
2.13
3.03
f1 (ppm)

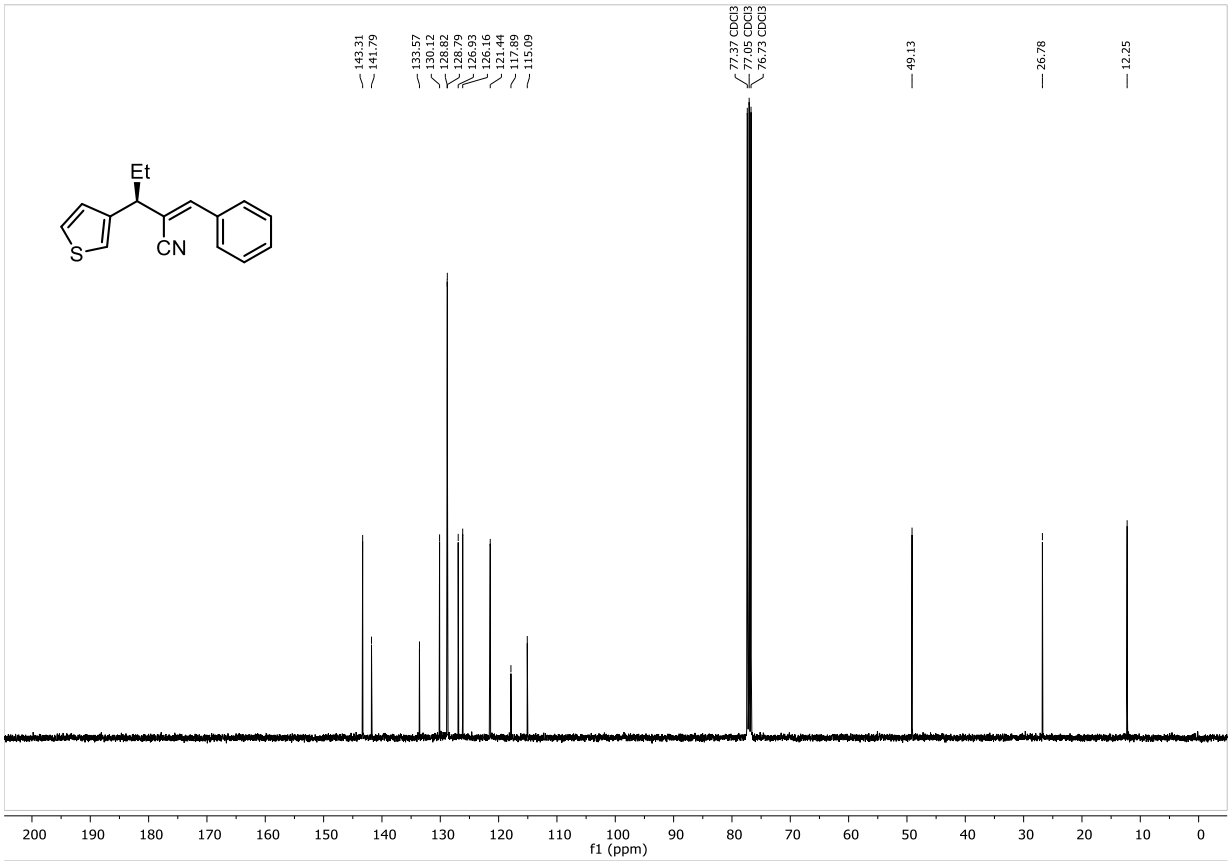
143.31
141.79
133.57
130.12
128.82
128.79
126.93
126.16
121.44
117.89
115.09
77.37 CDCl3
77.05 CDCl3
76.73 CDCl3
49.13
26.78
12.25
Et
CN
S
f1 (ppm)

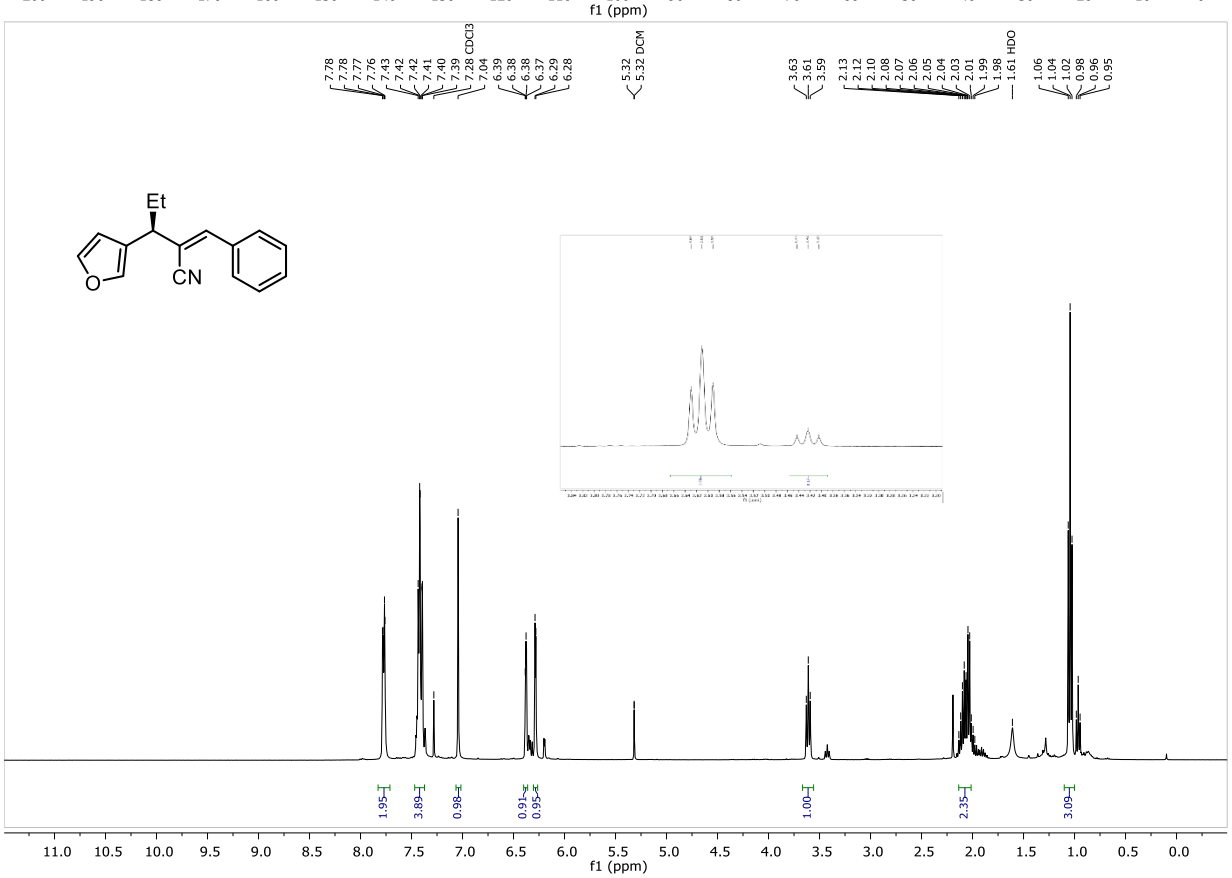
7.78
7.78
7.77
7.76
7.43
7.42
7.42
7.41
7.40
7.39
7.28 CDCl3
7.04
6.39
6.38
6.38
6.37
6.29
6.28
5.32
5.32 DCM
3.63
3.61
3.59
2.13
2.12
2.10
2.08
2.07
2.06
2.05
2.04
2.03
2.01
1.99
1.98
1.61 HDO
1.06
1.04
1.02
0.98
0.96
0.95
Et
CN
O
1.95
3.89
0.98
0.91
0.95
1.00
2.35
3.09
f1 (ppm)

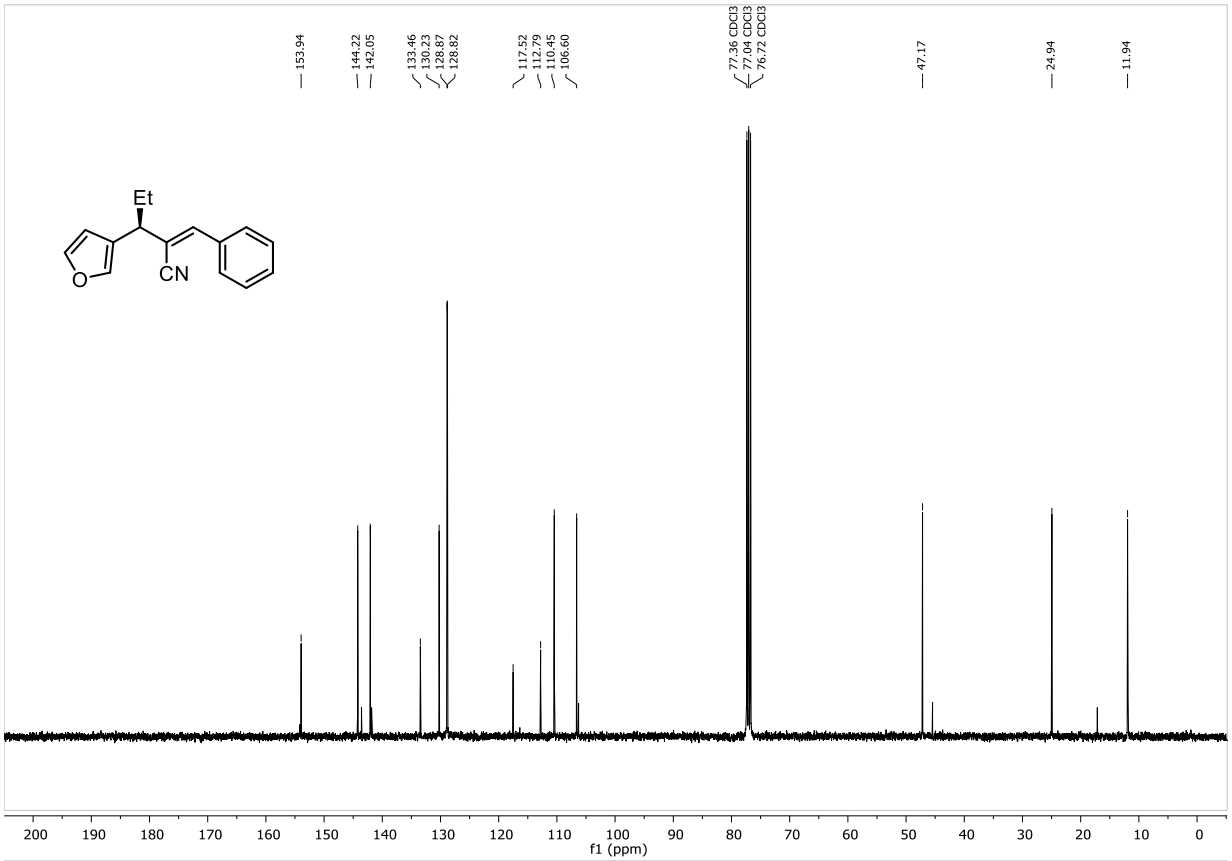
153.94
144.22
142.05
133.46
130.23
128.87
128.82
117.52
112.79
110.45
106.60
77.36 CDCl3
77.04 CDCl3
76.72 CDCl3
47.17
24.94
11.94
Et
CN
O
f1 (ppm)

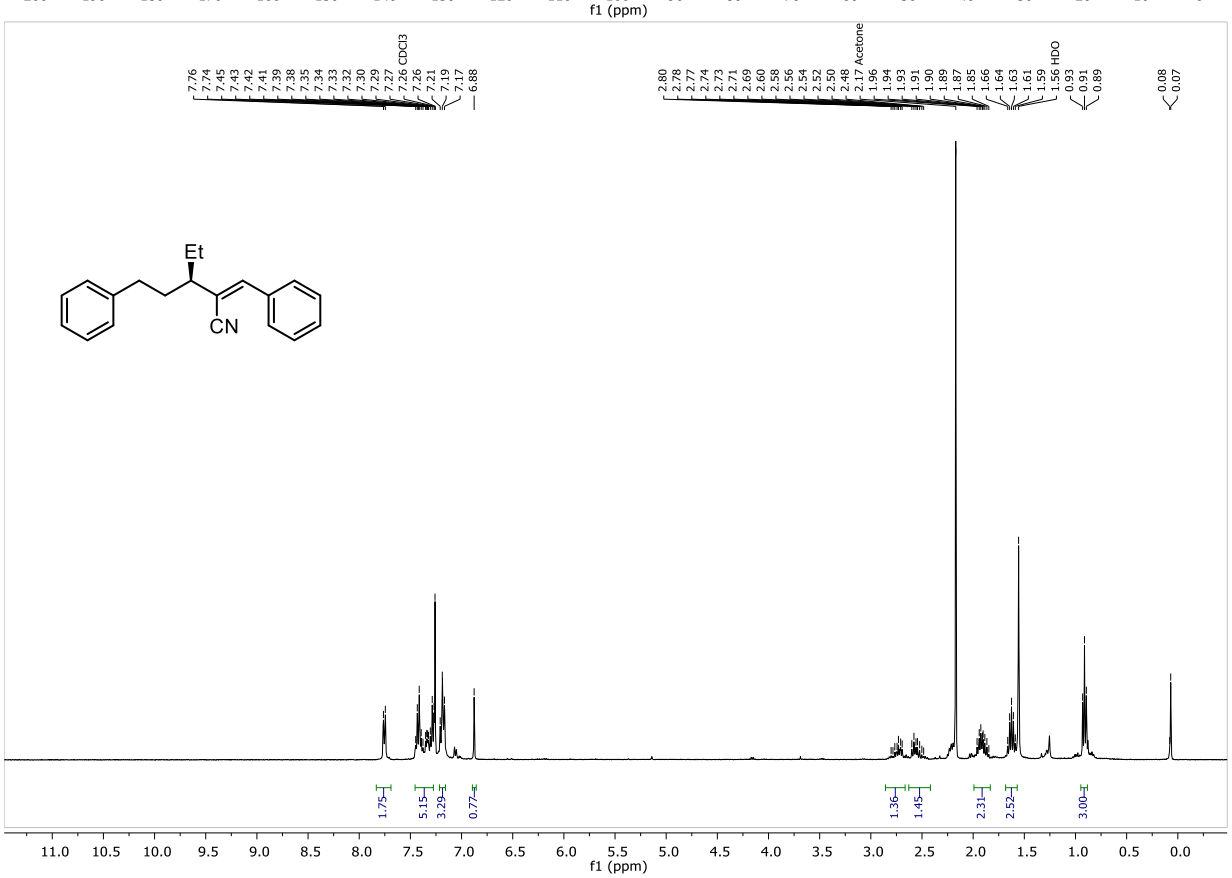
7.76
7.74
7.45
7.43
7.42
7.41
7.39
7.38
7.35
7.34
7.33
7.32
7.30
7.29
7.27
7.26 CDCl3
7.26
7.21
7.19
7.17
6.88
2.80
2.78
2.77
2.74
2.73
2.71
2.69
2.60
2.58
2.56
2.54
2.52
2.50
2.48
2.17 Acetone
1.96
1.94
1.93
1.91
1.90
1.89
1.87
1.85
1.66
1.64
1.63
1.61
1.59
1.56 HDO
0.93
0.91
0.89
0.08
0.07
Et
CN
1.75
5.15
3.29
0.77
1.36
1.45
2.31
2.52
3.00
f1 (ppm)

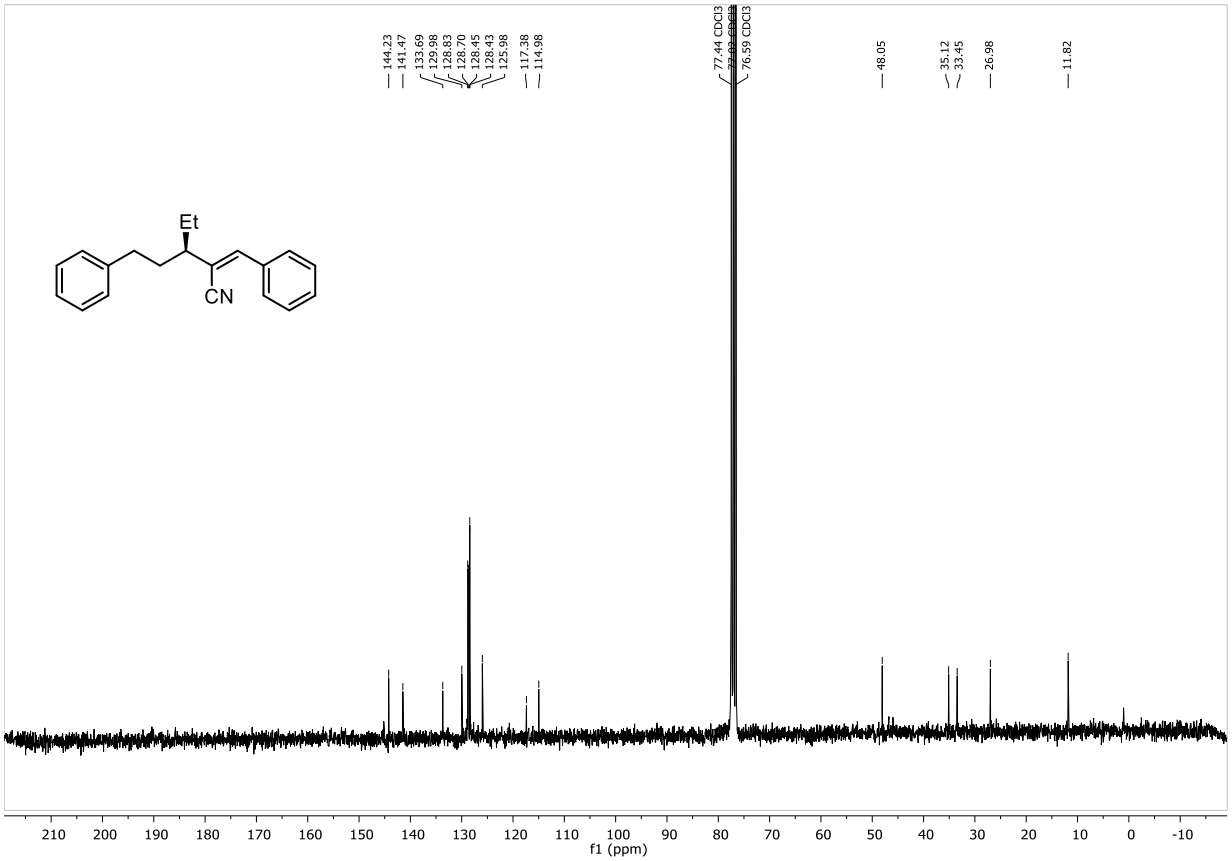
144.23
141.47
133.69
129.98
128.83
128.70
128.45
128.43
125.98
117.38
114.98
77.44 CDCl3
77.03 CDCl3
76.59 CDCl3
48.05
35.12
33.45
26.98
11.82
Et
CN
f1 (ppm)

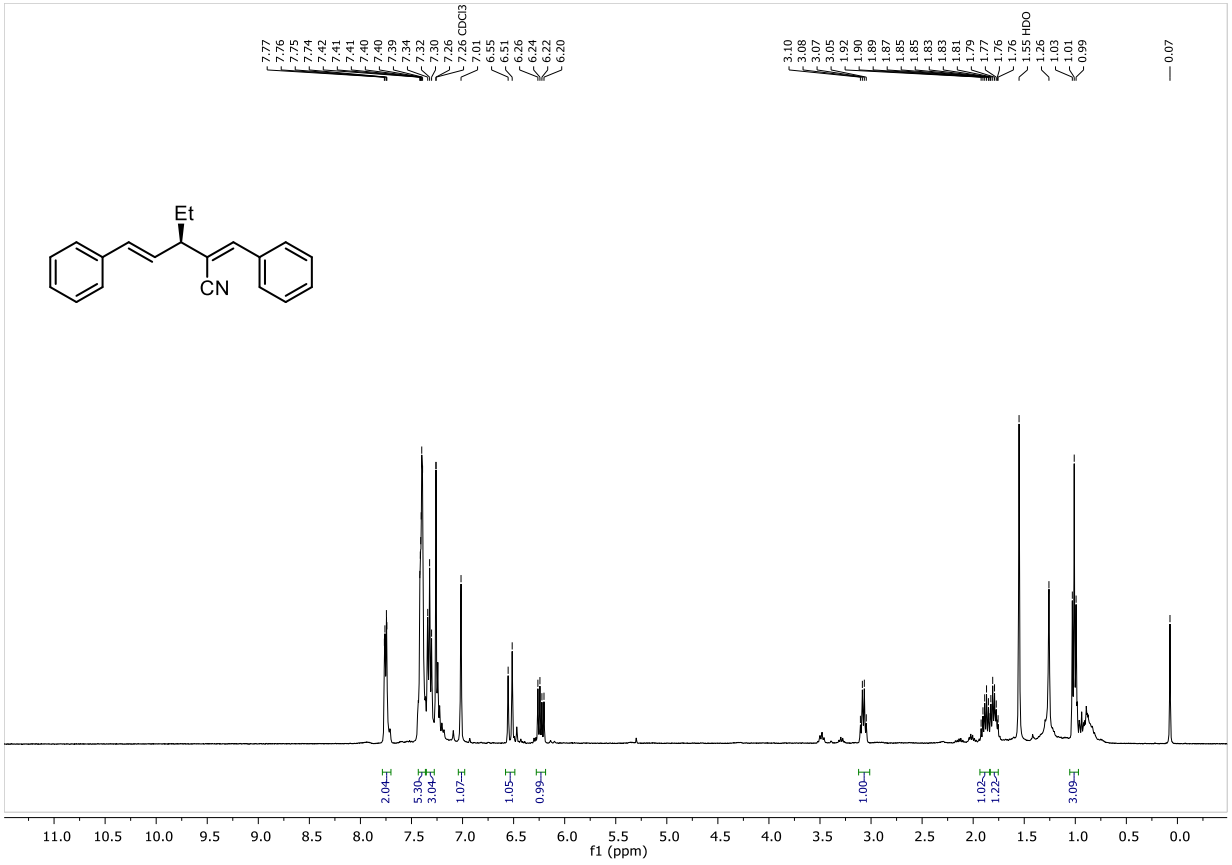
7.77
7.76
7.75
7.74
7.42
7.41
7.41
7.40
7.40
7.39
7.34
7.32
7.30
7.26 CDCl3
7.01
6.55
6.51
6.26
6.24
6.22
6.20
3.10
3.08
3.07
3.05
1.92
1.90
1.89
1.87
1.85
1.85
1.83
1.83
1.81
1.79
1.77
1.76
1.76
1.55 HDO
1.26
1.03
1.01
0.99
0.07
Et
CN
2.04
5.30
3.04
1.07
1.05
0.99
1.00
1.02
1.22
3.09
f1 (ppm)

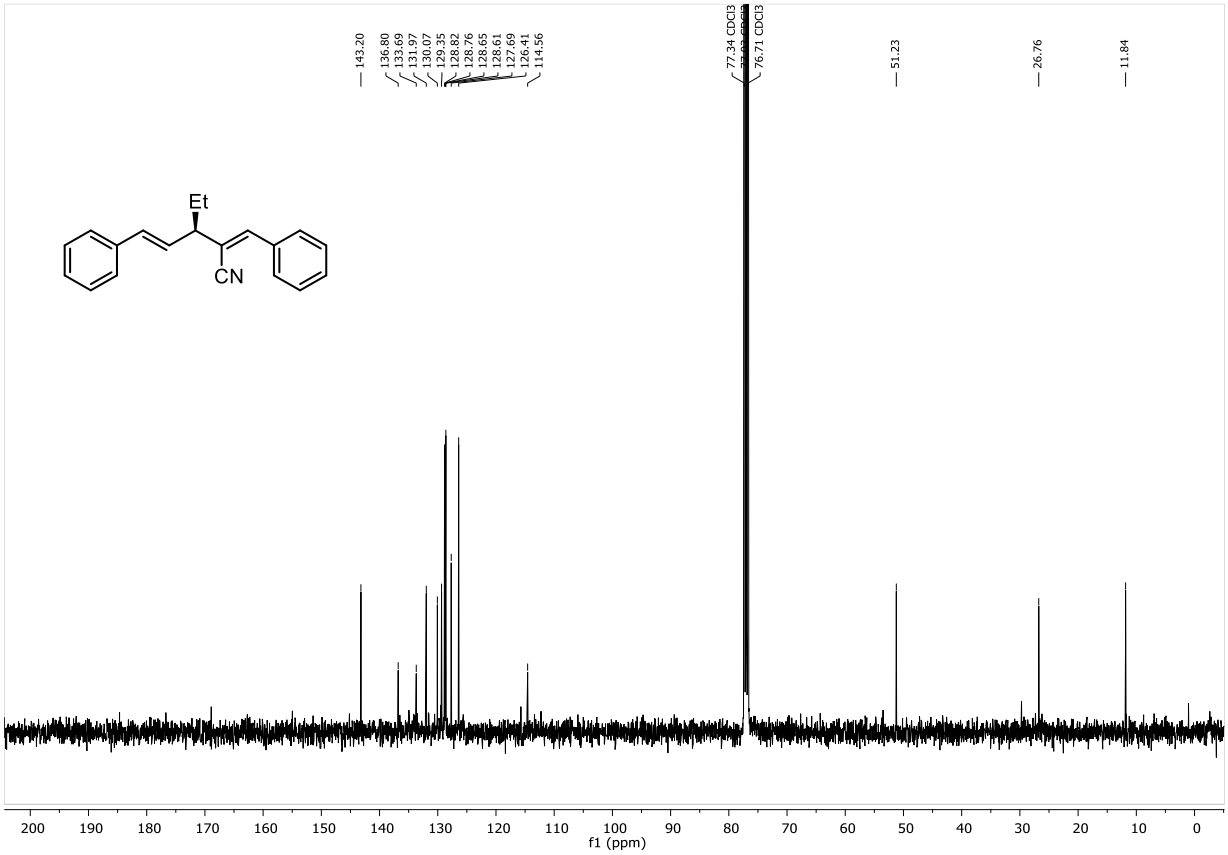
143.20
136.80
133.69
131.97
130.07
129.35
128.82
128.76
128.65
128.61
127.69
126.41
114.56
77.34 CDCl3
77.03
76.71 CDCl3
51.23
26.76
11.84
Et
CN
f1 (ppm)

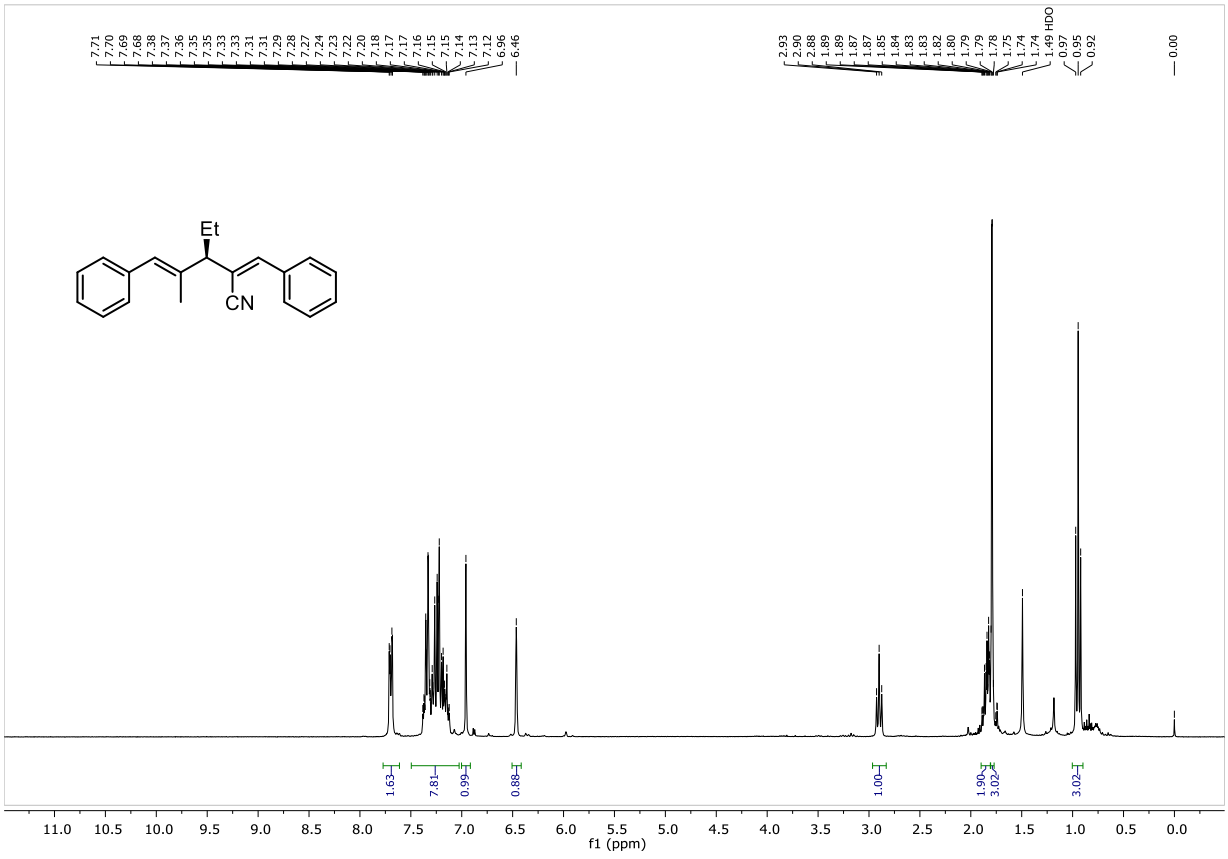
7.71
7.70
7.69
7.68
7.38
7.37
7.36
7.35
7.35
7.33
7.33
7.31
7.31
7.29
7.28
7.27
7.24
7.23
7.22
7.20
7.18
7.17
7.17
7.16
7.15
7.15
7.14
7.13
7.12
6.96
6.46
2.93
2.90
2.88
1.89
1.89
1.89
1.87
1.87
1.85
1.84
1.83
1.83
1.82
1.80
1.79
1.79
1.78
1.75
1.74
1.74
1.49 HDO
0.97
0.95
0.92
0.00
Et
CN
1.63
7.81
0.99
0.88
1.00
1.90
3.02
3.02
f1 (ppm)

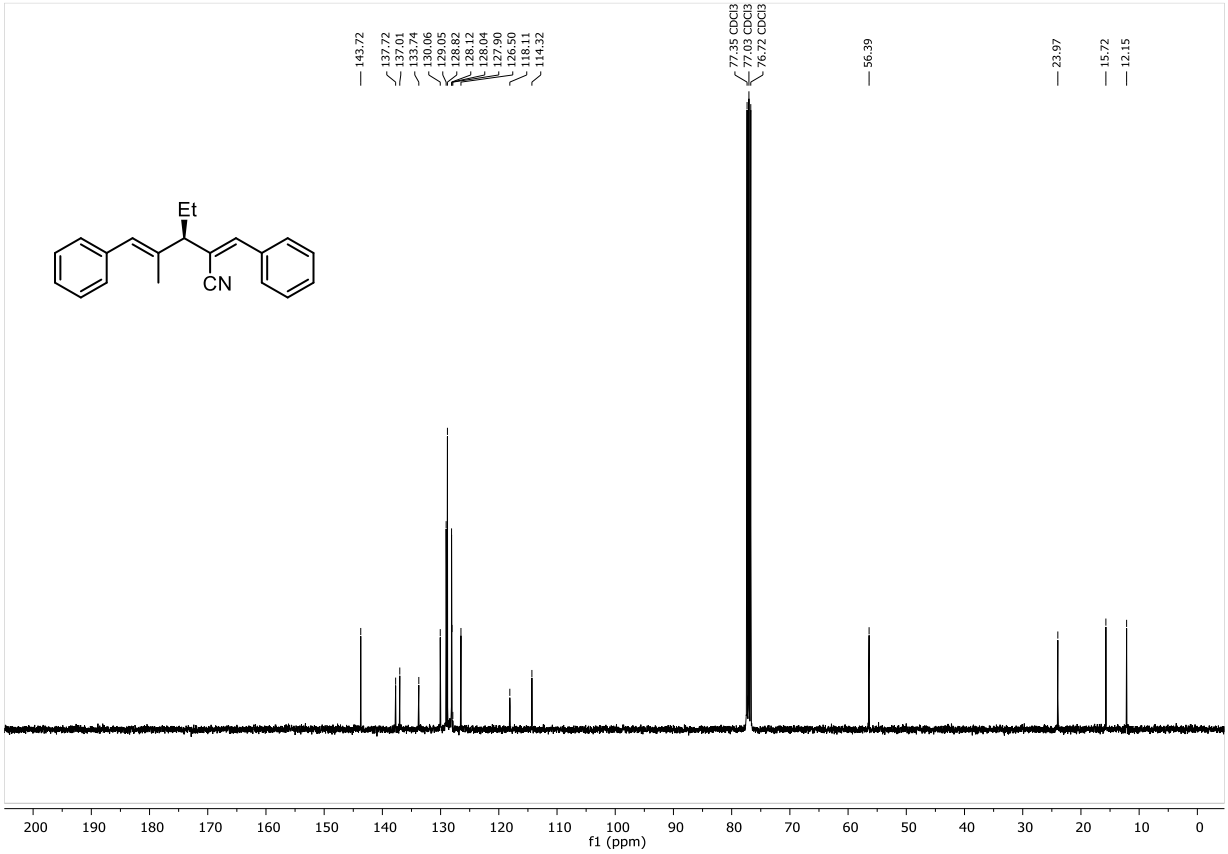
143.72
137.72
137.01
133.74
130.06
129.05
128.82
128.12
128.04
127.90
126.50
118.11
114.32
77.35 CDCl3
77.03 CDCl3
76.72 CDCl3
56.39
23.97
15.72
12.15
Et
CN
f1 (ppm)

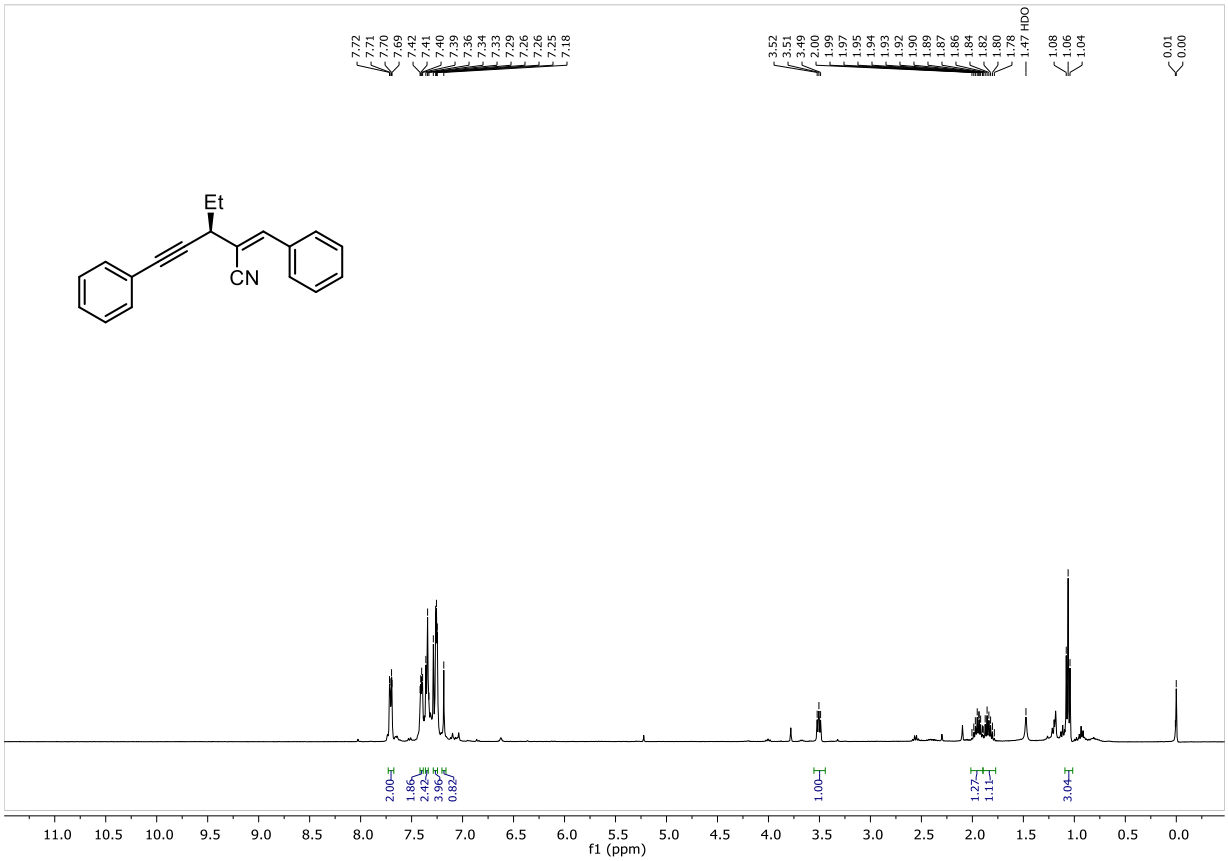
7.72
7.71
7.70
7.69
7.42
7.41
7.40
7.39
7.36
7.34
7.33
7.29
7.26
7.26
7.25
7.18
3.52
3.51
3.49
2.00
1.99
1.97
1.95
1.94
1.93
1.92
1.90
1.89
1.87
1.86
1.84
1.82
1.80
1.78
1.47 HDO
1.08
1.06
1.04
0.01
0.00
2.00
1.86
2.42
3.96
0.82
1.00
1.27
1.11
3.04
Et
CN
f1 (ppm)

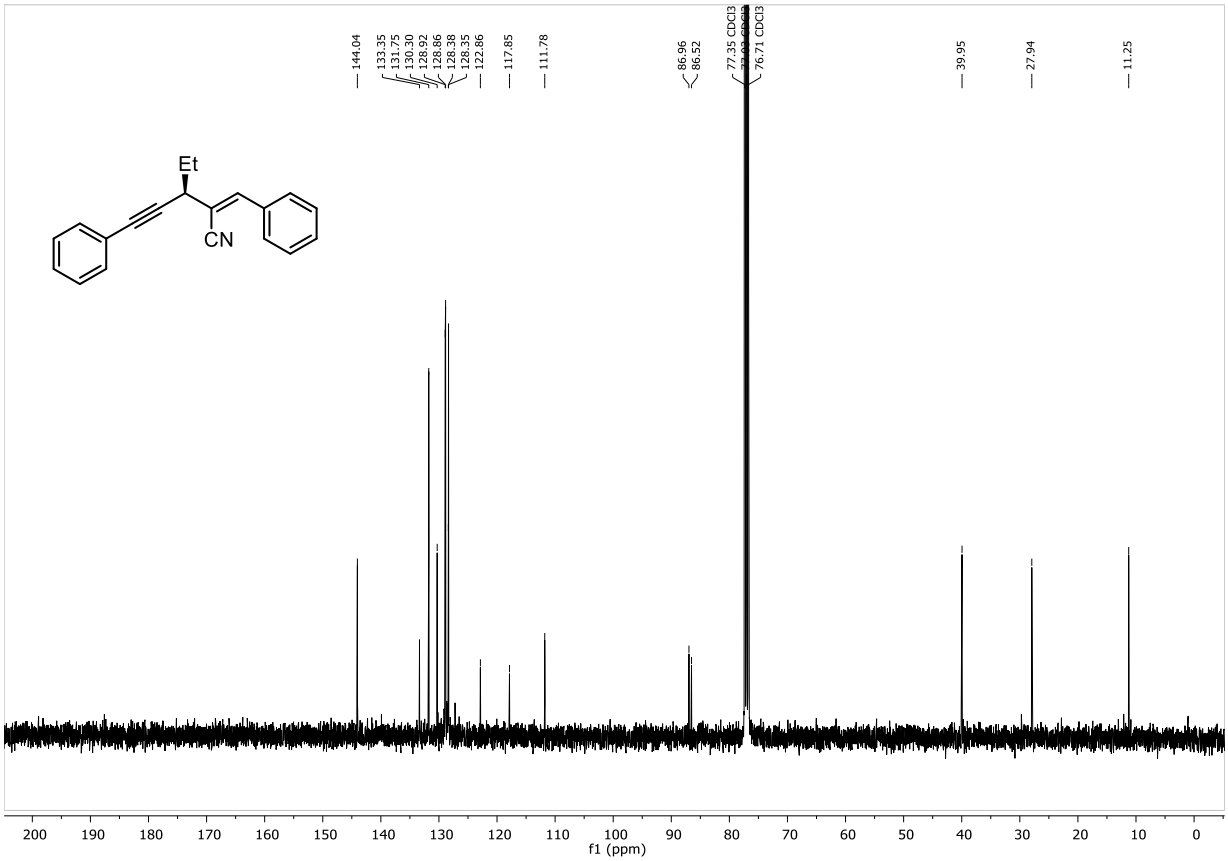
144.04
133.35
131.75
130.30
128.92
128.86
128.38
128.35
122.86
117.85
111.78
86.96
86.52
77.35 CDCl3
77.04 CDCl3
76.71 CDCl3
39.95
27.94
11.25
Et
CN
200 190 180 170 160 150 140 130 120 110 100 90 80 70 60 50 40 30 20 10 0
f1 (ppm)

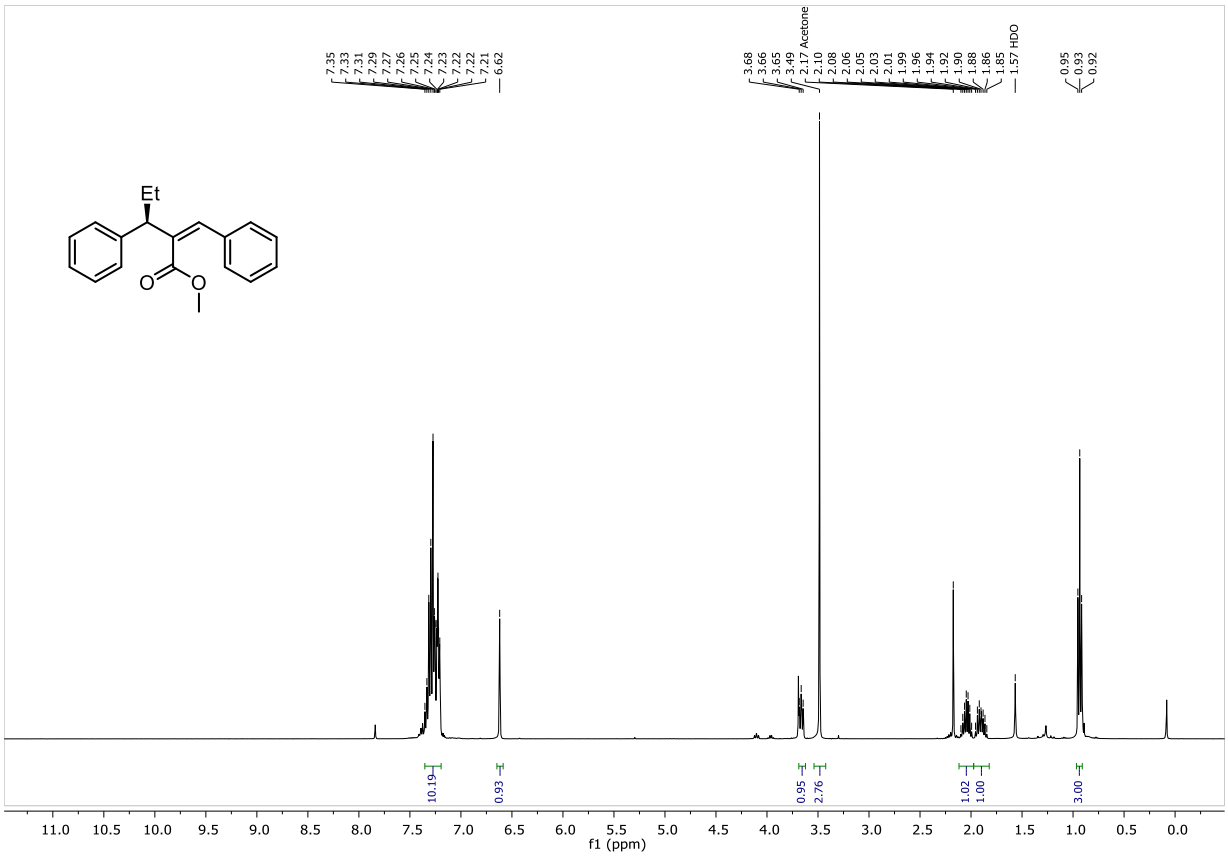
7.35
7.33
7.31
7.29
7.27
7.26
7.25
7.24
7.23
7.22
7.22
7.21
6.62
3.68
3.66
3.65
3.49
2.17 Acetone
2.10
2.08
2.06
2.05
2.03
2.01
1.99
1.96
1.94
1.92
1.90
1.88
1.86
1.85
1.57 HDO
0.95
0.93
0.92
Et
O
O
10.19
0.93
0.95
2.76
1.02
1.00
3.00
11.0 10.5 10.0 9.5 9.0 8.5 8.0 7.5 7.0 6.5 6.0 5.5 5.0 4.5 4.0 3.5 3.0 2.5 2.0 1.5 1.0 0.5 0.0
f1 (ppm)

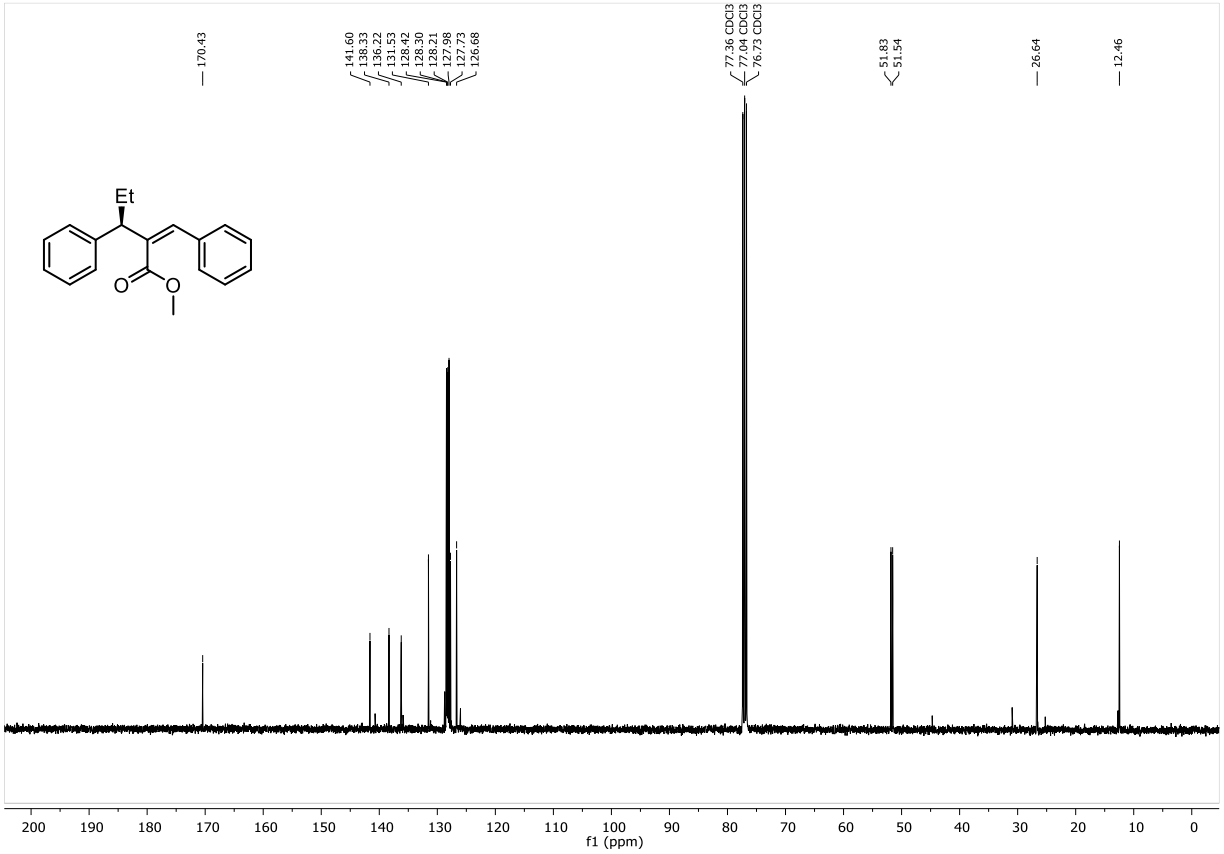
170.43
141.60
138.33
136.22
131.53
128.42
128.30
128.21
127.98
127.73
126.68
77.36 CDCl3
77.04 CDCl3
76.73 CDCl3
51.83
51.54
26.64
12.46
Et
O
O
f1 (ppm)

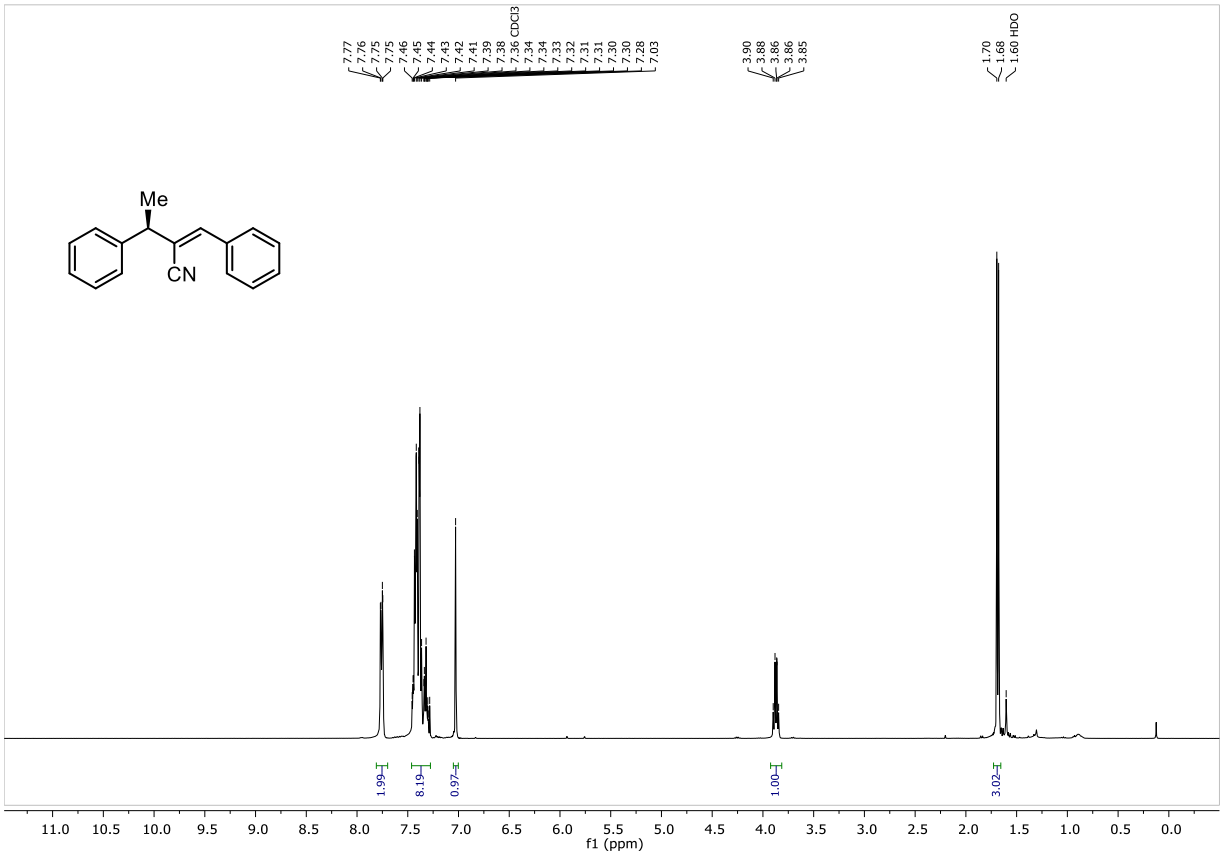
7.77
7.76
7.75
7.75
7.46
7.45
7.44
7.43
7.42
7.41
7.39
7.38
7.36 CDCl3
7.34
7.34
7.33
7.32
7.31
7.31
7.30
7.30
7.28
7.03
3.90
3.88
3.86
3.86
3.85
1.70
1.68
1.60 HDO
Me
CN
1.99
8.19
0.97
1.00
3.02
f1 (ppm)

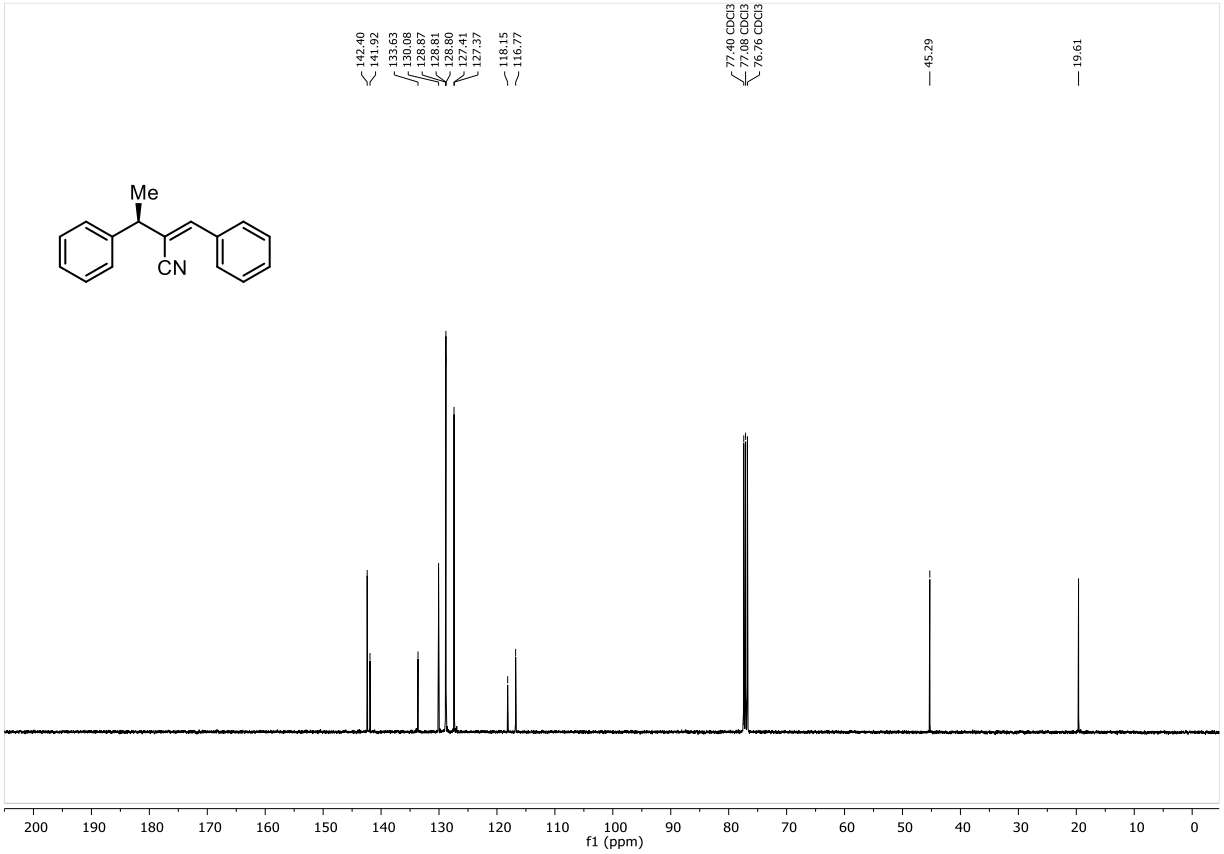
142.40
141.92
133.63
130.08
128.87
128.81
128.80
127.41
127.37
118.15
116.77
77.40 CDCl3
77.08 CDCl3
76.76 CDCl3
45.29
19.61
Me
CN
f1 (ppm)

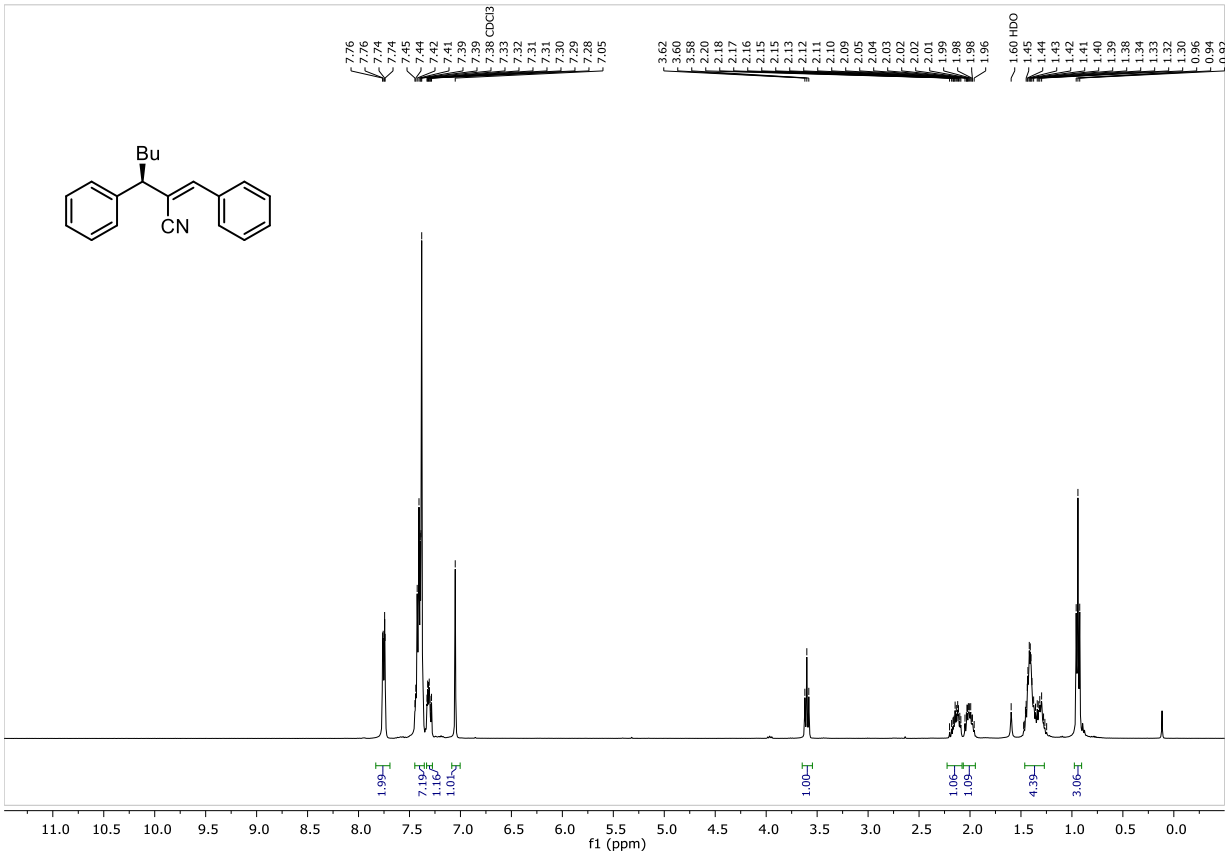
7.76
7.76
7.74
7.74
7.45
7.44
7.42
7.41
7.39
7.39
CDCl3
7.38
7.33
7.32
7.31
7.31
7.30
7.29
7.28
7.05
3.62
3.60
3.58
2.20
2.18
2.17
2.16
2.15
2.15
2.13
2.12
2.11
2.10
2.09
2.05
2.04
2.03
2.02
2.02
2.01
1.99
1.98
1.98
1.96
1.60 HDO
1.45
1.44
1.43
1.42
1.41
1.40
1.39
1.38
1.34
1.33
1.32
1.30
0.96
0.94
Bu
CN
1.99
7.19
1.16
1.01
1.00
1.06
1.09
4.39
3.06
f1 (ppm)

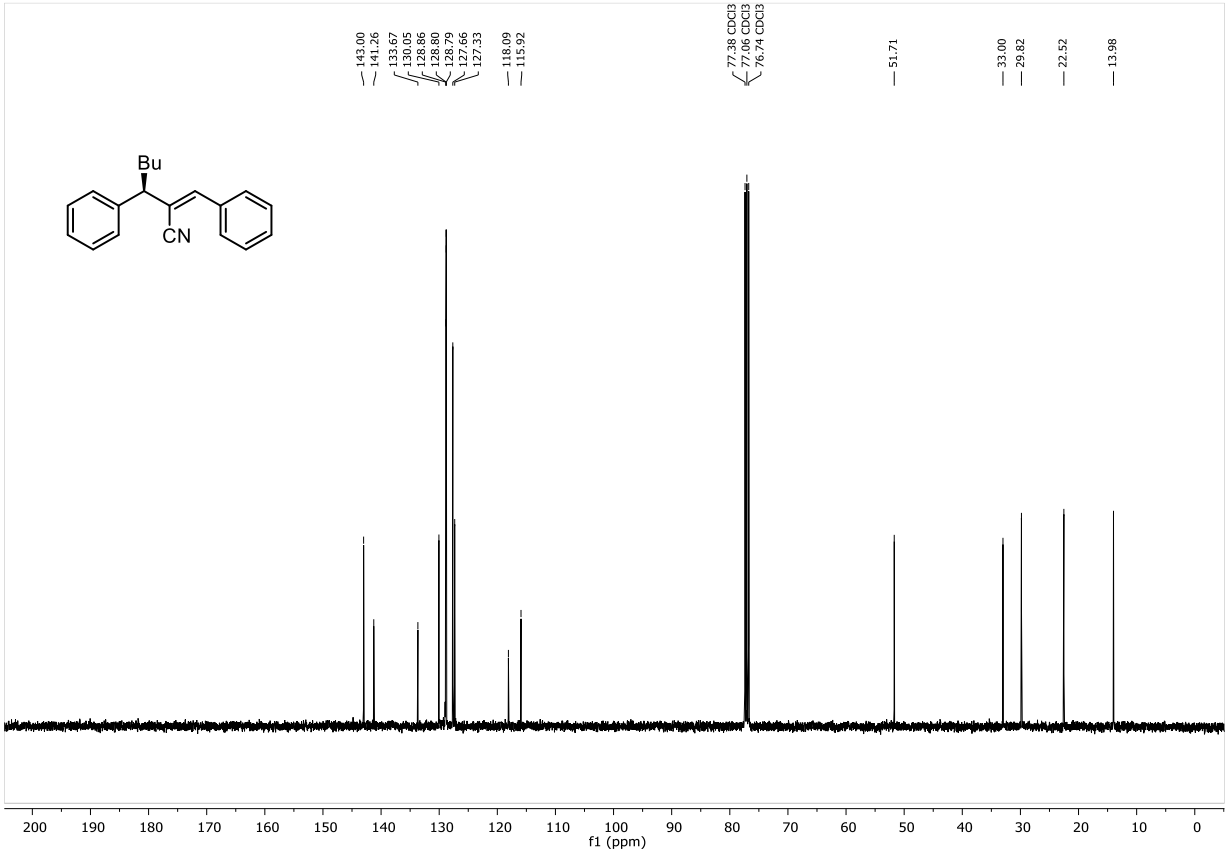
143.00
141.26
133.67
130.05
128.86
128.80
128.79
127.66
127.33
118.09
115.92
77.38 CDCl3
77.06 CDCl3
76.74 CDCl3
51.71
33.00
29.82
22.52
13.98
Bu
CN
f1 (ppm)

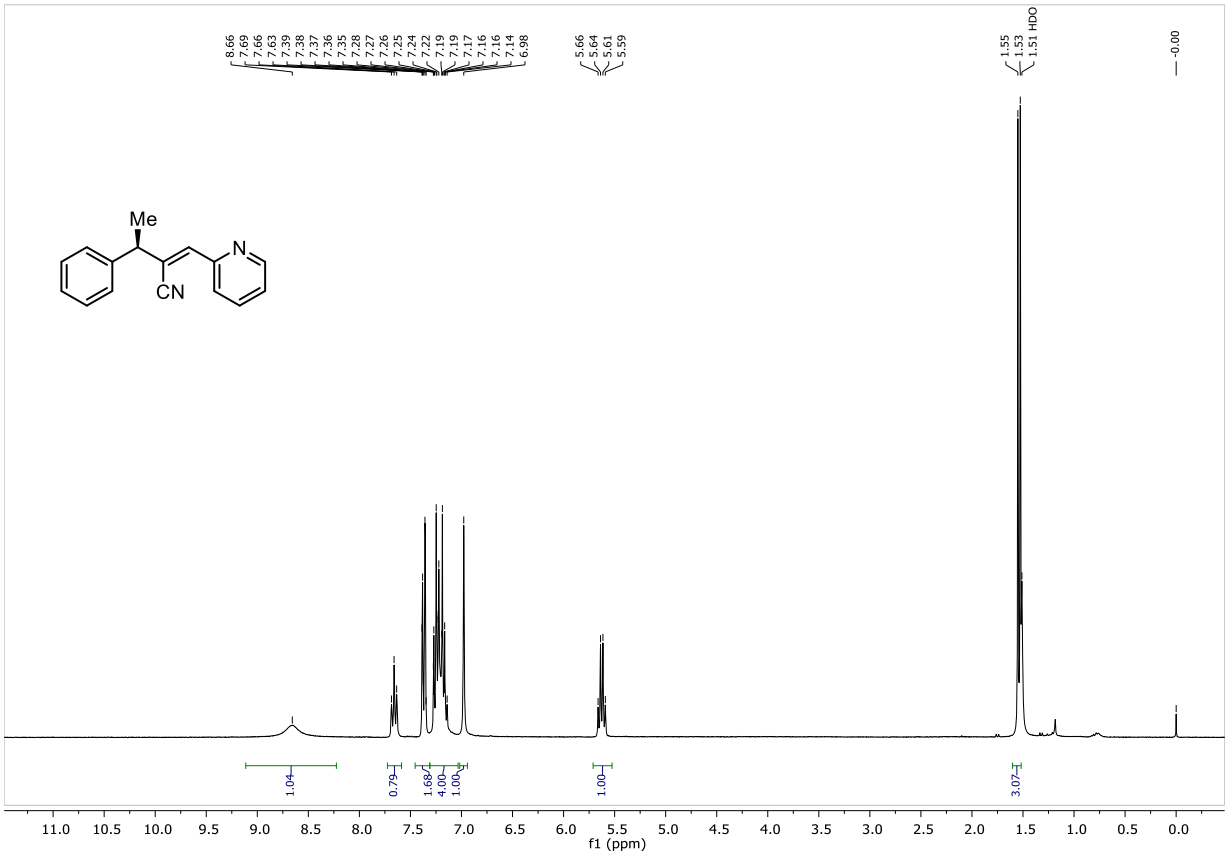
8.66
7.69
7.66
7.63
7.39
7.38
7.37
7.36
7.35
7.28
7.27
7.26
7.25
7.24
7.22
7.19
7.19
7.17
7.16
7.16
7.14
6.98
5.66
5.64
5.61
5.59
1.55
1.53
1.51 HDO
-0.00
Me
N
CN
1.04
0.79
1.68
4.00
1.00
1.00
3.07
f1 (ppm)

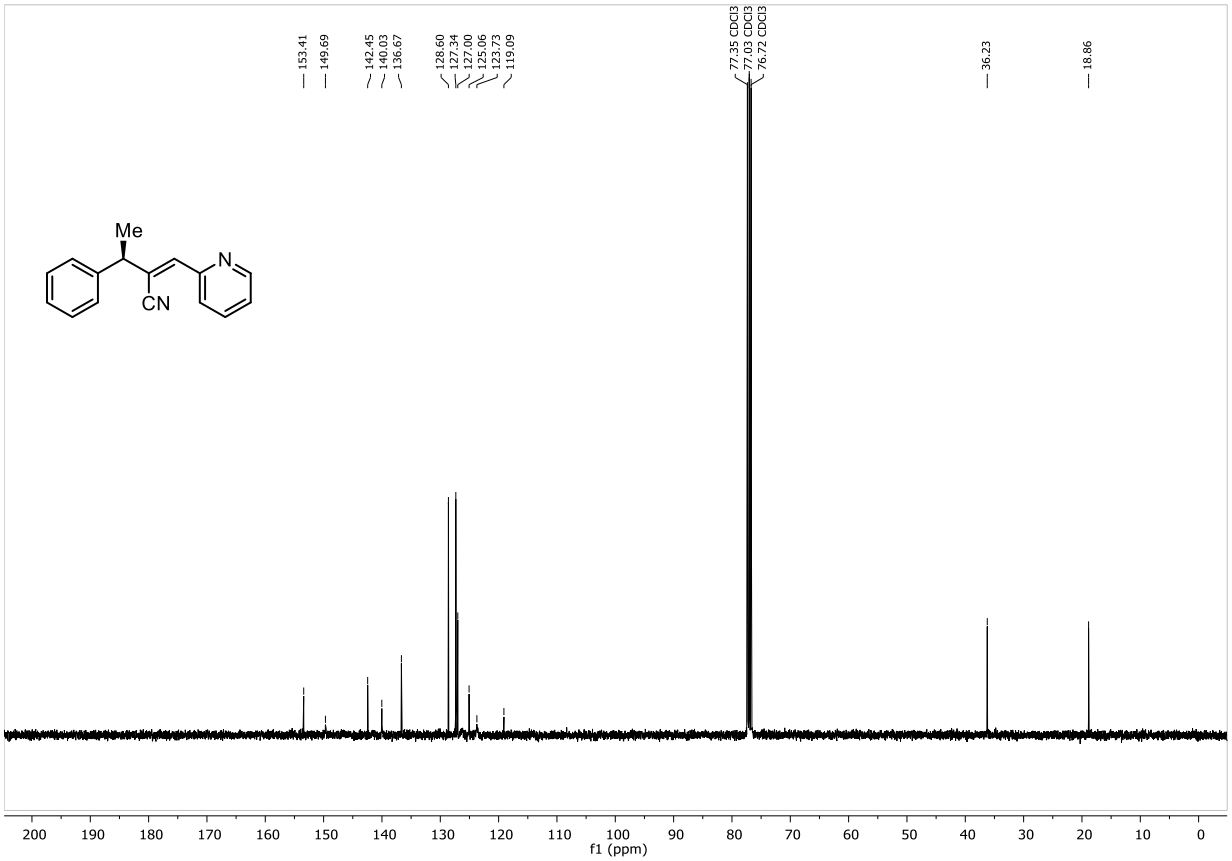
153.41
149.69
142.45
140.03
136.67
128.60
127.34
127.00
125.06
123.73
119.09
77.35 CDCl3
77.03 CDCl3
76.72 CDCl3
36.23
18.86
Me
N
CN
f1 (ppm)

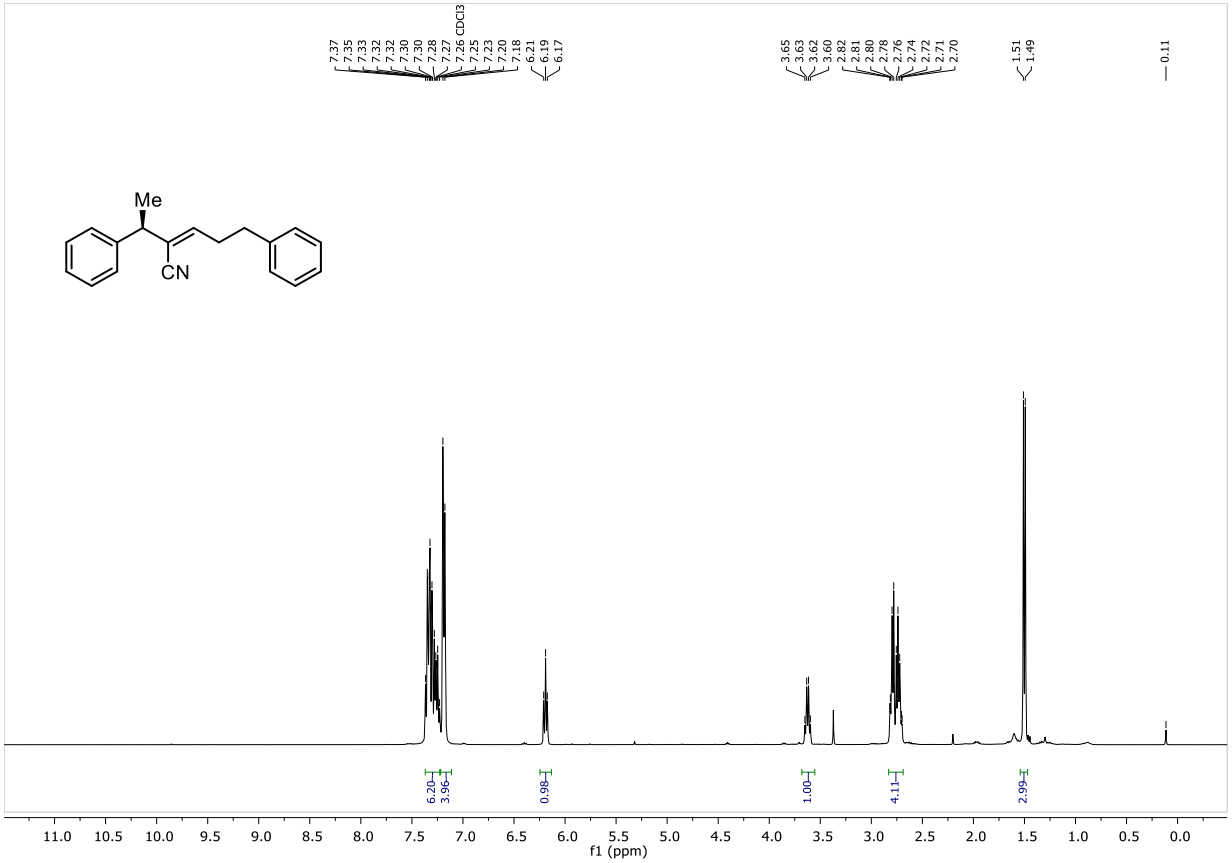
7.37
7.35
7.33
7.32
7.32
7.30
7.30
7.28
7.27
7.26 CDCl3
7.25
7.23
7.20
7.18
6.21
6.19
6.17
3.65
3.63
3.62
3.60
2.82
2.81
2.80
2.78
2.76
2.74
2.72
2.71
2.70
1.51
1.49
0.11
Me
CN
6.20
3.96
0.98
1.00
4.11
2.99
f1 (ppm)

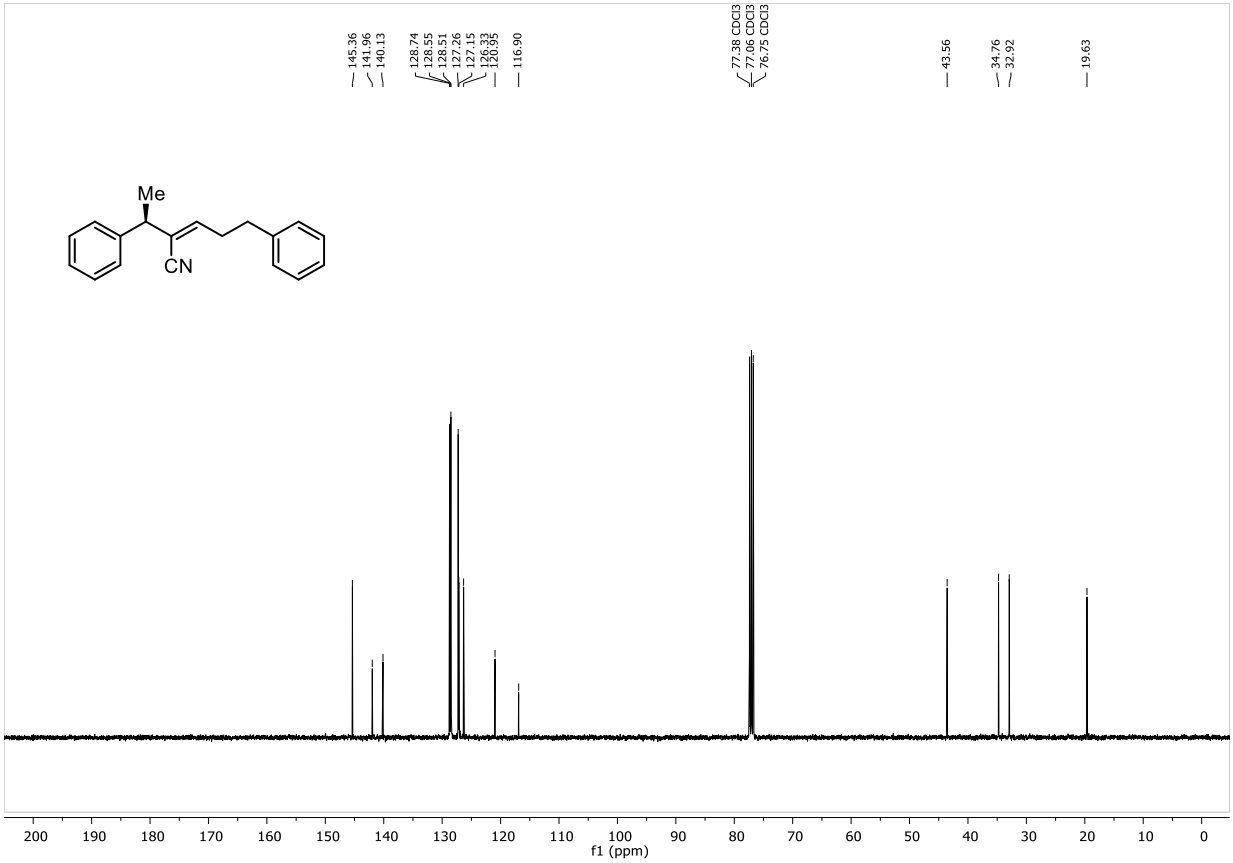
145.36
141.96
140.13
128.74
128.55
128.51
127.26
127.15
126.33
120.95
116.90
77.38 CDCl3
77.06 CDCl3
76.75 CDCl3
43.56
34.76
32.92
19.63
Me
CN
f1 (ppm)

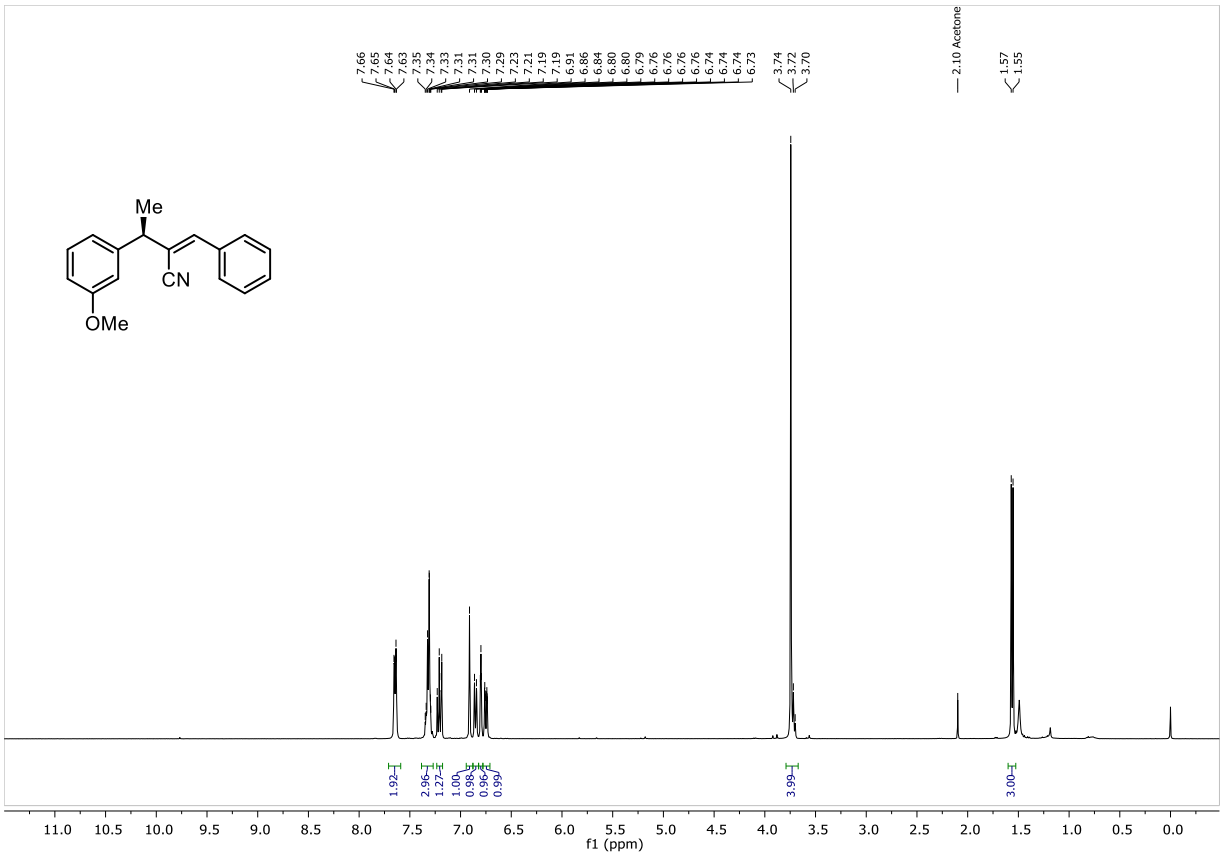
7.66
7.65
7.64
7.63
7.35
7.34
7.33
7.31
7.31
7.30
7.29
7.23
7.21
7.19
7.19
6.91
6.86
6.84
6.80
6.80
6.79
6.76
6.76
6.76
6.74
6.74
6.74
6.73
3.74
3.72
3.70
2.10 Acetone
1.57
1.55
Me
CN
OMe
1.92
2.96
1.27
1.00
0.98
0.96
0.99
3.99
3.00
f1 (ppm)

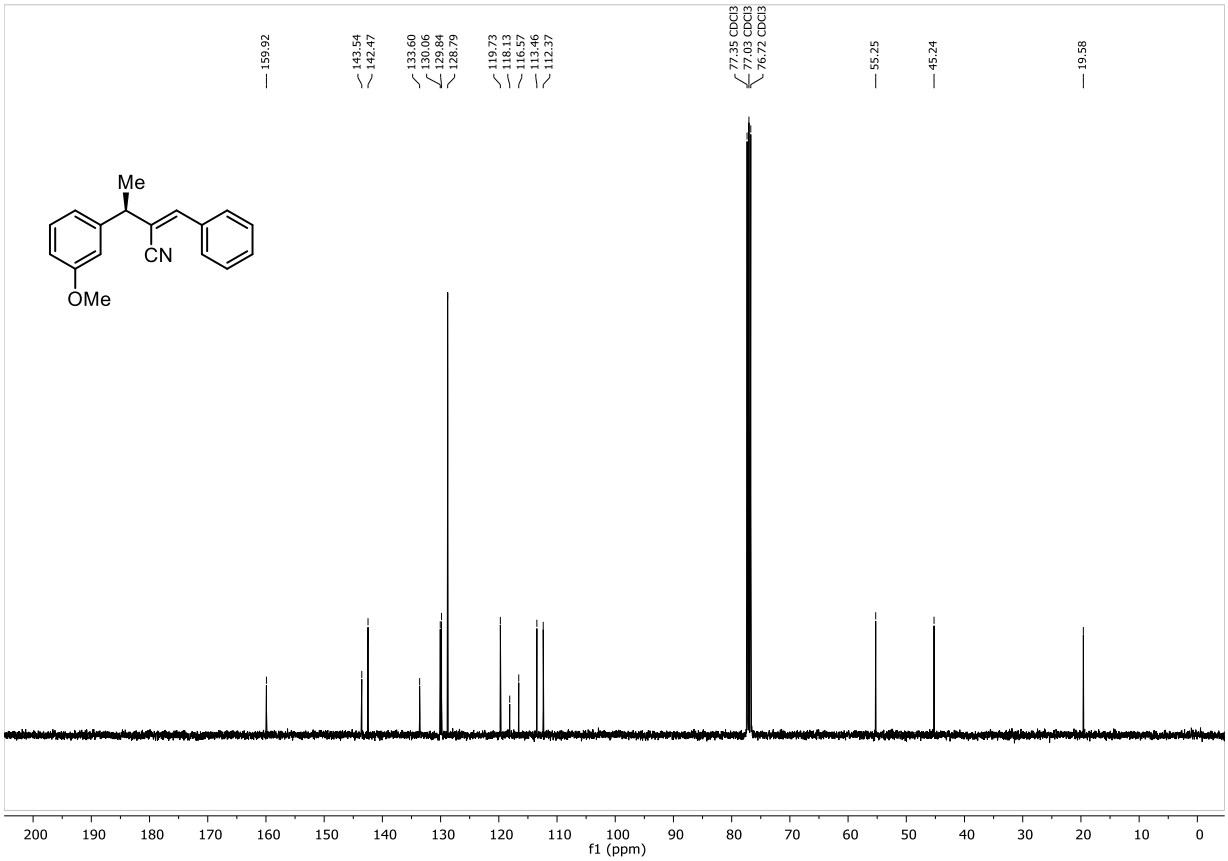
159.92
143.54
142.47
133.60
130.06
129.84
128.79
119.73
118.13
116.57
113.46
112.37
77.35 CDCl3
77.03 CDCl3
76.72 CDCl3
55.25
45.24
19.58
Me
CN
OMe
f1 (ppm)

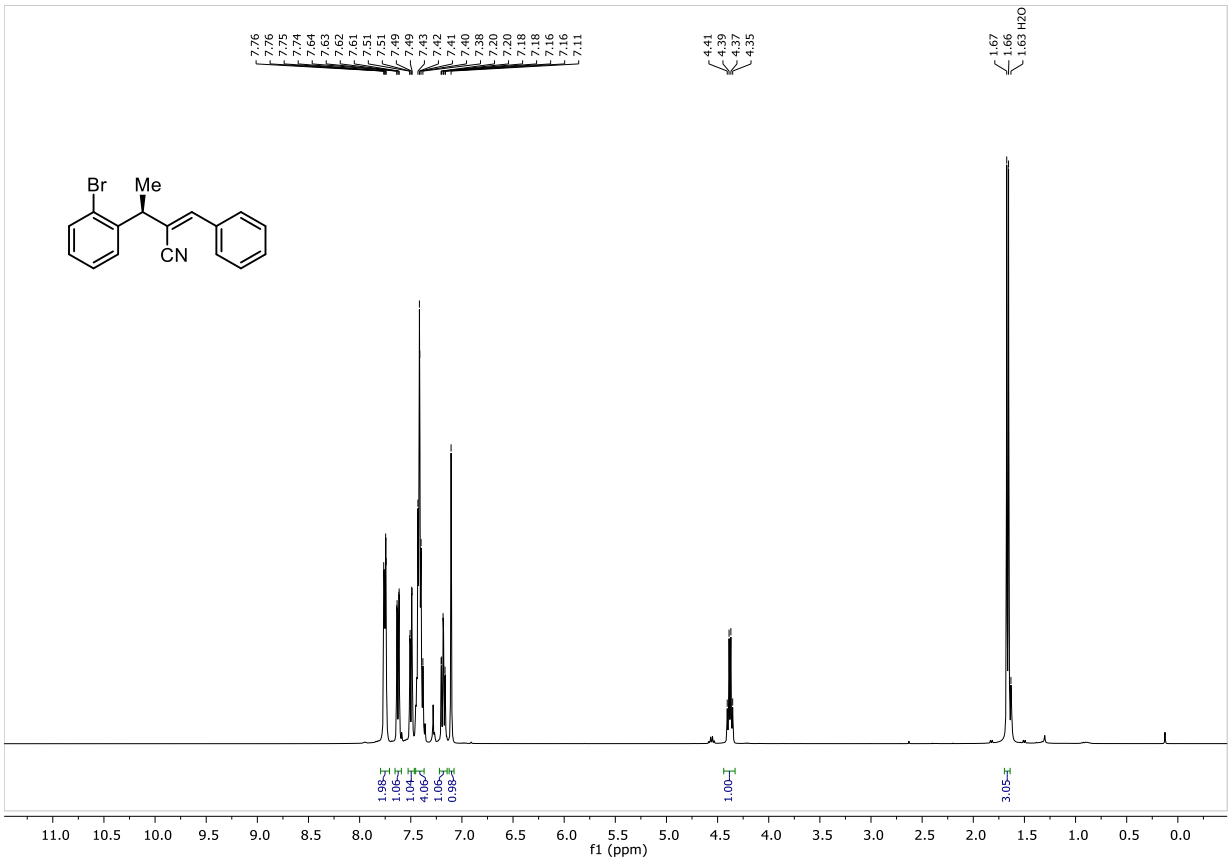
7.76
7.76
7.75
7.74
7.64
7.63
7.62
7.61
7.51
7.51
7.49
7.49
7.43
7.42
7.41
7.40
7.38
7.20
7.18
7.18
7.16
7.16
7.11
4.41
4.39
4.37
4.35
1.67
1.66
1.63 H2O
Br
Me
CN
1.98
1.06
1.04
4.06
1.06
0.98
1.00
3.05
f1 (ppm)

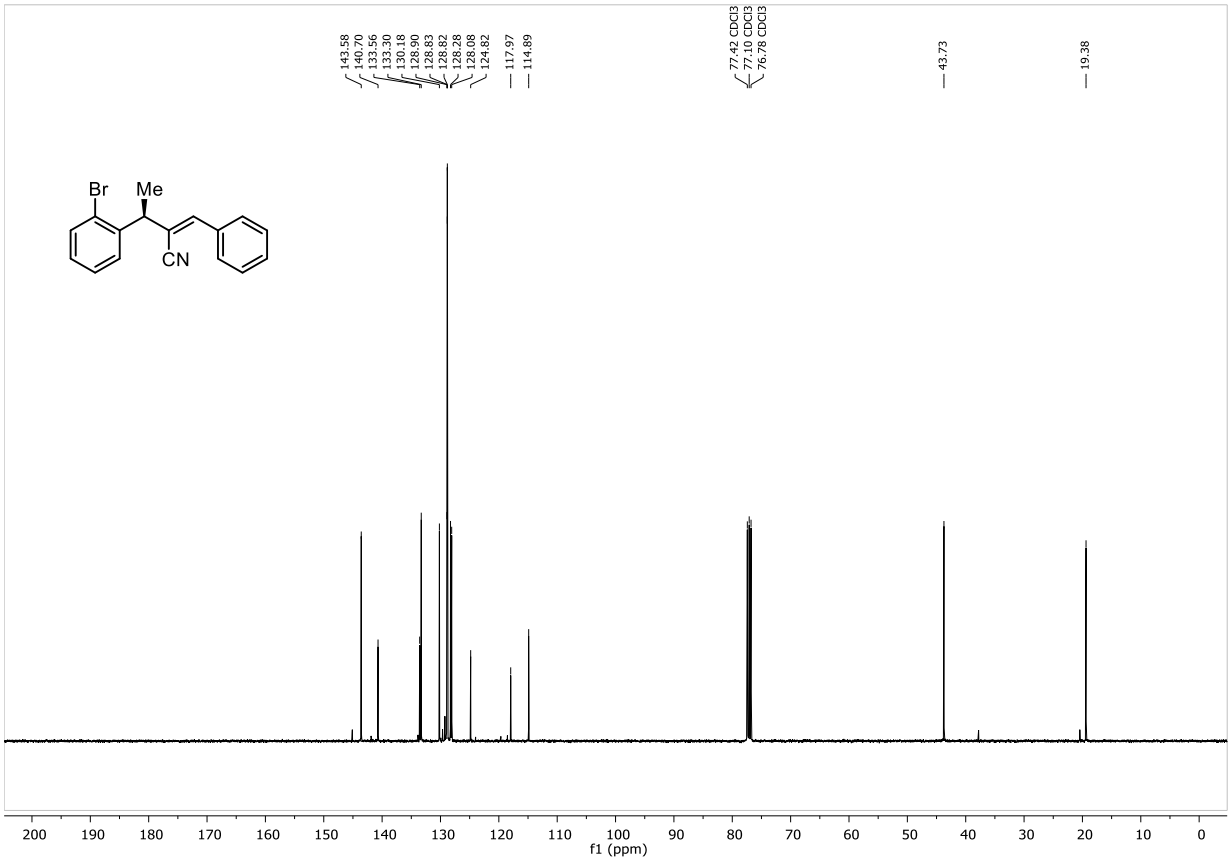
143.58
140.70
133.56
133.30
130.18
128.90
128.83
128.82
128.28
128.08
124.82
117.97
114.89
77.42 CDCl3
77.10 CDCl3
76.78 CDCl3
43.73
19.38
Br
Me
CN
200
190
180
170
160
150
140
130
120
110
100
90
80
70
60
50
40
30
20
10
0
f1 (ppm)

8. REFERENCES

1. Nozaki, H.; Moriuti, S.; Takaya, H.; Noyori, R. *Tetrahedron Lett.* 1966, 5239
2. Noyori, R. (2002), Asymmetric Catalysis: Science and Opportunities (Nobel Lecture). Angew. Chem. Int. Ed., 41: 2008-2022
3. Fulton, T. J.; Du, Y. E.; Stoltz, B. M. In *Catalytic Asymmetric Synthesis* 2022; pp 661-704
4. Pàmies, O.; Margalef, J.; Cañellas, S.; James, J.; Judge, E.; Guiry, P. J.; Moberg, C.; Bäckvall, J.-E.; Pfaltz, A.; Pericàs, M. A.; Diéguez, M. *Chem. Rev.* **2021**, *121*, 4373
5. a) Alexakis, A.; Bäckvall, J. E.; Krause, N.; Pàmies, O.; Diéguez, M. *Chem. Rev.* **2008**, *108*, 2796. b) Jerphagnon, T.; Pizzuti, M. G.; Minnaard, A. J.; Feringa, B. L. *Chem. Soc. Rev.* **2009**, *38*, 1039
6. Trost, B. M.; Crawley, M. L. *Chem. Rev.* **2003**, *103*, 2921
7. Falciola, C. A.; Alexakis, A. *European Journal of Organic Chemistry* **2008**, *2008*, 3765
8. Ohmiya, H.; Sawamura, M. *J. Synth. Org. Chem Jpn.* **2014**, *72*, 1207
9. Shintani, R. *Synthesis* **2016**, *48*, 1087
10. Feng, J.-J.; Mao, W.; Zhang, L.; Oestreich, M. *Chem. Soc. Rev.* **2021**, *50*, 2010
11. Hemming, D.; Fritzemeier, R.; Westcott, S. A.; Santos, W. L.; Steel, P. G. *Chem. Soc. Rev.* **2018**, *47*, 7477
12. Lonardi, G.; Parolin, R.; Licini, G.; Orlandi, M. *Ang. Chem. Int. Ed.* **2023**, e202216649
13. Yoshikai, N.; Nakamura, E. *Chem. Rev.* **2012**, *112*, 2339
14. Langlois, J.-B.; Alexakis, A. *Ang. Chem. Int. Ed.* **2011**, *50*, 1877
15. Calaza, M. I.; Yang, X.; Soorukram, D.; Knochel, P. *Org. Lett.* **2004**, 6, 4, 529-531
16. Ohmiya, H.; Yokobori, U.; Makida, Y.; Sawamura, M. *J. Am. Chem. Soc*. **2010**, *132*, 2895
17. Nagao, K.; Ohmiya, H.; Sawamura, M. *Synthesis* **2012**, *44*, 1535
18. Nagao, K.; Yokobori, U.; Makida, Y.; Ohmiya, H.; Sawamura, M. *J. Am. Chem. Soc*. **2012**, *134*, 8982
19. Whittaker, A. M.; Rucker, R. P.; Lalic, G. *Org. Lett*. **2010**, *12*, 3216
20. Ito, H.; Kunii, S.; Sawamura, M. *Nature Chemistry* **2010**, *2*, 972
21. van Zijl, A. W.; Szymanski, W.; López, F.; Minnaard, A. J.; Feringa, B. L. *J. Org. Chem.* **2008**, *73*, 6994
22. Alexakis, A.; Krause, N.; Woodward, S. In *Copper-Catalyzed Asymmetric Synthesis* 2014; pp 33-68
23. Alexakis, A.; Benhaim, C. *European Journal of Organic Chemistry* **2002**, *2002*, 3221
24. Hawner, C.; Alexakis, A. *Chemical Communications* **2010**, *46*, 7295

25. Vargová, D.; Némethová, I.; Šebesta, R. *Organic & Biomolecular Chemistry* **2020**, *18*, 3780
26. Guo, H.-C.; Ma, J.-A. *Ang. Chem. Int. Ed.* **2006**, 45, 354-366
27. de Vries, A. H. M.; Meetsma, A.; Feringa, B. L. Angew. Chem. **1996**, 108, 2526; Angew. Chem. Int. Ed. Engl. **1996**, 35, 2374
28. Feringa, B. L.; Pineschi, M.; Arnold, L. A.; Imbos, R; de Vries, A. H. M. Angew. Chem. **1997**, 109, 2733; Angew. Chem. Int. Ed. Engl. **1997**, 36, 2620
29. Alexakis, A.; Trevitt, G. P.; Bernardinelli, G. J. Am. Chem. Soc. **2001**, 123, 4358
30. Degrado, S. J.; Mizutani, H.; Hoveyda, A. H. J. Am. Chem. Soc. **2001**, 123, 755
31. Rathgeb, X.; March, S.; Alexakis, A. J. Org. Chem. **2006**, 71, 5737
32. Desrosiers, J.-N.; Bechara, W. S.; Charette, A. B. *Org. Lett.* **2008**, *10*, 2315
33. Bos, P. H.; Minnaard, A. J.; Feringa, B. L. *Org. Lett.* **2008**, *10*, 4219
34. Bos, P. H.; Maciá, B.; Fernández-Ibáñez, M. Á.; Minnaard, A. J.; Feringa, B. L. *Organic & Biomolecular Chemistry* **2010**, *8*, 47
35. Mauleón, P.; Alonso, I.; Rivero, M. R.; Carretero, J. C. *J. Org. Chem.* **2007**, *72*, 9924
36. Moure, A. L.; Gómez Arrayás, R.; Carretero, J. C. *Chemical Communications* **2011**, *47*, 6701
37. Nicotra, F.; Panza, L.; Russo, G. *J. Chem. Soc., Chem. Commun.* **1984**, 5
38. Li, N.-S.; Yu, S.; Kabalka, G. W. *Organometallics* **1999**, *18*, 1811
39. Baldwin, I. C.; Beckett, R. P.; Williams, J. M. J. *Synthesis* **1996**, *1996*, 34
40. Vieth, S.; Costisella, B.; Schneider, M. *Tetrahedron* **1997**, *53*, 9623
41. Barbot, F.; Paraiso, E.; Miginiac, P. *Tetrahedron Letters* **1984**, *25*, 4369
42. Roman, D.; Sauer, M.; Beemelmanns, C. *Synthesis* **2021**, *53*, 2713
43. Wang, Z. (2010). *Horner-Wadsworth-Emmons Olefination*. In *Comprehensive Organic Name Reactions and Reagents*, Z. Wang Ed.). doi: 10.1002/9780470638859.conrr332
44. Feringa, B. L.; Teichert, J. F. *Angew. Chem. Int. Ed.* **2010**, 49, 2486-2528
45. Matsunaga, S.; Das, J.; Roels, J.; Vogl, E. M.; Yamamoto, N.; Lida, T.; Yamaguchi, K.; Shibasaki, M. *J. Am. Chem. Soc*. **2000**, 122, 2252
46. Graves, C. R.; Zhou, H; Stern, C. L.; Nguyen, S. B. T. *J. Org. Chem.* **2007**, 72, 24, 9121-9133
47. Yang, F.; Wei, S.; Chen, C. A.; Xi, P; Yang, L.; Lan, J; Gau, H. M.; You, J. *Chem. Eur. J.* **2008**,14, 2223-2231
48. Shi, M.; Chen, L. H.; Li, C. O. *J. Am. Chem. Soc.* **2005**, 127, 11, 3790–3800

49. Alexakis, A.; Gille, S.; Prian, F.; Rosset, S.; Ditrich, K. *Tetrahedron Lett.* **2004**, 1449-1451
50. Song, J.; Yamataka, H.; Rappoport, Z. *J. Org. Chem.* **2007**, 72, 20, 7605–7624
51. Kaboudin, B.; Moradi, A.; Esfandiari, H.; Daliri, P; Kazemi, F.; Yanai, H.; Aoyama, H. ***Org. Biomol. Chem.***, **2022**, **20**, 2500-2507
52. Yao, Y.; Shu; H.; Tang, B.; Chen, S.; Lu, Z.; Xue; W. *Chin. J. Chem*. **2015**, 33, 601—609
53. Ishihara, K.; Kurihara, H.; Matsumoto, M.; Yamamoto, H. *J. Am. Chem. Soc.* **1998,** *120,* 6920-6930
54. Niu, D.; Buchwald, S. L. *J. Am. Chem. Soc.* **2015**, 137, 30, 9716–9721
55. Danion; Carrie *Bulletin de la Societe Chimique de France* 1972, p. 1130,1132, 1133, 1134